CONFIDENTIAL

164-7-26
Copy / of 3

[redacted] 25X1

Subject: FINAL REPORT

25X1 Reference: [redacted]

DICK S.

Dear Dick:

Enclosed are four copies of a report entitled "Automatic Image Recognition By Coherent Optical Techniques." This report is the final report on the referenced task. It is our understanding that you granted permission to release this report within the Company.

One copy of the report will be furnished to the contracting officer for his files.

[redacted] 25X1

Enclosures
(Four copies of Report No. 65-C-033,
25X1 [redacted] September 1965)

Declass Review by NGA.

GROUP 1
EXCLUDED FROM AUTOMATIC DOWNGRADING AND DECLASSIFICATION

CONFIDENTIAL

RECEIPT FOR CLASSIFIED MATERIAL

File 99738)

(AVOID INCLUSION OF CLASSIFIED INFORMATION ON THIS FORM)

Date: 30 September 1965

TO: Dick S.
Washington, D.C.

FROM: [redacted] 25X1

INSTRUCTIONS

1. ORIGINAL OF THIS RECEIPT TO BE SIGNED BY RECIPIENT AND RETURNED TO [redacted]
2. DUPLICATE TO BE RETAINED BY RECIPIENT
3. TRIPLICATE TO BE RETAINED BY SENDER IN SUSPENSE FILE

ACCOUNTABILITY NUMBER	IDENTIFICATION NUMBER	COPY NO. AND SERIES	CLASS.	DESCRIPTION (For documents, give type, pages, date, author, etc.)
	164-7-26	1&2	C	Letter, T. O. 99, 30 Sept 1965 and attachments. Final Report

CERTIFICATE

I have personally received the material as identified above. I assume full responsibility for the safe handling, storage and transmittal elsewhere of this material in accordance with existing security regulations.

SIGNATURE [redacted] 25X1

NAME

DATE 6 Oct 65

66# 99738.5

14 May 1965

The undersigned acknowledges receipt of the following material:

1 Roll of 9" film (Unclassified)

32 Strips of 5" film (Secret)
(RADC Control No. 65-S-13611)

25X1

Name

Company

Date 18 May 1965

Please Return signed Copy to Project Monitor.

[redacted]

CLASS 2

FILE COPY
FINAL REPORT
FILE 99738
P&D5/NPIC

AUTOMATIC IMAGE RECOGNITION BY COHERENT OPTICAL TECHNIQUES

by

[redacted]

25X1

Report No. 65-C-033 September 3, 1965

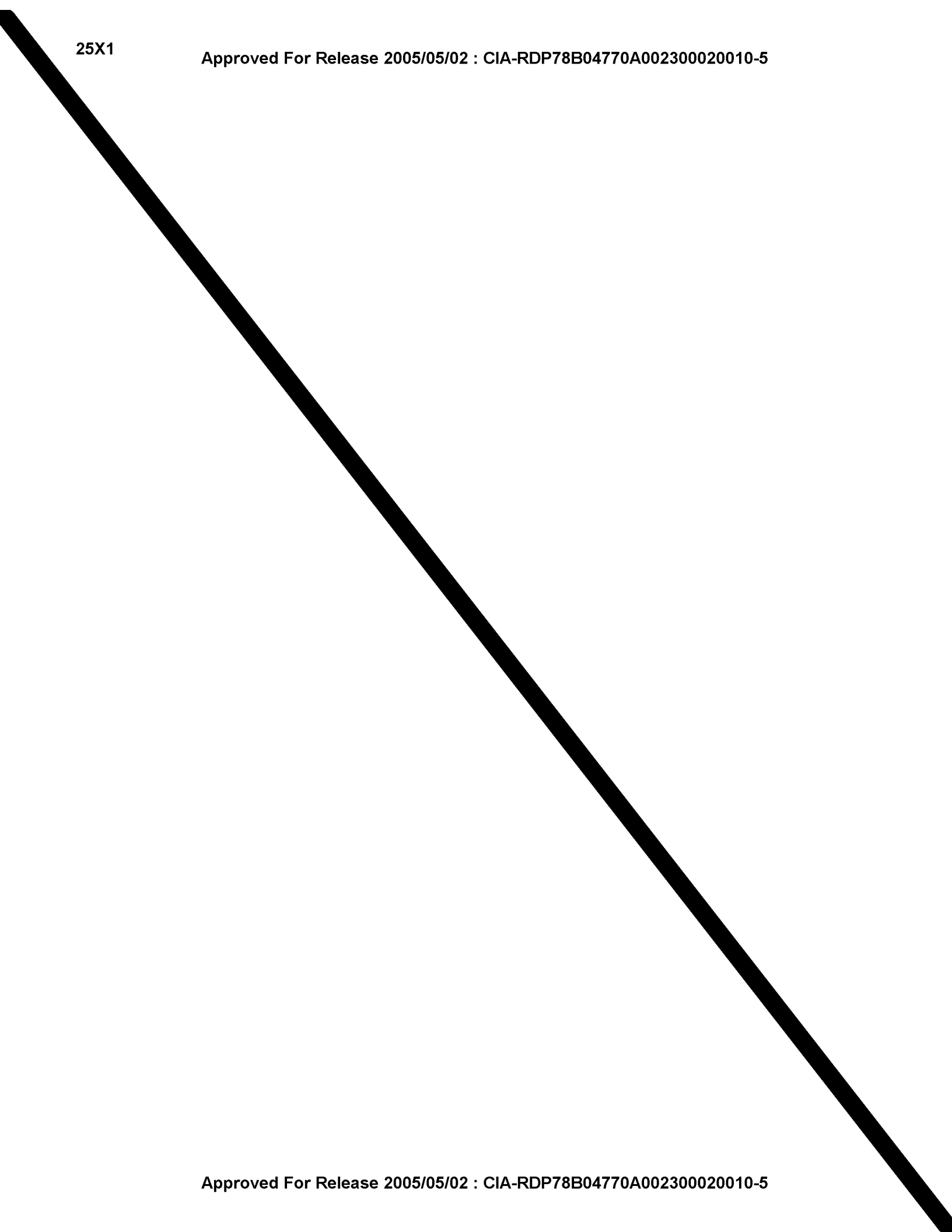

Approved For Release 2005/05/02 : CIA-RDP78B04770A002300020010-5

FILE COPY
FINAL REPORT

25X1

	SUBJECT Optical Image Recognition	NO. 65-C-033
		DATE 9/3/65
TITLE Automatic Image Recognition by Coherent Optical Techniques		II
		GOVT. CLASS None
		NO. PAGES 270

25X1

25X1

SUMMARY

This report covers a series of studies aimed at determining the technical feasibility of an automatic image recognition system employing coherent optical techniques. The overall study considered the theoretical limitations, the photographic or image problems, the equipment design problems and the problems of automating the recognition system. Twenty-three different image and system or equipment variables were studied. The results of this study indicate that image recognition by spatial filtering is technically feasible under the various conditions considered.

KEY WORDS

Image Recognition, Spatial Filtering, Optical Information Processing, Optics, Hologram

25X1

Approved For Release 2005/05/02 : CIA-RDP78B04770A002300020010-5

TABLE OF CONTENTS

Automatic Image Recognition by Coherent Optical Techniques

Introduction

It is assumed that the reader is familiar with the principles of optical processing of information by coherent light. This was described in an earlier 25X1 report "The 3-D Hologram Process and Image Recognition by Spatial Filtering" by [redacted] report no. 64GL159.* The theory and mathematics of the subject were described in "Signal Detection by Complex 25X1 Spatial Filtering" by [redacted] IEEE Transactions on Information Theory, April, 1964, page 139.

The vocabulary of this subject has been drawn from mathematics, information theory, radar, interferometery and optics, and is confusing to the beginner. All of the special terms used in this report are defined in the two references given above.

The purpose of the work covered in this report was to determine the feasibility of designing a completely automatic recognition device to search aerial camera film and detect the presence of specified objects or "targets" as they are called in this report. As conceived, the device would be loaded with a roll of film containing many frames and also one or several spatial filters for the targets of interest. The equipment would be turned on and would operate automatically until all the film was processed. The output would consist of a printed record or set of punched cards which would give the frame numbers on which the targets occurred, which targets were in what frames, the total number of targets found on the entire film and possibly other information. Not specifically covered in this study, but considered were such additional information as the x and y location of the detected targets in the proper frames. This could be recorded either as a pair of numbers or a photograph which would indicate the location of the targets in the frame.

25X1 * Internal [redacted] Report

Before such a piece of automatic equipment can be designed it is necessary to know a number of the engineering features of the system and this study was planned to cover as many of these as could be foreseen in 1964. The study was divided into four major portions:

A. Theory

B. Equipment

C. Automation

D. Picture Variables

Section A - Theory

The main problem considered here was to find if there were any theoretical limitations to the recognition process which would make an automatic device impractical. Specifically, one point was to find if the large amount of information produced by a highly detailed photograph would be too great for the optical system to handle. Also, it was desired to know if there was a limitation to the amount of information that could be stored in the spatial filter and if this would present a real restriction on the process. It was also desired to know whether theory indicated any difference in performance or limitation to spatial filters made by the [redacted] process of instant photography known as Photoplastic recording. 25X1

It was also desirable to calculate the expected signal-to-noise ratio which the process should produce and compare this to actual values.

These problems were separated into five subjects:

A-1 Maximum Information Content of a Spatial Filter.

A-2 Optimum Modulation Transfer Function for a Recognition System.

A-3 Use of a Phase Modulation Media for Recording Data and for Recording Spatial Filters.

A-4 Obtainable Signal-to-Noise Ratios.

A-5 Information Capacity of a Recognition System.

A-6 Effect of Image Size.

All of the theoretical work was done [redacted] 25X1

INFORMATION CONTENT OF A TWO-BEAM SPATIAL FILTER

1. Introduction

When spatial filters are used for signal detection in photo-records it is necessary to determine what information content the filters must have to adequately carry out the detection process. Generally, the information content of a filter is closely related to the space-bandwidth product of the filter. This close relationship is valid only, however, if the filter is a low-pass function. If the filter is a band-pass function, the information content and the space-bandwidth product may differ considerably. The two-beam process used to construct complex-valued filters as real valued functions on a carrier frequency is a band-pass process so that we can expect this difference to exhibit itself.

In the next paragraph we will define what we mean by information content and space-bandwidth product. In the following section we will carry out the analysis necessary to determine these quantities for spatial filters. The final section will summarize the results and state a few conclusions.

2. Definition of Space-Bandwidth Product and Information Content

The term "space-bandwidth product" (SBP) is the two-dimensional analogy to the term "time-bandwidth product" in an electronic system. It is the product of the area of a given signal and the number of resolution elements that it contains. If the signal has area A, and is limited in frequency to p_o, then SBP = $A\ p_o^2$. In any optical system having bandwidth at least as great as p_o, the SBP of the signal is the same in any plane normal to the optical axis. Thus, the SBP of a signal is dependent only on the area of the signal and the highest frequency that it contains.

The term "information content" implies that we know the area of the signal, its bandwidth, and the number of states that a resolution element can occupy. Note that in the definition of information content involves the use of the bandwidth of the signal which is the difference between the highest and lowest frequencies in the signal. If the signal is a low-pass function, the lowest frequency is zero and the bandwidth B is simply p_o. If the signal is a band-pass function with lowest frequency p_1, then the bandwidth $B = p_o - p_1$.

In the noise-free case, a resolution element might occupy any one of N states. If the probabilities associated with these states are denoted by p_i, then we can say that each element can contain:

$$H = -\sum_{i=1}^{N} p_i \log_2 P_i$$

bits of information. If all the p_i are equal, $H = \log_2 N$. The information content of the filter is then said to be:

$$IC \text{ (Information Content)} = AB^2H \text{ bits of information}$$

where $B = p_o$ or $B = p_o - p_1$ depending on whether the signal is a low-pass or a band-pass function.

The information content of the signal part of the filter is not altered by the presence of noise in the input because, for the type of filtering considered here, the filter is constructed from a noise-free signal. The noise-rejection part of the filter is dependent on the types of noise present in the input, and its effect on the IC of the filter will be considered near the end of the next section.

Further, the estimate of the IC of the signal was based on a discreet system analysis. It could equally well be based on a continuous system analysis with an integral replacing the sum in the computation of H.

3.0 Analysis of the Space-Bandwidth Product and the Information Content of Spatial Filters

In this section we will consider the space-bandwidth product and the information content of spatial filters. To get precise answers to this problem we must develop some fundamental parameters of the problem. In particular, we are interested in detecting arbitrary signals in photo-records. We assume that the signals are known and that the noise is additive, isotropic and homogeneous (See Reference 1). Under these conditions it is appropriate to operate on the input data f(x,y) with a filter whose transfer function is:

$$H(p,q) = \frac{k\ S^*(p,q)}{N(p,q)} \qquad (3.1)$$

where $S^*(p,q)$ is the conjugate of the Fourier transform of the signal of interest $s(x,y)$

$N(p,q)$ is the Fourier transform of the autocorrelation function of the noise $n(x,y)$

k is a constant.

These functions are defined by the following relationships:

$$S(p,q) = \iint s(x,y)\ e^{j(px + qy)}\ dx\ dy$$

$$N(p,q) = \iint R_n(x,y)\ e^{j(px + qy)} dx\ dy$$

and:

$$R_n(x,y) = \iint n(u,v)n^*(u+x,\ v+y)\ du\ dv$$

In general H(p,q) is a complex-valued function and is difficult to realize in practice. However, the two-beam method allows H(p,q) to be recorded on ordinary energy detectors. The method is based on the fact that a complex-valued function can be recorded as a real valued function on a carrier frequency. It will be seen later that the price paid for this method of realizing H(p,q) is the need for more SBP in the filter function than the SBP present in the signal.

The most elegant method for realizing H(p,q) is probably the use of a modified Mach-Zehnder interferometer as mentioned in Reference 1. An equivalent technique and one better suited to the problem from a practical viewpoint is the modified Rayleigh interferometer diagrammed in Figure 3.1. It is convenient to divide the optimum filter function represented by Equation 3.1 into two parts - a part due to the noise, and a part due to the signal:

$$H(p,q) = \frac{k_1}{N(p,q)} \cdot k_2 \, S^*(p,q) \qquad (3.2)$$

The noise part of the filter function $k_1/N(p,q)$ is a non-negative function because it is the Fourier transform of an autocorrelation function. Thus, it can be recorded on a suitable medium by normal techniques and does not require the use of interferometric techniques. The signal part of the filter $k_2 \, S^*(p,q)$ is complex-valued if s(x,y) is asymmetric, and interferometric techniques are necessary to record it on energy-sensitive devices. The two parts of the filter can be made separately and placed in contact after they are recorded to produce H(p,q).

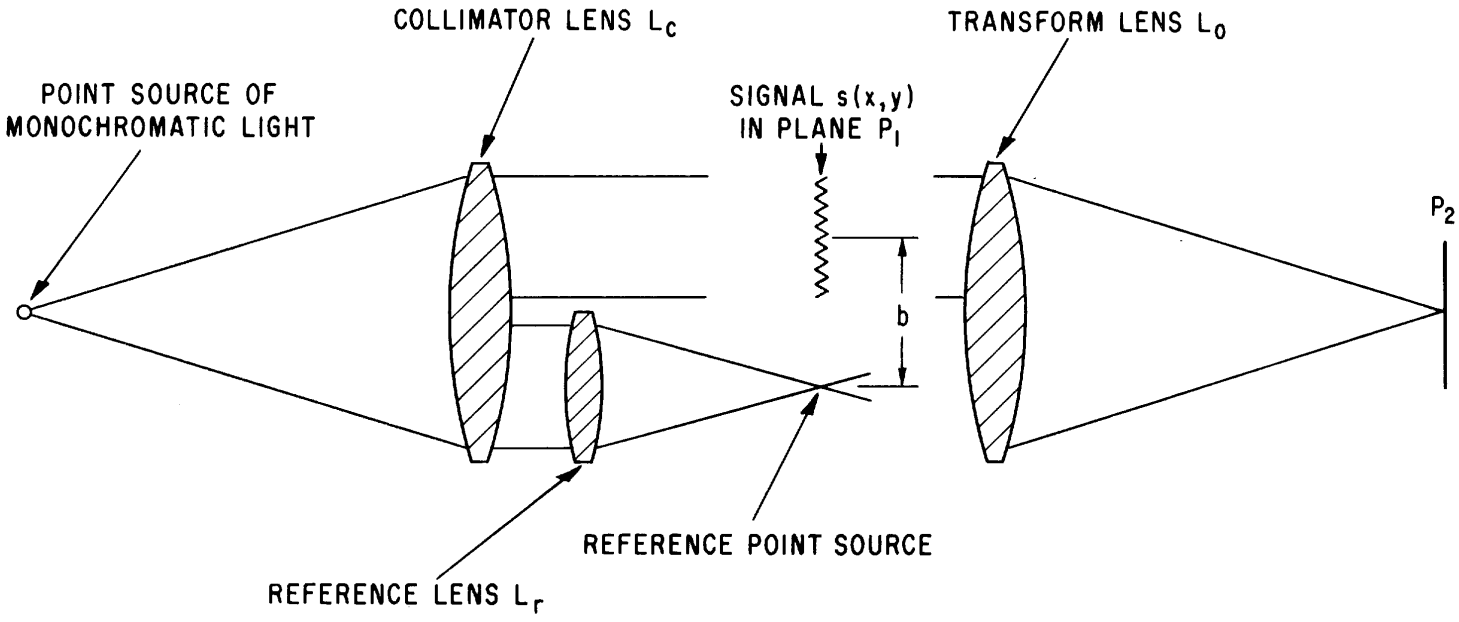

FIGURE 3.1

The signal whose filter we desire is placed in one-half of the light beam in plane P_1 of the system shown in Figure 3.1. A small lens called the reference lens is placed in the other half of the beam so that it produces a point focus of light in plane P_1, a distance b from the center of the signal in the x-direction. For purposes of this discussion, the light distribution in the point focus can be represented by a delta function of strength R_o. If the center of the signal defines the x = y = 0 point of plane P_1, then the total light distribution in that plane is:

$$g(x,y) = s(x,y) + R_o \delta (x-b,y) \qquad (3.3)$$

Lens L_o takes the two-dimensional transform of g(x,y) and displays it in plane P_2 as G(p,q) where:

$$G(p,q) = S(p,q) + R_o e^{jpb} \qquad (3.4)$$

The recording medium used in plane P_2 is always an energy detector that senses intensity or $|G(p,q)|^2$. It is not necessary that the detector be silver photographic material, but we will use it for sake of illustration. A detector can also be used that produces a phase variation rather than a transmission variation without changing the results of this analysis. The photographic material is exposed and developed so that its specular amplitude transmission is proportional to the exposure or:

$$T_a(p,q) = a - bE(p,q) \qquad (3.5)$$

where a and b are photographic constants as diagrammed in Figure 3.2.

By appropriate choice of R_o and the exposure, we can insure that E(p,q) lies on the linear portion of the curve between E_1 and E_2. Since the exposure is proportional

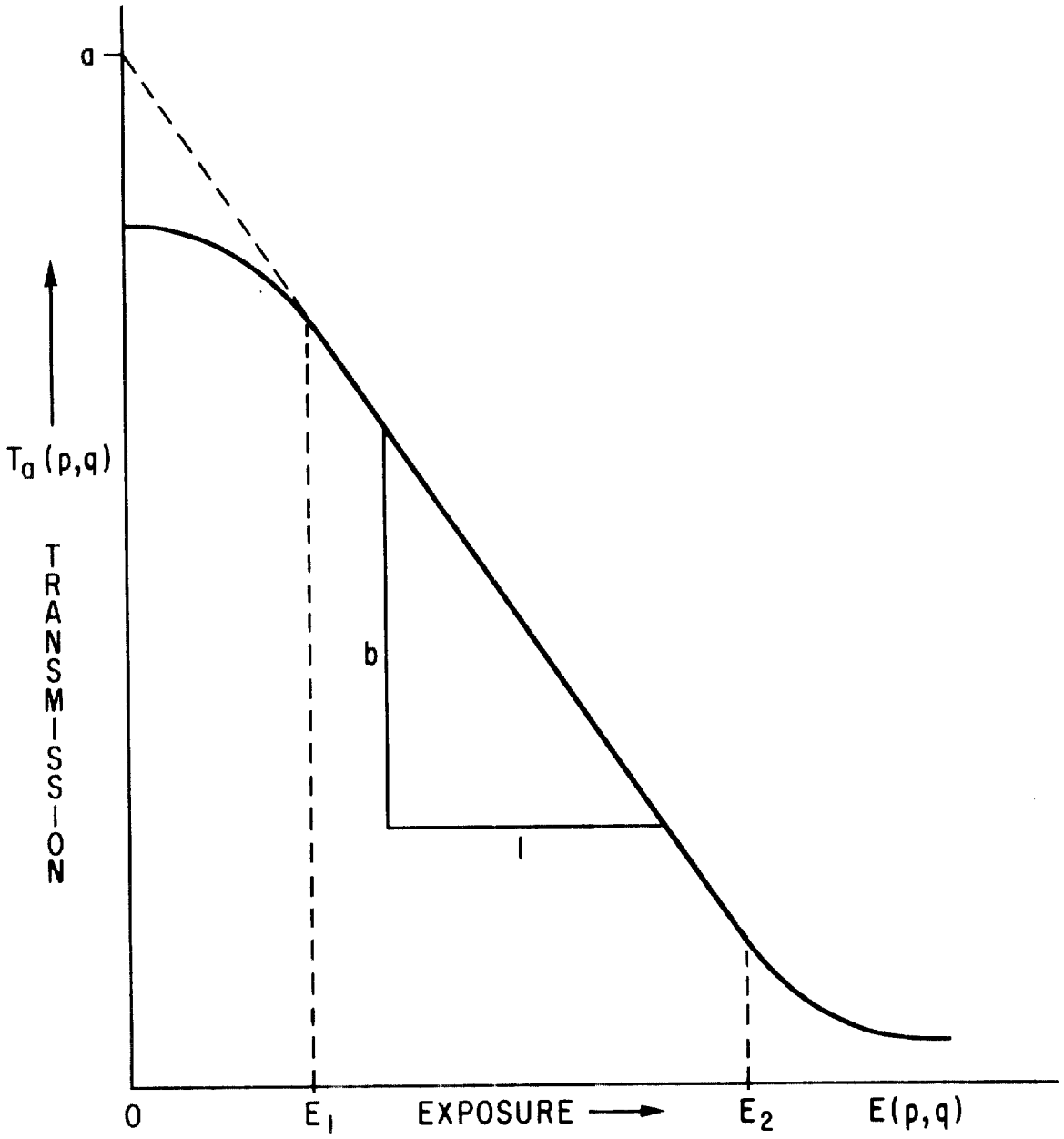

FIGURE 3.2

to $|G(p,q)|^2$, the transmission of the film is:

$$T_a(p,q) = a - b\,|G(p,q)|^2 \qquad (3.6)$$

where $G(p,q)$ is given by equation 3.4.

Substituting equation 3.4 in equation 3.6 and expanding, we have

$$T_a(p,q) = a - b\left[R_o^{\,2} + |S(p,q)|^2 + R_o\, e^{-jpb}\, S(p,q) + R_o\, e^{jpb}\, S^*(p,q)\right] \qquad (3.7)$$

We note that the last term in equation 3.7 is proportional to the second part of the optimum filter function as represented by equation 3.2. It is, however, multiplied by a linear phase factor, and is comingled with other terms. The optical system that is used to process the data $f(x,y)$ uses this linear phase factor to automatically separate the term of interest from the others. This optical system is shown in Figure 3.3. The data to be processed $f(x,y)$ is placed in plane P_1. Lens L_o displays its Fourier transform $F(p,q)$ where $F(p,q)$ is modified by $T_a(p,q)$. Lens L_i takes the Fourier transform of this modified distribution and displays it in plane P_3 where:

$$O(-x,-y) = \frac{1}{4\pi^2} \iint F(p,q)\; T_a(p,q)\; e^{j(px\,+\,qy)}\; dp\; dq \qquad (3.8)$$

By using the convolution theorem, equation 3.8 can be rewritten as:

$$O(-x,-y) = \iint f(u,v)\; t_a\,(u+x,\; v+y)\; du\; dv \qquad (3.9)$$

The negative signs associated with x and y result from the fact that successive transforms in optical systems always introduce a positive kernel function. In the following discussion for convenience we will drop the practice of noting this rotation of the image through π radians.

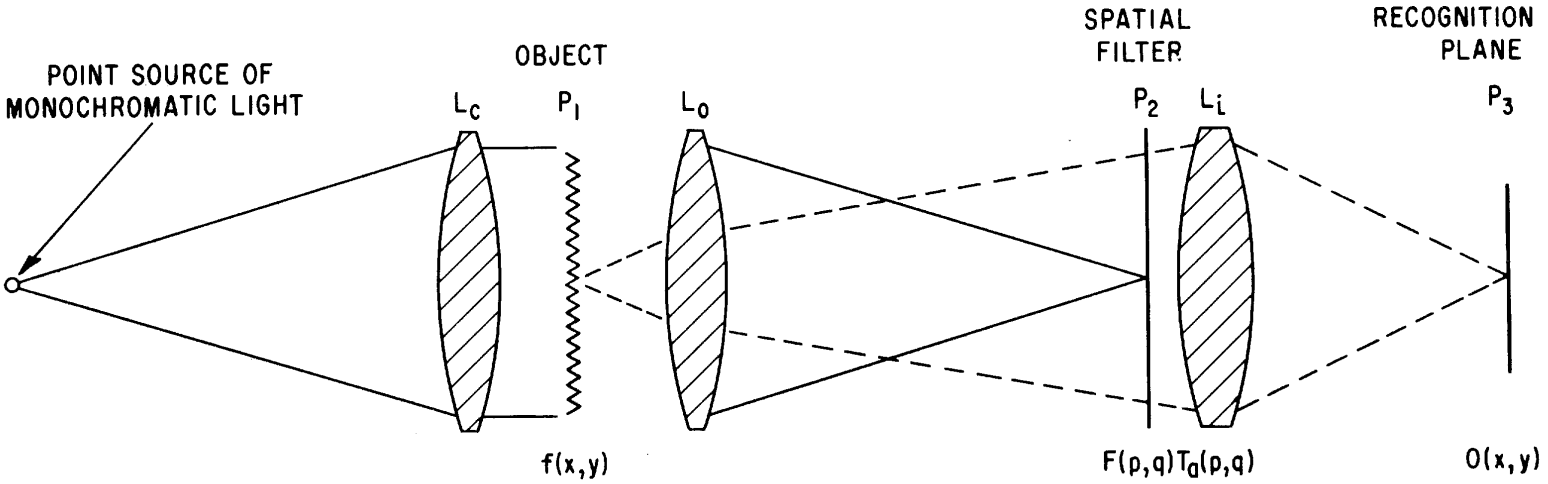

FIGURE 3.3

A-1-12

Our primary task at this point is to determine what minimum value of b will allow the system to operate successfully. For this purpose it is easier to use the representation of the output $O(x,y)$ as given in equation 3.9. The first step is to find the impulse response of the total filter function. This is done by removing $f(x,y)$ from the system, and inserting a lens that will produce a point source of light on the optical axis in plane P_1. The light distribution in plane P_3 will then be the Fourier transform of $T_a(p,q)$. In this analysis we assume unity magnification for convenience, but the results are unaffected by this assumption.

The Fourier transform of $T_a(p,q)$ is:

$$t_a(x,y) = \frac{1}{4\pi^2} \iint T_a(p,q)\, e^{j(px + qy)}\, dp\, dq \quad ,$$

and by making use of equation 3.7 we have:

$$t_a(x,y) = \frac{1}{4\pi^2} \iint (a - bR_o^2)\, e^{j(px + qy)}\, dp\, dq$$

$$- \frac{b}{4\pi^2} \iint |S(p,q)|^2\, e^{j(px + qy)}\, dp\, dq$$

$$- \frac{bR_o}{4\pi^2} \iint S(p,q)\, e^{j[p(x-b) + qy]}\, dp\, dq$$

$$- \frac{bR_o}{4\pi^2} \iint S^*(p,q)\, e^{j[p(x+b) + qy]}\, dp\, dq \qquad (3.10)$$

The first term of equation 3.10 is a δ-function of magnitude $a - bR_o^2$ located at $x = y = 0$. The second term is the autocorrelation function of $s(x,y)$ and is

centered on the optical axis:

$$-\frac{b}{4\pi^2}\iint |S(p,q)|^2 e^{j(px+qy)}\,dp\,dq = -b\iint s(u,v)\,s^*(u+x,\,v+y)\,du\,dv \qquad (3.11)$$

If the signal has length ℓ_x in the x-direction, then the right hand side of equation 3.11 has length $2\ell_x$ in the x-direction.

The third term of equation 3.10 is $bR_o\,s(x-b,y)$ which is the signal displaced from the optical axis by a distance b. Similarly, the fourth term of equation 3.10 is $bR_o\,s^*(-x-b,-y)$ which is the conjugate of the signal with reversed coordinates displaced from the optical axis by a distance -b. Each of the latter two distributions have length ℓ_x in the x-direction. The impulse response of the total filter function is illustrated in Figure 3.4. Thus, $t_a(x,y)$ is given by:

$$t_a(x,y) = (a-bR_o^2)\,\delta(x,y) - bs(x,y) * s^*(-x,-y)$$
$$- bR_o\,s(x-b,y) - bR_o s^*(-x-b,-y) \qquad (3.12)$$

From equation 3.9 we see that if we remove the impulse function from the system and replace it by f(x,y), the output of the system is given by:

$$O(x,y) = f(x,y) * t_a(x,y) \qquad (3.13)$$

where * denotes convolution. (Note that * also denotes complex conjugate, but it should be clear from the usage which operation is intended).

Using equation 3.12 in equation 3.13 yields:

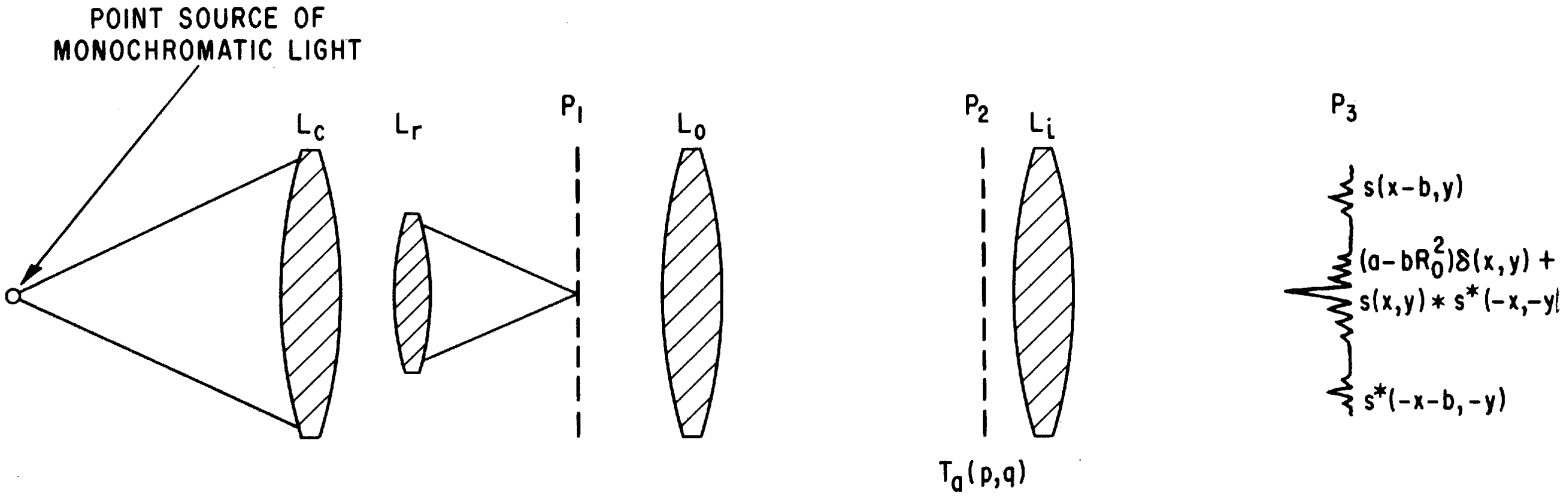

FIGURE 3.4

$$O(x,y) = (a-bR_o^2)\, f(x,y) * \delta(x,y)$$

$$- \; bf(x,y) * s(x,y) * s^*(-x,-y) - bR_o f(x,y) * s(x-b,y)$$

$$- \; bR_o\, f(x,y) * s^*(-x-b,-y) \qquad (3.14)$$

The first term of equation 3.14 has length L_x in the x-direction where L_x is the length of $f(x,y)$. The second term has length $L_x + 4\ell_x$. The third and fourth terms each have length $L_x + 2\ell_x$, but they are centered at $x = \pm b$. The minimum value of b is chosen so that the various terms do not overlap. Both the first and second terms of equation 3.14 are centered on the optical axis, but since the second term occupies more space in the x-direction it determines the minimum length of b. Thus, we have the condition for non-overlap as:

$$|b| \leq \frac{1}{2}\left[L_x + 4\ell_x\right] + \frac{1}{2}\left[L_x + 2\ell_x\right]$$

central order one side order

or,

$$|b| \leq L_x + 3\ell_x \qquad (3.15)$$

The minimum value of b occurs when the inequality holds, thus $b = L_x + 3\ell_x$.

This has been a somewhat lengthy analysis merely to determine the minimum value of b, but it is needed to gain an accurate picture of the SBP and the IC of the spatial filter. It has also served as a review of the fundamental concepts and gives some insight into the operation of the system.

We are finally in a position to determine the SBP and the IC of the filter. The optical system used to construct the filter was shown in Figure 3.1. It is shown again in slightly modified form in Figure 3.5. To determine the SBP and the IC of the filter we must find the value of four parameters. These parameters are the area A of the filter, the highest frequency p_o that it contains, the bandwidth B of the filter, and the number of states that each resolution element must be able to assume.

The area of the filter is determined by the maximum frequency contained in the signal. We regard the filter as a limiting aperture of a lens (effectively the aperture of lens L_i in Figure 3.3). The application of Rayleigh's criterion for resolution shows that the filter must have a radius $R = \frac{1}{2} \lambda D p_o$, where λ is the wavelength of the illumination, D is the distance from plane P_1 to plane P_2 in Figure 3.5, and p_o is the highest frequency contained in the signal. Thus the area of the filter is $A = \frac{\pi}{4} \lambda^2 D^2 p_o^2$.

The highest frequency that the filter must record is determined by the signal length ℓ_x and the data length L_x, both lengths measured in the x-direction (or the direction normal to the carrier frequency). From figure 3.5 we see that the maximum distance from the reference point to the edge of the signal is $b + 1/2 \ell_x$, but $b = L_x + 3\ell_x$ so that the maximum distance is $L_x + 7/2 \ell_x$. Referring to Figure 3.6, we have two points separated by a distance $L_x + 7/2 \ell_x$, lying in a plane a distance D from the filter plane.

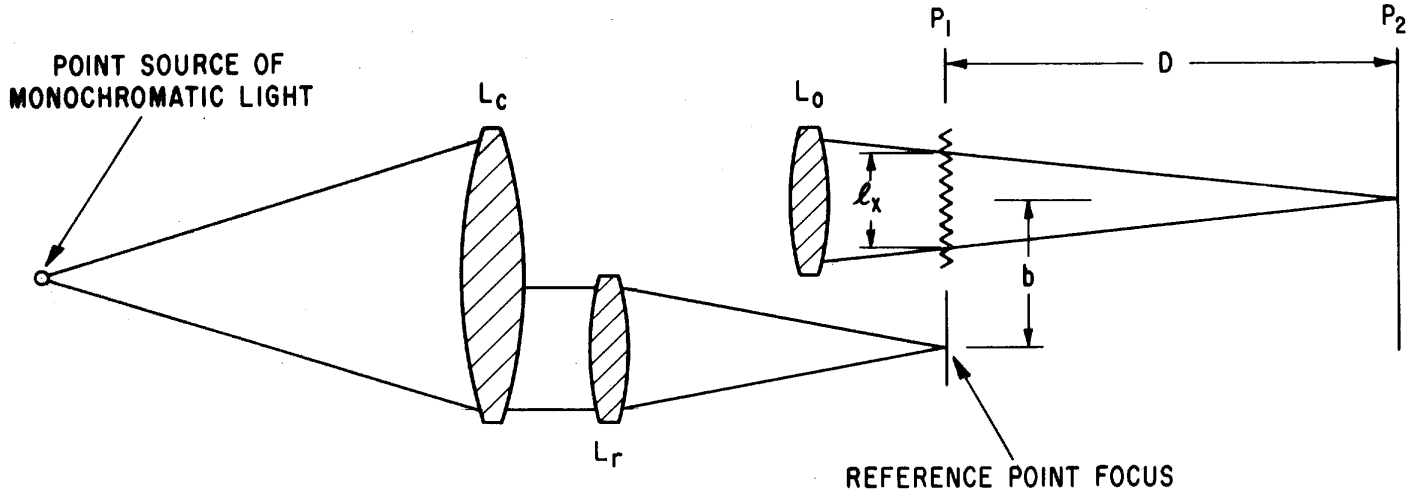

FIGURE 3.5

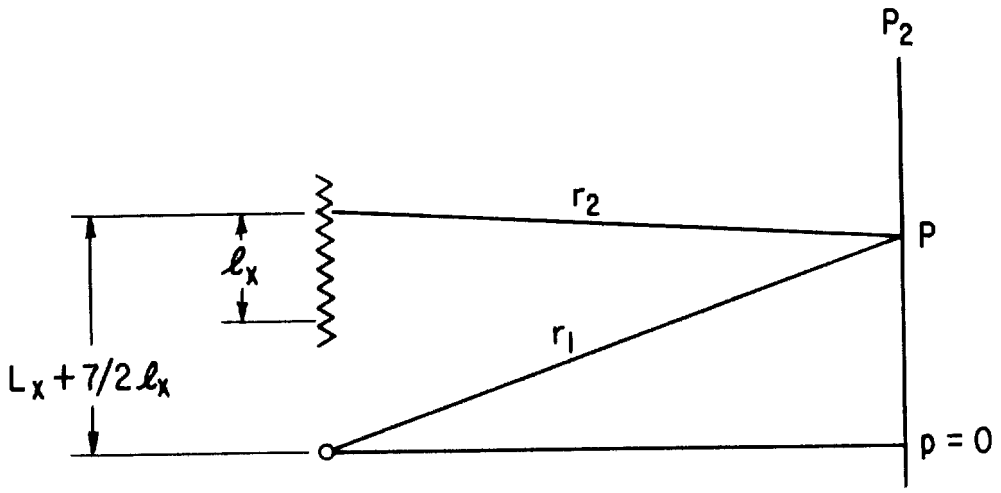

FIGURE 3.6
(SEE FIG. 3.5 FOR DETAIL)

Let us denote a ray from the reference source image to an arbitrary point p by r_1 and a ray from the extreme edge of the signal to the point p by r_2. The light distribution in plane P_2 as a function of p due to these two points whose amplitudes are normalized to unity for convenience, is:

$$f(p) = e^{jkr_1} + e^{jkr_2}$$

We are interested only in the magnitude of f so we have:

$$\left| f(p) \right|^2 = \left| e^{jkr_1} + e^{jkr_2} \right|^2 = 2 \left[1 + \cos k (r_1 - r_2) \right] \quad (3.16)$$

Writing r_1 and r_2 in terms of p and D, we have:

$$\begin{aligned} r_1 &= D\left[1 + 1/2 \left(\frac{p}{D}\right)^2 + \ldots \right] \\ r_2 &= D \left[1 + 1/2 \left(\frac{p - L_x - 7/2\, \ell_x}{D} \right) + \ldots \right] \end{aligned} \quad (3.17)$$

We can truncate the binomial expansions after the second term because $D \gg p$. Using equation 3.17 in equation 3.16 gives:

$$\left| f(p) \right|^2 = 2 \left[1 + \cos \frac{kD}{2} \left\{ (p/D)^2 - \left(\frac{p - L_x - 7/2\ell_x}{D} \right)^2 \right\} \right] \quad (3.18)$$

The frequency is obtained by differentiating the argument of the cosine function with respect to p:

$$\begin{aligned} p_{x_{max}} &= \frac{1}{2\pi} \frac{d}{dP} \left[\frac{kD}{2} \left\{ (p/D)^2 - \frac{p - L_x - 7/2\ell_x}{D}^2 \right\} \right] \\ &= \frac{1}{2\pi} k D \left[p/D^2 - \frac{p - L_x - 7/2\ell_x}{D^2} \right] \\ &= \frac{1}{\lambda D} \left[L_x + 7/2\ell_x \right] \end{aligned} \quad (3.19)$$

Similarly, the minimum frequency in the x-direction is found by using the reference point and a point taken at the nearest edge of the signal. This frequency is given by

$$p_{x_{min}} = \frac{1}{\lambda D}\left[L_x + 5/2\ell_x \right] \qquad (3.20)$$

The bandwidth in the x-direction is given by $B_x = p_{x_{max}} - p_{x\,min} = \ell_x/(\lambda D)$ The bandwidth in the y-direction is $B_y = \ell y/(\lambda D)$ where ℓy is the signal length in the y-direction. Since we have computed the bandwidths in two orthogonal directions, it is also customary to compute the area of the filter as though it were a square of side 2R rather than a circle of radius R. The area of the filter then becomes $A = \lambda^2 D^2 p_o^2$.

Finally, we must determine the number of states that each resolution element must be able to assume. As stated in section 2, the information content of a signal must be equal in every plane in an aberration-free system that has adequate bandwidth. Recall that the IC of the signal was equal to $Ap_o^2 H$ bits, where A is the area of the signal p_o is its maximum frequency, and $H = -\sum_{i=1}^{N} p_i \log_2 p_i$ The IC of the signal is then given by:

$$IC_s = \ell x \ell y\, p_o^2 H_s$$

where the area of the signal is $\ell x\ \ell y$.

The IC of the filter is given by $IC_f = A\ B_x\ B_y\ H_f$ or:

$$IC_f = \lambda^2\ D^2 p_o^{\,2} \left(\frac{\ell x}{\lambda D}\right)\left(\frac{\ell y}{\lambda D}\right) H_f$$

$$= \ell x\ \ell y\ p_o^{\,2}\ H_f \qquad (3.21)$$

By comparing the IC of the signal with equation 3.21 we see that we must have $H_f = H_s$. In the event that each state has equal probability of occurrence in both the signal and filter, we have:

$$H_f = \log_2 N_f = H_s = \log_2 N_s \qquad (3.22)$$

or that each resolution element in the filter must be able to assume exactly the same number of states as each of the resolution elements in the signal.

The space bandwidth product of the filter is given by:

$$SBP_f = p_{x\ max}\ p_{x,y} \lambda^2 D^2 p_o^{\,2}$$

$$= (L_x + 7/2\ell_x)\ell_y\ p_o^{\,2} \qquad (3.23)$$

whereas the space bandwidth product of the signal is:

$$SBP_s = \ell_x\ \ell_y\ p_o^{\,2} \qquad (3.24)$$

It can easily be seen that the SBP_f must be much larger than the SBP_s. This is due to the fact that the filter is effectively a band-pass function while the signal is a low-pass function. The filter contains a band which is "empty" between zero frequency and $(L_x + 5/2\,\ell_x)/(\lambda D)\ell$ /mm which is needed in order to properly process the data. Thus it is seen that the IC's of the filter and signal are equal whereas the SBP's are not. In many cases $\ell_x \ll L_x$ so that the ratio of SBP_f to SBP_s is:

$$\frac{SBP_f}{SBP_s} = \frac{(L_x + 7/2\ell_x)\ell_y\, P_o^2}{\ell_x \ell_y\, P_o^2} \cong \frac{L_x}{\ell_x} \qquad (3.25)$$

Thus the ratio of the SBP's is approximately equal to the ratio of the data length to the signal length.

So far the estimate of the IC of the filter have been based on only the second part of the optimum filter as given in equation 3.2. We should also consider the information content needed to record k_1 /N(p,q). The problem is complicated somewhat by the fact that the dynamic range of the recording medium is greater than that usually available. This is due, in part, to the concentration of N(p,q) at very low frequencies. One might correctly argue that no information is contained in the zero frequency term, but the problem is still complicated by the frequencies near, but not at, zero frequency.

Further, since the available dynamic range of any recording medium is intrinsically linked to the noise level of that medium, this problem also needs attention. Since the noise process is a low-pass function and the noise filter

realization is not complicated by any unusual interferometric techniques, I feel that it would be better for some of your people [redacted] who are versed in information theory to try their hand at this part of the problem. One possible attack is to consider the noise to be a continuous process and compute the noise and signal power levels. Then one could consider the filter to be an information channel and use the two power levels to determine its capacity.

25X1

It is my opinion that this part of the problem is not of as much interest from a practical viewpoint as determining the IC and SBP of the filter due to the signal. Experience shows that one can always do a respectable job of realizing $k_1/N(p,q)$, whereas that is not necessarily true of realizing $k_2\ S^*(p,q)$.

4.0 Summary and Conclusions

In this analysis we have shown that the information content of the filter is equal to that of the signal and is given by:

$$IC = \ell_x \ell_y \quad p_o^2 H$$

where

$\ell_x \ell_y$ are the signal lengths in the x and y directions

P_O is the highest frequency contained in the signal

H is the number of bits of information per resolution element

We have also found the space-bandwidth product for both the signal and the filter and have shown that they may differ appreciably when the filter is constructed by the interferometric carrier-frequency method used here.

The results of this analysis are not dependent on the use of any specific recording medium for the signal, the input data, or the filter. For example, a phase modulating medium would be subject to the same general restrictions as were obtained under the assumption that photographic film was used.

In conclusion, this analysis shows that, from a practical viewpoint, the necessary information content of the filter is quite easily obtained. The practical difficulty lies in obtaining sufficient space-bandwidth product in the filter. In particular, the most severe requirement placed on the recording medium is that it be able to resolve the carrier frequency. The artifice of the two-beam technique thereby places a demand on the recording material but considerably improves the processing operation.

25X1

Optimum Modulation Transfer Function for a Recognition System

1.0 Introduction

The recognition system consists of two main parts: the optical processor that actually performs the recognition and an optical subsystem that constructs the filters to be used in the optical processor. In this section we will discuss the optimum modulation transfer function for the various optical elements, or place other specifications on those elements for which the transfer function notation is not convenient. In order to keep this study of reasonable length, it will be necessary to refer to the literature for details on some aspects of the problem.

In a recognition system of the type discussed here, it is important to optimize the modulation transfer function for each element separately. In some systems aberrations introduced by one element in the system can be compensated by other elements, but this system does not belong to this class. Obviously, loss of information transfer will result in reduced capability to carry out the recognition process.

Since we are dealing with systems that operate with coherent illumination, it will be assumed at the outset that good care of the optical elements will be observed. The surfaces must be kept free from dirt, dust, films, residues, fingerprints and other contaminants; and they must be constructed from glass that is free from blemishes, bubbles, strain, etc. In some cases it is possible to eliminate the effects of these defects by proper use of apertures, but steps taken to prevent de-phasing defects and diffraction artifacts are still necessary.

2.0 Analysis of the Optical Processor

A typical optical processor contains those elements shown in Figure 2.1. In general a laser is chosen for the light source because of its high degree of spatial coherence and high intrinsic brightness. It might be noted here that temporal coherence is not a necessary feature of the light source to be used in the processor. The beam emitted from the laser must be uniphasal (TEM_{oo} mode) for maximum system performance. At the laser this beam is either parallel or slightly divergent due to the use of confocal mirrors and has a diameter of only 2 or 3 millimeters. In order for the system to process an appreciable amount of data or cover moderate size object transparencies this small beam must be expanded so that it is 125 mm in diameter. This can be accomplished in either of two ways. The first is to use a strong negative lens in the beam to expand it so that the beam fills the collimator lens, as shown in Figure 2.2. This method suffers from several difficulties. The overall performance of the system is highly dependent on the lateral position of the negative lens. The "point source" is a virtual image and is not physically accessible for reducing unwanted diffraction effects produced by the laser. Finally, the longitudinal position of the negative lens must be accurately maintained to keep the system in collimation. If a different laser is substituted that has a slightly differing rate of divergence, the collimation is also affected. Thus, there is no convenient bench mark in this system.

The second method overcomes most of these difficulties, although it takes more length along the optical axis. This method employs a strong positive lens that brings the small beam of light to a primary focus as shown in Figure 2.3. Since the beam from the laser has a relatively small diameter, the positive lens must

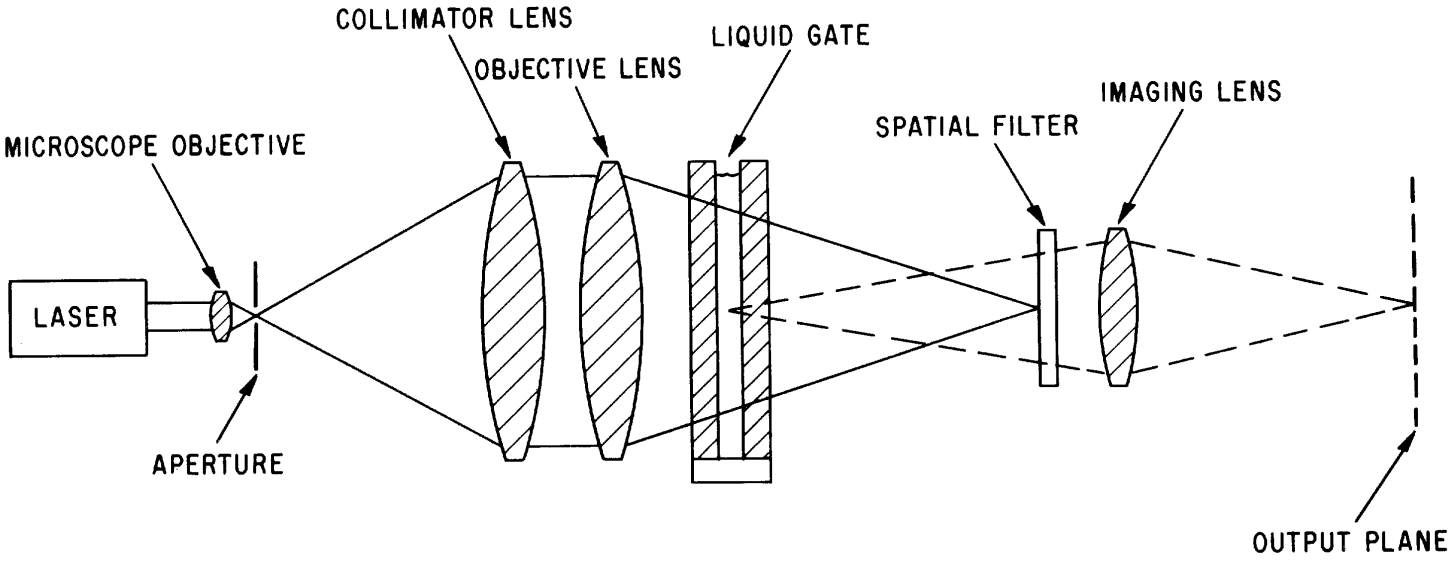

FIGURE 2.1

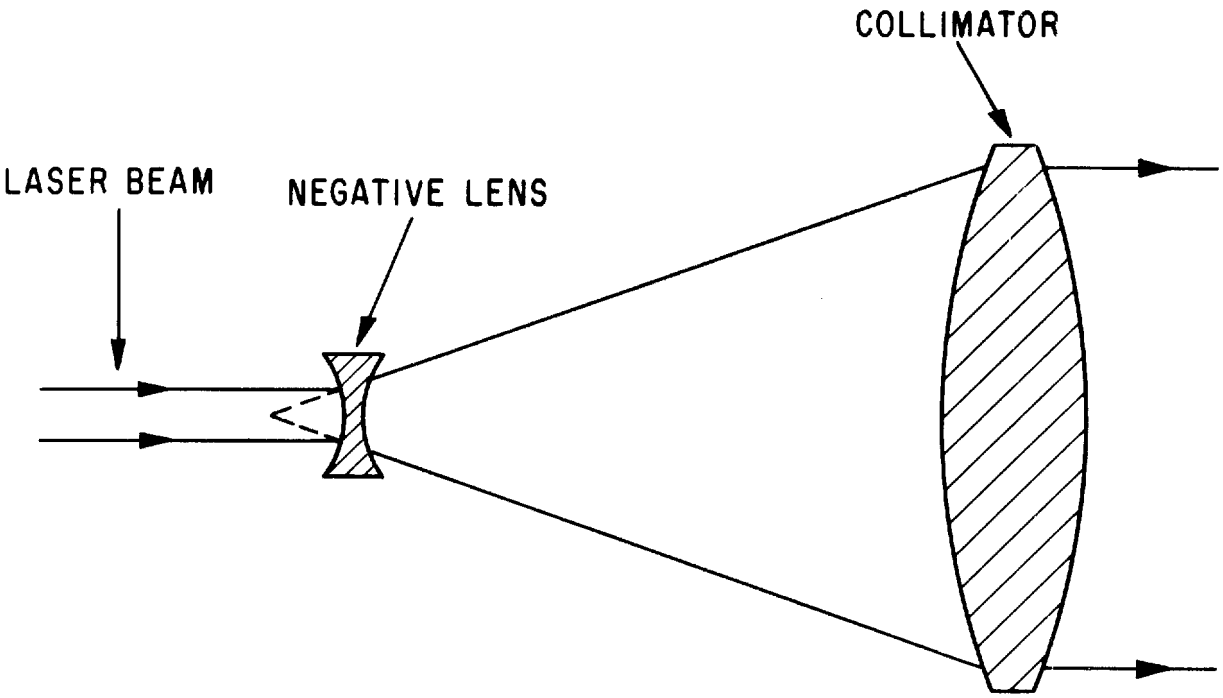

FIGURE 2.2

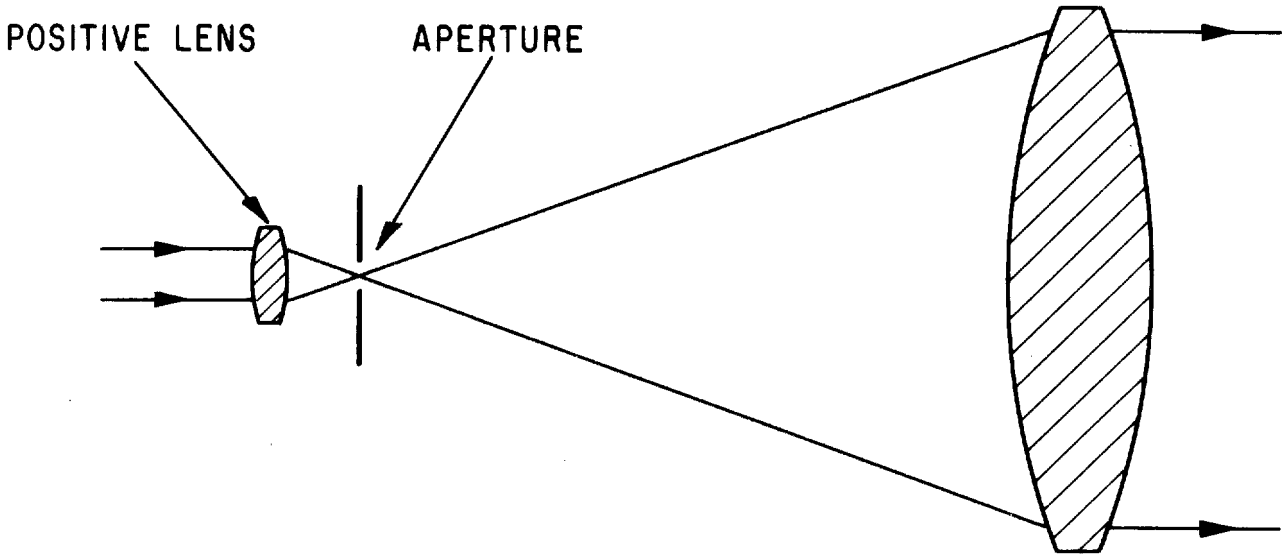

FIGURE 2.3

have a relatively short focal length in order that the resultant cone of light fill the collimator. In general, the aperture ratio of the positive lens has to be considerably higher than the collimator in order to over-fill it with light.

The presence of a real primary focus offers the advantage that an aperture can be placed in the plane of focus to prevent scattered light from propagating into the processing system. This scattered light may be due to apertures in the laser, the aperture of the positive lens or dust particles on any of the laser surfaces. This aperture also acts to remove the blue light that usually leaks through the mirrors of neon gas lasers and must be excluded because of its high actinic value.

It is not the function of the aperture to produce an adequate degree of spatial coherence as is often the case when conventional light sources are used. Thus, there is some latitude in selecting its size. Its size should be small enough to block the scattered light, yet large enough to allow some moderately high frequencies to pass through so that the beam beyond the aperture is as uniform as possible. An aperture whose diameter is approximately ten times the diameter of the airy disk in the primary focus will perform adequately in most cases, and will, at the same time relieve the tolerance on positioning.

Finally, the use of an aperture provides a convenient reference point in the system because it can be fixed on the optical axis in the front focal plane of the collimator. If the laser is replaced by one having slightly different properties, the condenser lens can be adjusted to return the system to normal operation.

The beam that is emitted by a neon laser is not uniform in intensity across its section, even though it may be collimated. The beam normally shows a rotationally symmetrical Gaussian distribution. Since we require the beam to be a uniform in section at the collimator, steps must be taken to insure this. The ideal method would be to use an optical system near the laser aperture that would redistribute the Gaussian distribution into a uniform one. Such a device has been invented (Reference 1) and is sketched in Figure 2.4 but is not commercially available due to the difficulty making the very small aspheric surfaces required. The use of this device would allow nearly all of the available light to be utilized in the processing system.

An alternate scheme that works fairly well is to overfill the collimator such that only the central part of the beam is used. Unfortunately, much of the light is wasted by such a technique, the exact percentage lost depends on how uniform the final distribution is required to be. In some cases the remaining light may be adequate for the type of sensor used at the output, particularly if it is an image orthicon tube. The percentage light utilized by the system can be derived rather easily. The Gaussian light distribution is described by the rotationally symmetrical function:

$$I(r) = I_o e^{-r^2/2\sigma^2}$$

where I_o is the peak intensity, r is the radius of the distribution, and σ is the standard deviation. We now find the integral of I(r) as a function of the radius of the collimator R:

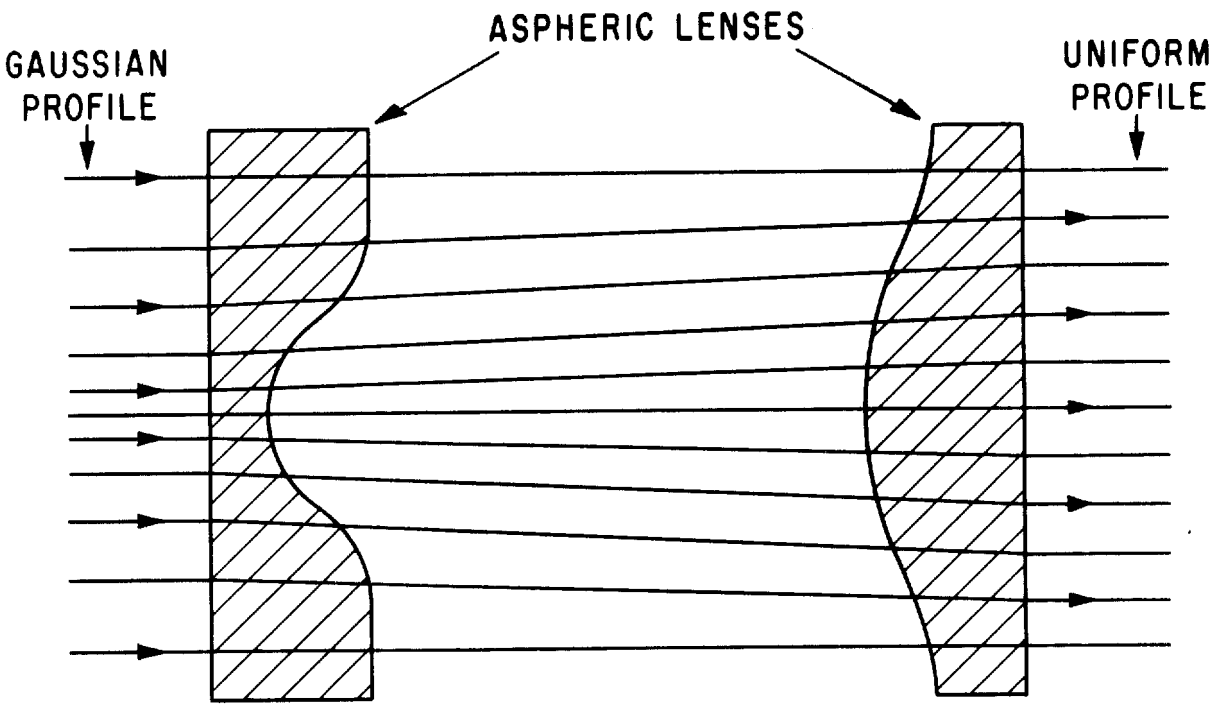

FIGURE 2.4

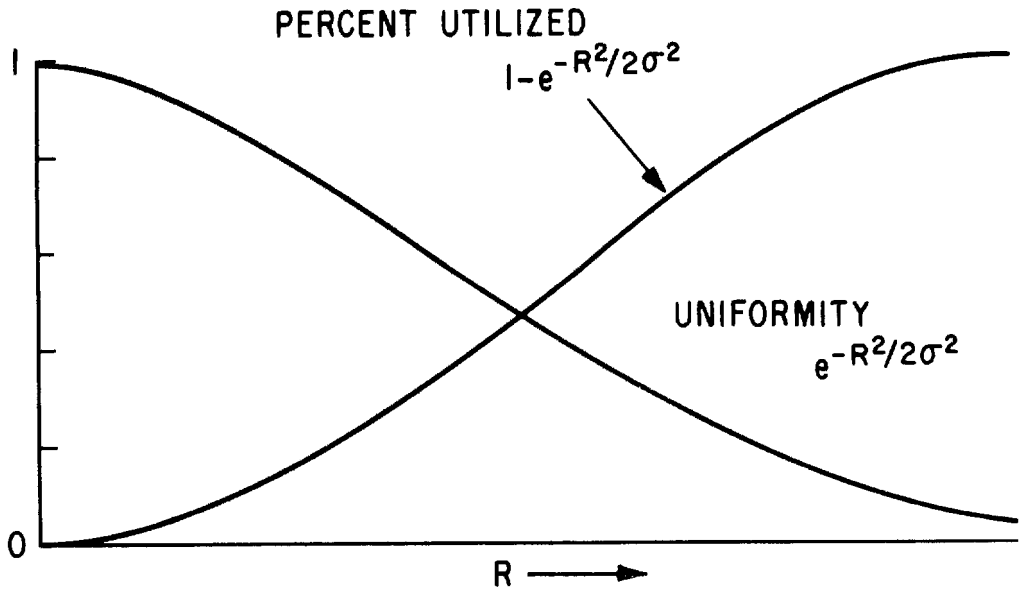

FIGURE 2.5

$$\int_0^R \int_0^{2\pi} I(r)\, r\, dr\, d\theta = I_o \int_0^R \int_0^{2\pi} e^{-r^2/2\sigma^2}\, dr\, d\theta$$

$$= 2\pi\, I_o \int_0^R r\, e^{-r^2/2\sigma^2}\, dr$$

$$= 2\pi\, I_o \sigma^2 \left[1 - e^{-R^2/2\sigma^2} \right]$$

If $R \to \infty$, we capture the total available light or $2\pi\, I_o\, \sigma^2$. Thus, to find the percentage light utilized we have:

$$\% \text{ utilized} = 1 - e^{-R^2/2\,\sigma^2}$$

A graph of I(r) and the light utilized is sketched in Figure 2.5. From this figure we can estimate immediately how much light is utilized for any given degree of uniformity over the aperture of a given system.

Another method for producing a uniform beam is to use a graded neutral density filter at the collimator that is weighted inversely with respect to the Gaussian distribution. This method is no more efficient, and we have the added problem of possible light scattering by the filter. The scattering problem could be solved by placing the filter prior to the condenser lens, but then the filter would have to be designed for each particular laser. In any event, this method is no more efficient than the previous one due to losses by absorption in the filter material.

It should be clear that the Gaussian cross-section of the laser beam leads to strong illumination of the center of the object and weak illumination of the edges and corners. This, in itself is bad because it leads to a weaker recognition signal

for off-axis points, so that objects near the edges of the record may be missed. It should also be clear that the vignetting which is normal in all optical systems tends to compound this effect so that it is very easy to produce a system which shows good recognition on-axis and poor recognition off-axis.

It has become common practice to call the lens plus aperture device a "noise eliminator" because it effectively eliminates the "noise" or diffraction artifacts due to dust and defects on the preceding optical elements. Without the noise eliminator the holograms or spatial filters are filled with bull's eye patterns of optical noise which tend to take up the information capacity of the recording medium. The device to produce a uniform light cross-section from the Gaussian distribution of the laser is called a "de-Gausser". We have found it practical to combine both of these in a single unit which can be attached to the laser and produce an essentially noise-free beam that is reasonably uniform in cross-section.

The principle of the device illustrated in Figure 2.4 is to introduce a known amount of spherical aberration of the correct sign. This takes energy out of the center of the beam and spreads it out to the edges resulting in a more uniform section. The usual choice of a short focus lens to be used in the arrangement shown in Figure 2.3 is a microscope objective. These lenses are corrected for spherical aberration in green light for the usual microscope conjugates which allows 160 mm of back focus. When used with a laser having confocal mirrors the effective back focus is slightly more than 1000 mm and the image is formed in red light. Both of these departures tend to introduce spherical aberration, but of the wrong sign. It is possible to place a negative lens between the laser and microscope objective and adjust the effective back focus to any desired value. When the back focus is

less than the designed 160 mm, spherical aberration of the correct sign is introduced to produce an improved light distribution. No recommendation can be given that is universally applicable because different makes of microscope objectives have different residual aberrations and perform in unpredictable ways when the balance is upset by changing the conjugates. We have obtained our best results by using a minus 4-inch focal length lens with a Unitron 10X objective.

In summary a lens must be used which is capable of producing a point focus of light from a uniphasal beam of light that is either parallel or slightly divergent. It need only be corrected for a point on the optical axis, which suggests the use of an aspheric lens, but a well-corrected microscope objective provides satisfactory performance at a minimum cost. Further, since these are corrected over a small field, some decentering is permissible before the response drops appreciably. The aperture should be round, and as thin as possible. It should have a diameter approximately ten times that of the Airy disk computed as though the beam entering the lens were uniform. The normal Gaussian intensity profile must be improved upon before the beam is suitable for the recognition system.

The next optical component is the collimating lens. Its purpose is to render the wavefronts plane and parallel to the optical axis. Although it is possible to replace the collimator and objective lenses by a single element, this would not provide flexibility nor reduce the total cost by an appreciable margin. Thus we will discuss these elements separately.

Since the collimator need only render the light from an axial point in plane wavefronts, it should be a single element aspheric lens. One might wish to correct for a small amount of coma in order to ease the tolerance on lateral positioning, but this is normally not necessary. Hence, the optimum modulation transfer function for the collimator is:

$$H_c(u,v) = e^{-j\frac{k}{2f}(u^2+v^2)} \quad (u^2+v^2) < R^2$$
$$= 0 \quad (u^2+v^2) \geq R^2 \qquad (2.1)$$

where R is the radius of the lens

u and v are coordinates in the plane of the lens

f is the focal length

$k = 2\pi/\lambda$

λ is the wavelength of light

Since the illumination is monochromatic, this lens, as well as all other optical elements, need only be corrected for a single wavelength of light.

The next optical component is the objective lens. Its design is complicated by the presence of the liquid gate used to correct phase errors in the record film. In the event that photographic film were not used in the system, the effects of the glass substrates still have to be considered. Since this glass is in a convergent part of the beam, it introduces spherical aberration. The lens must be so designed to compensate this aberration and produce a diffraction-limited point focus at its back focal plane when a dummy glass plate is installed. In general, its surface will still be aspheric, but slightly different from the collimator. The situation is illustrated in Figure 2.6.

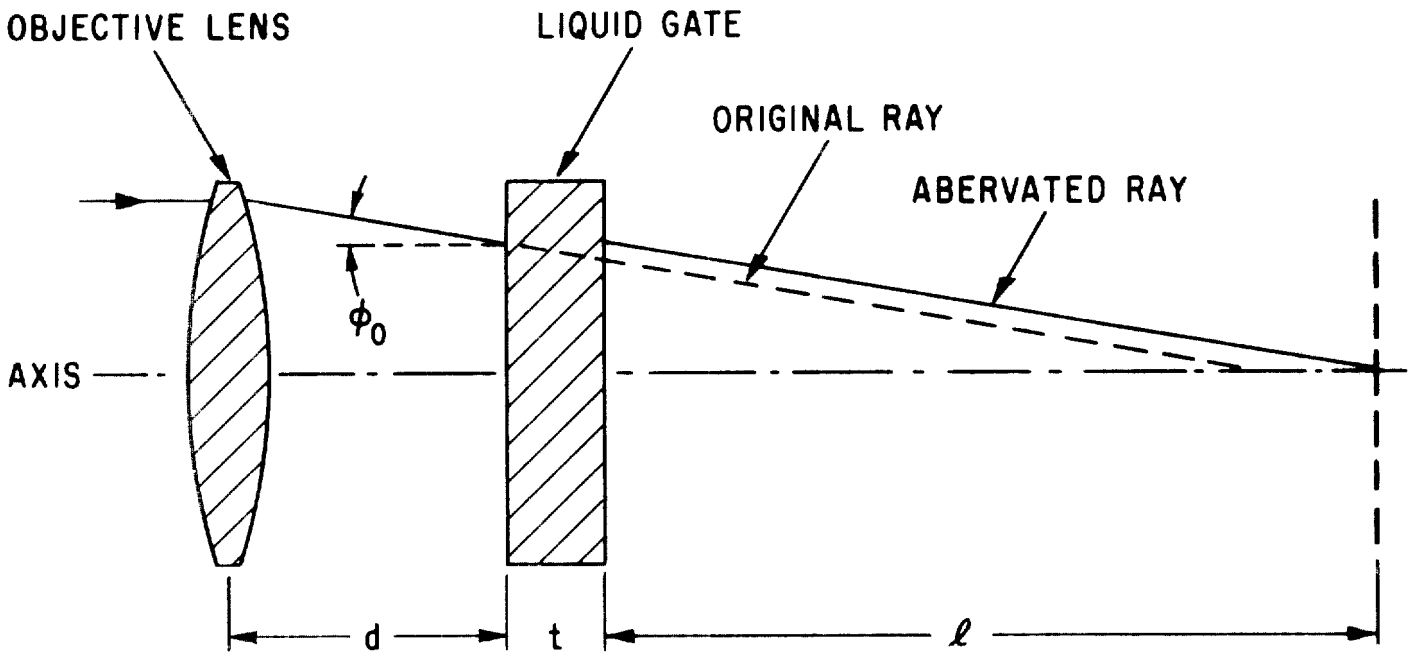

FIGURE 2.6

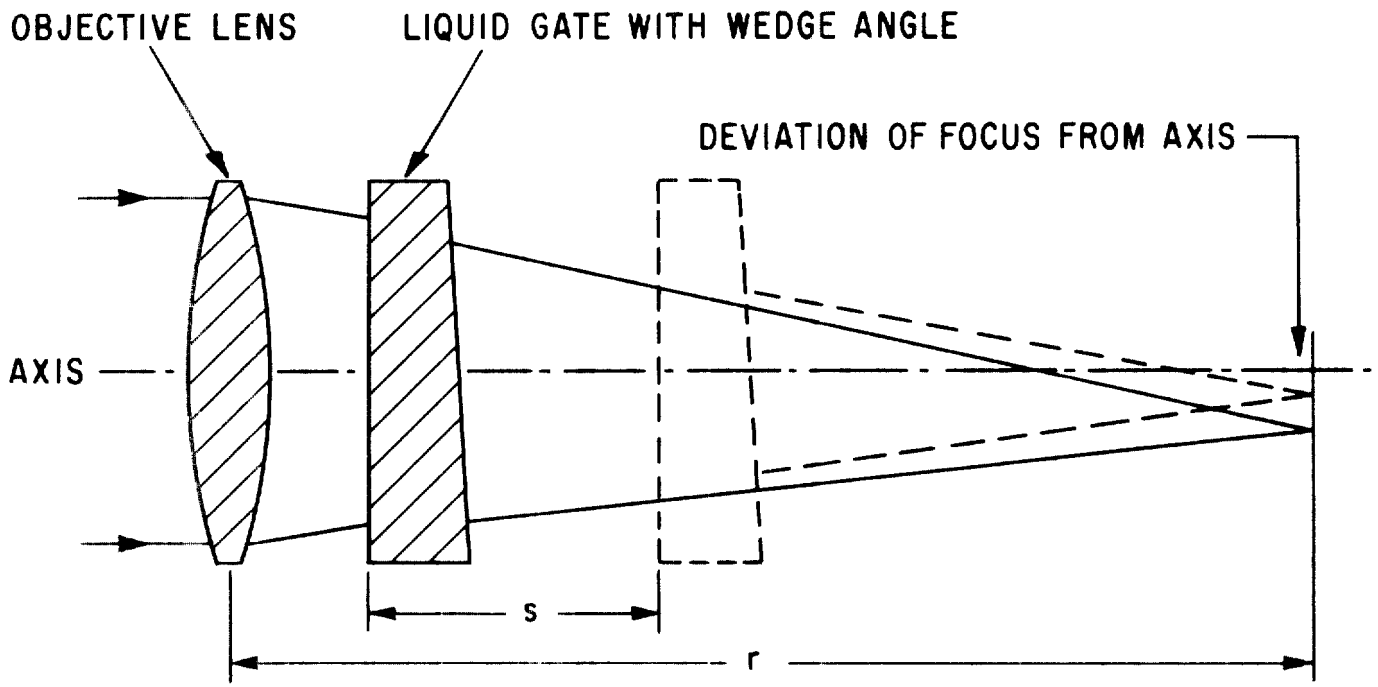

FIGURE 2.7

We will now determine what this added correction should be for the case where a single piece of glass of thickness t and refractive index n_1 is used. The refractive index of air will be assumed to be unity. Consider a ray leaving the lens at an angle ϕ_o and at an arbitrary height x. It intersects the first surface of glass at a height x_1 where:

$$x_1 = x - d \tan \phi_o \tag{2.2}$$

By Snell's law:

$$\sin \phi_o = n_1 \sin \phi_1 \tag{2.3}$$

The ray leaves the glass at a height x_2 where:

$$\begin{aligned} x_2 &= x_1 - t \tan \phi \\ &= x - d \tan \phi_o - t \tan \phi_1 \end{aligned} \tag{2.4}$$

The distance to the point where this ray intersects the optical axis is ℓ where:

$$\begin{aligned} \ell &= x_2 / \tan \phi_o \\ &= \frac{x}{\tan \phi_o} - d - t \frac{\tan \phi_1}{\tan \phi_o} \end{aligned} \tag{2.5}$$

Using Snell's law we have:

$$\ell = \frac{x}{\tan \phi_o} - d - t \frac{\cos \phi_o}{n_1 \cos \phi_1} \tag{2.6}$$

We now find the optical path-length r of any ray and require that it be constant in terms of ϕ_o. We have:

$$r = (\ell + d) \; / \; \cos\phi_o + t/\cos\phi_1$$

From (2.6) we can substitute for $\ell + d$ to get:

$$r = \frac{x}{\cos\phi_o \tan\phi_o} - \frac{t}{n_1 \cos\phi_1} + \frac{t}{\cos\phi_1}$$

$$= \frac{x}{\sin\phi_o} + \left(\frac{n_1 - 1}{n_1}\right)\frac{t}{\cos\phi_1} \qquad (2.7)$$

From Snell's law we find $\cos\phi_1 = \left(1 - \frac{\sin^2\phi_1}{n_1^2}\right)^{1/2}$ so that (2.7) becomes:

$$r = \frac{x}{\sin\phi_o} + \left(\frac{n-1}{n_1}\right) t \left[1 - \frac{\sin 2\phi_o}{n_1^2}\right]^{-1/2} \qquad (2.8)$$

But,

$$\sin\phi_o = \frac{x}{(x^2 + f^2)^{1/2}}, \text{ so}$$

$$r = (x^2 + f^2)^{1/2} + \left(\frac{n_1 - 1}{n_1}\right) t \left[1 - \frac{x^2}{n_1^2 (x^2 + f^2)}\right]^{-1/2} \qquad (2.9)$$

Expanding (2.9) by the binomial theorem and retaining only the first two terms we have:

$$r = f + \frac{x^2}{2f} + \left(\frac{n_1 - 1}{n_1}\right) t - \left(\frac{n_1 - 1}{n_1}\right) t \; \frac{x^2}{2 n_1^2 f^2 (1 - x^2/f^2)}$$

$$= f + \left(\frac{n_1 - 1}{n}\right) t + \frac{x^2}{2f} - \left(\frac{n_1 - 1}{2 n_1^3}\right) t \frac{x^2}{f^2} - \frac{(n_1 - 1) f x^4}{2 n_1^3 f^4} \qquad (2.10)$$

Equation (2.10) reveals several interesting facts. Letting $x \rightarrow 0$ shows that the focus occurs at a distance r from the lens where:

$$r = f + \left(\frac{n_1 - 1}{n_1} \right) t \qquad (2.11)$$

which was anticipated.

Further, it shows that the lens should have a phase factor of:

$$- \frac{k}{2f} (x^2 + y^2) \left[1 - \frac{(n_1 - 1)\, t}{n_1^3\, f} \right]$$

which is similar to that of the collimator except for the fact that the focal length is increased somewhat. In addition we have the correction term:

$$+ \frac{(n_1 - 1)\, t\, x^2}{2\, n_1^3\, f^4}$$

which is opposite in sign to the normal phase factor of the lens. Both of these correction terms are small for lenses with low relative apertures, but must be considered for faster systems.

Finally, the optimum modulation transfer function for the objective lens is:

$$H_o(u,v) = \exp - \frac{jk}{2f} \left\{ (u^2 + v^2)\left(1 - \frac{(n_1 - 1)\, t}{n_1^3\, f}\right) \quad \frac{(n_1 - 1)\, t\, (u^4 + v^4)}{n_1^3\, f^3} \right\} \qquad (2.12)$$

for $u^2 + v^2 < R^2$

for $u^2 + v^2 > R^2$

where: R is the radius of the lens

f is its focal length

u,v are coordinates in the lens plane

$k = 2\pi/\lambda$

t is the thickness of the glass

The solution when a practical liquid gate is used follows this same line of analysis except that we have two such glass plates and a space filled with a liquid of refractive index n_2. In passing, we should note that the amount of spherical aberration introduced by the glass is independent of its axial position.

We are now ready to place requirements on the liquid gate itself. First, every surface should be flat to at least $\lambda/4$, with a $\lambda/8$ requirement preferable. The critical tolerance on the gate is the permissible wedge angle. This is not of importance if the gate is stationary, but if a scale search is carried out by moving the gate axially in the system, then the wedge angle is important. The reason is that the point focus created by the objective lens will shift as a function of the axial position of the gate due to varying optical levers. The situation, greatly exaggerated, is shown in Figure 2.7.

Suppose we wish to move the gate over a range as to carry out some given percentage scale search. Denote the wedge angle of the gate by α and the distance from the lens to the frequency plane by r. The deflection of the point focus when the gate is very close to the lens is $\delta = r \sin \alpha$. The deflection when the gate is in the other extreme position is $\delta_1 = (r-s) \sin \alpha$. For the system to perform well, the difference between δ and δ_1 should be less than 1/10th the diameter of the Airy disk produced by the objective lens. The size of this disk is:

$$d = \frac{1.22 \lambda r}{R} \tag{2.13}$$

where R is the radius of the lens. Using this criterion gives:

$$\begin{aligned} \delta - \delta_1 &\leq d/10 \\ &\leq \frac{1.22 \lambda r}{10R} \end{aligned}$$

or

$$\sin \alpha \leq \frac{1.22 \lambda}{10R} \tag{2.14}$$

Equation (2.14) then sets the limit on the maximum amount of total wedge angle that the gate may have when it is filled with liquid of the proper refractive index.

The next element in the optical processor is the spatial filter. From a performance viewpoint this element must not introduce excessive phase errors. If photographic film is used, it must not introduce more than $\lambda/4$ wavelength of aberration over its aperture. Film thickness variations must be reduced to this level by immersion in a liquid of matching index or by using a thin emulsion coated on glass plates of suitable flatness. If photoplastic film is used, the combination of the substrate and coating must also satisfy these requirements. A few comments on the required positional accuracy of the filter will be given at the end of this section.

The next element in the system is the imaging lens. Since it is the only element in the system that must operate over a large field, its design has to be different from the other elements. First, its aperture must be adequate to receive all the diffracted rays, unless some auxiliary elements are used to bring the important diffracted bundle of rays parallel to the optical axis. The thickness of the glass substrates for the record and spatial filter must be considered as possible sources of aberration.

Since the imaging lens will be used axially along with the input liquid gate and the output sensor, it need only be corrected for one pair of conjugates and one wavelength of light. The resolution capability of the lens must be adequate to image the input scene well over the entire field. The image plane should have as little

curvature as possible, or could be designed for a particular type of sensor that might be curved. The demagnification of the lens should be made compatible with the size of the input record and the sensitive area of the detector.

The final element in the processor is the output sensor. Its resolution capability as a function of its size should be adequate to resolve the input record at the required amount of demagnification. Its sensitivity should be such that it can handle data at the chosen rate.

3.0 Analysis of the Filter Making Subsystem

The optimum modulation transfer functions for the elements in the filter making subsystem are very similar to those placed on corresponding elements in the processor. In fact, some of the elements can be identical to those used in the processor. Whereas the configuration of the processor is fixed, the configuration of the filter maker is not. However, a typical subsystem will contain the elements shown in Figure 3.1.

The laser, condenser lens, aperture and collimator are subject to the same requirements placed on these respective elements in the processor; in fact, they can be duplicates to save on cost. However, the laser should have a fair degree of temporal coherence as well as spatial coherence in order for this instrument, which is basically an interferometer, to work well. Generally 500-600 mm of temporal coherence is adequate.

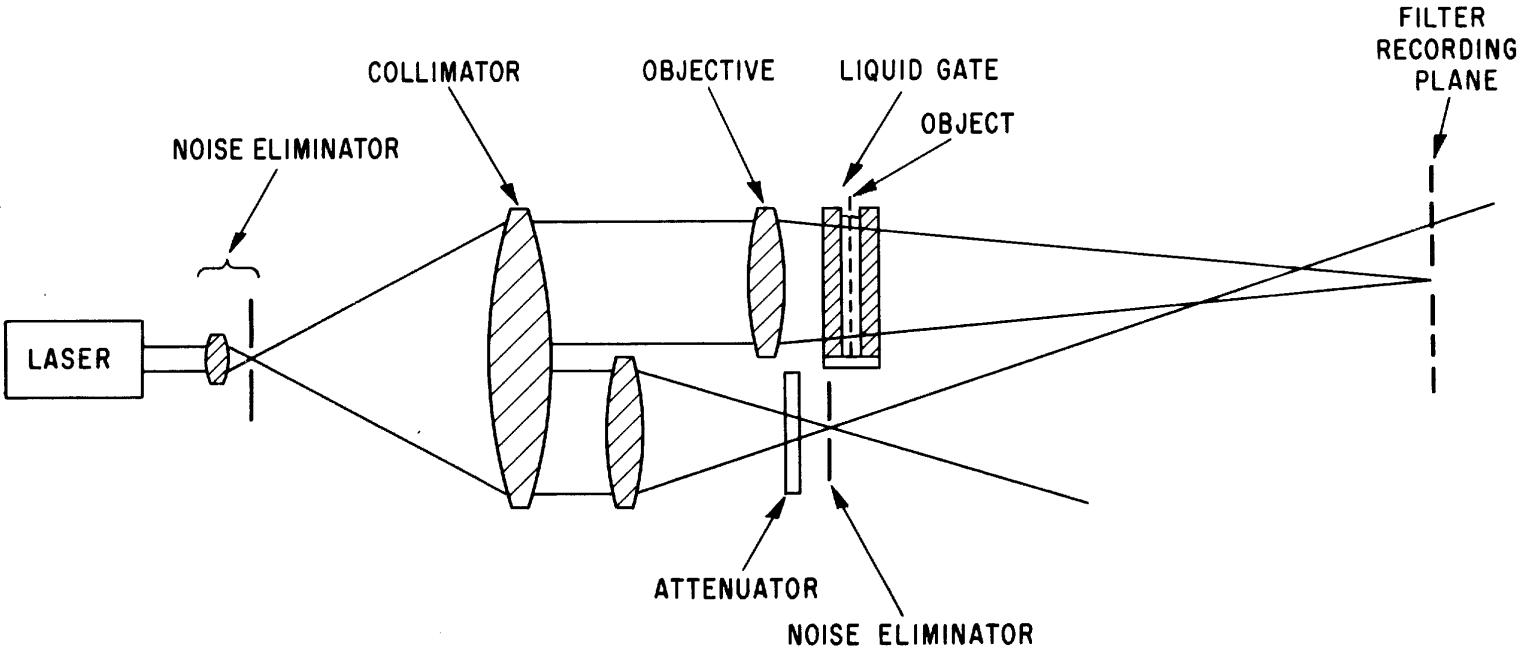

FIGURE 3.1

The objective lens is identical to the one used in the processor except that it can be of smaller aperture if the signals to be detected are small compared to the field of view used in the processor. In fact, it may not be necessary to correct this lens for the spherical aberration introduced by the liquid gate that contains the signal, particularly if the effective relative aperture of this lens is f/50 or less. Hence, a simple single element aspheric lens with transfer function similar to that given in equation 2.14, but with smaller aperture, is adequate. Note, that because of the scale changing feature of the processor, it is not necessary that the two objective lenses have matched focal lengths.

The liquid gate has the same flatness requirement as the one used in the processor, but the wedge angle is not critical. A small amount of wedge in this gate merely changes the carrier frequency by an insignificant amount. Also, because of the scale change feature, it is not necessary to match the thicknesses of the two gates.

The reference lens can also be a single element aspheric because its purpose is to create a diffraction-limited point focus of light. This point focus should occur in such a plane that the optical paths from the frequency plane to this plane and the signal plane are equal. An aperture used at the focus will reduce the "noise" in the reference beam. We may also wish to place an attenuator in the reference beam to control its amplitude. This element should be placed near the point focus, but ahead of the aperture to minimize aberrations. The use of attenuating media in the signal beam is not recommended.

Finally, the maximum performance of the optical processor will not be realized unless the photographic film is positioned properly in the filter making subsystem. The offset frequency present on the filter acts much the same as a thin prism if the light is monochromatic, and will introduce astigmatism in the processor. This astigmatism can be reduced to a minimum by positioning the film in the filter making subsystem such that it is normal to the bisector of the angle between the signal and the reference point as seen from the film plane. This technique is equivalent to using a thin prism at its minimum deviation angle.

4.0 Summary and Conclusions

In this memorandum we have analyzed the requirements to be placed on each optical element in the recognition system and the filter making subsystem. All of the lenses except one can be single element aspherics. The use of single element lenses reduces reflections in the system to a minimum. All elements should be coated with anti-reflectant coatings to further reduce reflections. All elements should be made of highest quality glass to avoid bubbles and striae. Polishing operations should be done with extra care to produce a blemish-free surface.

The care of the optical elements after construction is almost as important as the design and construction phases. Fingerprints and smudges are irreversible processes and cleaning with solvents is likely to leave residues. All components should be fitted with lens caps when not in use to prevent contamination.

In conclusion, the optical systems described here are not sophisticated ones in terms of the types of lenses used. The nature of the process requires, however, that the individual elements be well designed and kept in good alignment and clean throughout the operation of the system.

Note on Position Accuracy of Spatial Filter

This problem is technically not one of determining optimum transfer functions because the optimum position for the filter is obvious. The problem is one of great practical interest, however, and will be briefly discussed here. In practice it is often desirable to rotate or change filters while the system is in operation. The question becomes one of determining how accurately this must be done to prevent degradation below a certain point.

This problem is not an easy one to answer and cannot be solved by simple analysis except for the white noise case. The non-white noise case can be formulated, but requires the aid of a computer as well as knowledge of the noise statistics to get any meaningful results. Personnel at the [redacted] 25X1 have performed such an analysis on its Air Force and Army contracts, and the results are available in the classified literature. (References 2 and 3)

Although the white-noise case is of little interest in itself, it is interesting when compared to the non-white noise results. We are essentially interested in four different results; the lateral and longitudinal positioning tolerances for both the white and non-white noise cases.

We first treat lateral positioning errors for the white noise case. The final results is that:

$$SNRD = \frac{\iint |s(u,v)|^2 \, e^{j(\Delta pu + \Delta qv)} \, du \, dv}{\iint |s(u,v)|^2 \, du \, dv} \qquad (A\text{-}1)$$

where SNRD is the signal-to-noise degradation; i.e. it is the ratio of the SNR when the filter is displaced from the ideal SNR. Also, $s(u,v)$ is the signal; $(\Delta p, \Delta q)$ are the amounts of displacement in the p and q directions in the frequency plane and are measured in radians/mm.

The next case is longitudinal positioning errors for the white noise case. The result is:

$$SNRD = \frac{\iint |s(u,v)|^2 \, e^{j(\Delta p' u + \Delta q' v)} \, du \, dv}{\iint |s(u,v)|^2 \, du \, dv} \qquad \text{(A-2)}$$

where $\Delta p' = \frac{2\pi x_o}{\lambda \ell 2} \Delta Z \, p$

$\Delta q' = \frac{2\pi y_o}{\lambda \ell 2} \Delta Z$

ΔZ is the displacement of the filter

x_o , y_o are the coordinates of the center of the signal in the input

ℓ is the distance from the input to the frequency plane

It is clear from equation (A-2) that the SNR is a function of the location of the signal as well as the displacement of the filter. This illustrates that the frequency plane is the only plane in which a filter can be placed without the need for scanning. It should be stated that the result represented in equation (A-2) is based on the assumption that the displacement is not so large that S(p,q) varies appreciably. In view of the small relative apertures of the signals typically used, this assumption is valid.

We now treat the case where the noise spectral density is not uniform. The result for lateral positioning errors is:

$$SNRD \quad \frac{\int S(p-\Delta p) \, S^*(p) T_n(p) \, dp}{\frac{\int N(p-\Delta p) \, |T_n(p) S^*(p)|^2 \, dp}{\int |S(p)|^2 \, T_n(p) \, dp}} \qquad \text{(A-3)}$$

$$\int N(p) \, |T_n(p) S^*(p)|^2 \, dp$$

where S(p) is the signal spectrum

Δp is the lateral positioning error

N(p) is the noise spectral density

$T_n(p)$ is the transmission of the noise rejection part of the filter

Finally, we have the result for longitudinal positioning errors for the non-white noise case:

$$\text{SNRD} \quad \frac{\int S\,(p-\Delta p')S^*(p)\,T_n(p)\,dp}{\int N(p,\Delta z)\,|\,T_n(p)\,S^*(p)\,|^2\,dp} \Big/ \frac{\int |S(p)|^2\,T_n(p)\,dp}{\int N(p)|T_n(p)\,S^*(p)|^2\,dp} \qquad \text{(A-4)}$$

where $\Delta p' = \frac{2\pi x_o}{\lambda \ell^2}\,\Delta z$

$N(p, \Delta z)$ is the noise spectral density in the plane of the filter.

Note, that we have written equations (A-3) and (A-4) in one-dimensional notation for convenience. The two-dimensional versions can be written by inspection.

Admittedly equations (A-3) and (A-4) are of limited usefulness unless $N(p,q)$ is known, and certain assumptions are made about the construction of $T_n(p,q)$. The work mentioned in References 2 and 3 arrives at results for a specific case.

References

1. J. Kreutzer, paper given at Fall Meeting of the Optical Society of America, New York City, New York.

[redacted]

25X1

3. Same as above except Report No. 6318-10-P, December 1964.

The Use of Phase Modulating Media for Recording Data and for Recording Spatial Filters

1. Introduction

In this memorandum we will consider the feasibility of using phase modulated media in the optical processor to replace conventional photographic film. The most important advantage to be gained is that certain phase modulating media have the capability of operating in real time or near real time. Also, there should be a fair increase in the amount of usable light, and no chemical processing treatments are necessary to obtain an image. Possible disadvantages are the potential increase in the noise introduced into the system and the fact that phase media tend to be band-pass operators. The latter property is not a problem if the phase media are used for recording spatial filters which are themselves bandpass functions.

Our major purpose in this memorandum is to lay the theoretical ground work for using phase functions and to determine whether any unusual techniques are necessary to fully use the potential of such functions. Under separate headings we will discuss the use of phase functions in the input plane for recording the data to be processed and its use in the frequency plane for recording filter functions.

2. Use of Phase Modulating Media in the Input Plane

The basic optical system under consideration is shown in Figure 2.1. Its operation has been described elsewhere and will not be repeated here. Suffice it to say that the data to be processed is normally placed in plane P_1 and will be denoted by $f(x,y)$. It is this element of the optical system that we wish to consider here. In conventional systems $f(x,y)$ is the specular amplitude transmission of photographic film, and its related in some (usually non-linear) way to a given property of the real world. The optical system is designed to display the two dimensional Fourier transform of $f(x,y)$ in plane P_2 as $F(p,q)$.

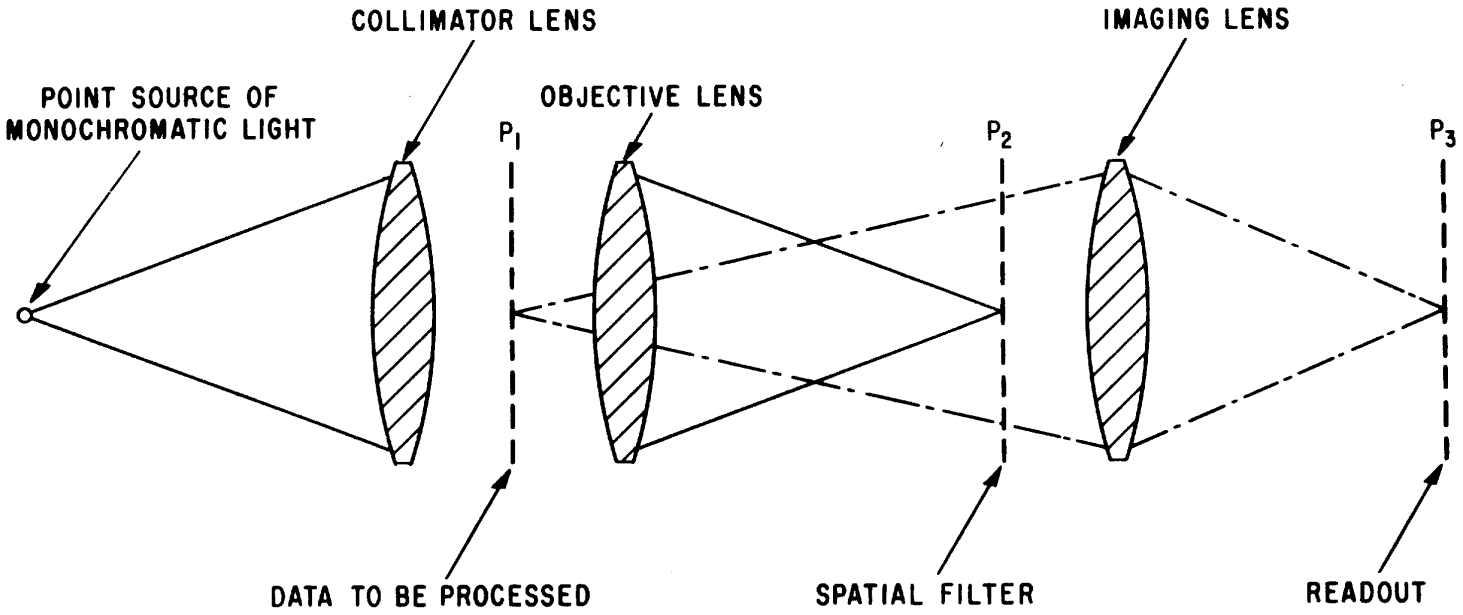

FIGURE 2.1

There are two ways to approach the problem at hand. One is to inquire whether it is possible to convert f(x,y) into a phase function g(x,y) such that the rest of the system's operation remains unchanged. This approach is of interest if one has great quantities of data recorded on photographic film and wishes to process a phase modulated version of it. The conversion can be carried out by reliefing the film or by changing it into a refractive index variation. The exact method for doing this is not of interest here.

The second approach is to use the phase modulating media to record the same property of the real world that the photographic film recorded. In this case we are not particularly interested in whether the resulting phase function is identical to f(x,y) because the system's operation can be predicated on the use of this process. The same comment could equally well apply to the first approach if the rest of the system's operation has not yet been specified.

We will confine ourselves to the second of these two approaches. Suppose the property of the real world that we wish to record is f(x,y). If this function is recorded on a phase modulating media, we have for the phase function:

$$g(x,y) = \exp\left[\, jc\, f(x,y)\right] \qquad (2.1)$$

where c is a constant. If the total phase variation is less than $2\pi/\lambda$, where λ is the wavelength of light, we can expand equation (2.1) to obtain:

$$g(x,y) = 1 + jc\, f(x,y) + \ldots \qquad (2.2)$$

We can drop the higher order terms in the expansion if the restriction is met. The Fourier transform of g(x,y) is:

$$G(p,q) = \delta\ (p,q) + jc \iint f(x,y)\ e^{j(px + qy)}\ dx\ dy \qquad (2.3)$$

We note that the DC term is $\pi/2$ radians out of phase with the Fourier transform of f(x,y). This fact is normally unimportant in practice.

So far we have tacitly assumed that the phase modulating media has a perfect frequency response function for all frequencies contained in f(x,y). Some such media (e.g. thermoplastic and photoplastic processes) are unable to record very low frequencies because they cannot maintain long-term depressions. A typical response curve might look something like that shown in Figure 2.2. We have also allowed for some fall off at higher frequencies. Thus, the Fourier transform of f(x,y) will not contain frequencies below the lower frequency cutoff P_o of the media. In many cases the inability to record extremely low frequencies is not serious, but if the lower cutoff is very much above one line/mm, the performance of the system will be reduced somewhat. The main point of interest here, however, is that the two terms in equation (2.3) do not overlap when bandpass media are used. Consequently, a small blocking spot can be placed on the optical axis in the frequency plane to prevent the δ function from continuing to the output. The inverse Fourier transform of G(p,q) then becomes:

$$g_1(x,y) = jc\ f_1(x,y) \qquad (2.4)$$

where $f_1(x,y)$ is now considered to be a modified version of f(x,y) due to the modulation transfer curve of the phase media.

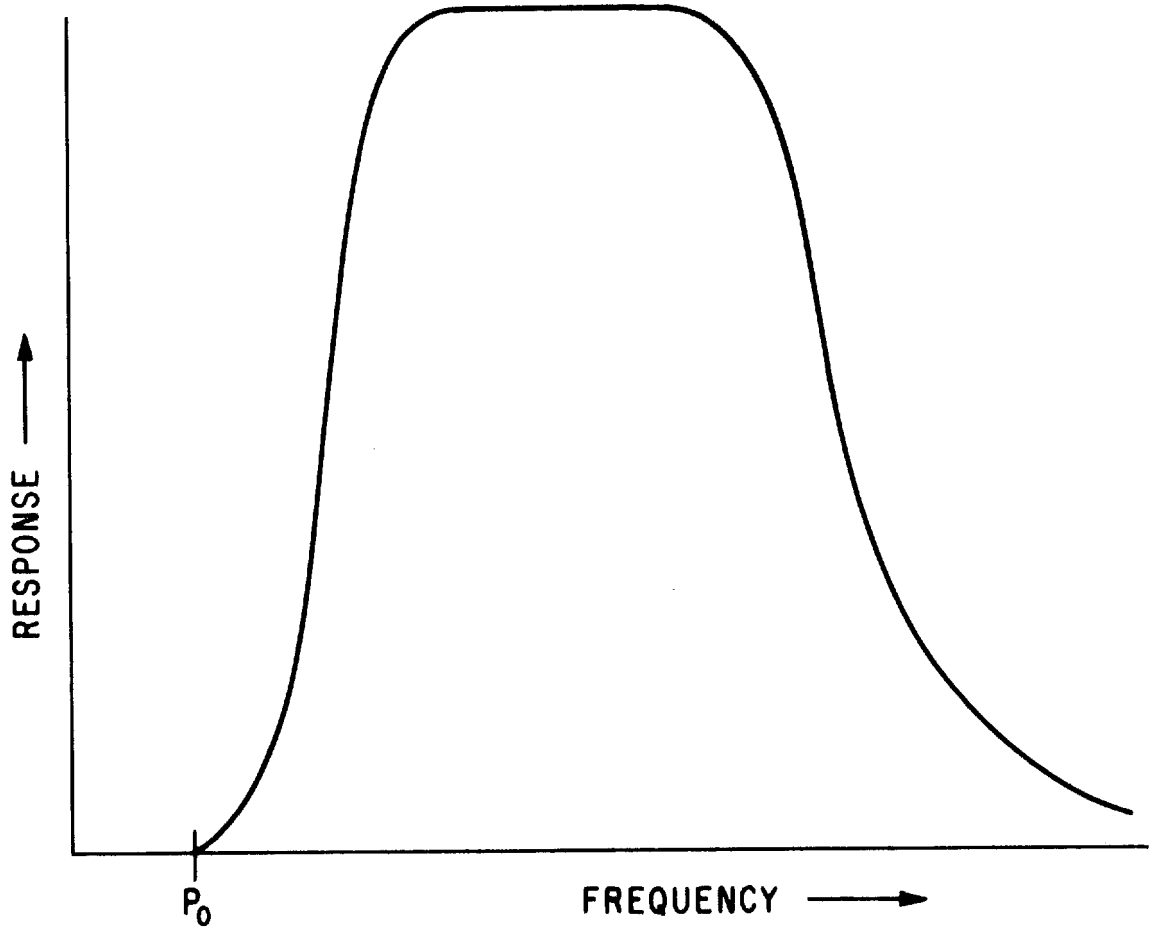

FIGURE 2.2

Thus, it appears that no unusual techniques are required to use phase modulating media in the input plane for recording the data to be processed. Since the input experiences two Fourier transforms, the light amplitude distribution in the output plane is proportional to f(x,y) except that it is modified by the transfer function of the phase media.

If the phase medium are to be used in the input plane, it must satisfy some other general requirements. If it is supported by a substrate, that substrate must not introduce more than $\lambda/4$ wavelength of phase error into the system and of course the phase medium itself must also satisfy this requirement. The questions of speed of handling, ability to store information for long periods of time, resolution capability, dynamic range, etc., must also be considered before phase media can be substituted for photographic films. Some possible problems due to over-modulation will be treated in Section 4.

The fact that some phase media are inherently bandpass operators does not necessarily limit their usefulness for recording data. It is a question of how low is the low cutoff. If it is of the order of the reciprocal aperture in ℓ/mm, the effect will be quite negligible; in fact, even if it is as high as 1/4 to 1/2 ℓ/mm, the phase media may still have a great deal of usefulness in typical recognition systems. This is so because the noise rejection part of the optimum filter for signal detection normally attenuates these frequencies anyway. They contain very little information and usually will not be missed.

3.0 Use of Phase Media in the Frequency Plane

Much of what was said in the previous section about the general requirements of the phase media also applies here. From a theoretical viewpoint we have an interesting variation in the problem, viz., the phase media will only work in the frequency plane if the function to be recorded is a bandpass function. (This is not to be confused with the fact that the phase medium itself is of a bandpass nature.) To see that this is so, consider a low-pass frequency function H(p,q) that might be a candidate filter function. The associated phase function is:

$$G(p,q) = \exp\left[\, jc\ H(p,q)\right] \tag{3.1}$$

$$\cong 1 + jc\ H(p,q) \tag{3.2}$$

The impulse response of this candidate filter is:

$$g(x,y) = \iint \left[\, 1 + jc\ H(p,q)\right]\ e^{j(px + qy)}\ dp\ dq$$

$$= \delta\,(x,y) + jc\ h(x,y) \tag{3.3}$$

Note that g(x,y) is the sum of the desired impulse response h(x,y) and an out of phase δ-function. Since only one Fourier transform is carried out in going from the frequency plane to the image plane, we have no opportunity to separate these two images as we did in the previous case. Even if the phase medium is inherently bandpass, we cannot separate the effects of the two terms of equation (3.3), even though the two terms themselves may be separated. The reason for this is that the output of the system is the convolution of the input function and g(x,y) i.e. if the input function is denoted by f(x,y) and the output is denoted by r(x,y), then:

$$r(x,y) = f(x,y) * [\delta\,(x,y) + jc\ h(x,y)]$$

$$= f(x,y) + jcf(x,y) * h(x,y) \tag{3.4}$$

It is the second term of equation (3.4) that contains the useful information. The first term is added to it and can be considered to be noise. Hence, if H(p,q) is a low-pass function, phase media in the frequency plane will not yield the desired operation.

Fortunately the filters used in the recognition system are themselves bandpass functions. The use of phase media is not only possible, but in some sense is better suited for this application than for recording the input data because it is a bandpass media. Recall that the signal part of the optimum filter is given by:

$$H(p,q) = R^2 + |S(p,q)|^2 + R\,e^{-jpb}\,S(p,q) + R\,e^{jpb}\,S^*(p,q) \qquad (3.5)$$

The associated phase function is:

$$G(p,q) = \exp\ [jc\ H(p,q)]$$

$$\approx 1 + jc\ H(p,q)$$

$$\approx 1 + jc\ [R^2 + |S(p,q)|^2 + R\,e^{-jpb}\,S(p,q) + R\,e^{jpb}\,S^*(p,q)] \qquad (3.6)$$

Taking the impulse response of G(p,q) yields:

$$g(x,y) = \delta(x,y)\ [1 + jc\ R^2] + jc\ s(x,y) * s^*(-x,-y)$$

$$+ jc\ R\ s(x-b,y) + jc\ R\ s^*(-x-b,y) \qquad (3.7)$$

Now we see the effect of the bandpass nature of the filter function. The interesting parts of the filter are on a carrier frequency so that they are automatically separated from the objectionable δ function that occurs on the optical axis. The effect of the δ function is exhibited in the zero order image term that is of no interest.

Although the phase medium can be used to record the signal part of the filter, it is not so clear how it can record the noise-rejection part i.e. $1/N(p,q)$. One way that it could be done is to use the required noise-rejection function in the filter making system so that the signal spectrum is already modified by $1/N(p,q)$ and the effect thus recorded on the filter. This normally leads to difficult mechanical problems unless the filter maker is constructed so that it has two frequency planes. Then the noise-rejection filter could be placed in one frequency plane and the film in the other, but this also leads to systems with mechanical difficulties.

An alternate approach is to expose the phase medium twice, once to record the signal spectrum and once to introduce $1/N(p,q)$. One would then hope that the second exposure reduced the modulation frequency by the proper amount and in the proper places to get optimum overall performance.

Still another way is to use both photographic films and phase media in the recognition system. The noise-rejection filter could be recorded on the photographic film and placed in contact with the phase medium. Since the noise-rejection filter does not have to be changed very often, we can maintain whatever dynamic modulating characteristics the phase media might have. This approach would require some changes to the filter making subsystem and the optical processor to obtain good results.

It appears that the problem of introducing the proper noise-rejection function into the system when required, will be the main difficulty in using phase media in the frequency plane for recording filters.

4.0 Phase Modulation Requirements

In this section we will consider the effect that over-modulation might have on each of the two processes. The effect of over-modulation in the input plane can be seen from equation (2.2). If c f(x,y) is not small compared to unity (meaning that the phase modulation is small compared to $2\pi/\lambda$), we cannot truncate the series expansion after the second term. The more complete expansion for g(x,y) is:

$$g(x,y) = \left[1 + jc\, f(x,y) - \frac{c^2 f^2(x,y)}{2!} - \frac{j c^3 f^3(x,y)}{3!} + \frac{c^4 f^4(x,y)}{4!} + \ldots \right] \qquad (4.1)$$

Thus, when the medium is over-modulated, terms appear which essentially add more noise to the process. The signals are distorted and will not, in general, correlate with the filter. Finally, the various terms are out of phase with each other and will lead to unusual interference effects in the output. The solution to the problem obviously is to insure that over-modulation does not occur.

The effects of over-modulating the phase medium in the frequency plane are slightly more difficult to obtain but are of greater interest. The basic equation that we will deal with here is (3.6). For convenience it will be rewritten as:

$$g(p,q) = \left[1 + jc \left\{ A(p,q) + B(p,q) \cos \left[\phi(p,q) - pb \right] \right\} + \ldots \right] \qquad (4.2)$$

where $A(p,q) = R^2 + |S(p,q)|^2$

$B(p,q) = 2R\,|S(p,q)|$

$\phi(p,q)$ is the phase part of $S(p,q)$

It will be helpful in carrying out the expansion of equation (4.2) to simplify even further by dropping the arguments of the functions. Then equation (4.2) becomes:

$$G = \Big\{ 1 + jc\,[A + B\cos(\phi - pb)] - \frac{c^2}{2!}[A + B\cos(\phi - pb)]^2 - j\frac{c^3}{3!}[A + B\cos(\phi - pb)]^3 + \ldots \Big] \tag{4.3}$$

$$= \Big\{ 1 + jc\,[A + B\cos(\phi - pb)] - \frac{c^2}{2}[A^2 + 2AB\cos(\phi - pb) + B^2\cos^2(\phi - pb)] - j\frac{c^3}{6}[A^3 + 3AB^2\cos(\phi - pb) + 3AB^2\cos^2(\phi - pb) + B^3\cos^3(\phi - pb)] + \ldots \Big] \tag{4.4}$$

Further expansion followed by a collecting of terms gives:

$$G = 1 + jcA - \frac{c^2A^2}{2} - j\frac{c^3A^3}{6} - j\frac{c^3AB^2}{4} - \frac{c^2B^2}{4} + (jcB - c^2AB - j\frac{c3A2B}{2} - j\frac{c3B3}{8})\cos(\phi - pb) + (-j\frac{c^3AB^2}{4} \quad \frac{c^2B^2}{4})\cos(2\phi - 2pb) - j\frac{c^3B^3}{24}\cos(3\phi - 3pb) + \ldots \tag{4.5}$$

First we note the presence of the expected harmonic terms. These terms do not overlap with the terms of interest and can be disregarded. They do, however, contain some energy and contribute to the inefficiency of the process. In passing we also note that the harmonic terms have both amplitude and phase distortion and are unacceptable for any use.

The first term of equation (4.5) is equivalent to the zero order term. The distortion terms cause some spreading of the central image in the output plane. For example the term c^3AB^2 is actually $c^3 [R^2 + | S(p,q)|^2] 4R^2 | S(p,q)|^2$. The length of the central image in the output is $L_x + 8\ell_x$, where L_x is the length of the input signal and ℓ_x is the length of the signal to be detected, both taken in the x-direction. When over-modulation is not present the length of the central image is $L_x + 4\ell_x$, as described in Information Content of Spatial Filters. Thus, the carrier frequency would have to be increased somewhat to counteract this phenomenon. Further, the presence of the distortion terms tends to use up the available dynamic range of the phase media.

It is the second term of equation (4.5) that is of greatest interest because it contains the desired information. Writing it with the appropriate arguments and in ascending powers of $|S(p,q)|^2$ we have:

$$\Big\{ \left(- jc - c^2 R^2 - j\, c^3 R^4 \right) |S(p,q)| + \left(- c^2 R - j\, 2\, c^3 R^2 - j\, \frac{c^3 R^3}{8} \right) |S(p,q)|^3 + (- c^3 R) |S(p,q)|^5 \Big\} \cos (\phi(p,q) - pb)$$

First note that no phase distortion is introduced by the over-modulation. However, two of the three terms contain amplitude distortion. This distortion produces what might be termed a small signal suppression effect. The exact opposite might appear to be the case from an examination of the terms given above, but it must be remembered that less of the usable portion of the dynamic range is available for the term in $|S(p,q)|$. It can then be seen that those regions of $|S(p,q)|$ that have low amplitudes tend to be suppressed by the distortion terms.

It has been shown that over-modulation of the phase medium in either the input plane or the frequency plane must be avoided if possible. While it is true that the amplitudes of the distortion terms are lower than the amplitudes of the terms of interest, the distortion reduces the efficiency of the process and increases the noise factor.

It should be pointed out that over-modulation of photographic films will produce similar results, except that the various terms will not be out of phase, so that this phenomena is not unique to phase modulating media. Whether the effect is more or less severe in the phase method depends on the available dynamic range. This, in turn, is dependent on the amount of noise inherent in the phase media. These questions cannot be answered without some experimental results on which to base such calculations.

Section A-4

Obtainable Signal-to-Noise Ratios

1. Introduction

The ultimate factor in determining how well an automatic recognition system operates is the signal-to-noise ratio (SNR) at the output of the system. A threshold or decision level cannot be set and automatic detection is not possible unless the SNR is sufficiently large. In this memorandum we will discuss the SNR that can be expected from an optical recognition system. The problem will first be solved in its most general form and then specific (although reasonable) assumptions will be made in order to provide a few figures.

2. Mathematical Background

The input data $f(x,y)$ is considered to be the sum of a signal of interest $s(x,y)$ and a noise background $n(x,y)$. The noise background is said to be homogeneous if any subportion of the data has approximately the same statistics as any other subportion. The noise is said to be isotropic if the statistics show no preferred orientation.

The property of homogeniety guarantees that any particular image will have the same noise statistics as any other image from the same general area. As a refinement, one could divide the backgrounds into a subset of backgrounds - natural terrain, urban areas, thermal backgrounds of IR images, etc. - to obtain somewhat more accurate results. In this case the noise is assumed to be homogeneous within any particular subset.

The signal is a Fourier transformable function of two space coordinates. Its Fourier transform is given by:

$$S(p,q) = \int_{-\infty}^{\infty} \int s(x,y)\, e^{j(px + qy)}\, dx\, dy \qquad (2.1)$$

The noise has an autocorrelation function $R_n(x,y)$ defined by:

$$R_n(x,y) = \lim_{\substack{\ell y \to \infty \\ \ell x \to \infty}} \frac{1}{A} \int_{-\ell y}^{\ell y} \int_{-\ell x}^{\ell x} n(u,v)\, n^*(u + x, v + y)\, du\, dv \qquad (2.2)$$

where $A = 4\, \ell x\, \ell y$. In view of the assumption of homogeneity, it does not matter whether $n(u,v)$ in equation (2.2) is a complete subset of noise backgrounds or any element selected from the subset. The noise can also be characterized by a noise spectral density $N(p,q)$ defined by:

$$N(p,q) = \int\int_{-\infty}^{\infty} R_n(x,y)\, e^{j(px + qy)}\, dx\, dy \qquad (2.3)$$

It is desired to find the optimum filter function $H(p,q)$ that will maximize the ratio of peak signal energy to mean square noise energy. The signal part of the output is:

$$r_s(x,y) = \frac{1}{4\pi^2} \int\int_{-\infty}^{\infty} S(p,q)\, H(p,q)\, e^{j(px + qy)}\, dp\, dq \qquad (2.4)$$

and the mean square noise (MSN) is:

$$MSN = \frac{1}{4\pi^2} \int\int_{-\infty}^{\infty} N(p,q)\, |\, H(p,q)\, |^2\, dp\, dq \qquad (2.5)$$

We want to find the $H(p,q)$ that will maximize the ratio $|\, r_s(0,0)\, |^2 / MSM$, where the peak signal is evaluated at $x = y = o$. The peak value of the signal is not dependent on its location so we can set $x = y = 0$ for convenience. From equations (2.4) and (2.5) we have:

$$\frac{r_s(0,0)^2}{MSN} = \frac{\frac{1}{4\pi^2} \left| \int\int_{-\infty}^{\infty} S(p,q)\, H(p,q)\, dp\, dq \right|^2}{\int\int_{-\infty}^{\infty} N(p,q)\, |\, H(p,q)\, |^2\, dp\, dq} \qquad (2.6)$$

Since N(p,q) is the Fourier transform of an autocorrelation function, it is non-negative and can be used as a weighting function in the Schwarz inequality. Applying this inequality to equation (2.6) we have:

$$\frac{|r_s(0,0)|}{MSM}^2 \leq \frac{1}{4\pi^2} \int_{-\infty}^{\infty}\int \frac{|S(p,q)|^2}{N(p,q)} \, dp \, dq \qquad (2.7)$$

with equality if, and only if:

$$H(p,q) = \frac{k \, S^*(p,q)}{N(p,q)} \qquad (2.8)$$

where k is some constant. If H(p,q) satisfies equation (2.8), the SNR is:

$$SNR = \frac{1}{4\pi^2} \int_{-\infty}^{\infty}\int \frac{|S(p,q)|^2}{N(p,q)} \, dp \, dq \qquad (2.9)$$

Equation (2.9) gives the most general result for the obtainable SNR. The SNR can be calculated as soon as S(p,q) and N(p,q) are known. Unfortunately, the calculation of SNR cannot be done by hand in most practical cases. Before passing on to a specific problem that can be calculated by hand, it should be noted that if N(p,q) is constant (white noise case), then the SNR is dependent only on the total signal energy - and not dependent on the signal shape. This fact has some relevance in determining what signal shape to use in the calculations of the next section.

3. Specific Examples

The general formulation for the SNR was given in Equation (2.9). In this section we will assume a specific form for both the signal and the noise spectral density that are not too far from reality. First, the fact that the noise is isotropic implies that N(p,q) has rotational symmetry. We will replace N(p,q) by

by $N(\rho)$ where $\rho^2 = p^2 + q^2$. The noise spectral density can be quite closely approximated in some cases by a function of the form:

$$N(\rho) = c_1 \quad \frac{1}{1 + (\rho/a)^2} \tag{3.1}$$

where c_1 is the average noise energy n^2, and a is a constant that determines the shape of $N(\rho)$.

A somewhat better approximation to $N(\rho)$ might be attained by using a function of the form:

$$N(\rho) = c_1 \quad \frac{1}{1 + a_1 |\rho| + a_2 \rho^2 + a_3 |\rho|^3 + \ldots} \tag{3.2}$$

where $a_1, a_2, \ldots a_n$ are chosen to fit the particular $N(\rho)$ that is present. We will use Equation (3.1) in the calculations of this section, although the use of Equation (3.2) would not change the basic methods involved.

To simplify the calculations, we will choose a signal shape that also has rotational symmetry so that we can replace $S(p,q)$ by $S(\rho)$. Then Equation (2.9) becomes:

$$\begin{aligned} SNR &= \frac{1}{4\pi^2} \int_0^{\infty} \int_0^{2\pi} \frac{|S(\rho)|^2}{N(\rho)} \rho \, d\rho \, d\phi \\ &= \frac{1}{2\pi} \int_0^{\infty} \frac{|S(\rho)|^2}{N(\rho)} \rho \, d\rho \end{aligned} \tag{3.3}$$

The choice of signal shapes is, at best, a compromise. We must have a signal shape that will lead to conservative estimates of the SNR, but will, at the same time, allow us to compute the SNR in closed form. A signal form that

satisfies both these requirements is:

$$s(x,y) = c_2\, e^{-b(x^2 + y^2)} \tag{3.4}$$

where c_2 is the peak amplitude of the signal and b is a constant. The Fourier transform of s(x,y) is:

$$S(p,q) = c_2 \int_{-\infty}^{\infty}\int_{-\infty}^{\infty} e^{-b(x^2 + y^2)}\, e^{j(px + qy)}\, dx\, dy$$

$$= 4c_2 \int_0^{\infty} e^{-bx^2} \cos px\, dx \int_0^{\infty} e^{-by^2} \cos qy\, dy$$

$$= 4c_2 \left(\frac{1}{2}\frac{\pi}{b}\, e^{-p^2/4b}\right)\left(\frac{1}{2}\frac{\pi}{b}\, e^{-q^2/4b}\right)$$

Substituting $\rho^2 = p^2 + q^2$, we have:

$$S(\rho) = \frac{c_2\,\pi}{b}\, e^{-\rho^2/4b} \tag{3.5}$$

Substituting (3.5) and (3.1) into (3.3) gives:

$$SNR = \frac{1}{2\pi} \int_0^{\infty} \frac{\left|\frac{c_2\,\pi}{b}\, e^{-\rho^2/4b}\right|^2}{c_1 \frac{1}{1 + (\rho/a)^2}}\, \rho\, d\rho$$

$$= \frac{c_2^2\,\pi}{2\,b^2\,n_o^2} \int_0^{\infty} (\rho + \rho^3/a^2)\, e^{-\rho^2/2b}\, d\rho$$

$$= \frac{c_2^2\,\pi}{2b^2\,n^2} \left[b + \frac{2b^2}{a^2} \right]$$

$$= \frac{c_2^2\,\pi}{2n_o^2} \left[\frac{1}{b} + \frac{2}{a^2} \right] \tag{3.6}$$

Equation (3.6) gives the expected SNR in terms of the peak signal amplitude in the input, the average noise in the input, and the parameters a and b. Figure 3.1 gives a plot of $\left(\frac{N(\rho)}{n_o^2} \right)$ for four values of the parameter a. Past experience indicates that a should take on values around 1/2 for some real world backgrounds. Thus, we use a = 1/8, 1/4, 1/2 and 1 for our plots of the noise spectral density.

In Figure 3.2 we have plotted $\left(\frac{2n_o^2 \, SNR}{c_2^2 \, \pi} \right)$ as a function of b for the four values of a. These curves are asymptotic to 1/b for small values of b and are asymptotic to $(2/a^2)$ for large values of b.

To get some meaningful results, it is necessary to determine what values a and b are likely to assume in an actual system. From some data we acquired some time ago, it appears that a $\approx$ 1/8 for aerial photographs of natural terrain at a 2500:1 scale. The value of b can be determined from Equation (3.4) if we know the length of the target (actually, the "diameter" of the target because we are working with rotationally symmetric signals). Here we will use that value of b that will cause s(x,y) to drop to its half value point at the edge of the signal (see Figure 3.3). Any other assumption, say using the half power point will also be acceptable as long

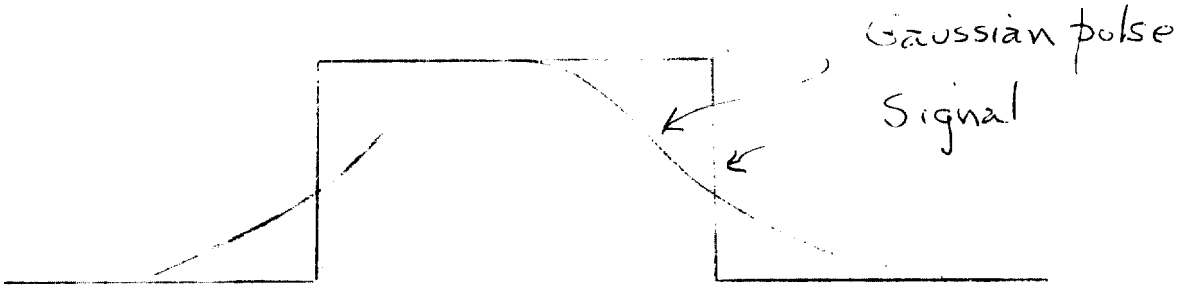

Figure 3.3

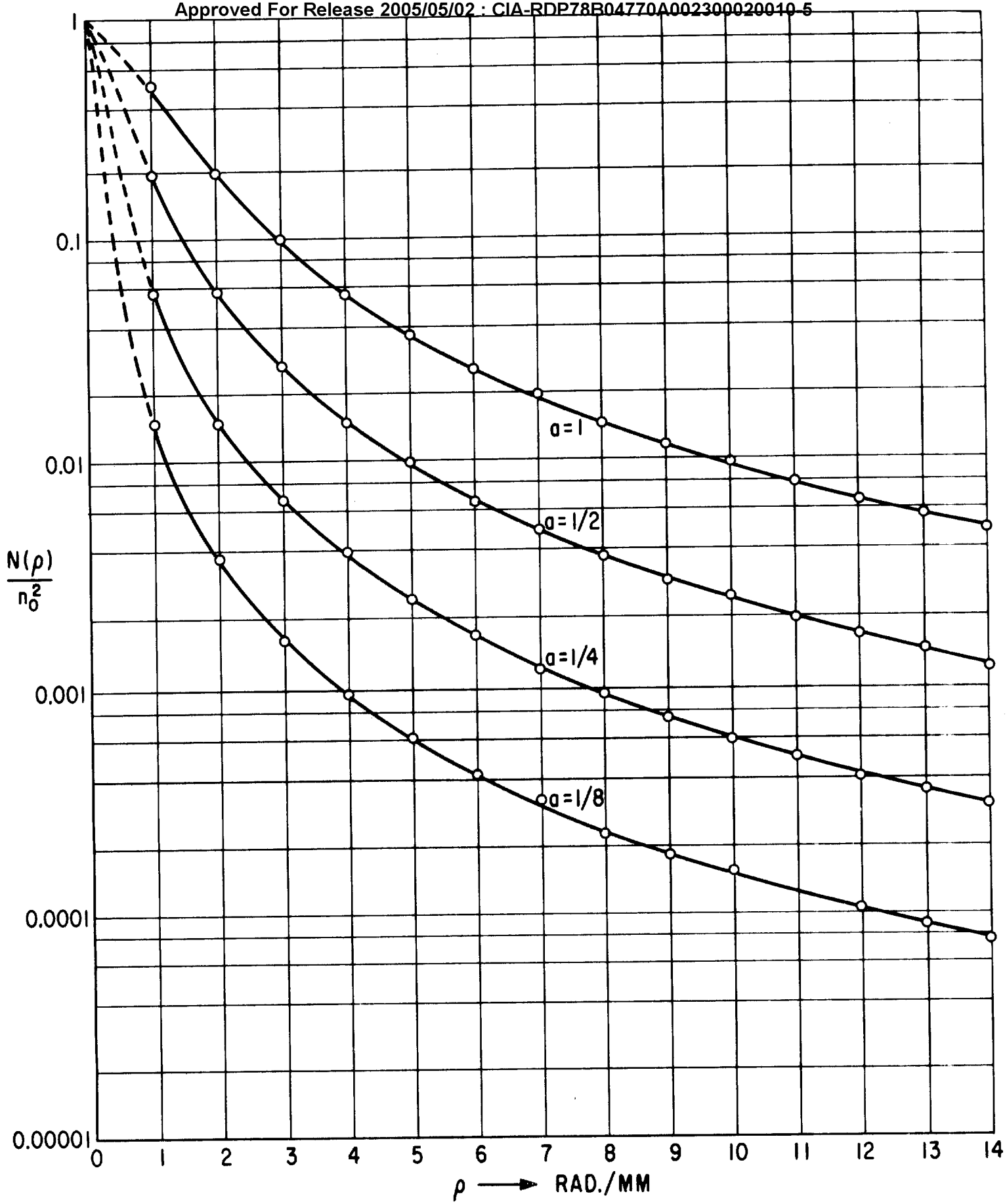

FIGURE 3J

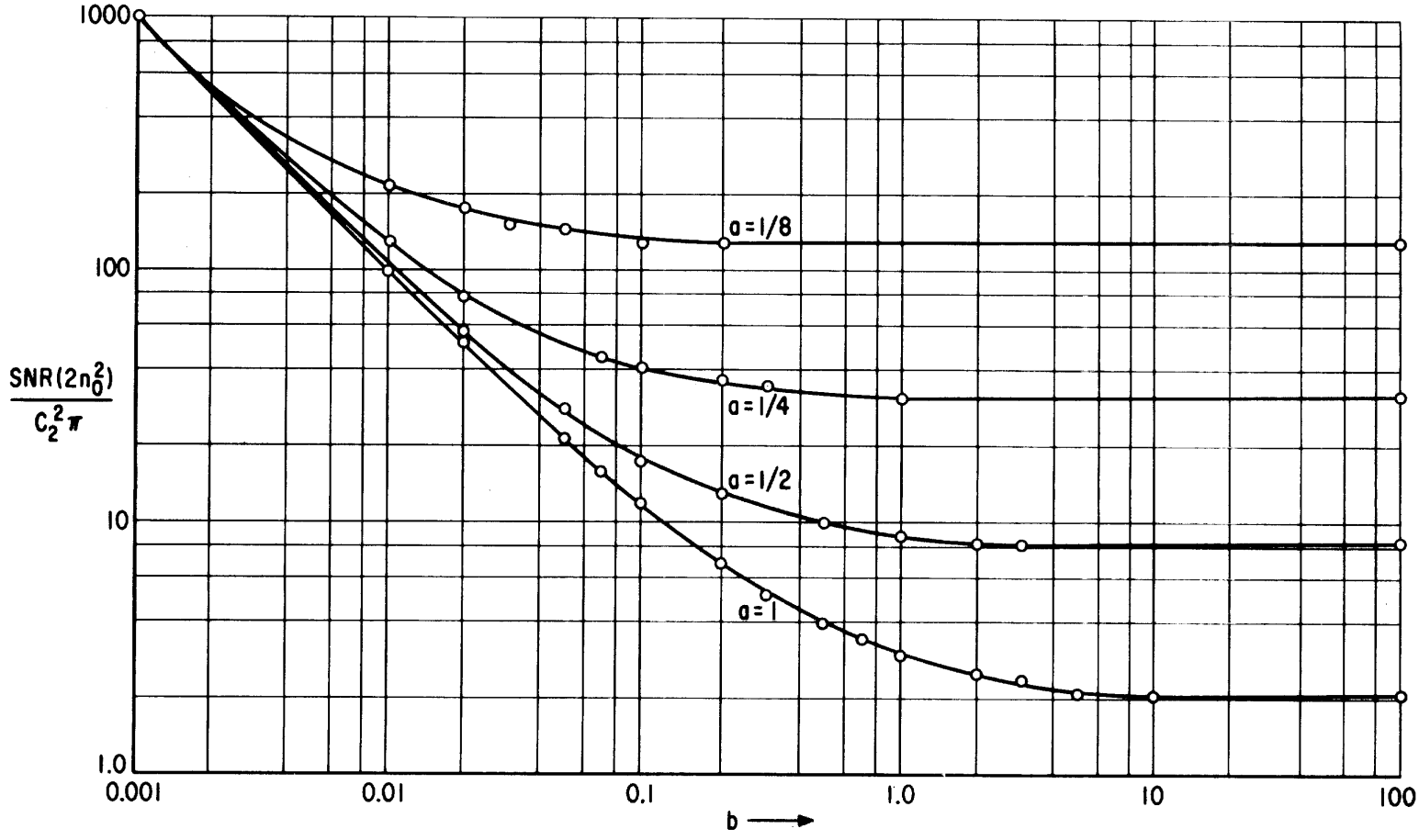

FIGURE 3.2

as it is consistent. I choose to use the half value point because this results in a half power point when we use the signal <u>energy</u> in the computations. The value of b that satisfies this requirement is:

$$b = \frac{4}{2}\left(\frac{1.18}{D}\right)^2 = 2.8/D^2$$

where D is the diameter of the target. In an aerial photograph at 2500:1 scale, a target of 20 ft. diameter will have an image size of about 2.5 mm. Thus, for that target b = 0.45. From Figure 3.2 we see that:

$$SNR = \frac{c_2^2 \pi}{2n_o^2}(128)$$

If the peak signal amplitude in the input is $c_2 = 0.5$ and the average noise is $n_o = 0.5$, then:

$$SNR = \frac{\pi}{2}(128) \approx 200$$

$$= + 23db$$

It is reasonable to assume that $c_2 \gtrless n_o$ in the input so that the output SNR will vary accordingly.

Before concluding this section we must examine the validity of equation (3.6) for both large and small values of b. A large value of b implies that the signal is very small and a small value of b implies that the signal is large. The result expressed in equation (3.6) is valid at least up to the point where the signal fills the system's aperture. The value of b can be obtained by requiring that the signal as given by equation (3.4), be less than or equal to 0.223 at the edge of the aperture

so that we do not lose more than 5 percent of the signal's energy. If the system's aperture is 2A, we have:

$$b\,A^2 \geq (1.05)^2/2$$

If 2A = 100 mm, then

$$b \geq \frac{(1.05)^2}{2\,(50)^2}$$

$$b \geq 0.0002$$

Thus, it is safe to use Figure 3.2 for any small value of b that is shown. The validity of equation (3.6) for large values of b can be estimated from equation (3.5). Again, if $S(\rho)$ is less than or equal to 0.223 at the frequency plane aperture cutoff, no more than 5 percent of the signal's energy will be lost. Suppose the system is band limited at ρ_o rad/mm. Then from equation (3.5) we have:

$$\rho^2/4b \geq \frac{(1.05)^2}{2}$$

For $\rho_o = 2\pi$ (50 /mm) we have:

$$b \leq \frac{2(314)^2}{4(1.05)^2}$$

$$\leq 50{,}000$$

This value of b is well outside the range of values of b as shown in Figure 3.2. Thus, the curves shown in Figure 3.2 can be used for all values of b as given.

4. Summary and Conclusions

In this memorandum we have derived a general expression for the SNR at the output of an optical recognition system. The SNR can only be calculated in closed form for certain signal shapes and for certain noise spectral densities. For the more general case a computer is ususally necessary to compute the SNR. A computer

solution also has the advantage that the SNR as given in equation (2.9) can be found as a function of finite limits so that the effect of the system's bandwidth can be seen.

An estimate of the SNR for assumed signal and noise spectral density functions was made in Section 3. The results indicate that the SNR can vary widely depending on the exact form of the signal and noise functions. In practice we have found SNR of about 15 db, so these estimates are fairly realistic.

A note of caution is in order, however, when using these results. We have assumed that the entire system is linear. The filter function, however, is recorded on a physical medium that of ten is non-linear. Again, this refinement of the analysis can only be made with the assistance of a computer.

Section A-5

Information Capacity of a Recognition System

1. Introduction

The problem is one of showing that the optical processor can handle large, highly detailed images. We will also consider the limitations that may be introduced by some of the system parameters.

This case is closely related to the material covered in "Information Content of Spatial Filters", except we cannot properly consider the information capacity of a noise-free system. We can, however, talk about the space-bandwidth product (SBP) of such a system. The major problem is that the types of noise in an optical can vary widely and cannot be very well defined. The noise may be due to stray light, blemishes on the optical elements, or noise in the recording media or sensor. The effects of noise have been described by G. Toraldo di Francia in Optica Acta, Vol. 2, No. 1, April 1955.

2. Space Bandwidth Product of the Optical System

In the section on Information Content of Spatial Filters we considered the SBP of the signal to be detected and the SBP required of the spatial filter. We did not consider the SBP of the input data, but it can be obtained by a simple extension of that analysis. Recall that the SBP of any signal is equal to the product of the area of that signal and the highest frequency that it contains. We will assume that the input data is a low-pass function, as is almost always the case.

At this time we are only interested in matching the SBP of the optical system with the SBP of the input data. We will use the system shown in Figure 2.1 as the basis for this analysis. The data to be processed $f(x,y)$ is placed in plane P_1, a distance ℓ from the frequency plane P_2. The Fourier transform of $f(x,y)$ appears

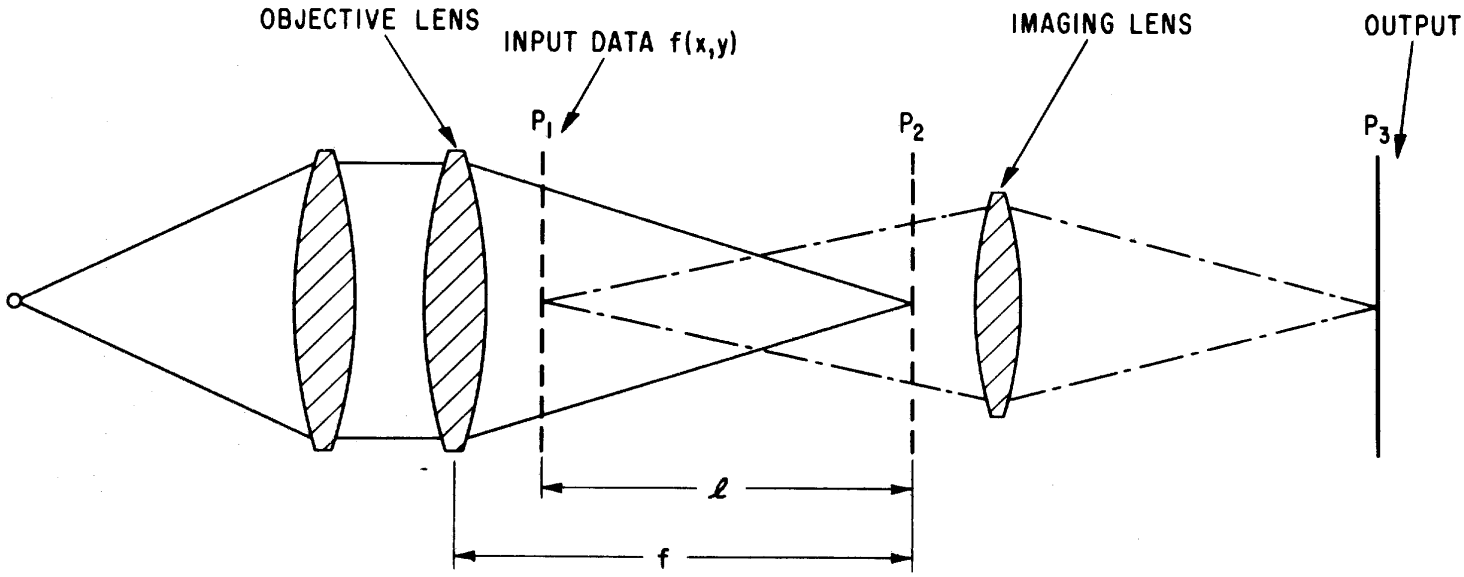

FIGURE 2.1

in plane P_2 as:

$$F(\epsilon, n) = g(\epsilon, \ell) \iint f\left(\frac{x\ell}{f}, \frac{y\ell}{f}\right) e^{j\frac{k}{f}(\epsilon x + ny)}\, dx\, dy \qquad (2.1)$$

$$\text{where } g(\epsilon, \ell) = \frac{-jA}{\lambda \ell} e^{j\frac{k}{\ell}(\epsilon^2 + n^2)}$$

In this case ϵ, n are the actual distance variables in plane P_2, $k = 2\pi/\lambda$, λ is the wavelength of light, f is the focal length of the objective lens, and A is the amplitude of the light in the collimated region. The presence of the factor $g(\epsilon, \ell)$ is not of importance in this analysis and will be neglected. Equation (2.1) exhibits the scale varying transform relationship; but since the input data has its smallest effective scale and its largest effective area when $\ell = f$, we will consider only that case.

We will first consider what requirements must be placed on the size of the frequency plane due to a small patch of the input data centered on the optical axis. The size of the frequency plane is determined solely by the highest frequency in this patch. Suppose the input data is band-limited to a frequency p_o ℓ/mm, then the radius of the frequency plane must be:

$$R = (\epsilon_o^2 + n_o^2)^{1/2} = p_o \lambda f \qquad (2.2)$$

Thinking of it in other terms, suppose the frequency plane is limited in size to radius R_o or more likely, the aperture of the imaging lens is the limiting radius, then the maximum frequency that can be passed by the system is:

$$p = \frac{R_o}{\lambda f} \quad \ell/\text{mm} \qquad (2.3)$$

Thus, the limit on how highly detailed the input data can be is ultimately determined by the aperture of the frequency plane or the aperture of the imaging lens, whichever is smaller. This is exactly what one might expect because, in the absence of a filter, the resolution of the total system is limited by the imaging lens.

It is clear from a consideration of equation (2.1) that the location of this small patch in the input plane has no effect on the required size of the frequency plane. Again, in other terms, for a given bandwidth, the patch can be just as highly, detailed regardless of its location in the input. Thus, it will not make any difference if there are many such patches in the input plane. In fact, the entire aperture of the system can be used to illuminate the signal. Hence, we have shown that the optical system can process large, highly-detailed images without sub-dividing them into smaller images for processing.

A good analogy to this situation can be made by considering an electronic system. If the system has some given bandwidth, the duration of the signal is of no importance. In general the bandwidth requirements are independent of the duration of the signal, except for very short duration signals.

Perhaps the only question generated by this chain of reasoning is that it might appear that the frequencies from the various subportions of the input will interfere and produce some anomalous effect. This is not the case. The maximum frequency that can be produced by these interference effects in the frequency plane is:

$$W = \frac{\lambda f}{A} \qquad (2.4)$$

Any frequency so generated can be passed by the imaging lens provided it does not vignette the field of view. Proper placement of stops in the lens can prevent this occurring.

Finally, there is an upper limit as to how highly detailed the input data can be. If the highest frequency p_o approaches $2/\lambda$ ℓ/mm, the diffracted waves will be evanessent and will not propogate into the system. Very few recording media have resolution capabilities that will produce such an effect, and no image transmitted by a realizable lens can contain such frequencies. It should be pointed out, however, that such frequencies can be obtained in holograms when the field of view extends to very large angles.

EFFECT OF IMAGE SIZE

1. Introduction

In this section we will discuss the performance of the optical recognition system as a function of the actual image size. This material is closely related to the section discussing the obtainable signal-to-noise ratio (SNR) in an optical system. The reason for this is that the same measure of performance will be used, i.e., the minimum required SNR will determine the minimum signal size. It differs from that discussion in that we are now concerned with microscopic noise (film grain noise) as well as macroscopic noise (the background terrain). One expects the background terrain noise to enter this analysis in much the same way as before and expects the film grain noise to further reduce the SNR.

The fundamental problem is to construct a good mathematical model of film grain noise. We know, for example, that film grain noise is a multiplicative process. This means that the amount of noise is dependent on the signal strength and that the total input data must be described by a function f(x,y), where:

$$f(x,y) = s(x,y)n_1(x,y) + n_o(x,y)$$

In this representation $n_o(x,y)$ is the background terrain noise, $s(x,y)$ is the signal, and $n_1(x,y)$ is the film grain noise. Since $n_o(x,y)$ is considered to be macroscopic in nature, we can assume that it is not affected to any great extent by the film grain noise. As the signal size decreases we can expect the system's performance to be quite highly dependent on the exact nature of the film grain noise process.

As has been shown elsewhere (Reference 1), we cannot formulate the mathematical theory for matched filtering when the noise process is multiplicative. The best we can do is (1) make some approximations that reduce the problem to one of additive noise or (2) use a computer to try to optimize the filter under the multiplicative

noise restriction. There is no guarantee that matched filtering is optimum, of course, but the problem gets out of hand from the analytical viewpoint.

There is one feature about the types of signals usually detected in recognition systems that allows us to pursue the former approach. The signals tend to be uniformly illuminated. For example, if the signal is of the form shown in Figure 1.1a, one could expect that the difference between the multiplicative noise process and an assumed additive noise process would be significant. However, if the signal is more like that shown in Figure 1.1b, the difference between the multiplicative and additive cases should be small.

The way in which the many different methods of describing photographic film noise enter into this problem is not at all clear. Researchers have discussed the accutance, granularity, definition, resolution, etc., of photographic film, but it is difficult to incorporate such quantities into the calculations of the SNR. It appears that the best method of describing the film grain noise for the purposes of this study is to say that the film grain noise spectral density is uniform for all frequencies of interest. Different films will then be characterized by the amount of noise that they introduce.

For the type of signal shown in Figure 1.1b, we will assume that we can write the total input function as:

$$f(x,y) = c\ s(x,y)\ n_1(x,y) + s(x,y) + n_1(x,y) + n_o(x,y)$$

where c is some constant. Here we have divided the multiplicative noise process into a sum of signal times noise and a sum of signal and noise. We will assume that c is sufficiently small so that we can neglect the first term of f(x,y) as a first order approximation to the true situation. Thus, if $N_o(p,q)$ is the spectral

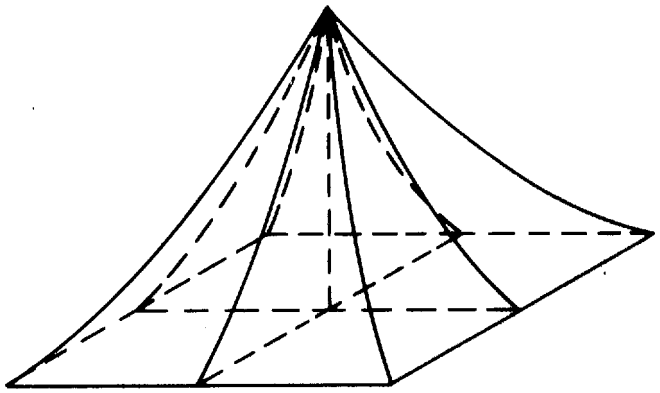

(a)

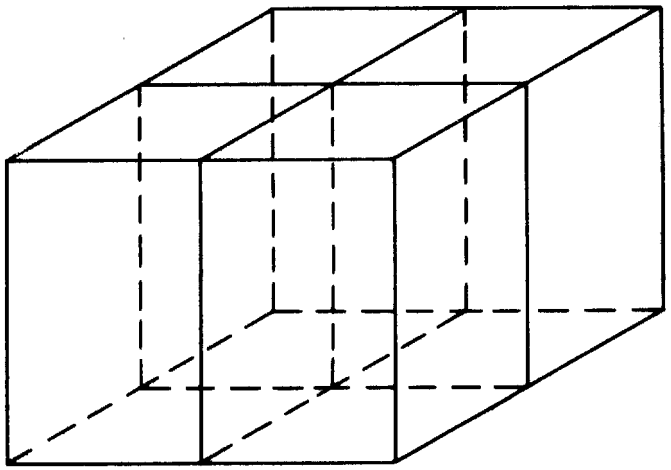

(b)

FIGURE 1.1

density of the background terrain and $N_1(p,q)$ is the spectral density of the film grain, the total noise process is $N(p,q) = N_o(p,q) + N_1(p,q)$.

It is admitted that the approach taken here is less than what would be desired. Under the circumstances it is about all that can be done, but it is hoped that this approach represents at least one step toward the real solution to the problem.

2. Mathematical Solution

We will draw on the results presented in the section "Obtainable Signal to Noise Ratios" as a starting point for this discussion. Recall that the SNR was given as:

$$SNR = \frac{1}{2\pi} \int_o^\infty \frac{\rho |S(\rho)|^2 d\rho}{N(\rho)} \tag{2.1}$$

where both the signal and noise were assumed to have rotational symmetry. The signal has the form:

$$s(x,y) = c_2 \, e^{-b(x^2 + y^2)} \tag{2.2}$$

with Fourier transform:

$$S(\rho) = \frac{c_2 \pi}{b} \, e^{-\rho^2/4b} \tag{2.3}$$

The macroscopic noise spectral density due to the background terrain was assumed to be of the form:

$$N_o(\rho) = \frac{n_o^2}{1 + \rho^2/a^2} \tag{2.4}$$

The microscopic noise spectral density $N_1(\rho)$ due to film grain noise will be of the form $N_1(\rho) = n_1^2$. Thus, we are assuming that the microscopic noise has a flat spectrum which agrees favorably with experimental observations. The total noise spectral density is then:

$$N(\rho) = \frac{n_o^2}{1 + \rho^2/a^2} + n_1^2$$

$$= \frac{n_o^2 + n_1^2 + n_1^2\ \rho^2/a^2}{1 + \rho^2/a^2} \tag{2.5}$$

Substituting equations (2.3) and (2.5) into (2.1) gives:

$$SNR = \frac{c_2^2\pi}{2b^2} \int_o^\infty \frac{(1 + \rho^2/a^2)\ \rho e^{-\rho^2/2b}\ d\rho}{n_o^2 + n_1^2 + n_1^2\ \rho^2/a^2} \tag{2.6}$$

$$= \frac{c_2^2\pi}{2b^2} \int_o^\infty \frac{\rho e^{-\rho^2/2b}\ d\rho}{n_o^2 + n_1^2 + n_1^2\ \rho^2/a^2}$$

$$+ \frac{c_2^2\pi}{2b^2a^2} \int_o^\infty \frac{\rho^3 e^{-\rho^2/2b} d\rho}{n_o^2 + n_1^2 + n_1^2\ \rho^2/a^2} \tag{2.7}$$

The two integrals of equation (2.7) can be solved by letting $\rho^2 = u$, $2\rho d\rho = du$, to get:

$$SNR = \frac{c_2^2\pi}{4b^2} \int_o^\infty \frac{e^{-u/2b}}{n_o^2 + n_1^2 + n_1^2\ u/a^2}\ du$$

$$+ \frac{c_2^2\pi}{4b^2a^2} \int_o^\infty \frac{u\ e^{-u/2b}}{n_o^2 + n_1^2 + n_1^2\ u/a^2}\ du \tag{2.8}$$

These integrals can be put into standard form by letting $n_1^2\, u/a^2 = t$. Then we have:

$$SNR = \frac{c_2^2 \pi\, a^2}{4b^2 n_1^2} \int_0^\infty \frac{e^{-\frac{ta^2}{2bn_1^2}}}{n_o^2 + n_1^2 + t}\, dt$$

$$+ \frac{c_2 \pi\, a^2}{4b^2\, n_1^4} \int_0^\infty \frac{t\, e^{-\frac{ta^2}{2bn_1^2}}}{n_o^2 + n_1^2 + t}\, dt \qquad (2.9)$$

From the "Tables of Integral Transforms", Vol. 1, Edited by A. Erdelyi, McGraw-Hill, 1954, pg. 137, we have the following integral transform:

$$\int_0^\infty t^v (t+\alpha)^{-1}\, e^{-pt}\, dt = \Gamma(v+1)\, \alpha^v\, e^{\alpha p} \Gamma(-v, \alpha p) \qquad (2.10)$$

Thus we can solve the two integrals of equation (2.9) by letting $v = 0$ and $v = 1$ respectively. Further, we let $p = \frac{a^2}{2bn^2}$ and $\alpha = n_o^2 + n_1^2$. Then equation (2.9) becomes:

$$SNR = \frac{c_2^2 \pi\, a^2}{4b^2\, n_1^2} \left[\Gamma(1)\, e^{\alpha p} \Gamma(0, \alpha p) \right]$$

$$+ \frac{c_2^2 \pi\, a^2}{4b^2 n_1^2} \left[\Gamma(2)\, \alpha e^{\alpha p}\, \Gamma(-1, \alpha p) \right] \qquad (2.11)$$

We also have the following relationships for the incomplete gamma functions:

$$\Gamma(1) = \Gamma(2) = 1 \qquad (2.12)$$

$$\Gamma(0, \alpha p) = E_1(\alpha p) \qquad (2.13)$$

$$\Gamma(-1, \alpha p) = -E_1(\alpha p) + \frac{e^{-\alpha p}}{\alpha p} \qquad (2.14)$$

where:

$$E_1(x) = \int_0^\infty \frac{e^{-t}}{t}\, dt \qquad (2.15)$$

Using (2.12) - (2.14) in (2.11) we have:

$$SNR = \frac{c_2^2 \pi a^2}{4b^2 n_1^2}\left[e^{\alpha p} E_1(\alpha p) \right]$$

$$+ \frac{c_2^2 \pi a^2}{4b^2 n_1^4}\left[\frac{\alpha e^{\alpha p} e^{-\alpha p}}{\alpha p} - \alpha e^{\alpha p} E_1(\alpha p) \right] \qquad (2.16)$$

$$= \frac{c_2 \pi a^2}{4b^2 n_1^2}\left[e^{\alpha p} (1 - \alpha/n_1^2) E_1(\alpha p) + \frac{1}{n_1^2 p} \right]$$

Using the values given previously for α and p, we have:

$$SNR = \frac{c_2^2 \pi a^2}{4b^2 n_1^2}\left[e^{\frac{a^2(n_o^2+n_1^2)}{2bn_1^2}} \left[1 - \frac{n_o^2+n_1^2}{n_1^2} \right] E_1\left[\frac{a^2(n_o^2+n_1^2)}{2bn_1^2} \right] + \frac{2b}{a^2} \right] \qquad (2.17)$$

Note that the first term of equation (2.17) is zero if $n_o^2 = 0$, i.e. if the macroscopic noise is zero. Thus we can also obtain the "white noise" solution from equation (2.17).

Equation (2.17) is plotted as curve A in Figure 2.1 for the following values of the parameters:

$$n_o^2 = 0.29$$

$$n_1^2 = 0.01$$

$$a = 0.1$$

$$c_2^2 = 0.30$$

We note that curve A is asymptotic to $c_2^2/2b^2n_1^2$ for large values of b. The asymptotic behavior for small values of b cannot be found because $E_1(x)$ is not tabulated for $x < 0.01$. It appears that the SNR is growing very slowly as would be expected. In any event, this region is not of particular interest because it

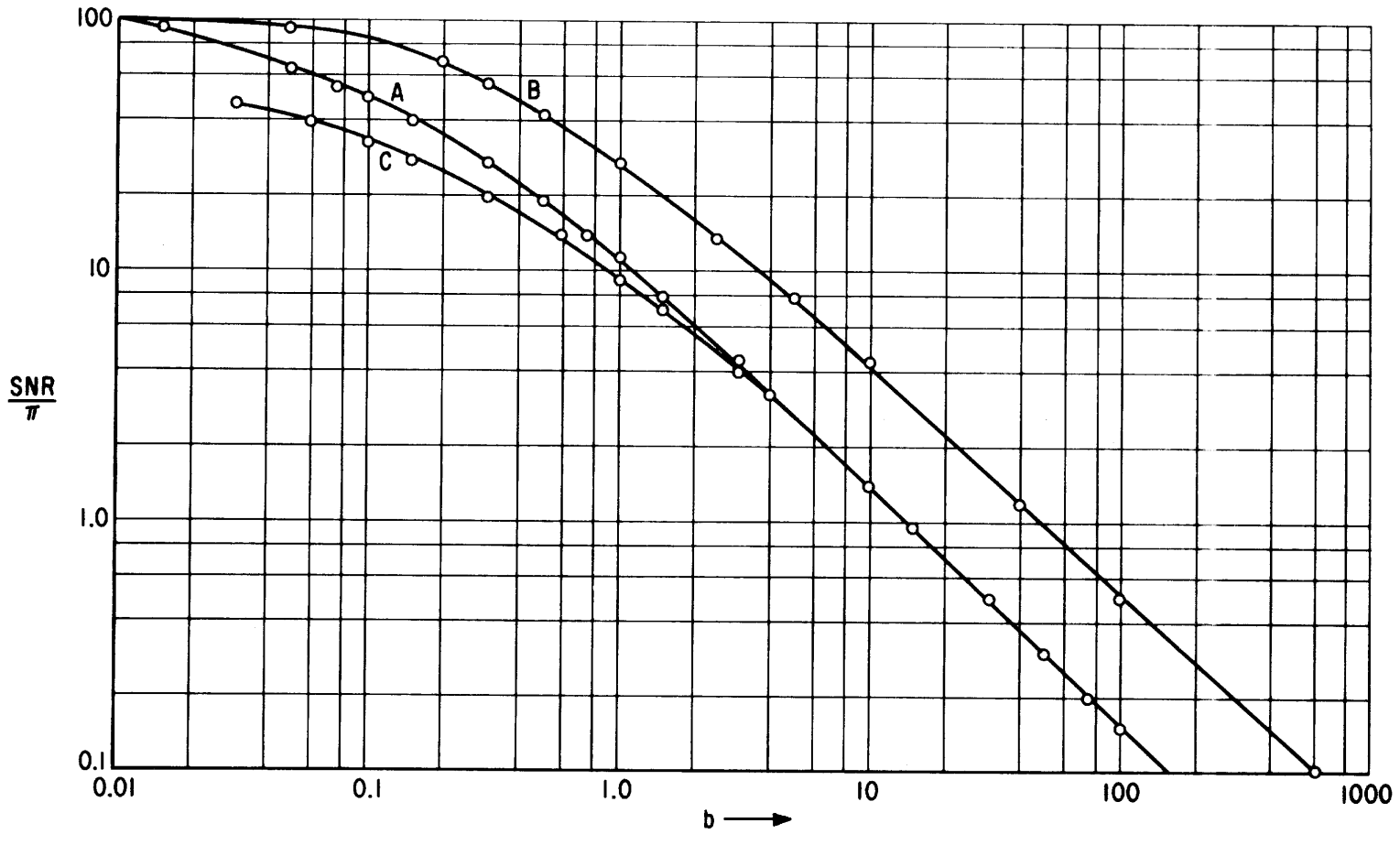

A-6-8

FIGURE 2.1

represents large signals. We are interested in the behavior of the SNR for large values of b, corresponding to small signals.

Suppose we require a SNR of + 3db for adequate detection of the signals. From curve A we see that b must be less than or equal to approximately 23 for the given values of the parameters. This value of b gives a lower limit to the signal size (to the half value points) of 0.35 mm.

The number of parameters is too large to give a comprehensive family of curves of SNR. We will, however, plot two other curves to get some idea of how a change in these parameters changes the SNR. First, suppose $\frac{n_o^2 + n_1^2}{n_1^2}$ increases, i.e. we have a film with less grain noise. In curve B of Figure 2.1, we have $n_o^2 = 0.297$, $n_1^2 = 0.003$, $a = 0.1$ and $c_2^2 = 0.30$. The overall effect is to move the curve to the right of the first curve without affecting its shape. As we would expect, the maximum value of b increases for a given SNR which shows that the image size can be smaller when fine grain films are used. The opposite effect will be experienced for coarse grain films.

Next we observe the effect of the change of the parameter a i.e. a different form of the macroscopic noise. In curve C of Figure 2.1 we have $n_o^2 = 0.29$, $n_1^2 = 0.01$, $c_2^2 = 0.30$ and $a = 1/7$ i.e. the same parameters as for curve A except that we have increased the parameter a. The curve for the SNR is not affected for large values of b (the film grain noise is predominant here), but is somewhat lower for small values of b. This denotes reduced detectability of large signals. This could be anticipated because less signal energy is received in the output plane. Also, the opposite effect is expected for a decrease in the value of the parameter a.

3. Summary and Conclusion

In summary, we have attempted to find the minimum signal size that can be detected when one considers film grain noise as the limiting factor. In order to make an analytical treatment of the problem it is necessary to make some approximations and assumptions with respect to the nature of the noise process. Although the film noise is generally thought of as a multiplicative process, it can be approximated by an additive process if the signals to be detected are nearly uniformly illuminated. Under these conditions an equation was derived for the signal-to-noise ratio. In using this equation it is first necessary to determine the value of the average microscopic noise power n_o^2 and the value of the parameter a that controls its shape. These two parameters are not affected, in general, by the particular film used. It is then necessary to determine the value of n_1^2 for the particular film used. The value of n_1^2 is not independent of the signal amplitude, but it varies in accordance with a curve similar to that shown in Figure 3.1. Thus, given a value of c_2^2, one can determine the proper value of n_1^2 for the type of film to be used. Equation (2.17) can then be plotted as a function of the signal size as reflected in the parameter b.

In spite of the assumptions that were made, equation (2.17) exhibits all the properties that one would expect from such a noise process and no unusual results are in evidence.

25X1

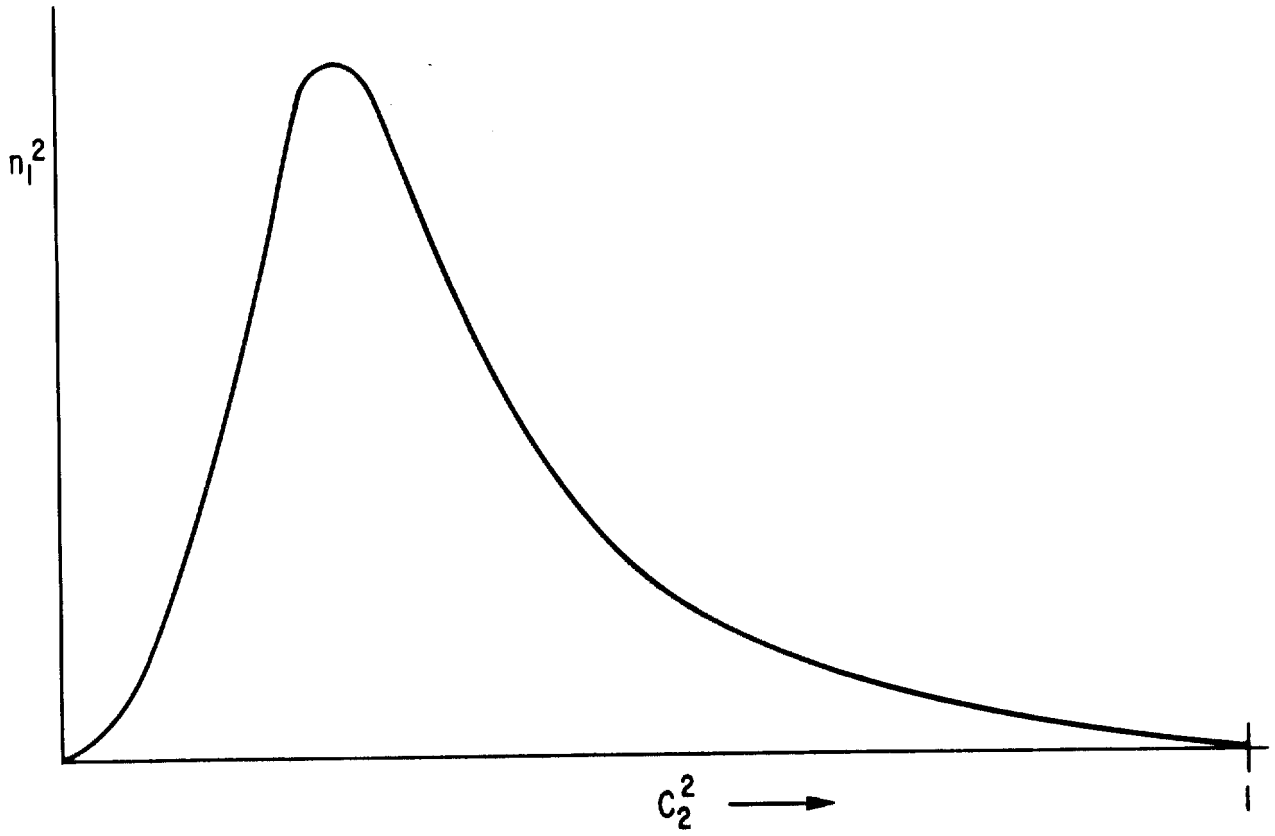

FIGURE 3.1

Section A

Conclusions

1. There should be no difficulty in obtaining the necessary information content in the spatial filter. The highest resolution requirement is that of the carrier frequency which is the interference fringe pattern produced in the two-beam filter. This usually amounts to 125 to 250 lines per millimeter which can easily be recorded on any of several fine-grained emulsions.

2. The optical requirements of the processing device involve no impossible conditions. The necessary optical quality is easily obtained and results in a modulation transfer function that appears adequate for any purpose that can be envisioned at present.

3. Phase-modulating material such as [redacted] Photoplastic film can be used to make spatial filters which perform in a manner very similar to amplitude-modulating silver photographic filters. Mathematically, the two are interchangeable. 25X1

4. To calculate the theoretical signal-to-noise ratio it is necessary to assume a grain size for the film and a noise level due to extraneous objects. Making reasonable assumptions for aerial film the conclusion is that a signal-to-noise ratio of 15 db should be obtainable. Translated into optical terms this is adequate for automatic detection and agrees with experimental findings.

5. It has been shown that the upper limit of detail in the photograph which the process can handle is 2000 lines per millimeter. At present there are few lenses or emulsions in common use which will realize as much as 200 lines per millimeter in the finished photograph, therefore the principle is adequate for a purpose considered in this report.

6. The minimum size of detectable objects in an aerial photograph is about .3 mm or .012 inch. This calculation was based on assumptions for typical grain size and

noise. For fine-grained film the minimum size would be less, and for noise-free subjects such microfilmed printed copy the minimum size is much less.

7. The general conclusion we have drawn from this theoretical study is that the process is capable of much more than is needed at present, the real problems are materials and techniques.

Section B-Equipment

The purpose of these tests was to settle several equipment design and material problems which appeared serious in 1964. These covered such questions as the effects of irregular glass or plastic emulsion support on the optical system and the relative merits of glass and film spatial filters.

The individual tasks were:

B-1 The Effect of Poor Quality Glass Plates in a Recognition System.

B-2 The Effect of Aberrations due to Glass Plates in a Recognition System.

B-3 Effect of Vibration on the 20-Foot Optical Bench.

B-4 Means for Attenuating the Reference Beam.

B-5 A New Means for Attenuating or Intensifying the Reference Beam.

B-6 Relative Merits of Glass and Film for Spatial Filters.

B-7 Use of Liquid Gates.

B-8 Test of S.O. 243 Film for Spatial Filters.

Effect of Poor Quality Glass Plates in Recognition System

Definition

Poor quality in a flat glass plate is defined as any factor that may cause the plate to show wavefront deformations in a beam of light. These may be surface - quality defects such as lack of flatness of the faces resulting in variations in thickness of the glass, and hence variations in phase retardation of a coherent plane wave or they may be material quality defects such as variation in refractive index. In thin glass plates the surface defects predominate.

Statement of the Problem

Glass plates can be introduced in the "perfect" system of the recognition apparatus in the following ways:

1. Use of a glass plate transparency as an object to make the spatial filter.

2. Use of a glass plate transparency of the objects to be recognized.

3. Use of a spatial filter on a glass plate.

1. Glass plate transparency of an object. In general, the objects from which the filters are made are small. The quality of most plates will not vary much over this small area so that this is rarely a problem. If severe, the effect will produce a poor spatial filter. If the object is a simple one resulting in well defined diffraction spectra, microscope examination of such a filter will show distorted spectra. In the case of complex objects distortion is difficult to recognize.

So far, in our experience we have had only one object on a glass support which had defects serious enough to cause trouble. This piece of glass was unusually bad and should not have passed inspection as photographic plate material. The condition of the surfaces is difficult to describe except that they were "rough", a condition rarely seen in fire-polished, rolled or polished glass. It appears that 99 percent of any sort of glass photographic plates will be adequate for objects up to 10 mm size.

2. Glass plate transparency of objects to be recognized. There is considerable variation in the surface-quality of the glass in any box of ordinary plates. These plates are made of "rolled" glass which tends to have a wavy surface in the direction of rolling and these waves produce astigmatism. The plates may also be wavy crosswise and these two effects can combine to produce:

a. Areas in which the surface results from two crossed cylinders. If both cylinders have the same sign the surface is approximately spherical.

b. Areas in which the surface results from two crossed cylinders of different sign. This produces a lens positive in one meridian and negative in the other and is known as "saddle-shaped" astigmatism.

c. Areas in which the crossed cylinders are skewed and random in sign. This is known as an "irregular" surface.

When an appreciable amount of any of these aberrations is added to the diffracted beam the diffraction spots will not fall on the proper areas of the spatial filter and poor recognition will result. In small transparencies, 1 inch square and less, the defects due to using commercial plates appear negligible, except in the case of an unusually bad piece of glass. For 4 by 5 inch transparencies the defect in commercial plates seriously degrade the recognition. This case was examined in detail and is reported under experimental tests.

3. Use of spatial filter on a glass plate. The equipment we have used produces a spatial filter not over 26 mm in diameter with most of the information in an area about 5 mm in diameter. It appears that the small area allows the use of commercial plates or film with good results.

Scope of the Investigation

In experimental work such as described in this report it is convenient to use glass photographic plates for transparencies. Glass is usually a more uniform substrate than film, glass plates are generally coated more uniformly, they do not show linear coating effects usually detectable in film and glass plates do not curl or shrink due to processing or storage.

The purpose of this tests was to determine if the commercially available glass photographic plates were satisfactory in the recognition system. These plates are coated on selected rolled glass and can be expected to show the same optical defects as window glass. If possible, it would be desirable to use them because they are easily available in many types, low in cost and fairly easily cut to smaller sizes once the user has mastered the art of cutting glass in total darkness. The two alternatives were the use of microflat plates which are expensive, difficult to obtain and hard to cut, or the use of liquid gates to compensate for irregularities in the substrate.

Original Plan of Experiments

It is fairly clear that when wavefront deformations take place in the transparency to be searched that some of the diffracred rays will be deviated from their normal paths and will no longer fall on corresponding points of the spatial filter. The result will be twofold, a loss of signal strength and a gain in noise or leakage. The total result will be a reduced s/n ratio and poor recognition. The original plan was to select a typical simulated aerial photograph on a plate known to be nearly perfect, then using a spatial filter for one of the objects to produce a recognition spot. The intensity of the spot and its surroundings would then give the s/n of a "perfect" plate. Then additional clear glass plates containing known and measured defects would be added one at a time and the s/n measured for each case.

Several tests were made in this manner and useful results obtained, but two practical difficulties made the work slow. Most of the plates contained appreciable wedge angle which deviated the zero order and required repositioning the spatial filter to compensate. It was difficult to align the filter with the badly aberrated image produced by the worst plates. The increase in the "noise" component appeared in all sorts of unexpected places due to the random location of local defects in the plates. This made it necessary to search the entire picture area for increases in background leakage. It was decided to postpone this part of the test until the T.V. readout system was in use as this would largely automate the measurement of s/n ratios. In the meantime a simpler test was used which appeared reliable and correlated well with the measurements already made.

Revised Plan of Experiments

In the last paragraph the defects in the glass plate were found to deviate the rays diffracted by the transparency resulting in a loss of signal and a gain in noise. It had already been calculated that any deviations greater than half the diameter of the diffraction disc size would be detrimental. The diffraction disc of the basic system is determined by the entrance aperture, the aperture ratio of the collimator lenses, their quality and alignment. It is about 20 microns in either of our instruments. If clear glass plates were placed in the beam of the instrument their defects would increase the size of the diffraction image and this could be measured. Assuming the aberrated image to be uniform in intensity by neglecting "streamers", it should be possible to estimate the area covered by this image and the resulting attenuation of the signal. This tests tells nothing about the "noise" component except that it increases. It does not seem practical to calculate the noise increase, but since this is spread over a large area of the picture it is of relatively less importance than the loss of signal in determining s/n ratio.

Source of Glass Plates

Forty 4 by 5 inch glass plates, most of which had been used as transparencies were selected. These plates were graded as to whether it had been possible to obtain good, poor or no recognition from them in previous tests. The emulsion was dissolved and the plates carefully cleaned by a procedure designed to prevent etching or scratching the glass. All of the plates were then tested in an interferometer adjusted to produce a single fringe. If the plate were perfect the view would remain a single fringe. Most of the plates contained appreciable wedge angle which required readjusting the interferometer to the single fringe condition. If the plate contained defects the distortion of the wavefront was shown by the number and pattern of the fringes. This was recorded. The two sets of results; the performance of the plate as a transparency and the test

of the glass support agreed in almost every case, acting as a double check on the glass quality. The results fell into three categories, important for the present purpose:

1. Transparencies which had shown good recognition all showed minor wavefront deformations, usually less than one wavelength and this "regular" meaning cylindrical or spherical.

2. Transparencies which had shown poor recognition showed one to two and a half wavelengths of deformation, usually regular, or up to one wavelength of irregular deformation.

3. Transparencies which had shown no recognition showed more than three wavelengths of wavefront deformation.

Numerical Results

In the following Table the first column gives the wavefront deformation measured in the interferometer. The second column gives the area of the aberrated diffraction disc produced by this plate compared to the normal disc area. On the basis of simple theory and the assumption of uniform illumination, the intensity of the recognition spot should vary inversely with this area. Actually the aberrated image is most intense at its center so that the recognition signal does not decrease this rapidly. The column "Measured Signal" gives the results of the original plan of the experiment described earlier. The values are arbitrary based on the intensity of the unaberrated signal as 100 units. The column "Measured Noise" is also the result of the originally planned experiment and gives arbitrary values, not related to the signal values, but based on the intensity of the unaberrated noise as 1.

Measured Wavefront Deformation	Type of Deformation	Relative Area Image	Relative Intensity Recognition Signal	Relative Noise
None	-	1	100	1
1/8	Regular	1	100	1
1/4	Regular	1	100	1
1/2	Regular	1	100	1
1	Regular	4	60	2
1 1/2	Cylindrical	7	40	3
2 1/2	Cylindrical	14	10	4
2 1/2	Irregular	20	5	5
4	Astigmatic	32	-	-
3 1/2	Astigmatic	15	-	-
3/4	Cylindrical	6	-	-
2 1/2	Astigmatic	11	-	-
2 1/2	Irregular	14	-	-
5	Regular	32	-	-
3/4	Cylindrical	8	-	-
1 1/2	Irregular	24	-	-
3/4	Irregular	10	-	-

Conclusions

1. The glass on which commercial photographic plates is coated contains surface irregularities which result in wavefront deformations in the recognition process which can reduce the s/n ratio of the signal.

2. For very small systems where the area of the plate is not over one square inch, most plates will be satisfactory. For larger systems, specifically 4 by 5 inch, these plates will in general not be satisfactory.

3. Microflat glass which usually shows less than half a wavelength of deformation is satisfactory.

4. If 4 by 5 inch commercial plates or film are used, then a liquid gate may be necessary.

Approved For Release 2005/05/02 : CIA-RDP78B04770A002300020010-5

Section B-2

The Effect of Aberrations Due to Glass Plates in a Recognition System

Introduction

The apparatus used to make the two-beam spatial filter and the recognition system both employ high quality lenses to obtain small well-defined diffraction images of the point source.

The size of the pinhole used is nominally .001 inch or 25μ, but the size of the Airy disc of the image as measured by a microscope (10X objective and 10X eyepiece) was measured as being 20μ, showing that the two lenses are quite good.

However, the spatial filters we plan to use consist of emulsion deposited on a transparent base of a certain thickness, and we may use liquid filled cells up to an inch thick. Such a thick plate, placed in a convergent beam of light, increases the size of the image, because rays passing through it at greater angles to the axis come to a focus at a point on the axis farther from the lens than the focus of rays passing through the cell at smaller angles. Thus the addition of a thick plate in the converging case of rays causes rays from successively greater zones in the converging cone to come to a focus at points distributed along the axis, instead of all coming to a common focus. The envelope of such a cone of light comes to a minimum diameter W and then increases. The object of this work was:

(a) to calculate the position, along the axis, of the focus of rays of various inclination, and

(b) calculate or estimate the enlargement W of the focus spot due to this, and

(c) set up an experiment on the six-foot optical bench to check the calculations.

Derivation of Equations

Figure 1 shows a ray of light, part of a converging cone, passing through a flat plate of thickness t and index of refraction Ng and, because of displacement in the plate, coming to a focus at e, instead of the original focus C. The displacement d along the axis I is the distance between C and e. Distance j is the distance from the plate to C, but as j doesn't appear in the equation derived below, its value doesn't affect d.

From Figure 1, equation 1 can be derived: (see page 5)

$$d = t\left(1 - \frac{\cos i}{Ng \cos r}\right) \text{ ----------(1)}$$

in which the value of r can be computed from Snell's law, viz:

$$\sin r = (Na/Ng) \sin i \text{ ----------(2)}$$

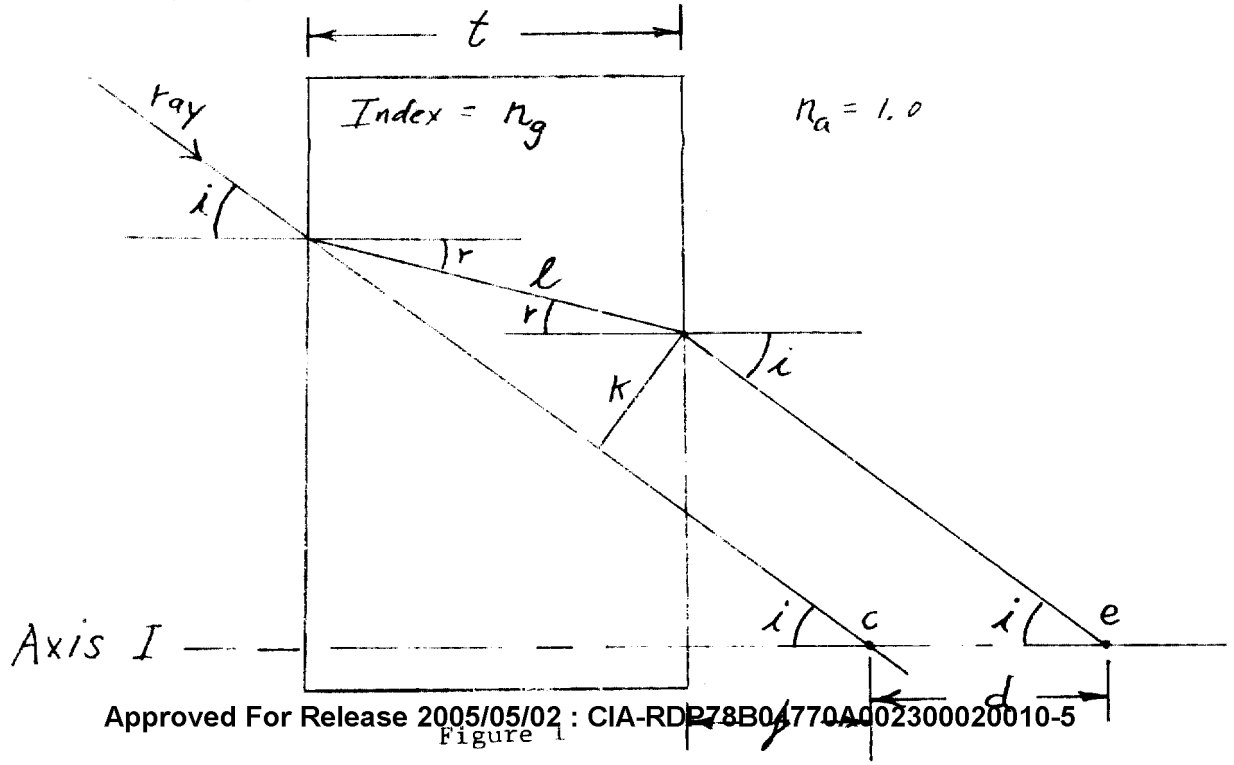

Figure 1

Calculations

These tests were made on the small system, not the 20-foot system. The small system has more nearly perfect lenses and operates at a higher aperture ratio so the effects should be more easily seen. In this instrument the convergent cone of light was 26 mm diameter at lens L-2, and converged 350 mm away. To select values for i, the lens was divided into three zones of equal area and the three radii used to establish three values for i. Equations 1 and 2 were used to calculate 3 corresponding values for d as shown in Table 1, where other values assumed were:

$t = 24$ mm
$Ng = 1.51$
$Na = 1.00$

Table 1

Case	Angle i	d
1	2° 8'	8,112.1 microns
2	1° 44'	8,110.0 microns
3	1° 14'	8,108.0 microns

Results of calculations tabulated in Table 1.

(a) The distance along the axis between the three foci of these three sets of rays is only 2 microns.

(b) A further calculation of W, the enlargement of the focus spot, showed W = 0.12 micron.

Such an enlargement is too small to measure, the chief purpose to be served by an experiment was to look for an observable enlargement, which would check on the calculations.

Experimental Setup

The six-foot optical bench was brought into the best possible adjustment, with the laser beam passing through the pinhole purifier, through a collimating lens L-1, through converging lens L-2, through an observing microscope having three translational motions (from the Gaertner lens testing bench) and fitted with a 10X objective and 10X eyepiece, and then through a neutral density filter and into the observer's eye.

The thick plate, placed between L-2 and the microscope, was a high quality glass cell filled with Decalin, a liquid with an index of refraction 1.51 matching that of the glass in the cell. The cell was 24 mm thick.

Results of Experiment

The value of d was measured as 7.68 mm (instead of 8.11 as calculated in Table 1). The probable cause of this discrepancy is that the value of Ng is not precisely known.

The image of the pinhole, in a well adjusted system, consists of central disc (Airy disc) plus concentric diffraction rings. Some 83% of the energy lies in the Airy disc, and its diameter is what was measured.

With cell omitted, disc diameter = 20μ.

With filled cell in place, disc diameter = 16 to 18μ.

This indicates that the aberrations added by the cell have a sign opposite to residual aberration in the lenses; unless the apparent reduction in disc size is due to inaccurate measurement.

Experimental Setup

The six-foot optical bench was brought into the best possible adjustment, with the laser beam passing through the pinhole purifier, through a collimating lens L-1, through converging lens L-2, through an observing microscope having three translational motions (from the Gaertner lens testing bench) and fitted with a 10X objective and 10X eyepiece, and then through a neutral density filter and into the observer's eye.

The thick plate, placed between L-2 and the microscope, was a high quality glass cell filled with Decalin, a liquid with an index of refraction 1.51 matching that of the glass in the cell. The cell was 24mm thick.

Results of Experiment

The value of d was measured as 7.68mm (instead of 8.11 as calculated in Table 1.) The probable cause of this discrepancy is that the value of Ng is not precisely known.

The image of the pinhole, in a well adjusted system, consists of central disc (Airy disc) plus concentric diffraction rings. Some 83% of the energy lies in the Airy disc, and its diameter is what was measured.

With cell omitted, disc diameter = 20μ.

With filled cell in place, disc diameter = 16 to 18μ.

This indicates that the aberrations added by the cell have a sign opposite to residual aberration in the lenses; unless the apparent reduction in disc size is due to inaccurate measurement.

Appendix

Derivation of Equation 1

From Fig. 1 $k = l \sin (i-r)$

Expanding $k = l \sin i \cos r - l \cos i \sin r$

But $l = t/\cos r$

$$k = t \sin i - \frac{t \sin r \cos i}{\cos r}$$

By Snell's Law, if Na = 1 $\sin r = (\sin i)/Ng$

So $$k = t \sin i - \frac{t \sin i \cos i}{Ng \cos r}$$

$$k = t \sin i \left(1 - \frac{\cos i}{Ng \cos r}\right)$$

By Fig. 1 $k = d \sin i$

So $$d = t \left(1 - \frac{\cos i}{Ng \cos r}\right) \quad \text{---------- (1)}$$

VIBRATION ANALYSIS OF 20-FOOT OPTICAL BENCH

The vibration characteristics of the 20-foot optical bench were investigated by applying a variable frequency vibration force to the frame and observing the resultant vibration motion. The frequency of the input force was slowly increase and these frequencies recorded at which maximums in the vibration amplitude were noted. In this manner the resonant or critical frequencies up to 10 kilocycles per second were determined.

By holding the frequency constant at each of these resonant frequencies the vibration amplitude distribution throughout the bench was determined. The resonant frequencies and a sketch of this vibration amplitude distribution is shown in Figure 1.

When the effect of the various vibration modes on the operation of the optical system was studied it was found that only one at 45 cps was important. This is the first, or lowest frequency mode, and consequently the one with the largest displacement for the same energy input, of the modes that result in a distortion of the optical axis from bending stresses in the bench.

It was observed that, at 45 cps, if the center of the bench vibrated over .0004" peak to peak then the loss of light in the optical system was noticeable. Since there is a resonant amplification of 20, the maximum acceptable floor vibration at 45 cps without isolation is approximately 20 microinches peak to peak. However, with the vibration isolators between the bench and the floor the maximum floor vibration could be .001" (0.1g acceleration) peak to peak before the effects of the vibration were noticeable.

VIBRATION CHARACTERISTICS OF 20 FT. OPTICAL BENCH

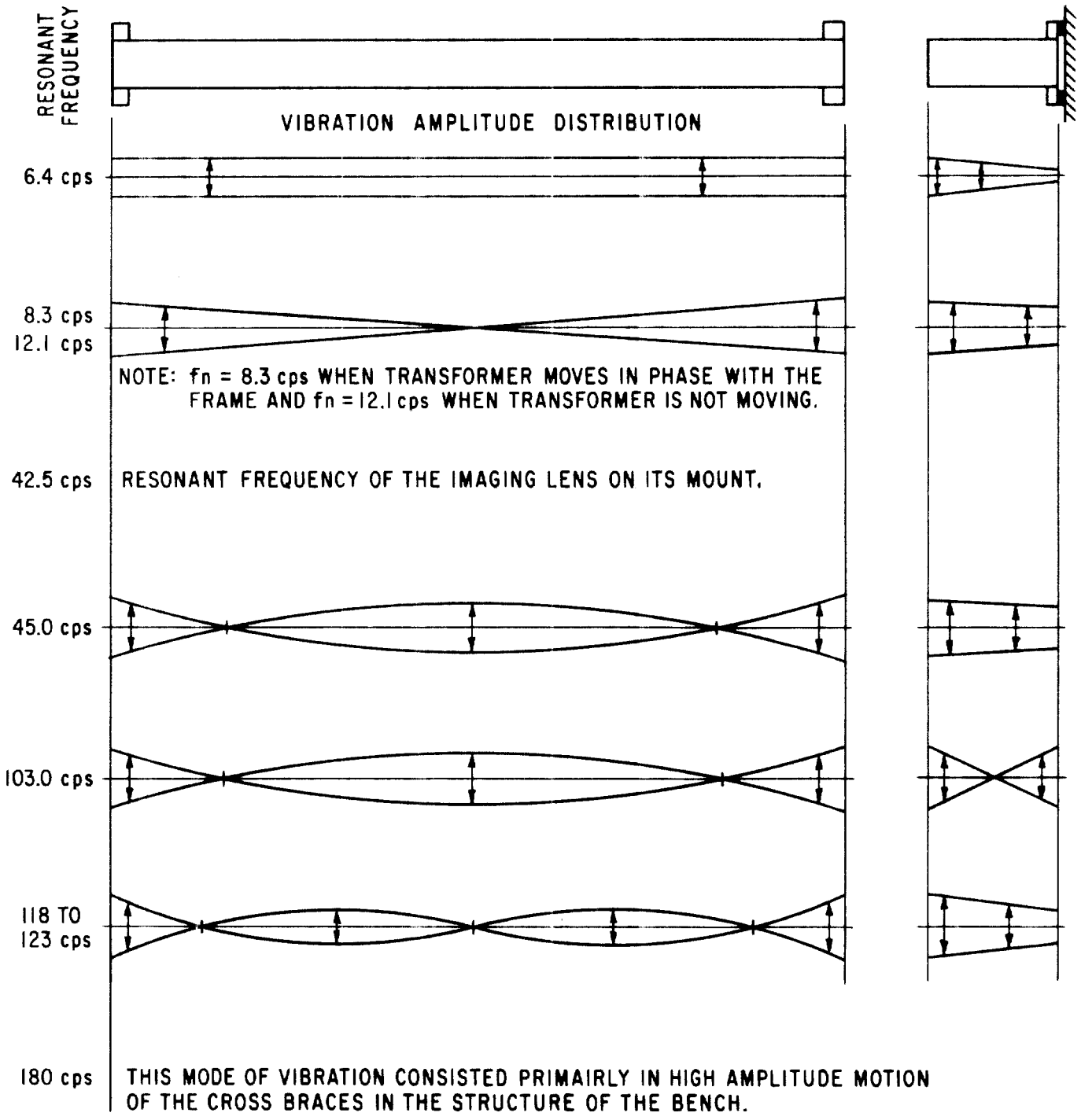

FIGURE 1

25X1

Note to [redacted] Report

During this testing program it was found that the only two parts that vibrated independently of the bench were the imaging lens mount and the "noise eliminator". Both of these parts were poorly supported. The imaging lens was on the end of a thin rod and the noise eliminator was cantilevered from the end of the laser on a rather insecure frame. Both of these parts were rebuilt in accord with the general solid construction of the lens mounts and no further vibration was noticed.

In general, the construction appeared insensitive to even very severe vibration, the equipment continued to operate as a recognition system all during the vibration tests and afterwards with no change of adjustment. So far as we can see, vibration is not a problem with the type of construction used.

Beam Attenuation Methods

Introduction

The apparatus required to make a two-beam spatial filter (Figure 14 of Reference 1) includes an attenuator to reduce the intensity of one of the light beams. This investigation concerns a search for the best material to use for this attenuator.

Desirable features of such an attenuator should include:

(a) the beam of light transmitted should be reduced in intensity but otherwise unchanged. That is, aberrations or scattering should be absent, or as small as possible.

(b) attenuation should be continuously variable, although for some applications, small steps would be equally useful.

Other features, such as cost, weight, size, reliability, life expectancy and maintainability depend too much on the specific application to be given much consideration here.

Attenuators Investigated

(a) thin Wratten neutral density gelatin filters mounted in cardboard holders without glass. ND=1.00.

25X1

(b) small (2 x 2 cm) Wratten neutral density filters, factory mounted in glass. ND=0.3.

(c) Bausch & Lomb N.D. filters (2" x 2") made by evaporating metal on glass. ND=0.30.

(d) continuous neutral wedge on 6" diameter circular glass plate, 5/16-inch thick. This was made by Eastman Kodak and cost $600.

(e) Polaroid type HN 38, plastic sheet 12" x 12" x .032". Sheet was unsupported and rather curled.

(f) Polaroid type HN 32, stiff plastic sheet. (Surplus pieces selected for use with 3-D Color TV Display System.)

(g) Kodak Polaroid filter for cameras, called Polascreen. Here the Polaroid is mounted between high quality glass plates.

Method of Investigation

The apparatus on our six-foot optical bench was set up as used for a 2-beam recognition system (Figure 15 of Reference 1). The imaging lens, the object and the spatial filter were removed, and an observing microscope having three translational motions (from the Gaertner lens testing bench) was set to look at the source image located in the plane where the spatial filter was. Various attenuators were placed in the beam, both at the image plane and nearer the converging lens. Observations were made at maximum effective magnification, 100X.

The method used to decide whether an attenuator would be satisfactory was to observe changes in the size and shape of the 20 micron diameter airy disc of the source image. These results are somewhat subjective, in that the degree of goodness or badness of the image could not be given on a scale of numbers, but judgements had to be made as to the general crispness and detail in the image and how these changed as the attenuators were moved in and out of the light beam. Each time an attenuator was moved in or out of the beam it was necessary to refocus the microscope to get the picture as sharp as possible, and this added somewhat to the difficulty of making comparisons. When a polarizer is used as an attenuator in the apparatus used to make a 2-beam spatial filter (Figure 14 of Reference 1), the system will be degraded unless two polarizers are used, with the second one (the one farther from the laser) permanently rotated around the optic axis so that its plane of polarization is parallel to the laser's plane of polarization. The reason for this is because:

(a) when several of plane polarizers (such as Polaroid sheets) are placed in series in a beam of light, the plane of polarization of the light transmitted through all of them will be parallel to the plane of polarization of the last polarizer.

(b) for the 2-beam spatial filter to be effective in doing its job it must contain many fine interference fringes created by the interaction of the upper and lower beams. The higher the contrast in this fringe pattern the more effective the filter will be. In order for two beams of light to interfere to form fringes their planes of polarization must be parallel, and as they are made increasingly non-parallel, the contrast between light and dark fringes decreases.

(c) Therefore, for maximum fringe contrast, as in (b), the plane of polarization of both beams must be kept parallel and the 2nd polarizer must, because of (a) be fixed, and the 1st polarizer rotated to cause variable attenuation of the beam.

In cases reported below a single polarizer was used (turned so its plane of polarization has approximately parallel with that of the laser beam) but in an actual attenuator two polarizers would have to be used with consequent doubling of the scattering or aberration of a single one. Therefore, in case h two polaroids were used. (In cases e, f, & g this was not done as only a single polarizer of each type was available).

Results of Experiments

All of the attenuators operated satisfactorily when placed at the focal point of the second lens, or within a few millimeters of the focal point. However, if a dust speck should happen to fall on the surface of an attenuator so located, the amount of light scattered from it would be large and hence such a location might not be a good one.

As an attenuator was moved from the focal point to positions nearer the focusing lens where the beam cross section was larger, the performance fell off in many cases. This is to be expected if an attenuator does not have sides that are flat, because lack of flatness will deviate a ray as it passes through, and the deviation will vary from one point to another. If the rays pass through a small area of the attenuator the deviation will be more nearly the same for all the rays than if they pass through a large area.

The results of the tests are tabulated below:

Material	Small Area of Beam	Large Area of Beam	Remarks
(a) Gelatin	Good	Good	Beam cross section can be any size with only slight image deterioratio noted. Max. beam size about 20mm.
(b) Small Wratten in glass	Good	Bad	
(c) B & L 2" x 2" glass	Good	Bad	
(d) EK Circular Wedge	Good	Good	Image deteriorates noticably only when beam cross section is 16 mm diameter or 640,000 X area when at focus.
(e) Polaroid Plastic Sheet Type HN 38	Good	Bad	Sheet poorly supported and rather curled. Might be OK if flat.
(f) Polaroid Stiff Plastic Sheet HN 32	Good	Bad	Beam diameter 2 mm when image deteriorated.
(g) Kodak Polascreen - Polaroid between high quality glass plates	Good	Good	Quite good at all beam diameters. Only had one Polaroid so couldn't test when crossed. Next item indicates 2 would be OK crossed.
(h) 2 Sheets HN 32	Good	Less Good	When beam diameter was 3 mm Airy disc was a 20 x 25 microns ellipse. When 1st sheet was rotated 90^{o} image got very dim but no change in image quality was noted.

Conclusion

Satisfactory attenuators would include:

1. A series of gelatin filters (item a).

2. A circular wedge (item d).

3. Two crossed polarizers - if mounted in flat glass plates (item g).

Section B-5

A New Means for Attenuating or Intensifying the Reference Beam

Introduction

In making spatial filters it is usually necessary to attenuate the reference beam to obtain optimum interference in the desired diffraction order. We have made a study of the conventional means such as neutral density filters and crossed polarizers. There are also times when it would be desirable to attenuate the sample beam, but this is not recommended because it is practically impossible to obtain an attenuator that will not introduce undesirable phase variations. The only recommendation has been that the apparatus should be designed so that this never happens or we should avoid large area objects which are likely to cause this situation. Needless to say, these recommendations are not entirely practical.

Possible Alternative Attenuators

1. Iris on the Rayleigh Lens. An iris placed on the Rayleigh or reference beam lens would allow control of the amount of light in the reference beam and act as an attenuator, but it also changes the diffraction pattern of the point focus. This point focus later becomes the recognition "spot", and hence changing this aperture would alter the size and structure of the recognition image. Since it is normal to attenuate the reference beam as much as 1:1000, the f value of the Rayleigh lens would become about f 2000 and the central disk of the focus and later the recognition spot would become large and diffuse. This solution appears impractical.

2. Vary Focal Length of the Rayleigh Lens. When the focal length of this lens is changed the reference beam at the filter plane becomes larger or smaller in diameter and hence its energy per unit area varies. This has some of the same difficulty as (1) above. The aperture remains constant but the f value will decrease with long focal lengths. This is not nearly so severe as in (1) and is a minor

objection. The major problem is finding a set of a dozen or more diffraction limited lenses, each three-inch aperture with the required focal lenghs. Even if the lenses were available, their use would be a considerable problem. Each time the focal length of the Rayleigh lens was changed the position of the object would have to be changed because the object and this focus must be in the same plane. In the "overlapping" system which we use in the object is not in collimated light this would change the object magnification and require a whole set of changes in the setup. This solution also appears impractical.

3. Add a Weak Lens Beyond Focus. If a weak simple lens such as a spectacle lens, is placed in the reference beam after the point focus it changes the diameter of the beam at the filter plane. The light intensity varies as the square of the diameter of the beam so that relatively weak lenses provide all the control required. Since the beam is small in cross section close to the focus, only a small portion of the lens is used and low-quality lenses are satisfactory. When negative lenses are used they spread the beam and act as attenuators, positive lenses compress the beam and increase the intensity of the reference beam which is better than attenuating the sample beam in terms of exposure.

In a test, this means of attenuating the reference beam or increasing its intensity appeared completely practical using a set of ordinary long focal length single element lenses.

In the case where the sample beam had to be attenuated by a filter (a practice that is not recommended) the exposure for a spatial filter was 4 minutes. Using the same equipment, but increasing the intensity of the reference beam by the auxiliary lens produced a better result with an exposure of 24 seconds.

Conclusion

The use of an auxiliary positive or negative lens in the reference beam can be used to attenuate its intensity or increase its intensity as required. This is the first practical means we have found to increase the intensity of the reference beam.

Section B-6

Use of Glass or Film to Make Spatial Filters

Introduction

All the spatial filters mentioned in this or previous reports from this laboratory were made on Eastman Kodak Spectroscopic Film type 649-F, 35 mm size. So far as known we are the only laboratory using this material and most others do not know it exists. The advantages of film are easy loading in a 35 mm camera, easy processing, easy identification of individual exposures.

We have been criticized for not using glass plates as others do. The disadvantages of plates are that it is impossible to buy them in the proper size, so they must be cut in the dark. Unless done with great care the emulsion surface can be damaged. Because cut plates vary in size and thickness they are difficult to hold during exposure. We have found it much more difficult to design a device to check the focus on these variable thickness plates than film.

Experimental Procedure

Spatial filters were made of the same object on both spectroscopic film, plates 0.40 inch thick and microflat plates .25 inches thick.

The exposure time to obtain the same density in the image was different for each material. This is normal in these special order emulsions. The emulsion on film has always been slower by a factor of 2 to 10 times than the same type emulsion on glass.

Examination of Images

Microscope examination of the images on the three substrates showed only one important difference. The images on plates showed ghost halation images due

to reflection from the back of the glass. Glass plates are not backed with anti-halation coating, though it is possible for the user to coat them himself. The film is backed with a very efficient coating which comes off between development and fixing.

Test of Filters

Three glass spatial filters and three corresponding film filters of the same object were compared to a photograph of ten similar objects. No difference could be detected between the performance of the two kinds of filters. The actual performance of two of the film filters was better in terms of signal strength, low noise and ability to reject similar targets, but this could be explained by slight differences in density. The remaining pair showed no difference.

Conclusion

It is impossible to hold spatial filters made on film perfectly flat. This appears to make little or no difference. Filters have been purposely bowed to a fairly short radius and they still operated. So long as the bowing does not cause appreciable foreshortening in one dimension or displace the filter from the plane of best focus, the effect seems negligible.

Filters made on film do not show reflections from the rear side of the substrate.

Glass filters appear to have no advantages for the present experiments.

Section B-7

Liquid Gate

Introduction

Most of the users of systems for optical processing of information in coherent light use liquid gates to hold their object transparencies. The reason usually given is that the liquid gate suppresses irregularities in the glass or film support or in the thickness of the emulsion coating. Other reasons we have seen in print are that liquid gates are useful to suppress the wedge angle of glass plates which would otherwise deviate the diffracted light beam from the spatial filter. Many thin glass plates also show appreciable lens power, either positive or negative so that it is necessary to adjust the position of the spatial filter axially to compensate for this change in focus. The liquid gate should remove this effect also.

Finally, we have seen the statement that liquid gates were useful to suppress the unwanted relief image of the transparency.

Not mentioned in any reports we have seen is the fact that a liquid gate should suppress the diffraction effects of scratches and defects on the surfaces of the emulsion and film support.

Liquid Gate Design

The gate used in these experiments was made with one fixed window and one adjustable so that the wedge angle could be reduced to practically zero. The windows were made from the best of several microflat glass plates and showed less than one-quarter wavelength phase distortion over the central two-inch area.

Attempts to use volatile solvents as immersion liquids were not successful. Evaporation at the surface resulted in cooling and convection currents so that the liquid-filled gate showed very bad optical astigmatism. This was due to a

convection pattern showing descending cooled liquid at the center and two rising columns of warmer liquid at the edges of the cell. The difference in temperature was not measured, but the result was about five wavelengths of phase distortion.

The only satisfactory liquid was mineral oil which is difficult to remove from the negatives.

Experiment

An aerial negative showing airplanes and a fair number of surface scratches was tested both in and out of a liquid gate filled with mineral oil. In several measurements there was no appreciable difference in either the signal level or the signal-to-noise ratio. Also, the surface scratches looked practically as bright when immersed as when in air.

This was an unexpected result; in all previous experiments immersion had suppressed the relief image and reduced the signal strength to about half its value in air.

Conclusion

In spite of the many advantages claimed for liquid gates, we have been able to obtain equally good results without them. In tests previously described in an earlier report, we also made spatial filters from objects in liquid gates and used spatial filters in liquid gates with no change in results.

Section B-8

Test of S.O. 243 Film for Spatial Filters

Introduction

This special order Eastman Kodak film was obtained in 35 mm size. This is described by the maker as "aerial film with ultra-fine grain and high acutance". The base is 5.25 mil triacetate without gelatin backing. This gray base does not provide the same high transparency as the base on which spectroscopic film is coated.

The sensitivity is panchromatic with extended red sensitivity. The spectral curve is practically smooth between 5500 and 6200 angstroms shows a dip at 6500 and a final peak at 7000 angstroms. The limit of sensitivity is about 7150 angstroms.

The RMS granularity in D-19 developer is rated at .016, in D-76 developer it is .013 for a density of 1.0

The resolving power for high contrast objects is as follows:

Developer	Resolution
D-19	465 1/mm
D-76	525 "

For low contrast subjects 1.6:1 the resolution is:

Developer	Resolution
D-19	205 1/mm
D-76	205 "

The ASA speed is rated at 1.6 which is 1000 times the rated speed of spectroscopic emulsion of .0015. However, we find little relation between the ASA rating and the effective exposure in laser light at 6328 A. For a particular spatial filter the optimum exposure on 649-F was 50 seconds, the optimum exposure on S.O. 243 was between .1 and .2 second depending on the development. This amounts to about 300 times the exposure speed.

It is possible to develop this film in D-19 for 5 minutes or D-76 for 8 minutes to obtain "normal" contrast. Both of these treatments appear to produce equivalent results. It is also possible to develop in D-76 for 2 minutes to obtain a very low contrast that requires doubling the exposure to obtain the same density and to reach the optimum diffraction efficiency. This treatment appears to improve the efficiency of the filters.

It would be desirable to have a fast film such as this available for spatial filters of poorly transmitting objects. For example, the exposure time on spectroscopic film for a 2 mm tank image is about 30 minutes. The only other fast film we have used is Kodak High Contrast Copy film which has an ASA speed of 32. For the spatial filter that required 50 seconds on 649-F and .15 seconds on S.O. 243, the correct exposure on HCC film was 1 second.

Experimental Work

The modulation efficiency of a spatial filter is the important property in determining the brightness of the recognition image. The optimum values we could obtain on the three emulsions were as follows:

Relative Modulation Efficiency

Emulsion	Development	Efficiency
649-F	D-19, 5 min.	100
S.O. 243	D-19, 5 min.	37
S.O. 243	D-76, 8 min.	50
S.O. 243	D-76, 2 min.	75
H.C.C.	D-19, 5 min.	50

These results indicate that S.O. 243 is faster than HCC film and with proper development can show a higher modulation efficiency.

Reconstructed Images

Some idea of the quality of a spatial filter can be gained from a microscope examination of the reconstructed image. For the subject tested, there was little

difference in the three films. The reconstructions from spectroscopic film were slightly more detailed and crisper with practically no difference between S.O. 243 and HCC film.

Graininess

When spatial filters of identical density were examined under the microscope the following results were obtained:

Apparent Graininess

Emulsion	Development	Graininess
649-F	D-19, 5 min.	Very low
S.O. 243	D-19, 5 min.	Low
S.O. 243	D-76, 8 min.	Same as above
S.O. 243	D-76, 2 min.	About same, different pattern
H.C.C.	D-19, 5 min.	Larger than above

It appears that the resolution cut-off due to graininess of spectroscopic film is 3 to 4 times as high as either SO 243 or HCC. The reported figures are as follows:

Resolution

Emulsion	Development	Resolution
649-F	D-19, 5 min.	+ 1000 1/mm (?)
S.O. 243	D-19, 5 min.	465 1/mm
S.O. 243	D-76, 8 min.	525 1/mm
HCC	D-19, 5 min.	360 1/mm

Relief Effects

Emulsion relief effects contribute to the efficiency of a spatial filter, but they are also believed to have undesirable phase effects. The noted relief effects were as follows:

Relief Effects

Emulsion	Development	Relief Image
649-F	D-19, 5 min.	Very low
S.O. 243	D-19, 5 min.	Higher with some roughness
S.O. 243	D-76, 8 min.	Still higher with more roughness
S.O. 243	D-76, 2 min.	Less relief, smoother
H.C.C.	D-19, 5 min.	Same relief as (2) above, rougher

It is impossible to decide whether high or low relief is desirable, but certainly roughness of the emulsion is undesirable since it contributes to scattering. S.O. 243 is superior to HCC in this respect.

Conclusions

S.O. 243 film can be used to make spatial filters. It does not show the extremely fine-grain and high modulation efficiency of spectroscopic emulsion and therefore does not make a filter as sharp or efficient. However, it requires an exposure only about one-three hundredth as long as would be useful for some objects. Proper processing will reduce the surface roughness and apparent graininess to acceptable values.

S.O. 243 appears to be superior to High Contrast Copy film in every respect including speed.

Section B

Conclusions

1. Poor quality glass plates in sizes 4 x 5 inches or larger can upset the operation of the system. At present this is no problem since we plan to work chiefly with film.

2. The spherical aberration introduced by glass plates or liquid gates is inconsequential in systems such as we have used.

3. Vibration effects can be avoided by proper design of the equipment.

4. Either of three methods can be used to attenuate the reference beam. The one favored is the use of unmounted gelatin filters.

5. By adding an auxilliary lens it is possible to either attenuate or intensify the reference beam.

6. The performance of spatial filters made on glass or film appears identical. Film is much easier to use.

7. Liquid gates have shown no advantages in experiments where they were used. We have obtained good recognition on aerial film with the film in air.

8. Emulsions other than slow spectroscopic 649-F can be used with comparable results and much shorter exposure time.

9. The general conclusion is that all of the equipment and materials problems considered appear to have simple solutions and are not limiting factors to the operation of the process.

Section C - Automation

It was established as early as 1963 that the spatial filtering process was capable of recognizing objects regardless of their complexity in photographs. Since that time a good deal has been learned about techniques and some data has been accumulated on what the process can and cannot do. It appears to have considerable potential, but it is of no economic value until it can be automated.

At the present time, using engineers to make the spatial filters, visually align the equipment and detect the recognition spots by eye it is far more expensive and time consuming to find an object in a photograph than a simple visual search using a magnifier.

If the system is ever to be used economically it must be automated to perform the search and recognition mechanically. There are many problems to the automation of a device this complex and in this study only a few critical items were considered.

Before these tests are described it is helpful to understand the present development of the manually operated equipment.

This section contains the following:

Section C-1

DESCRIPTION OF EQUIPMENT

Bench

The optical bench supporting the equipment used in these tests was designed and

25X1 built [redacted] and consists of two assemblies. One is a welded steel frame that acts as a rigid base, the other is a pair of accurate rails that form the locating surfaces for the bench carriages.

The frame was designed as a steel truss bridge 20-feet long, 4 1/2 feet high and 18 inches wide. It was made in two sections so that it could be transported on an elevator and bolted together on installation. It rests on four feet which are placed on vibration isolation pads. The frame is so rigid that no weight we would consider placing on it would deflect the frame as much as .001 inch. The mass of the frame is about 5000 pounds which effectively absorbs all vibration with frequencies above six cycles per second.

The rails are hardened and ground stainless steel rods 20-feet long supported in such a way that they can be straight even though the frame is not. Figure 1 shows an end view of the rails. They are fastened to 13 hardened and ground steel yokes which determine the spacing of the rails. One of these yokes is different (not shown) and is bolted directly to the frame. The other 12 yokes are supported on adjustable screws and also laterally adjusted by two other screws between angle plates. To facilitate initial adjustment, each yoke is held to the frame by a long bolt in the center which passes through a clearance hole in the frame and terminates in a coil spring and nut.

The rails were adjusted by autocollimating to a mirror placed on a carriage sliding on the rails. Vertical and lateral adjustment of the 12 sprung yokes was made until the rails were straight to at least .001 inch.

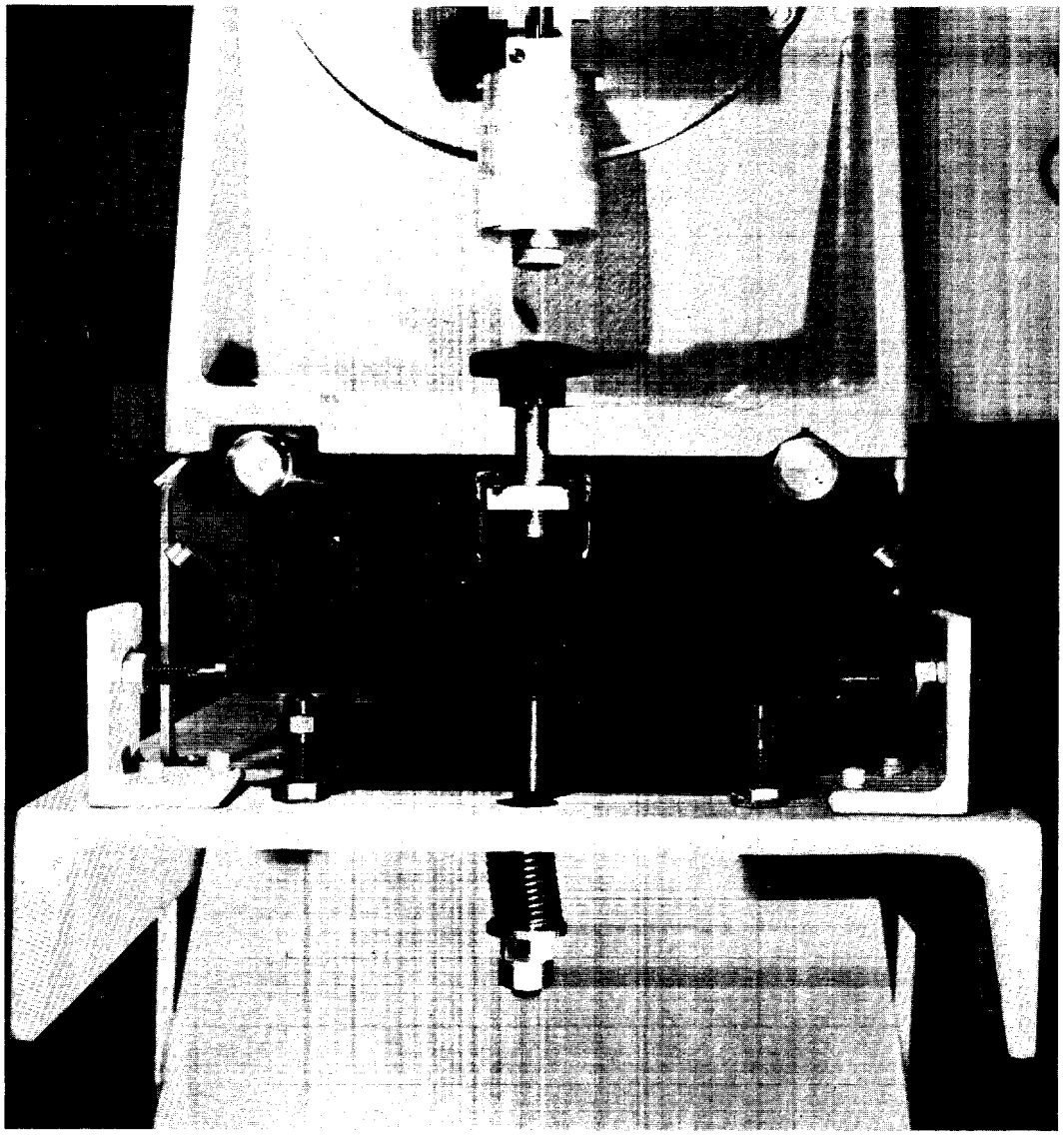

FIGURE 1 Clamping Arrangement

Between the rails and attached to the yokes in a commercial steel shape known as a "Unistrut". The carriages are clamped to the rails by a knurled-head screw which passes through the carriage and engages a special nut in the Unistrut. Large carriages have two clamps, small carriages have one.

Laser

The laser used in these experiments was a [redacted] Model 5300 D.C. excited neon gas laser. The nominal output was 10 milliwatts, but more than 5 was seldom obtained. Since operation in the principle mode is necessary for making spatial filters and no laser is completely stable, it would be desirable to use a laser with externally adjustable mirrors. 25X1

Laser Mounting

The laser is supported at its two ends. Both of these supports should be made adjustable to align the laser beam with the axis of the optical bench. Figure 2 shows the front end of the laser supported on two adjustment screws and retained by a sprung pin at the top. The laser we used was stable for the first six months of use, but thereafter required frequent adjustment.

Voltage Regulator

Not shown, is a Sorenson voltage regulator used to stabilize the laser. This unit was necessary to obtain a constant laser power output, which before regulation varied plus or minus 20 percent in a short term interval.

Noise Eliminator

This name is given to the device that brings the collimated laser beam to a focus and removes the "noise" caused by dust on the laser windows, mirrors and

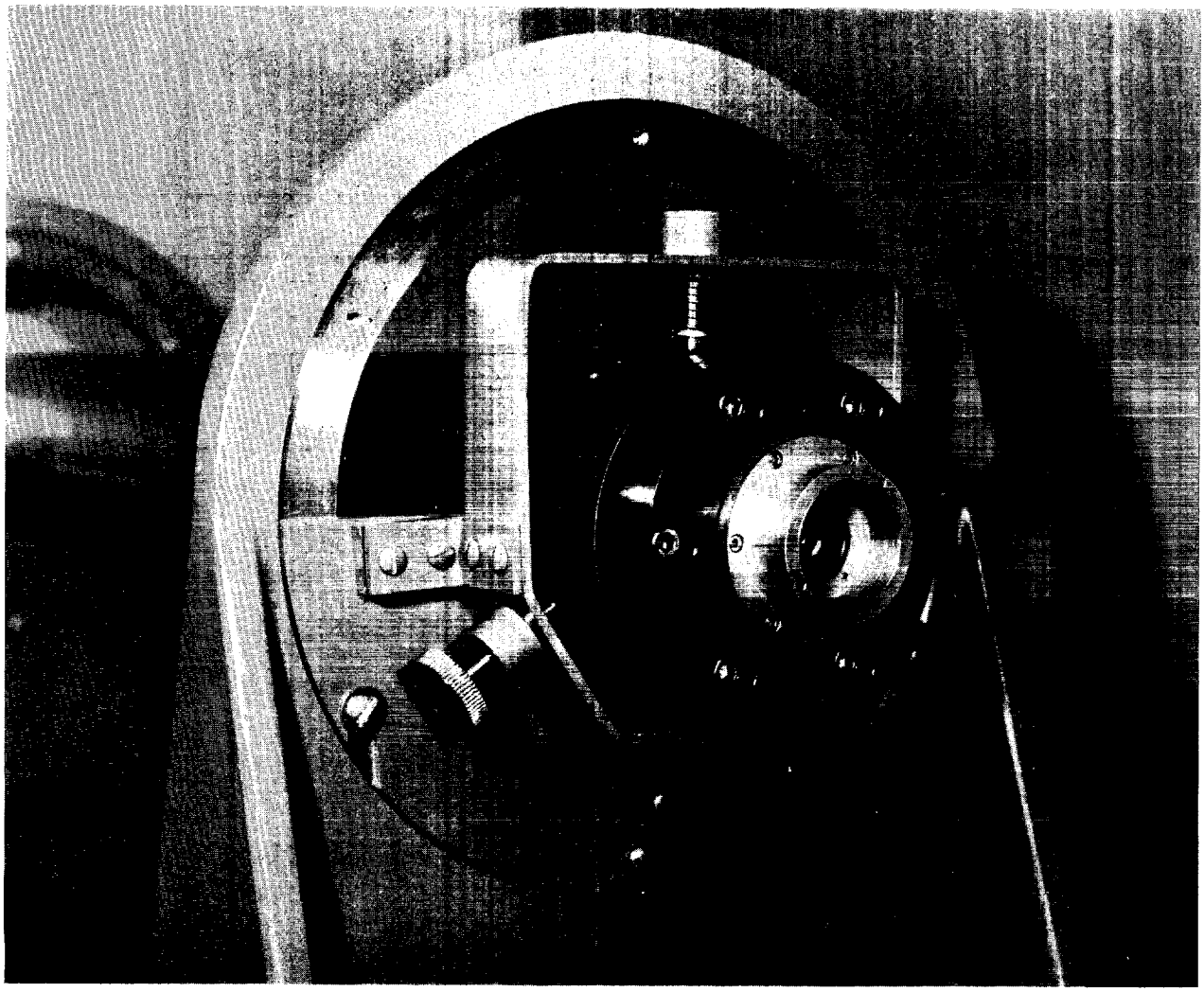

FIGURE 2 Laser Mounting

the focusing lens. Figure 3 shows this assembly which consists of a negative lens which spreads the 1.9 mm diameter laser beam so that it fills the back aperture of the focusing lens. This lens also improves the energy profile of the normally gaussian distribution of energy in the laser beam. The focusing lens is a Unitron 10X microscope objective in a focusing, centering mount. The laser beam is brought to a "point" focus on a .001-inch aperture in a very thin nickel foil. This is also mounted in a centering mount which is not necessary.

The combination of adjustments allows the laser beam to be focused exactly on the aperture and centered in it.

Attenuator

When experimental work is done where it is necessary to focus the intense laser beam by eye and also take diffraction photographs on extremely slow film it is necessary to have some control over the intensity of the light. This is done with a rotating disc containing different neutral filters. The disc in use has eight holes, one of which is open and used for all photographic work. The other holes contain Wratten gelatin filters in various densities from .3 to 5.0. This disc can be remotely stepped in either direction by a double-acting rotary solenoid. The two control switches are in a small box which is normally at the opposite end of the bench and which also contains eight indicator lights that show which filter is in the beam. This information comes from an eight pole rotary switch on the same shaft as the disc.

Figure 4 shows the disc at left, the two in-line rotary solenoids and the switch all on the same shaft. The box at right contains the two push button switches and indicator lights.

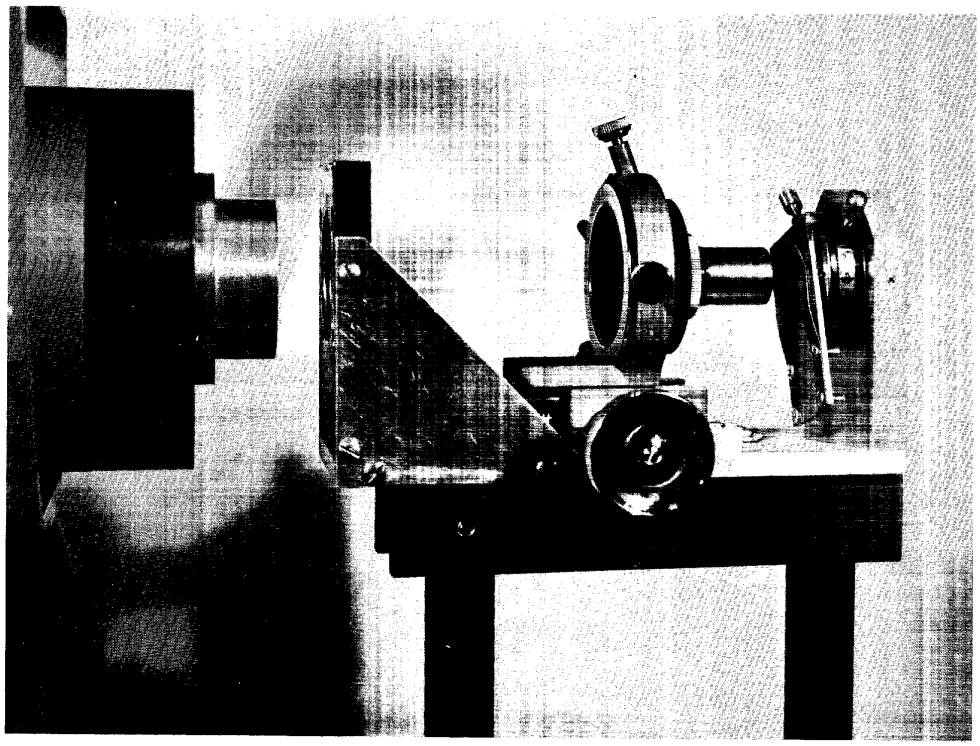

FIGURE 3 Noise Eliminator

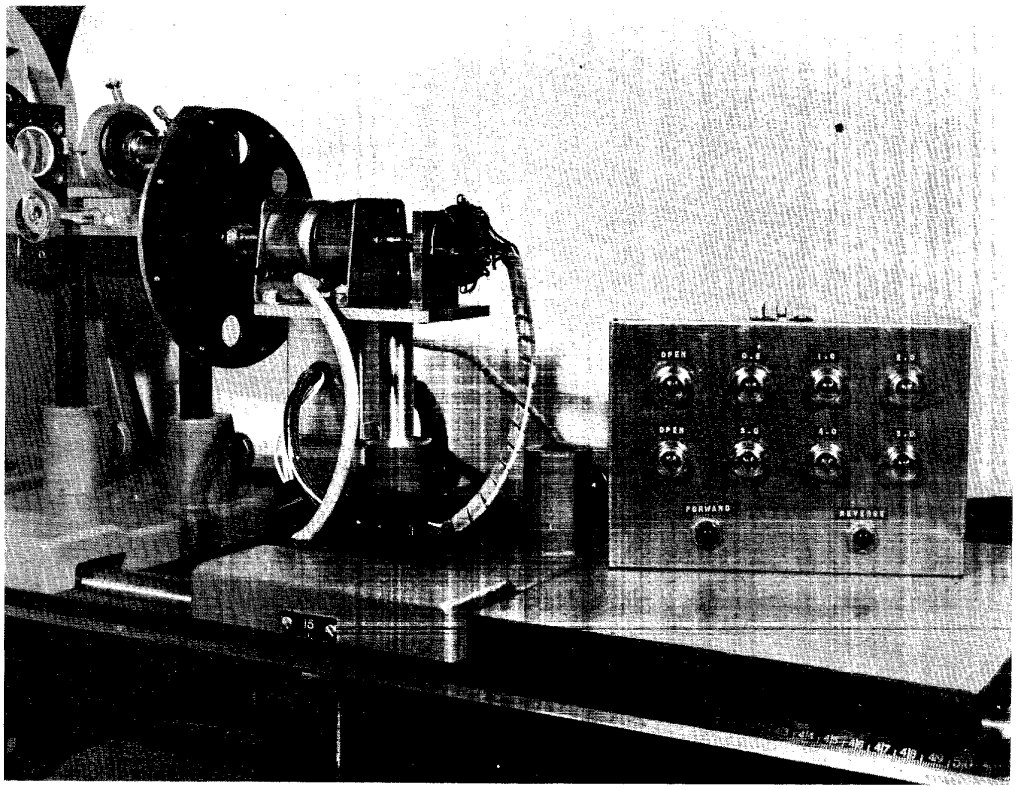

FIGURE 4 Light Attenuator

Light Monitor

Figure 5 shows a device used to keep the laser beam centered on the collimating lens. The lens is in the mount at the right side of the picture. Around the lens is a ring supporting four small cadmium sulphide photo cells. These are connected to four meters to read the intensity at the Top, Bottom, Right and Left sides of the lens. Initially, the laser is adjusted so that all four meters read the same, plus or minus 2 units. If the laser shifts or the bench warps the light spot will move off the lens and the light balance will be changed. These meters are normally at the opposite end of the bench and are consulted every time the measurement of a recognition spot intensity is made. Before this unit was available the beam would shift without our knowledge and assuming it was shifted upward; then recognition spots obtained in the lower half of the picture would read abnormally low. If all the meters read practically the same it can be assumed that the object transparency is uniformly illuminated.

Lens Mounts

All the lens mounts are aluminum castings similar to the one shown in Figure 5. Not shown in this view are the adjustments. The lens is in a cell which is mounted to a plate which fastens to the aluminum casting. The holes in the plate are oversize so that the lens can be centerd on the optical axis. The lens cell also incorporates three push-pull screws which can be used to tilt the lens in any direction to square it with the optical axis.

Rayleigh Lens

This lens is used only when spatial filters are being made and it then occupies the top half of the beam as shown in Figure 6. When not in use the lens is swung upward on a pivot out of the optical path. The lens has a mask around it to stop stray light which might pass around it.

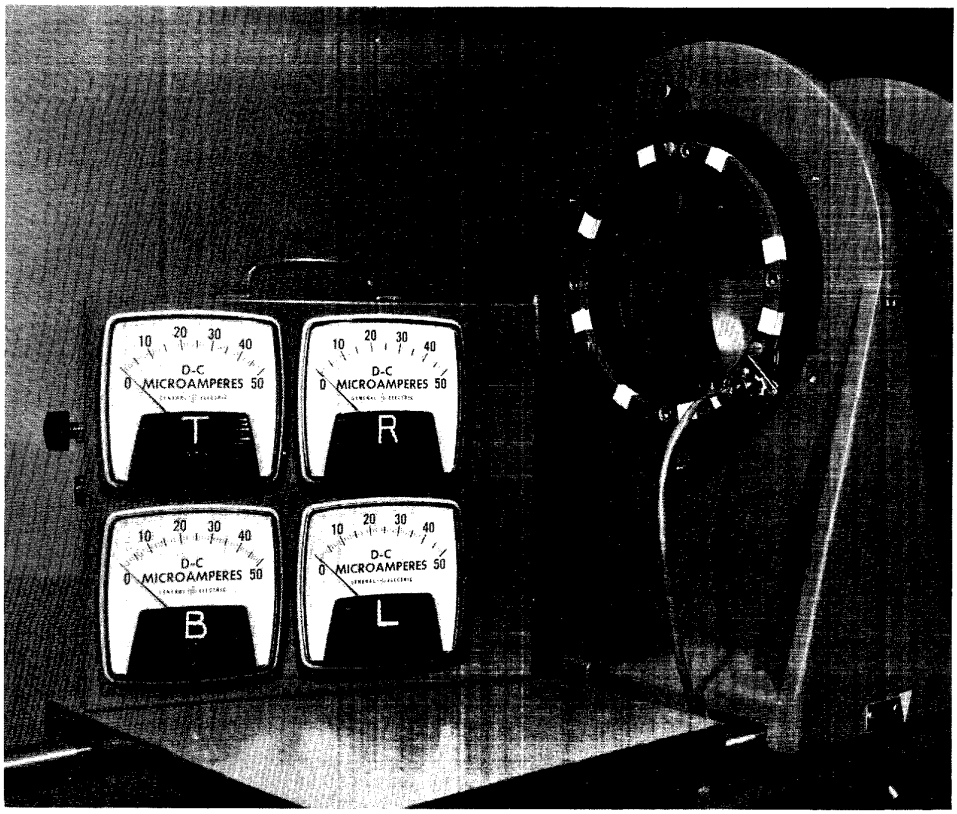

FIGURE 5 Light Monitor

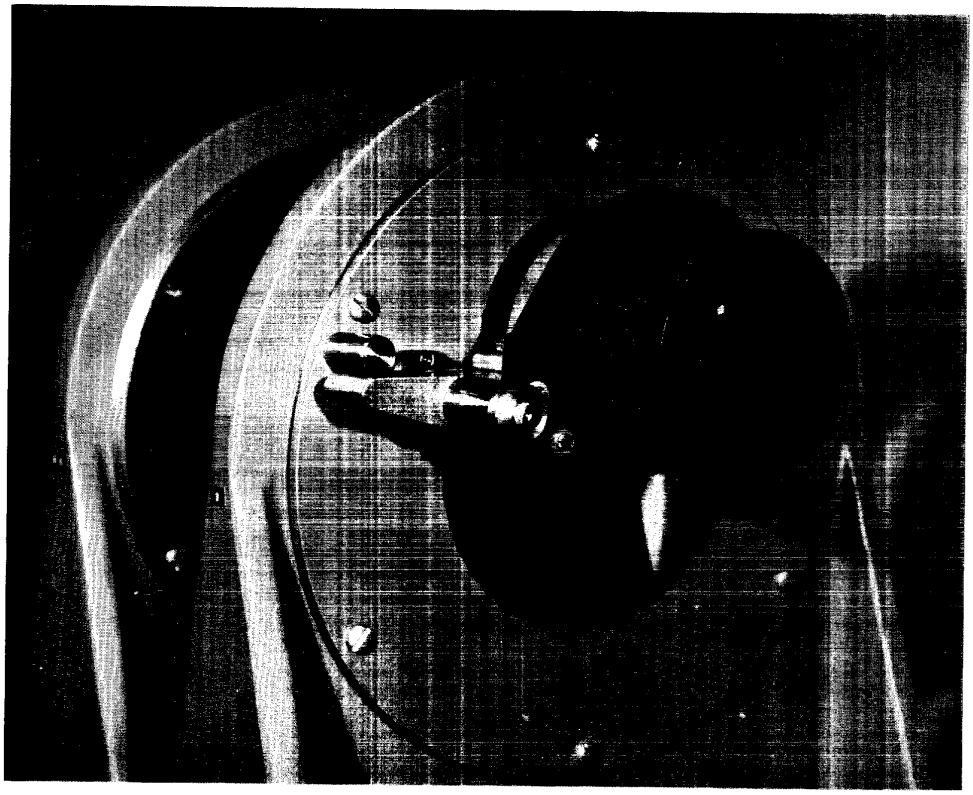

FIGURE 6 Rayleigh Lens

Object Holder

The holder for 4 x 5 inch glass plates is shown in Figure 7. The plates are retained between plastic supports and spring clamps. Other kinds of adapters can be used for film and the liquid gate.

The holder can rotate indefinitely in either direction on a light duty ball bearing. It is driven by a pulley around the outside and an "O" ring used as a rubber belt. The small 10 watt reversible clock motor at left also has a pulley for the rubber belt. The clock motor is one of a series and can be interchanged to obtain different speeds of rotation. The small black box on the right contains the controls and is normally at the end of the bench. The lower switch has three positions, clockwise, off and counter-clockwise.

The entire carriage can be translated on an auxilliary set of rails 3 feet long. The rails are precision ground stainless steel rods running in three ball bushings. The position of the carriage is determined by a ball-bearing lead screw which is driven by a pulley and belt arrangement from a reversible clock motor. This motor is also replaceable with other motors having different gear ratios. Two adjustable limit switches are provided to reverse the motion of the carriage. These switches are provided to reverse the motion of the carriage. These switches are attached to an auxilliary Unistrut shape between the rails. The switches can be adjusted so that the excursion of the carriage is the full length of the rails or only a short distance. The upper switch on the control box has two positions, on and off. There is also a manual reverse button on the left side of the box to reverse the direction of travel.

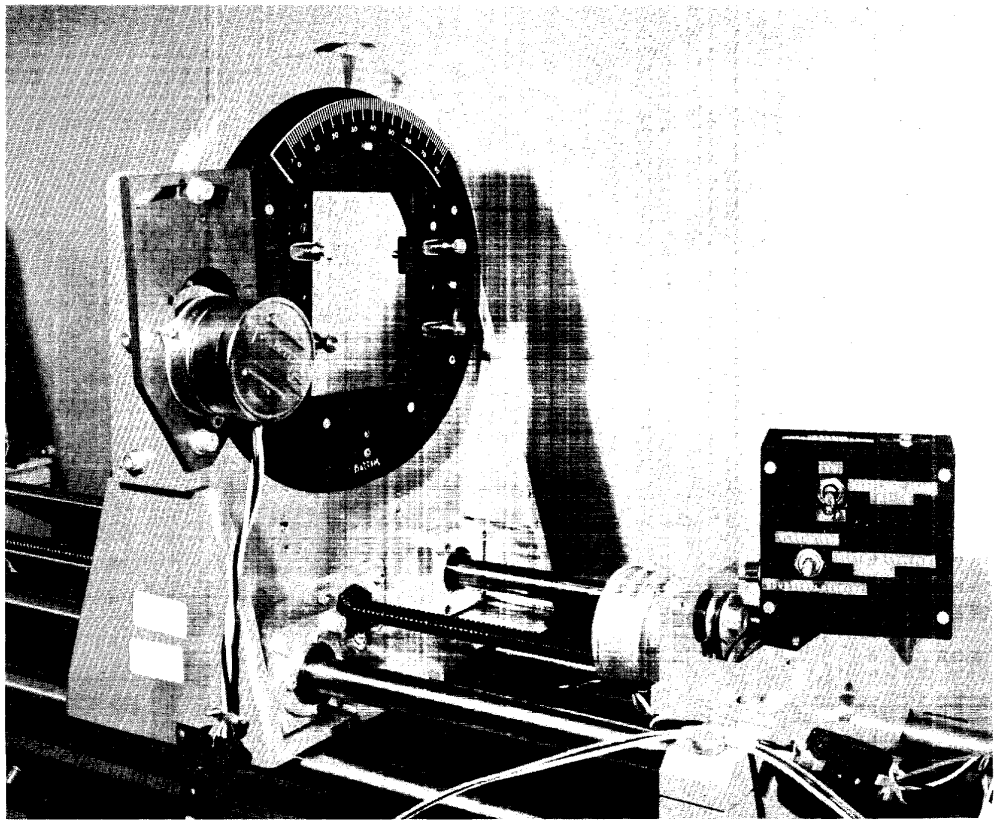

FIGURE 7 Object Holder

These two motions, rotation and traverse are used to provide the orientation and scale search of the object photograph.

The rotation of the object can be read to the nearest degree from the scale at the top. The translation and hence the relative magnification is read from an index mark on the moving carriage and a stationary steel tape which does not show in the photograph.

Reference Beam Attenuator

When spatial filters are being made the object holder shown in Figure 7 is used to support the transparency of the object in its lower half. The upper half of the aperture may contain a metal plate with a small hole which acts as a "noise eliminator" on the reference beam. In many cases it is necessary to reduce the intensity of the reference beam to obtain interference fringes in the desired diffraction orders. This is done by inserting a Wratten neutral density gelatin filter in the beam. It is essential that this filter be as close to the focus as possible. A means for doing this is shown in Figure 8. A metal plate painted light gray in the photograph is inserted against the back of the object transparency. This locks in place with two rotating sprung cleats, the dark colored objects in the photograph. Gelatin filters mounted in cardboard frames are inserted under the spring clips. In the figure a filter labelled N.D.0.50 is in place in the upper or reference beam and a small object transparency is in the lower sample beam.

Spatial Filter Holder

This device has precise X and Y motions controlled by large micrometer heads. This part was purchased as a stage for a small toolmaker's microscope and was intended to operate in a horizontal position. The two tension springs at the top

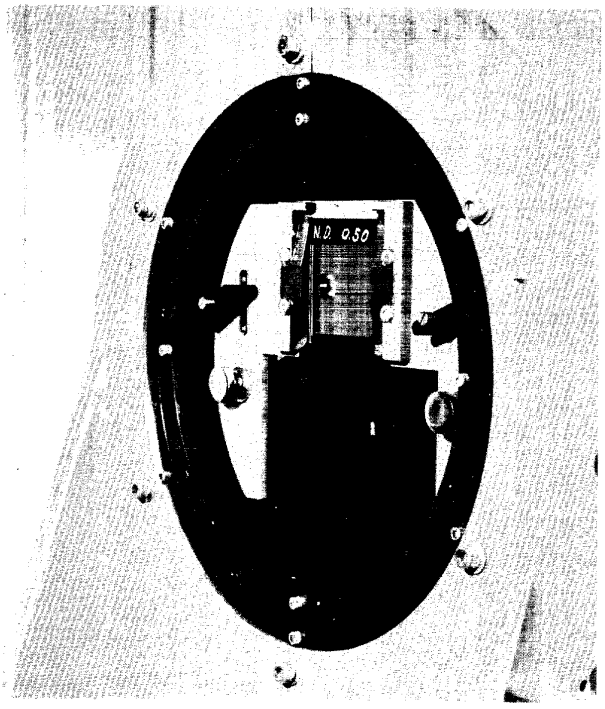

FIGURE 8 Reference Beam Attenuator

in Figure 9 are to take part of the weight off the lower micrometer.

The center part of this device can be rotated and the angle read in the curved window at the left by means of a vernier and magnifier. The angle can be measured to at least 1 minute of arc.

The spatial filter is attached to a metal plate with masking tape and the metal plate fits the aperture in the stage. Two spring clips retain the filter in use. The spatial filter shown in the figure is typical for a fairly simple object.

Imaging Lens

This lens is installed just behind the spatial filter and forms the images of the recognition spots. When the filter is changed or adjusted the lens swings up out of the way on a pivoted mount. Figure 10 shows the lens in its normal position.

Viewing and Photometric Microscope

The recognition images are viewed with a low-power microscope shown in Figure 11 which can also be used to measure their intensity. The microscope has a special mount which allows it to tilt so that it is in line with the off-set first order recognition image. The microscope also has rack and pinion motions in X, Y and Z. At the center of the field of view there is a single glass fibre built into the eyepiece. This fibre is bent at a right angle and makes contact with a 3-foot long multi-fibre light conductor. This goes to a phototube, not shown. The output of the phototube is read on the meter shown which has several scales. The power supply for the meter is battery operated to avoid live current variations. The entire microscope and meter are commercial items purchased from the [redacted] 25X1

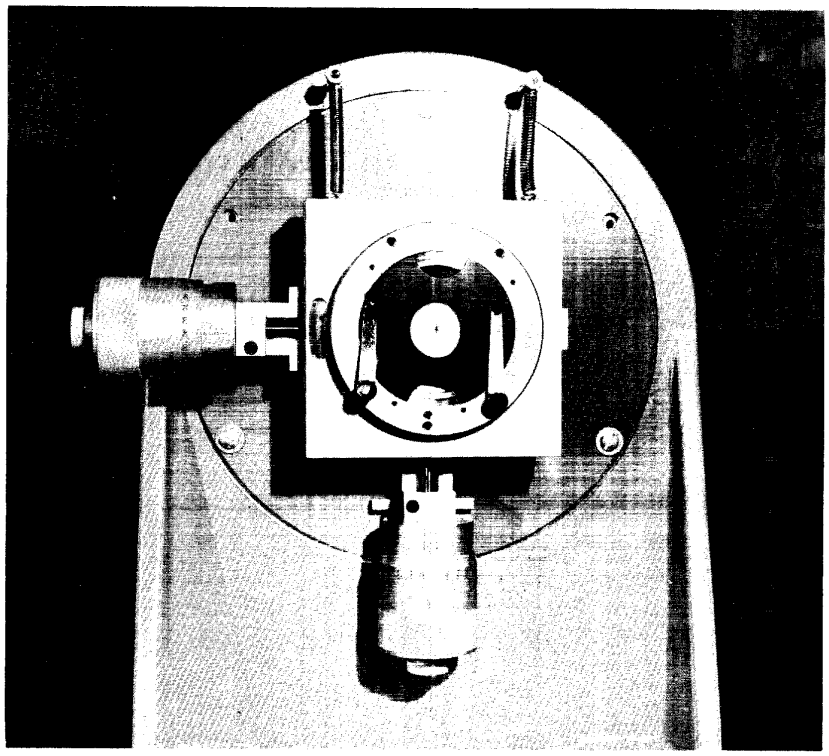

FIGURE 9 Filter Holder

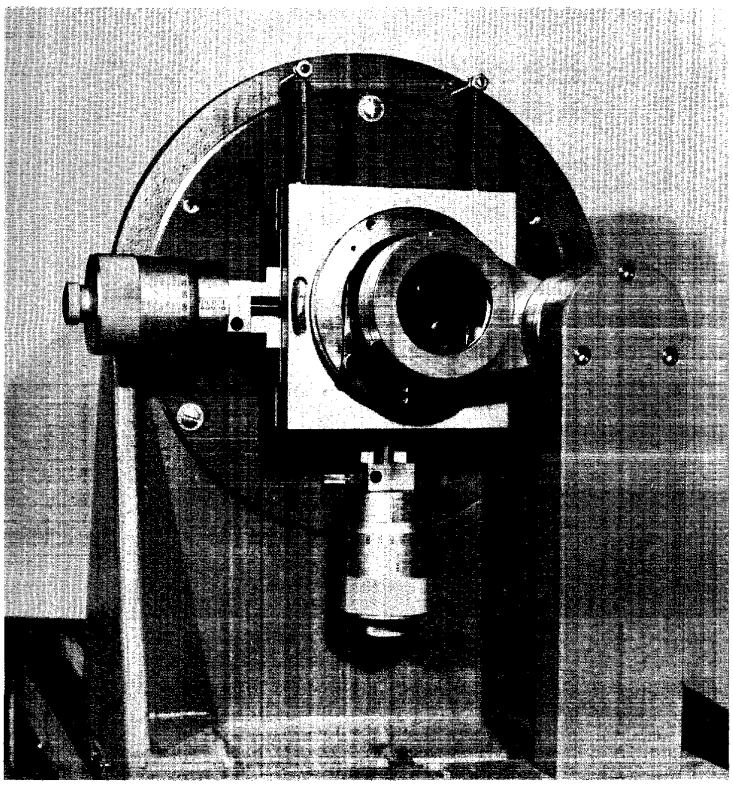

FIGURE 10 Imaging Lens

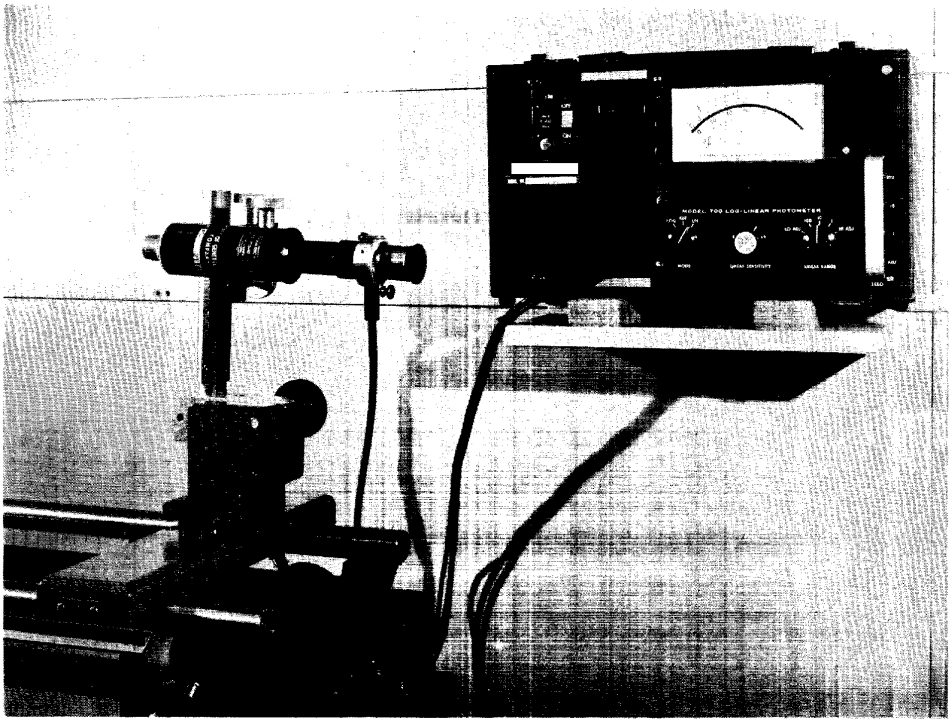

25X1

FIGURE 11 Photometric Microscope

There are several parts not shown in the figures which do not need explanation.

The camera used to make spatial filters is a 35 mm reflex camera without a lens. The reflex mirror is used to find the point of best focus and the normal magnifier is replaced by one of higher power.

The same camera is used to photograph recognition images.

Section C-2

Alignment Tolerance of Spatial Filter

Purpose

It is necessary to remove photographic spatial filters from the equipment for processing and then to replace them so that the image of the zero order is aligned with the optical axis. So long as this is a hand operation, the alignment tolerance is of no importance because the filter can be aligned by eye using a microscope and a suitable positioning device. If the recognition process is ever automated, then it will be necessary to have some means to do this automatically and to know the tolerances to which this device must operate.

Possible Automation Devices

In its present state of development the recognition process requires three separate optical systems, or with some loss of convenience these three can be incorporated in one by interchanging parts. These three systems are:

1. Filter making system using the Rayleigh lens to produce the two-beam filter.

2. Filter testing system to view the quality of the reconstructed image and measure its relative modulation efficiency.

3. Recognition system with equipment for measuring the intensity of recognition spots.

Thus, in the present equipment, the filter is made in one instrument and used in another so that some means would have to be devised for removing the filter, processing it, and returning it to an equivalent location in a second instrument.

If we are willing to ignore this advice and can build a single unit system, then the problem of alignment tolerance disappears. The filters would be exposed and if silver photographs would be rapid-processed in place and used there until discarded. Photoplastic filters could be processed in place and erased when no longer needed.

Considerations of automation seem to lead to two alternatives:

1. Separate instruments for making and using filters. Some mechanical device such as an accurate frame to allow the filter to be transferred from one instrument to another without realignment. Such a system appears more flexible and allows the user to establish a "filter bank".

2. A single instrument which processes and uses filters in one place.

At the present time our thinking favors the first alternative and hence the necessity for determining the alignment tolerance.

Experimental Approach

An obvious and simple means for determining alignment tolerance is to measure the intensity of the recognition signal and the signal-to-noise ratio when the filter is properly aligned and with different known amounts of misalignment. The problem is to choose a typical object and a typical filter.

Experimental Equipment

Spatial filters of various vehicles and other objects were carefully aligned with the diffraction images of photographs containing these

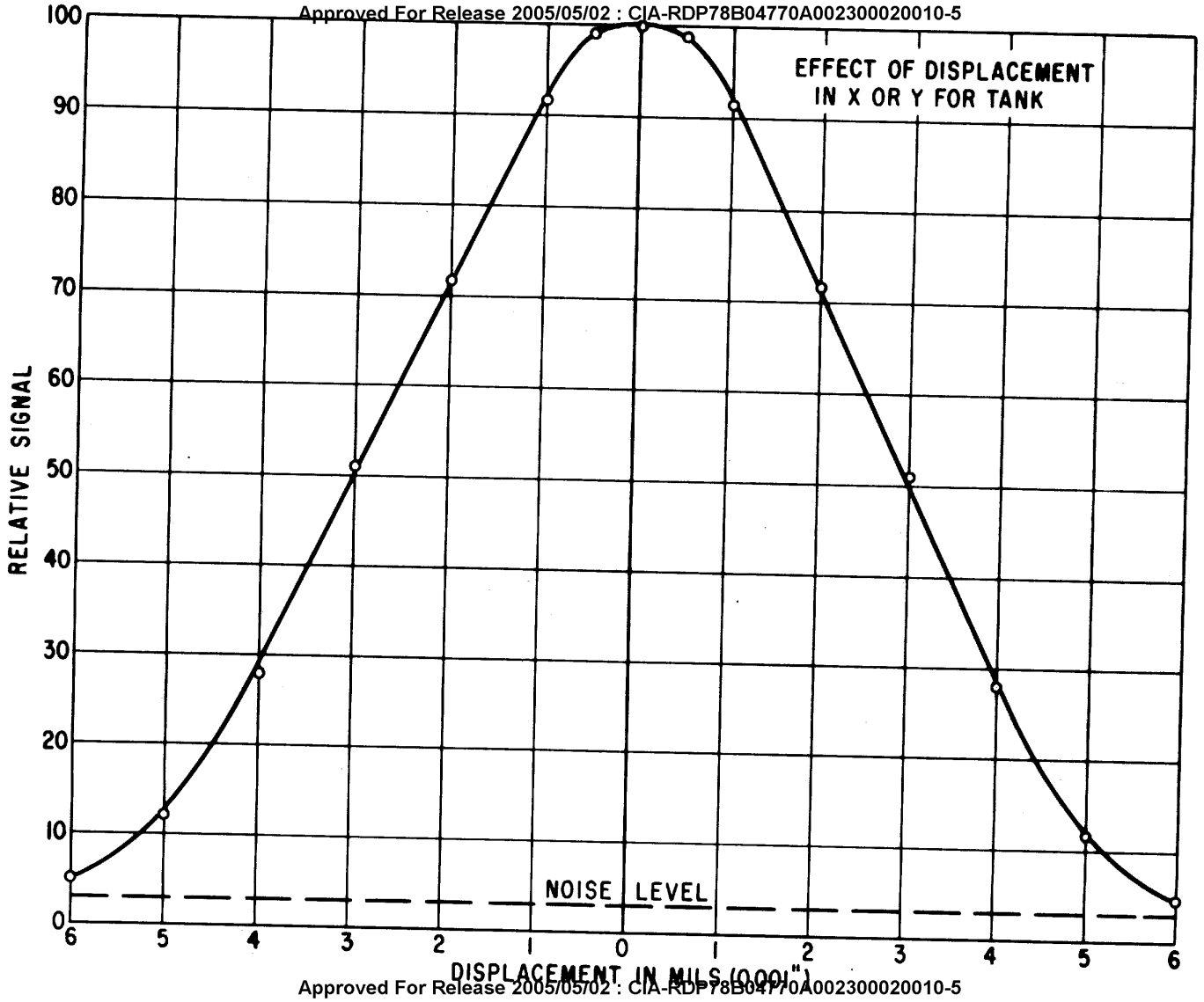

FIGURE 1

The part of the curve from the plateau down to the noise level is practically straight. The interpretation is that for alignment tolerance beyond the plateau, the loss of signal strength will be linear. At its lower end the curve joins the picture noise level in a gradual transition.

In every case we tested, the noise level did not change appreciably during the misalignment. It is quite possible to have a major misalignment of the filter which is much greater than any shown in the Figure 1 that can result in an increased noise background. Measurement of the noise in this case can be a difficult problem. Sometimes the recognition spot breaks up into several bright spots, or in some cases individual features of the object are locally recognized giving rise to a collection of scattered minor recognition spots. It could be argued that these are also "noise", but we have felt that if they were within the area occupied by the image of the object they were not background noise or false alarms and could be neglected. Actually, these confusing conditions did not arise in any of the tests designed to measure the alignment tolerance and therefore do not affect the interpretation of the data. In all of these tests, when the filter was misaligned from its proper location all that happened was that the recognition signal remained a single, practically round spot, but decreased in intensity.

Our conclusion, for the tests performed, is that alignment error results in a decreasing signal and a constant noise level and therefore a predictable decrease in signal-to-noise ratio.

It would be possible to continue these tests for objects of different sizes and shapes and finally to generalize some conclusions for the sizes of objects we might expect to search for in aerial photographs. These results are reported at the end of this section.

An experimental test was made to determine if the direction of the interference fringes had any effect on the relative x and y alignment tolerances. Normally, our system produces vertical shear between the reference and sample beams so that the fringes in the filter are horizontal. Also, it is our habit when making a filter to arrange the object square and with its long axis horizontal. It was realized that in some cases it would be advantageous to depart from this simple procedure. Particularly, in the case of a multiple filter for several similar vehicles it would not be desirable to arrange the vehicles parallel or in a neat square formation because this would result in a strong diffraction pattern for the arrangement. Since the purpose of the multiple filter is to detect individuals and not groups arranged in a particular pattern, such a filter would be less satisfactory than one in which the pattern was suppressed. Our means for subordinating this pattern is a random arrangement of vehicles. In this case the different vehicles produce diffraction patterns at random angles and with interference fringes at random angles.

Therefore, since this case appeared to be a real one, a test was made of the displacement tolerance of a set of filters of the same vehicle in which the interference fringes were parallel to the long dimension, perpendicular to the long dimension, at 45 degrees and at a random angle which turned out to be 32 1/2 degrees. As might be expected, there was no measurable difference, so that as a conclusion we can state that so far as alignment tolerance is concerned, it makes no difference how the object is oriented when the filter is made.

Analytical Approach

Another means to determine the alignment tolerance of a spatial filter is to analyze a typical example to find the function of the filter elements and to observe the effect of displacing these elements from the diffraction image. This analysis should result in a set of simple formulas which would allow the operator to calculate the tolerance for any possible situation.

ANALYSIS OF A SPATIAL FILTER

The problem is; can the various "spots" in a spatial filter be related to features in the object from which it was made? For very simple objects such as a slit or a round hole, the diffraction pattern is easy to predict and the analysis of the spatial filter presents no problem. For a complex object, the hologram is too complicated to analyze by eye. The object selected for study was a model M-48 tank. As seen in a vertical photograph the outline of the tank is a rectangle. The long sides of the rectangle are straight, but on closer examination the ends of the tank are not, one is rounded, the other is an offset straight line. The next major features are a turret which is approximately elliptical in outline and a gun barrel which is parallel-sided. The top surface of the tank also has cleats and other details.

Spatial filter Number 1077, which would recognize this tank or reconstruct a good image was examined. It consisted of 23 vertical orders of diffraction and 20 horizontal orders of diffraction or about 166 spots since each of the horizontal orders had two or more satellites. There were also sections of elliptical curves and curved lines intersecting the vertical orders.

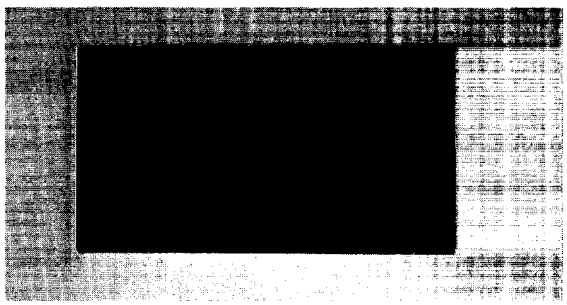

Tank Part 1

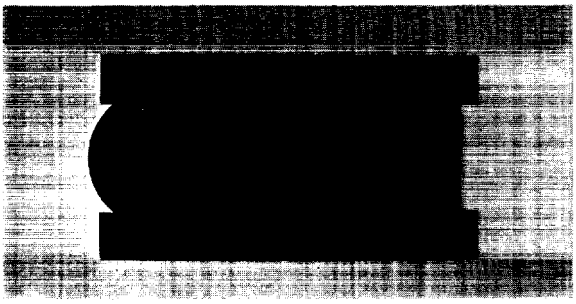

Tank Part 2

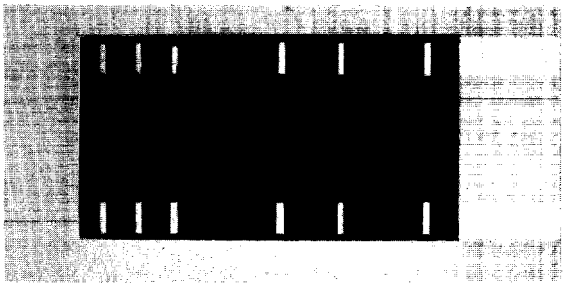

Tank Part 3

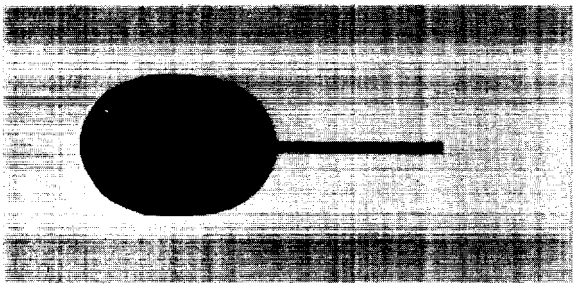

Tank Part 4

Tank

Figure 2 - Tank Parts Used in Spatial Filter Synthesis

In this experiment the filter was synthesized from its elements. Various simple parts of the tank, the rectangular outline, the turret and so forth were separately made into spatial filters with the idea that this would aid in identifying the elements responsible for these various features. This technique is not foolproof, as it may turn out that the diffraction pattern of two objects together is quite different from the two separately.

SYNTHESIS OF A SPATIAL FILTER

Four India ink drawings of tank parts were made to the same scale. These are shown in Figure 2 and show the following features:

Part 1 - Rectangular outline only, no details.

Part 2 - Outline with straight long sides and shaped ends. This is the entire outline of the tank.

Part 3 - Rectangular outline with 12 cleats on the surface. These cleats were considered to be the chief periodic elements and the most conspicuous features of the tank body.

Part 4 - Outline of elliptical turret and gun only. The turret is probably the most conspicuous feature of the tank except its outline.

These four drawings were reduced to transparencies the same size as the transparency of the tank used to make spatial filter Number 1077. Each of these transparencies was then made into a spatial filter. The following results were obtained:

Part 1, (Rectangular outline of tank only). The filter showed 23 vertical orders of regularly spaced spots, each spot decreasing uniformly in density. Each spot (order) was practically round and the spots were in a straight line. This filter is shown in Figure 3a.

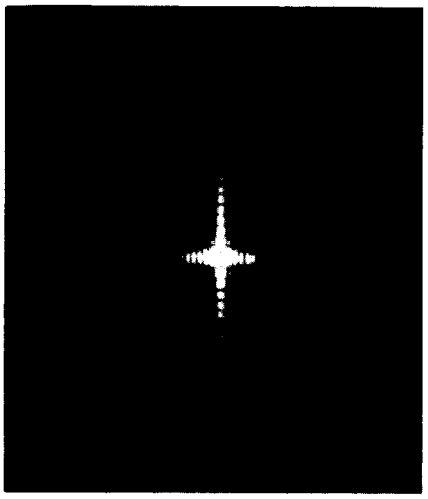

Fig. 3a - Tank Part 1

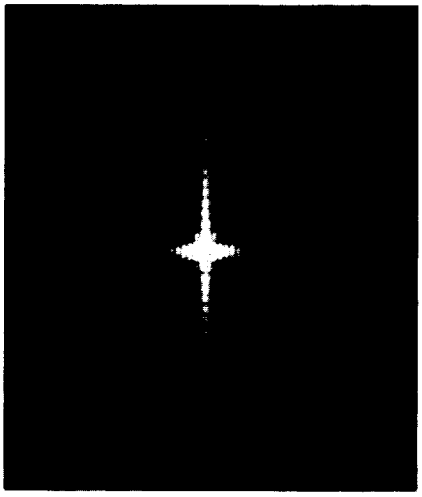

Fig. 3b - Tank Part 2

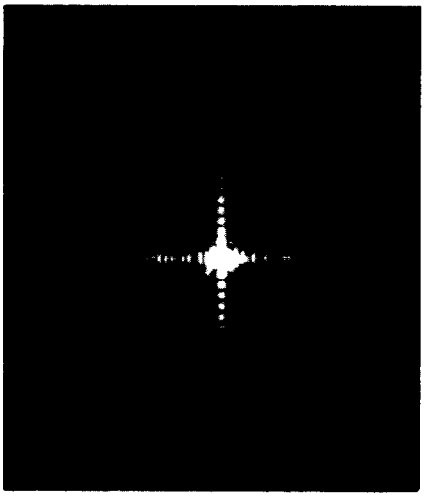

Fig. 3c - Tank Part 3

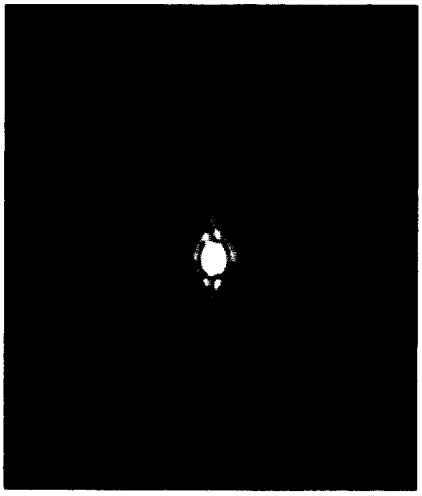

Fig. 3d - Tank Part 4

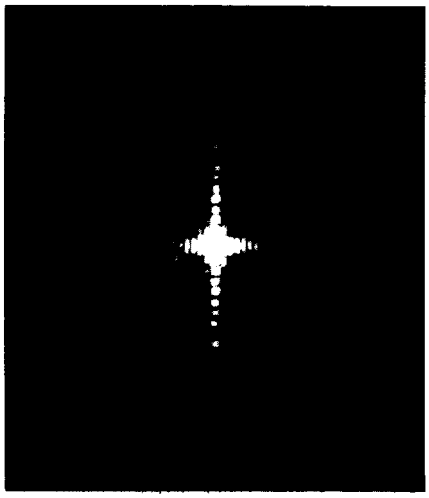

Fig. 3e - Tank Part 5

Figure 3 - Spatial Filters of Tank Parts

In the horizontal direction there were 25 orders of regularly spaced spots, each spot decreasing uniformly in density. Each spot was oval in outline. The entire pattern was rectilinear and symmetrical.

Referring to the description of spatial filter Number 1077 for a complete tank, it could be seen that the rectangular outline is the chief feature, and that the filter made from this outline only contained some 96 spots of which 86 compared to 86 spots in the filter for a complete tank. This left some 80 spots to account for.

Part 2, (Outline of tank with shaped ends). This filter, like Part 1 showed 23 vertical orders of regularly spaced spots, each spot decreasing uniformly in density. Each spot was practically round and the spots in a straight line. These vertical orders can be attributed to the diffraction of the long parallel sides of the tank and therefore are the same for Parts 1 and 2. This filter is shown in Figure 3b.

In the horizontal direction there were 13 orders or regularly decreasing density. Each order was composed of three to five spots, the central three of which were most dense. None of these spots was round, but varied from oval to banana-shaped. The spots were not in alignment, but were shifted in their relative positions. The pattern was essentially rectilinear and symmetrical.

Comparing this filter to Number 1077 for the whole tank it was found that about 130 of the spots could be accounted for. This indicates that the outline is the most important feature of the spatial filter and there were approximately 36 spots left to account for all other features.

Part 3, (Rectangular outline with cleats on top surface) like Parts 1 and 2 showed the same 23 vertical orders of regularly spaced round spots. This filter is shown in Figure 3c.

In the horizontal direction there were 23 irregularly spaced spots (the cleats are irregularly spaced) which tended to be oval. Different spots had two, four or six satellite spots. Between some sets of spots were dog-bone shaped spots. In general the order was as follows:

Order	Number of Satellites
1, 2	two
3, 4	four
5	two
6 to 10	six
11, 12, 13	none
14, 15, 16	four
17, 18, 19	two
20	none
20 to 23	two

This pattern is no doubt due to coincidences between diffraction patterns formed by individual pairs of cleats.

A new feature was that the density of the spots now did not decrease regularly as in the former simple cases. There was a maximum at about the 2nd spot and the 8th. Again this is probably due to coincidences in the spatial frequencies in the object.

The total number of spots in the spatial filter for Part 3 was about 184, or more than can clearly be seen in the filter for the entire tank. This indicates that the drawing showed the cleats in higher contrast than they appear in a photograph of a tank, and therefore their diffraction pattern has more energy and is capable of producing a larger number of orders. In general, the distribution of light in the spots and their satellites is much the same as the spatial filter for the tank and the differences between the filter for Part 3 and the whole tank are rather minor. It is possible to pick out about 12 spots in the tank filter which cannot be accounted for in Part 3. Therefore, we may say on a very simple basis, that there are 12 spots left to account for due to the turret and gun.

Part 4, (Turret and gun only). This spatial filter required a longer exposure than the previous objects. Parts 1 to 3 were all of the general tank outline and had an area on the transparency of about 15 sq. mm. The transparency of the turret and gun only had an area of about 5 sq. mm. The required exposure was about 50 percent longer. This part makes a very peculiar hologram. The turret as seen from above is elliptical in outline and produces a diffraction pattern that consists of concentric ellipses of diminishing density. If these ellipses are examined carefully they are seen to actually consist of broken arcs of circles which the eye joins together to make an ellipse. Apparently, the process analyzes the elliptical curves into a number of circular elements and each of these circular elements produces a bull's-eye pattern. The only unusual feature is that there were apparently only 5 orders of diffraction produced by the turret while the tank outline produced 23. The reason is probably the difference in light distribution. In the case of a rectangle the diffraction is in the form of spots in which the diffracted light is concentrated in a small area about .2 mm in diameter or an area of .03 sq. mm. In the case of the elliptical turret the diffracted light is in the form of "rings", the average diameter of each increasing with the order.

The area of the 3rd order "ring" for example is about 1.77 sq. mm which is 60 times the area of the spot produced by the rectangle. If the intensity is the same, the exposure will be distributed over a larger area and will be much less. This filter is shown in Figure 3d.

The gun barrel in Part 4 is parallel-sided and therefore acts as a slit in the negative and should produce parallel diffraction lines as long as the gun. The conclusion thus far is that the turret alone should produce a set of concentric ellipses, the gun alone should produce a series of parallel lines. However, the gun plus turret produced a very different pattern which consisted of four ellipses intersected by steep, nearly vertical lines at an angle of about 14 degrees. There were about 5 of these orders due to the gun in the spatial filter. This is a case where the sum of two diffraction patterns produced a pattern different from either component.

Spatial Filter of Complete Tank

We can now look at the filter for the tank as shown in Figure 3c and recognize all of the elements discussed.

Vertically there were 23 orders of diffraction, which did not decrease regularly in density, but followed the following pattern:

Order	Density
1 to 5	Strong
6, 7 and 9	Fairly Strong
8	Weak
10 to 16	Weak
17 to 23	Very Weak

Undoubtedly, the variations in density were due to the intersection of the ellipses and slanted lines of the turret and gun. If these were in phase they reinforced the vertical spots, if out of phase, they reduced the density of the spots.

The vertical spots were not all round. Orders 6 to 23 were practically round, but 1 to 5 were distorted. This is also due to intersection of the ellipses and slanted lines with the spots.

The vertical spots were not in a straight line. Orders 1 to 5 and 9 were approximately straight. Orders 7, 10, 12, 14 and 16 were deviated to the right. Orders 6, 8, 11, 13 and 15 were deviated to the left. This was probably due to phase interference between the turret-gun combination and the tank outline.

There were 20 horizontal orders which did not decrease uniformly in density. The progression was as follows:

Order	Density
1 to 5	Strong
6 to 11	Decreasing Uniformly
12 to 16	Stronger
17 to 20	Decreasing Rapidly

This can be explained as due to the irregular spacing of the cleats interfering with the odd-shaped ends of the tank.

Each of these horizontal orders was composed of from 3 to 5 oval or banana-shaped spots believed to be due to the cleats and one curved end of the tank.

There were four orders of broken ellipses due to the turret and five orders of slanted vertical lines due to the gun which intersected the 4th, 6th, 8th and 12th vertical order of spots.

Taken together, it was possible on a simple basis to explain the presence of every spot in the spatial filter of the tank from the four spatial filters of the tank parts.

ANALYSIS OF A SPATIAL FILTER

In the previous section a spatial filter was studied by synthesis; that is to say, putting it together from its elements. In this way it was possible, to some extent, to account for the presence of the 166 prominent spots and some of the structure. There is a lot that this study did not tell and some of these factors will be discussed in this portion which describes an analysis based on taking the filter apart.

The actual means by which this was accomplished was to successively mask different portions of a spatial filter of a tank using small pieces of opaque masking tape which were applied directly to the filter under a microscope. At each step the partially masked filter was reconstructed and this image photographed. The intensity of the reconstructed image was also measured. Finally, the masked filter was used to recognize a tank and the intensity of the recognition spot was measured. In every case the intensity of the reconstructed image and recognition spot were comparable within the accuracy of measurement so that only one set of figures is reported.

No tests were made of the noise background because, so far as could be seen, it remained unchanged in all the tests. No tests were made of the properties of the masked filters to distinguish between two similar objects because this was outside the present scope which was simply to determine the origin and function of each of the obvious elements of the filter.

General

The filter contained 23 vertical "spots" representing diffraction orders of the "slit" produced by the two long straight sides of the tank. It is fairly clear from a microscopic examination of the filter that many of these spots are doing little or no work in the recognition process. The first four orders are so much

overexposed that the bright lines in the interference fringes have irradiated or spread to join the next bright line so that the dark fringes have disappeared and the order is simply a solid black spot. Such a spot cannot produce diffraction or contribute to the reconstructed image of the filter or the intensity of the recognition image. These orders are said to be "plugged".

It is also apparent that the orders above the 10th are underexposed. The light amplitude across a set of interference fringes is ideally sinusoidal and the best diffraction appears to result when the exposure is such that the bright and dark fringes are recorded as equal in width. As the exposure decreases, only the most intense center portion of the bright fringe is recorded and therefore the grating consists of narrow opaque bars and wide transparent bars. These gratings appear to be much less efficient than the ideal grating with approximately equal width bars.

Finally, as the exposure decreases still further the bright fringe does not contain enough energy to completely blacken the film and the result is a grating made of thin gray bars. The efficiency of these gratings appears to be negligible.

It was therefore anticipated that a fair number of the spots could be masked or removed from the filter without producing any visible effect.

This simple concept is complicated by the fact that the light in the various vertical orders does not decrease regularly or according to any known function. Measured values of the light intensity in one set of vertical "spots" was as follows:

Order	Intensity
0	100
1	3.0
2	1.06
3	.46
4	.40
5	.29
6	.11
7	.12
8	.078
9	.10
10	.058
11	.044
12	.037
13	.033
14	.033
15	.018
16	.024
17	.010
18-23	.010-.004

It can be seen that these orders do not decrease in decades or even uniformly.

Masking the Vertical Low Orders

As just described, the first four vertical orders appear to be completely plugged and therefore non-functional.

Orders Masked	Relative Intensity Reconstructed Image	Appearance Reconstructed Image
1-4	.98	No difference
1-5	.97	No difference
1-8	.66	No difference

These results indicate as predicted, that the first four orders are non-functional, the 5th is only slightly useful and the 6th, 7th and 8th together contribute about one-third of the energy transmitted by the filter for this particular kind of information.

Masking the Vertical High Orders

As described earlier, the higher orders are so weakly exposed that the resulting gratings are inefficient. It should be possible to mask a good number of them with negligible loss.

Orders Masked	Relative Intensity Reconstructed Image	Appearance Reconstructed Image
23-15	1.00	No difference
23-13	1.00	Outline appear slightly rough
23-10	.98	Outline is rough, some loss of gun image
23-5	.10	Nearly total loss of information on tank sides and gun

The above results show that vertical orders 13 to 23, while distinctly present in the filter are practically non-functional and orders 10 to 12 diffract little energy. The fact that the outlines become rough as the higher orders are suppressed is predicted by Abbe's theory of the reconstruction of a diffraction image which states that resolution suffers if any of the higher orders are lost. Loss of resolution in this case results in a wavy or ragged outline. The reconstructed images are shown in Figures 4b and 5a, b, and c.

Conclusion on Vertical Orders

Taking these two experiments together it can be seen that so far as energy is concerned, that only the 6th to 9th orders are efficient at diffracting light and therefore, taking the average, this is a 7th or 8th order diffraction filter. It would appear that a much simpler filter showing only the four orders from 6th to 9th would probably be nearly as effective and certainly a filter showing only the eight orders from 6th to 13 would be as effective as the complete filter. This leads to the conclusion that it might be possible to make artificial spatial filters by photographing drawings of appropriate "spots" composed of black and white lines.

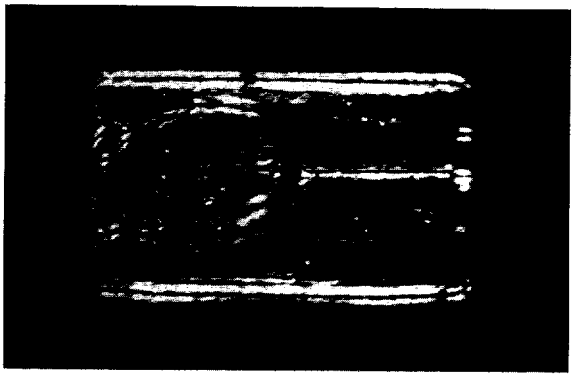

4a - No Vertical Orders Masked

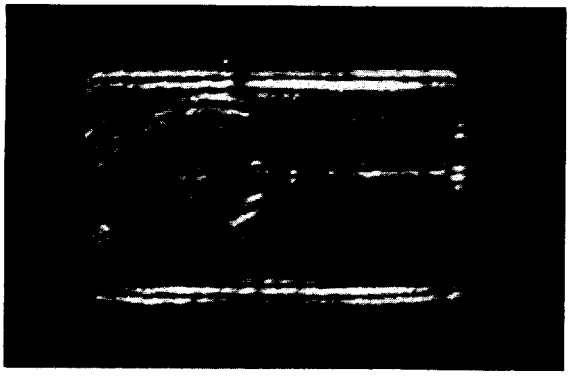

4b - 23rd to 15th Vertical Masked

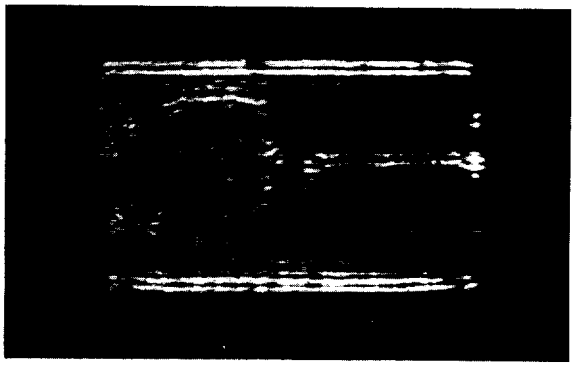

4c - 1st to 4th Vertical Masked

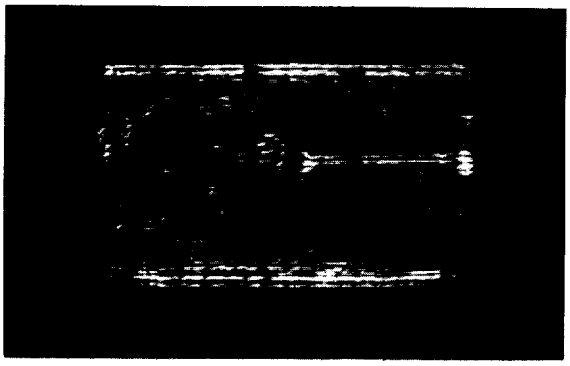

4d - 1st to 5th Vertical Masked

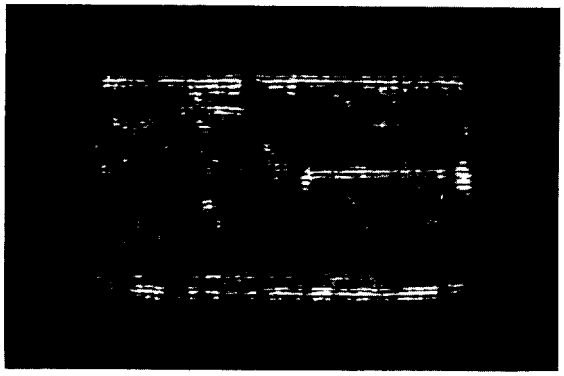

4e - 1st to 8th Vertical Masked

Figure 4 - Effect of Masking Horizontal and Selected Vertical Orders on a Spatial Filter

It also shows that it should be possible by some process of composite photography to produce a spatial filter in which all or most of the 23 orders were effective at producing diffraction. If this were achieved, then the filter would be about 5 times as efficient as the present filter having only about four function orders. There is also the possibility that a spatial filter made from a high-contrast drawing would be more efficient than one made from a photograph.

Masking Horizontal Orders

The spatial filter shows some twenty horizontal orders of diffraction, most of these orders having two to six satellites.

The results of masking these were as follows:

Orders Masked	Relative Intensity Reconstructed Image	Appearance Reconstructed Image
All	-	Total disappearance of details crosswise the tan
20-8	.97	No difference
20-5	.94	Little difference
20-4	.90	Details rough
1-2	.80	Little difference

The conclusion from these tests is that only the 2nd to 5th orders are effective in producing diffraction and the remaining orders are not serving any useful purpose. Reconstructed images are shown in Figures 4a and 5d.

General Conclusions

While the filter examined contains some 23 orders of diffraction and some 166 diffraction "spots", only about four or five of these orders are doing most of the work and only about 32 of the spots are effective in recognizing the rectilinear details. This study did not cover the 12 spots which represent the turret and it is not known how many of these are effective.

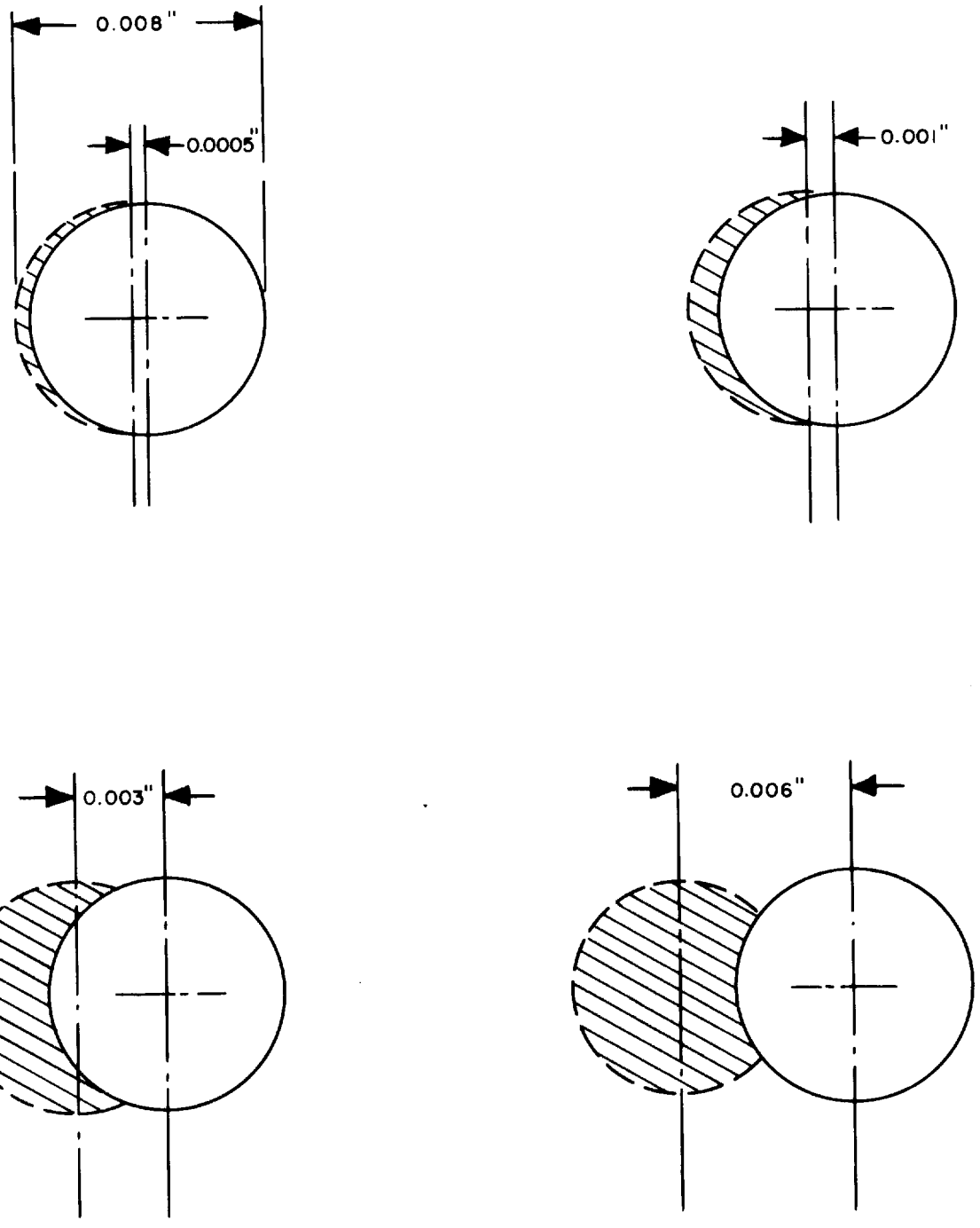

RELATIVE OVERLAP OF SPATIAL FILTER AND HOLOGRAM OF TANK

FIGURE 6

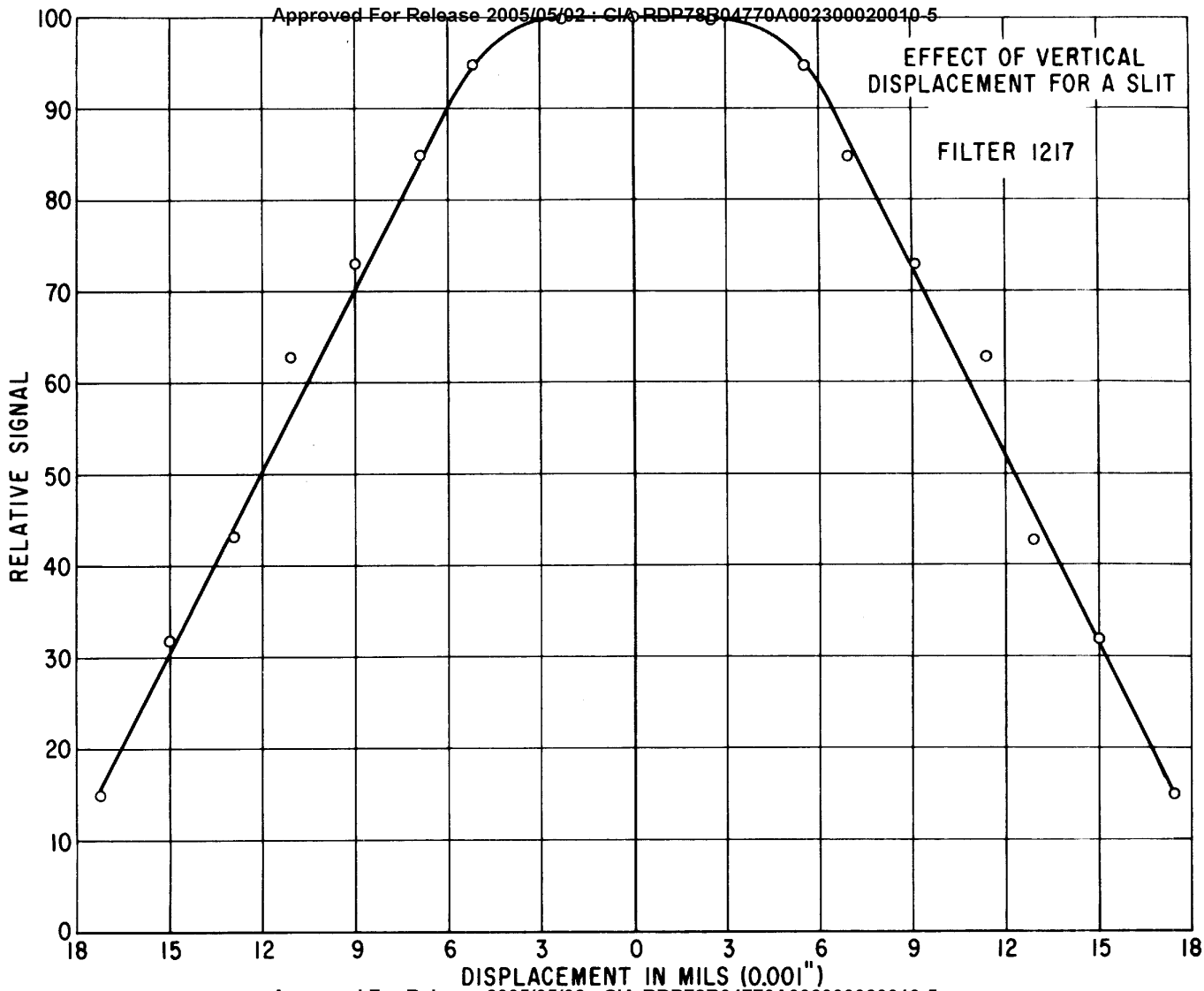

FIGURE 7

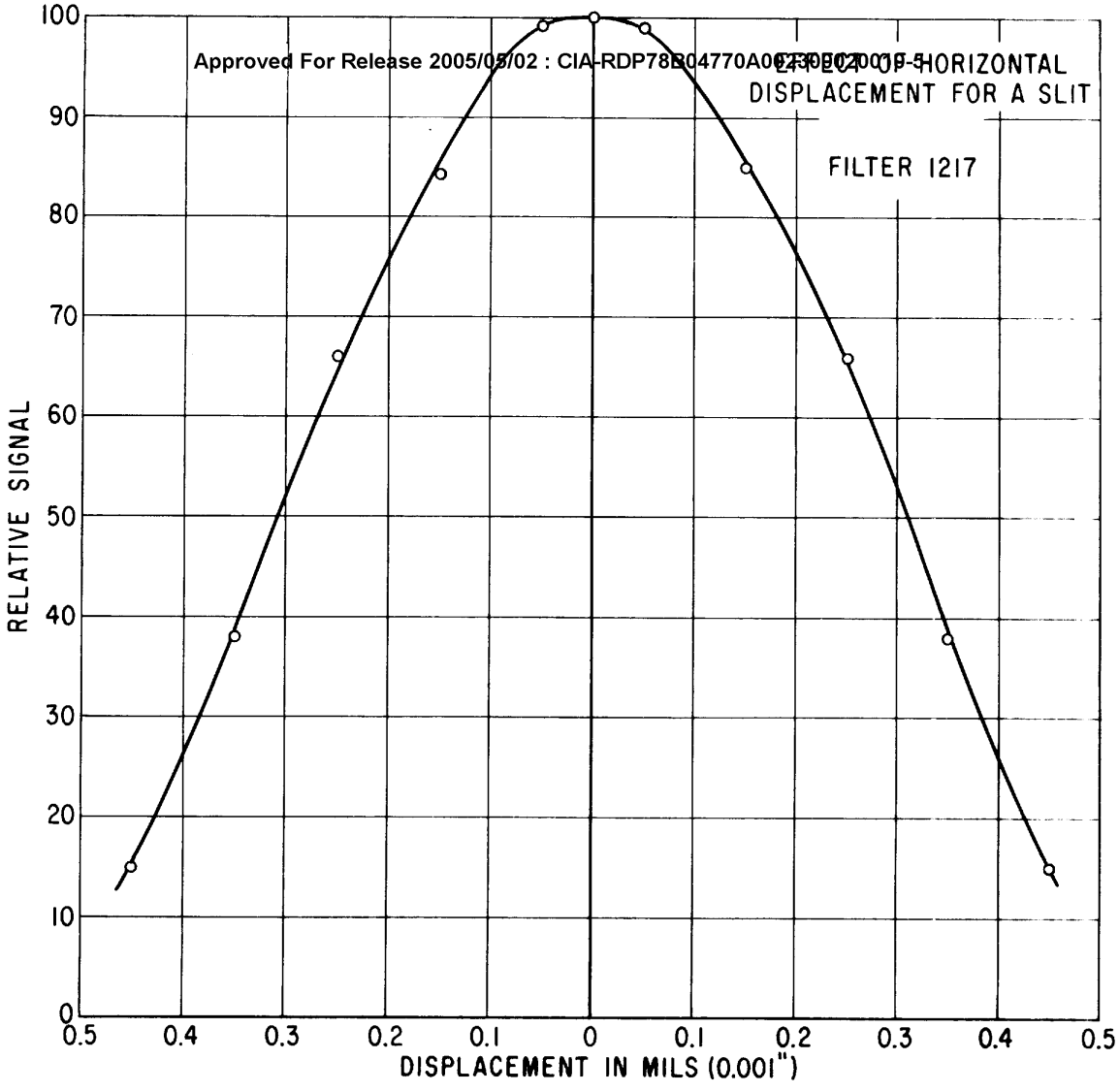

FIGURE 8

Conclusions on Spatial Filter Alignment Tolerance

1. The curve of recognition signal strength as a function of x or y error in alignment of the spatial filter is practically the same shape for any object that we would consider a "target".

2. This curve has a practically flat plateau at zero error and linear slopes. this means that small errors are insignificant and for larger errors the loss of signal is proportional to the displacement error.

3. For objects in the size range which we would consider as detectible "targets" an error of .001 inch results in negligible signal loss.

4. It should be possible to build an automated device to handle and change spatial filters to an accuracy of .001 inch.

5. A simple geometrical explanation for the observed error curve has been derived.

Section C-3

Rotation Tolerance of Spatial Filter

Purpose

If spatial filters are removed and replaced in the system or orientation alignment is a problem, or if the objects have to be scanned in orientation, then it is necessary to know the orientation or rotation tolerance of the filter.

Effect on Automation

If an automatic orientation search must be conducted it is necessary to know this tolerance to set a timing cycle.

Experimental Approach

A number of objects such as large and small vehicles, and characters were aligned with their spatial filters and the intensity of the recognition signal measured. The object or the filter was then rotated a small amount and the signal measured again. In this way a plot was made of signal as a function or orientation error. At the end of the work other objects such as slits were tested.

Experimental Equipment

The diffraction hologram of the object was carefully aligned with its spatial filter using a 60 power microscope. The spatial filter holder incorporated an accurately calibrated circular scale which can be read to 5 minutes of arc. Measurements of the signal were made with the Gamma Scientific photometric microscope which is linear to at least 1 percent.

Experimental Results

Every object and filter combination tested except one produced practically identical error curves. Figure 1 is typical and shows the result for an M-48 tank which measured 5 mm long on the object transparency.

The curves show a "plateau" near zero error and practically linear decrease in signal beyond this plateau. Examining this curve, it is possible to say that for objects of this general size and shape, 1/2 degree rotation error produces negligible signal loss, 2 degrees rotation error reduces the signal to about .80 its original strength, 4 degrees error results in a .50 signal loss and an error or 7 to 8 degrees usually reduces the signal close to the noise level.

All of the objects tested produced such similar results that it was decided to test two very unlikely objects. One of these was a slit 2 mm wide. The spatial filter of this object consisted of a series of very narrow lines in a straight line. Since these lines were not over .002" wide it was felt that a very small rotation of the filter would certainly cause the higher order elements to be displaced from their corresponding diffraction images and therefore a different error curve would result. The plot turned out to be practically identical to Figure 1 which seemed very surprising. The reason appears to be that it is possible to make a good spatial filter of a "wide" slit only if the lower spatial frequencies are included. These are located near the zero order and move on a short radius arm when the filter is rotated. If the spatial filter of a "wide" slit is made to include the higher frequencies only, it does not recognize the slit which is essentially a low frequency object. It does recognize the edges, but this recognition is very weak. To put

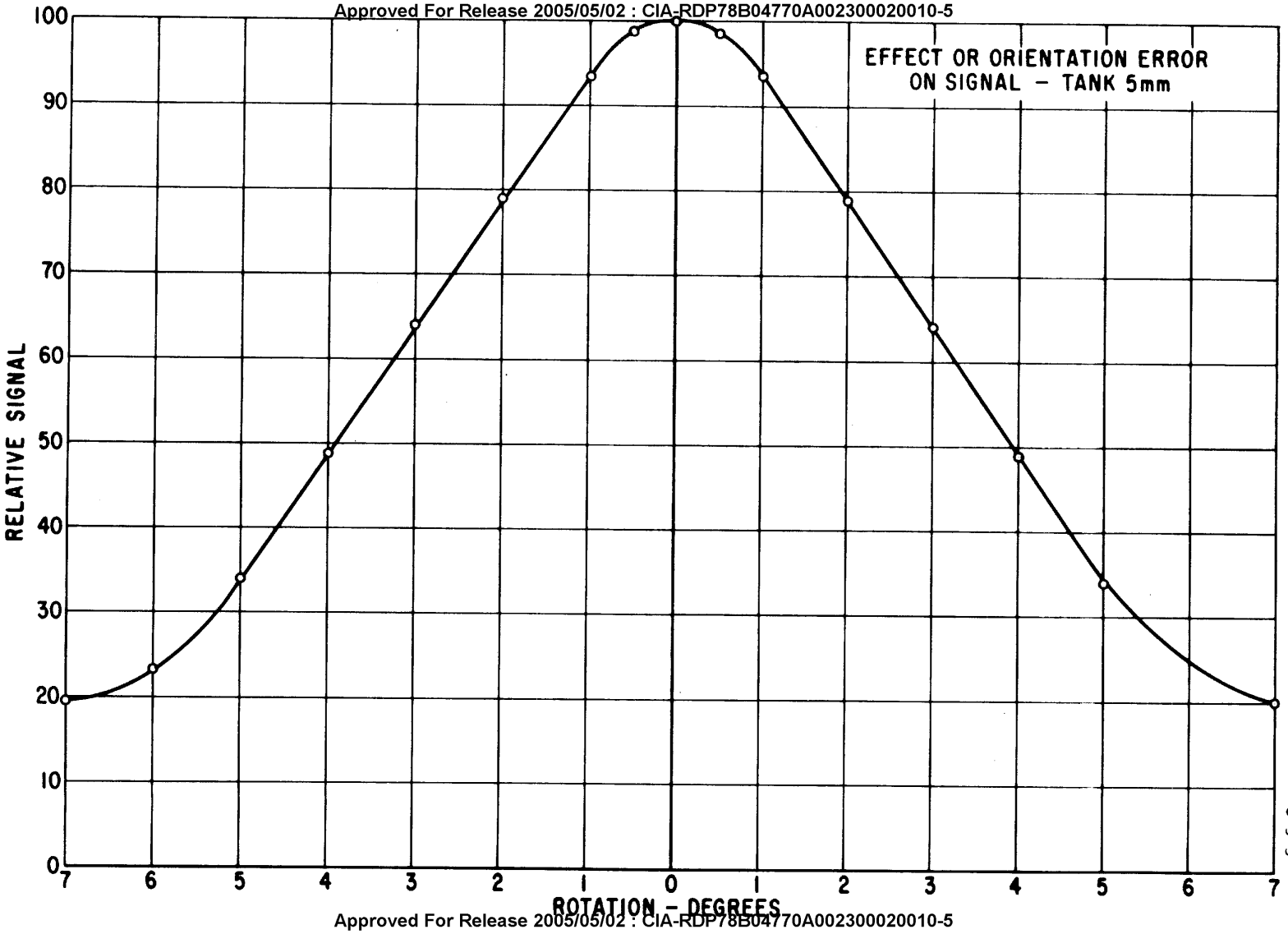

FIGURE 1

this conclusion in other words; the only part of the spatial filter of a wide slit that is effective is the part near the axis and since this rotates on a short arm the tolerance is relatively large. The higher diffraction orders are very conspicuous in the spatial filter, but appear to be completely inoperative.

A test was also made of a "narrow" slit only .2 mm wide. As might be expected, the first diffraction order is at a much greater distance from the zero order than in the case of the wide slit. It would appear that this would change the rotation tolerance, but the measured difference was insignificant. The explanation is that wide slits produce narrow, sharp images, but narrow slits produce wide fuzzy images. While it is true that the separation of the orders is greater in the case of the narrow slit and therefore the images move on a longer radius arm, the images are so much larger that the two effects practically compensate.

The only object for which we could obtain a noticeably different error function was a random noise pattern correlated with its spatial filter. This pattern consisted of about 40,000 irregularly shaped spots. A rotation error of 20 minutes of arc was enough to reduce the signal to .50 its normal value. At present we regard this as an example of a situation that would be unlikely to occur in aerial photographs.

Analytical Approach

In an earlier Section on Alignment Tolerance, a simple theory was developed to account for the observed error curve. Most of the same ideas are applicable here. Taking the spatial filter of a tank as an example, it consists of a number of "spots" which are the diffraction orders of the various details. It was found that only a few of the total number of spots were effective in the recognition process.

The following simplifying assumptions were made:

1. The only "spots" considered were the diffraction elements caused by the two parallel long sides of the tank.

2. The only orders considered were the 4th to 8th which were the only ones which showed appreciable modulation efficiency.

3. All the diffraction orders are shown equally spaced. The actual spacing is variable due to interaction of other diffraction elements.

4. All the diffraction orders are the same size. Actually the size varies with the intensity. The spots are drawn the average size for the 5th to 8th orders which appear to be ideally exposed and measure .200 mm diameter.

5. The interference detail in the filter has been omitted since it is not important in this interpretation.

Figure 2 shows the common area of the diffraction orders in the hologram of the object and the spatial filter with various amounts of rotation error between the two. It can be seem that the common area is approximately equal to the signal strength.

Conclusions on Rotation Tolerance

1. The curve of rotation error as a function of relative siganl intensity has a practically flat plateau at zero error and essentially linear slopes.

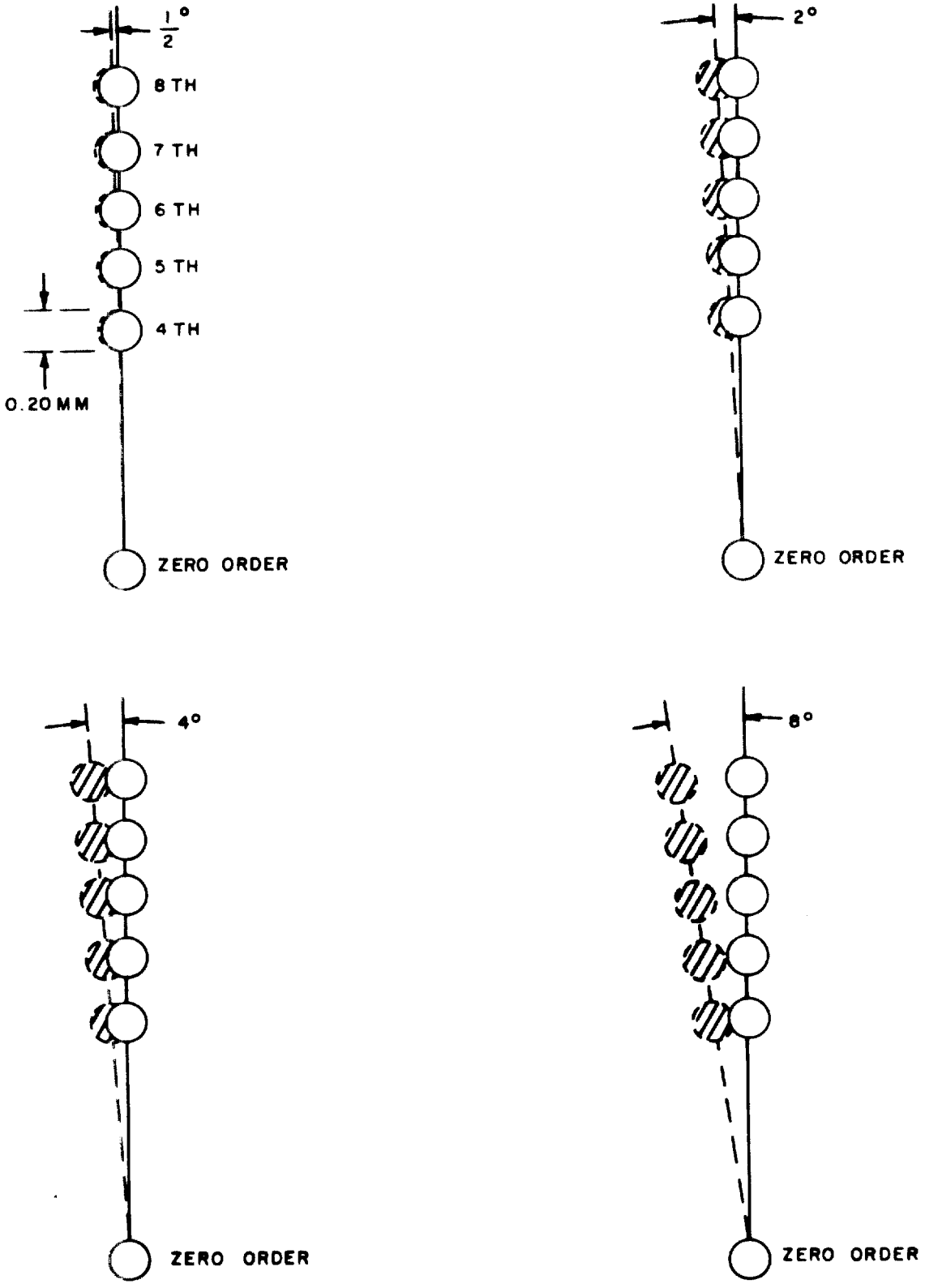

GEOMETRICAL EFFECT OF ROTATION ERROR
FIGURE 2

2. For the objects tested, a rotation error less than 1/2 of one degree results in negligible signal loss. Four degrees of rotation error reduces the signal to half its normal value.

3. The error curve is practically constant for many sizes and shapes of objects, even long slits.

4. It appears that a satisfactory mathematical solution for any orientation error can be derived from the geometry of the diffraction image.

Section C-4

Magnification Tolerance of a Spatial Filter

Purpose

In aerial photographs the size of the image on the film will vary with the altitude of the camera and the focal length of the lens. If the film is to be scanned with a spatial filter, then some way has to be found to bring the diffraction image of the object to the same size as the diffraction image in the filter. In the design of an automatic system it is necessary to know the tolerance on magnification in order to estimate the time cycle required to scan over a known degree of magnification change.

Experimental Approach

A transparency containing an object, vehicle or character was aligned with a spatial filter made for this object. The intensity of the recognition signal was measured. Then the relative magnification of the object was changed and the signal strength measured again. In this way it was possible to make a plot of magnification difference as a function of signal strength. A number of objects of different size and complexity were tested and the curves for all of them were close to that shown in Figure 1.

Experimental Procedure

The optical setup for these tests is not the usual one in which the object transparency is in collimated light because there is no simple way to vary the relative magnification. Instead the "overlapping" system shown in Figure 2 is used. The spatial filters for these tests also must be made on an overlapping system. As shown in the Figure, the transparency is installed in a converging beam and not in collimated light. If the filter was made with the object in the position shown, then it will detect the same object in this position. The diffraction angles of the various spatial frequencies in the object are fixed, but the size of the hologram

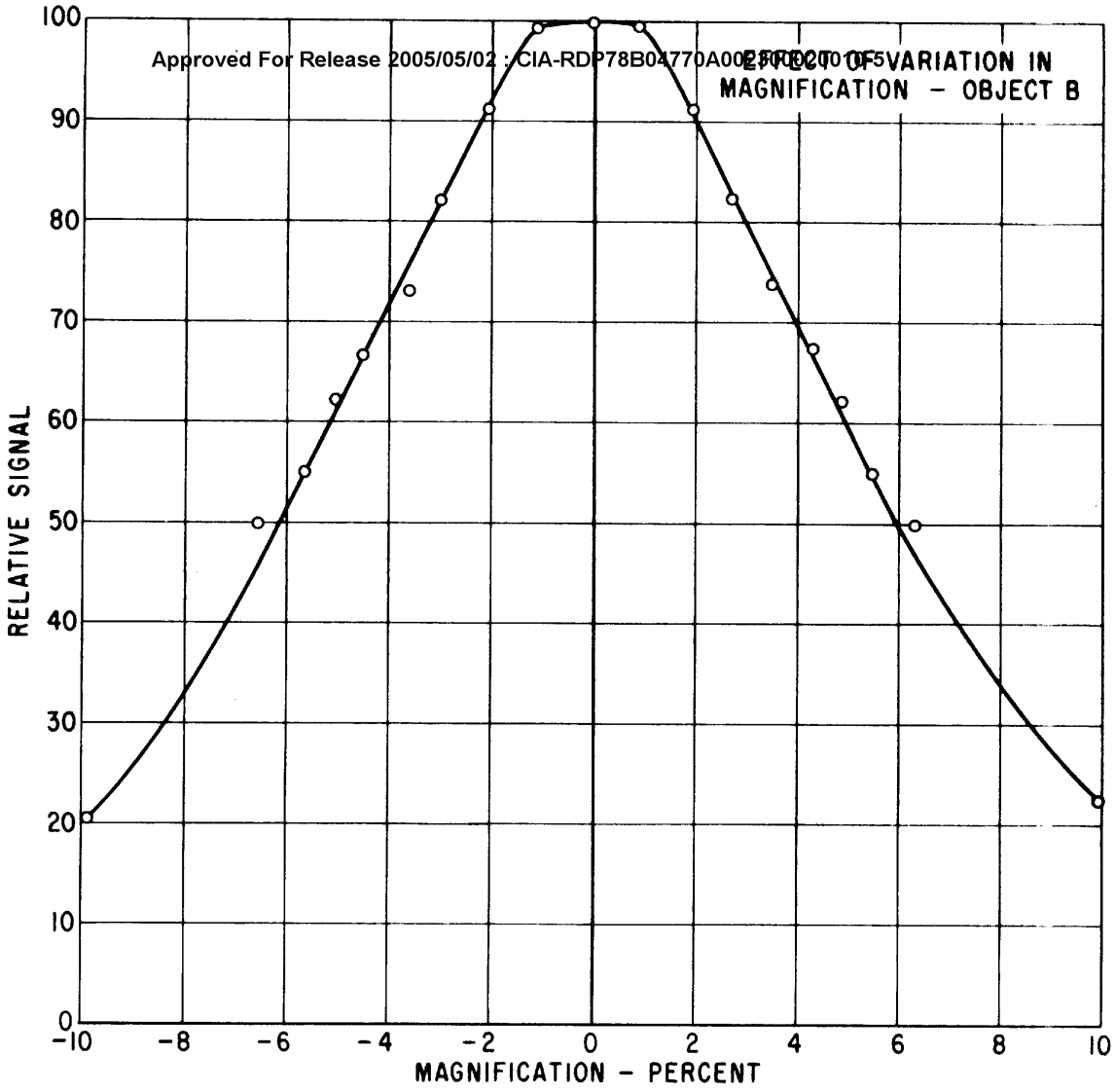

FIGURE I

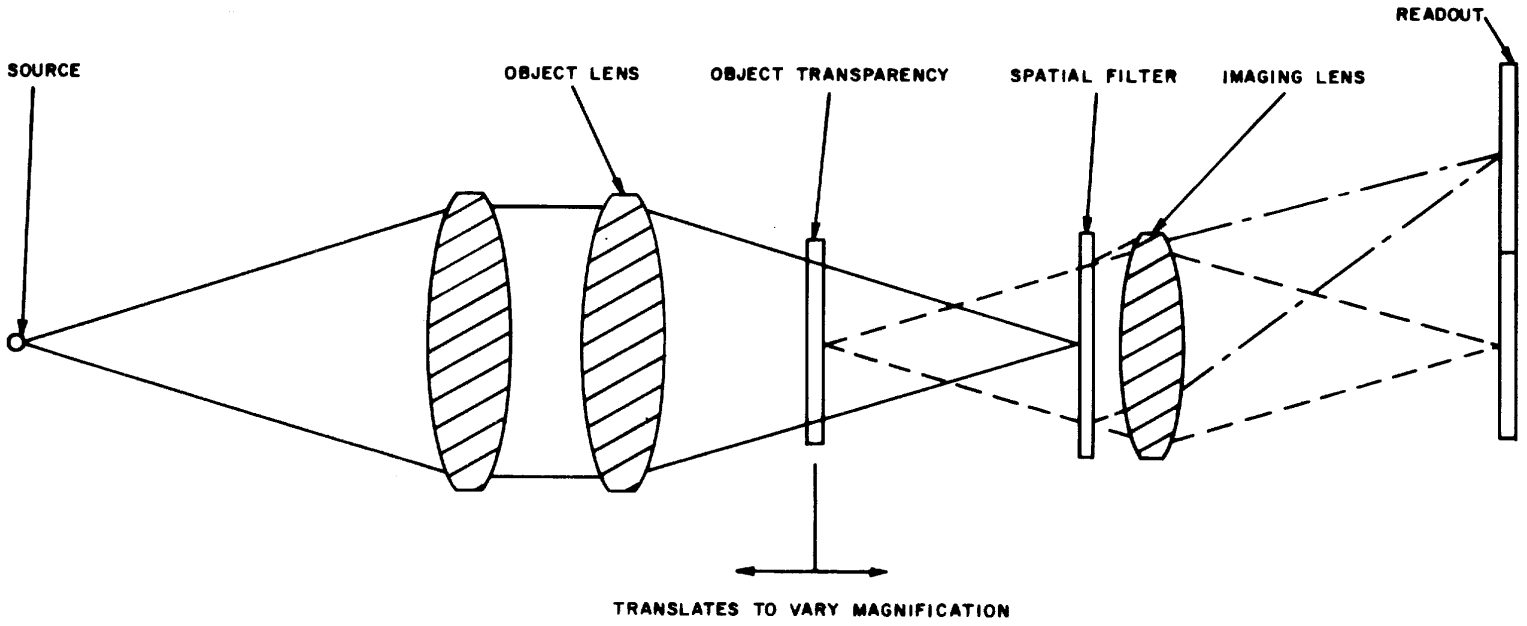

"OVERLAPPING" OPTICAL SYSTEM
FIGURE 2

depends on the distance between the object and the spatial filter. Thus, with the object as shown the diffraction image will fall exactly on the corresponding elements of the filter; as the separation is increased the diffraction angle stays the same but the size of the pattern gradually increases. Moved in the other direction the pattern decreases in size. By using a calibrated scale on the transparency slide it is possible to calculate the relative magnification knowing the focal length of the object lens and the original position of the transparency.

One peculiarity of any diffraction system is periodicity. When the object is twice its original size the diffraction image will be half as large and now the second order of the object will fall on the first order of the hologram and so forth. This is bound to happen in any system where the orders are uniformly spaced. For complex objects such as vehicles, these secondary maxima are barely detectable because the spatial filter contains size information on many different details and the orders are now complex. The probability of the 4th and 8th order for example, being exactly the same is less as the complexity of the object increases. To test this feature, a spatial filter was made of a round hole and in this case secondary recognition maxima occurred at exactly .5X and 2X magnification. In this simple case the intensity of these two secondary maxima were almost half, actually 42 percent of the correct size.

The purpose of mentioning this feature is that it may arise in trying to use spatial filters for simple shapes such as slits to detect roads in an aerial photograph.

Physical Explanation

No study was made of the physical causes of the phenomenon. It is fairly clear from the study of the models rotation and x and y translation what happens. As the relative magnification of the diffraction images and changes, less and less of them overlap.

Results

For all the objects tested, the results were practically the same. The strength of the recognition signal fell to .80 the maximum when the magnification varied plus or minus 3 percent, it fell to .50 when the magnification plus or minus 6 percent. For variations of magnification less than 1 percent the loss of signal strength was negligible.

Section C-5

Time Constants of a Scanning System

Purpose

If objects are randomly oriented in a transparency it is necessary to conduct a rotation or orientation "search" to recognize them. This is the process of rotating either the object transparency, the spatial filter or the image of the transparency until the two are in alignment. In an automatic system the readout would probably be a T.V. camera and it is necessary to perform the orientation search in such a way that no recognition spots are missed. If we assume the T.V. scan time to be .033 seconds, and we know the curve of recognition signal strength as a function of orientation error, then it is possible to calculate how long an orientation search will take.

In the same way, if objects may have a random size in the transparency it is necessary to conduct a scale search. This is usually done by changing the effective size of the objects by moving the transparency axially in a beam of convergent light.

The purpose of this section is to estimate the time to conduct an orientation and scale search in an automatic system.

Experimental Data

The necessary information on the effects of variation in orientation and scale on the signal strength were collected in two previous sections.

Discussion

It is necessary to decide what loss of signal is permissible. In the rotation experiments it was found that 1/2 degree of error produced negligible loss, 2 degrees of angle error reduced the signal to .8 its original strength and 4 degrees of error reduced it to .5. At present we believe that .8 signal is a safe minimum and this

results in an angle error of 2 degrees. The orientation search could be conducted either by rotation of one of the images 2 degrees per scan in a step-wise fashion, or by continuous rotation at the rate of 2 degrees per .033 seconds. It appears that continuous rotation is preferable from the point of view of less vibration. This means that if we wish to keep the signal strength at least .8 that a complete scan can be conducted in 180 x .033 or 5.04 seconds.

The figures for the scale search indicate that to obtain a signal not lower than .8 the value for a perfect match the magnification should not vary more than 3 percent. The time to make a scale search then depends on the range of scale to be covered. If it is plus or minus 25 percent then the scale search could be performed in 17 steps, each one requiring one complete orientation or 17 x 5.04 or 85.7 seconds for a complete orientation and scale search. Actually the scale variation would not be in steps, but would consist of changing the relative magnification gradually.

Result

For the case considered, where the signal should not drop below .8 of its maximum value and the scale is varied plus or minus 25 percent, a complete orientation and scale scan with a T.V. readout time of .033 seconds would require 86 seconds.

Clearly, none of these values is fixed and an automatic machine would have to have some sort of a variable programming device to adapt it to different conditions.

Conclusions

The search time for what is believed to be a typical case is about two minutes, including time to change transparencies.

Any automatic machine must be flexible to adjust to different conditions.

Section C-6

RECORDING MATERIALS STUDY

Purpose

The only satisfactory material for spatial filters known at the start of this project was Kodak spectroscopic plates 649-F. The normal time to process a filter on this material is one hour, though we believe this could be reduced to about 15 minutes by the use of an automatic processing machine.

Normally, the filters are removed from the equipment for processing and have to be returned to a position exactly on the optical axis.

The purpose of this study was to determine the feasibility of other materials with the objects of shorter exposure time, faster processing and no removal from the equipment.

Silver Photographic Materials

Spatial filters were made on spectroscopic plates type 103 and Kodak high-contrast copy film. The resolution of these emulsions was inadequate to produce a good record in interference detail.

Attempts were made to use Kodak High Resolution plates, but these were not sensitive at the laser wavelength.

Several other plates and films were tested without producing usable results.

Use of Photo Plastic Recording (PPR)

25X1 This term is used [redacted] to denote an electro-photographic process. One form of the recording material consists of a glass plate support and a thin plastic film on which the image is made. The glass support is normally 2 inches square and is coated with a transparent conductive film of tin oxide. At two edges of the support there are silver strips to contact the conductive coating. Resistance across a typical slide is 15 ohms and the light transmission is at least 85 percent. This support is coated with a thin film of a photoconductive thermoplastic. The coatings used in these tests varied in thickness from 11 to 20 microns.

PPR involves the following steps:

1. In the dark, the surface of the PPR plate is exposed to a corona discharge. This produces a surface charge in the range of 600-1000 volts. This charge can be retained for an hour or more if necessary.

2. The PPR slide is exposed to light. In the exposed portions the photoconductor allows the surface charge to leak through the plastic to the conductive coating which is grounded. The unexposed areas retain their charge.

3. The PPR slide is developed by heat. This can be done in a number of ways, but in the present experiments the plastic film was softened by resistive heating of the conductive film. The time required for development is .06 seconds. The effect of heating is to soften the thermoplastic so that the electrostatic effect of the surface charges will deform the film. On cooling these deformations are frozen. In general, the charged areas attract the ground plane and are depressed. The resulting image consists of ripples in the plastic surface, a completely transparent image, but one capable of refraction, diffraction and phase modulation.

After processing, the image may be erased by a longer heating cycle and the slide reused. This longer cycle melts the thermoplastic and heats the photoconductor to the point where it becomes a conductor. This completely discharges the slide and leaves it with a smooth surface.

Sensitivity of PPR

The #216 PPR slides are not red-sensitive. It was necessary to develop a special formulation known as PPR 334* containing a proprietary sensitizer to be used with laser light at 6328 Angstroms. Unlike normal PPR slides this material is not completely transparent, but blue in color and a fairly strong absorber of red light.

* The results to be reported were obtained with the very first #334 materials prepared. The data and inferences drawn from it must therefore be viewed as preliminary.

Theory of the Use of PPR Spatial Filters

The two-beam process for making a spatial filter uses the interference of two beams of coherent monochromatic light, one of which contains diffraction produced by the object. This complex image contains both phase and amplitude information about the object, and normally this is recorded on silver-bearing photographic emulsion. After processing, this filter can be used to recognize the same object in a larger body of information. The design of the equipment is such that both the phase and amplitude information can be recorded as light wave amplitude or variations in density in the photographic material. Such a filter is described as a "complex amplitude-modulating filter".

It is equally possible to record the phase and amplitude information on a transparent deformable material such as PPR so that the resulting filter modulates the phase of the incident light. This kind of filter is called a "complex phase-modulating filter".

So far as we can tell from theory, there is no essential difference between the two types of filters, there are, however, several practical differences.

Practical Differences between Amplitude and Phase-Modulating Filters

The amplitude-modulating or silver-bearing filter can exist in either a negative (exposed portions opaque) or positive (exposed portions transparent) filter. In some cases the performance of these two kinds of filters is quite different. In the case of phase-modulating filters it is difficult to tell a negative from a positive and there is no apparent difference in their performance.

The amplitude filter contains opaque material (silver grains) which obstruct part of the light incident on the filter, reducing the amount of light in all of the transmitted images. The phase filter can be completely transparent (neglecting surface reflection losses) and the total light in the transmitted images is essentially equal to the incident light.

A two-beam spatial filter produces a recognition image that is off-set from the optical axis or zero-order image. The ratio of the light in this off-set image, compared to the light incident on the filter is termed the modulation efficiency of the filter and is the chief factor in determining the intensity of the recognition image. The modulation efficiency of an amplitude filter, based on reasonable assumptions, is limited to about 16 percent. The efficiency of a phase-modulating filter can be over 40 percent. Therefore the brightness of the recognition images and in general the light efficiency of the whole process should be two to three times higher with a phase filter.

Relative Speed of PPR

"Speed" in this case refers to the idea of light sensitivity for a particular application. A light sensitive material is said to be "fast" if it requires a short exposure and "slow" if it requires a long exposure.

The recommended silver photographic material for making spatial filters is Kodak spectroscopic emulsion 649-F on either glass plates or film. There are several problems with this material. The sensitization curve falls off rapidly in the red so that the material is not efficiently used at the laser wavelength of 6328A. In spite of several experiments, no better commercially available material has been found.

The most undesirable feature of 649-F is its slow speed. A typical spatial filter on our 5-inch aperture system requires an exposure 2 to 10 minutes.

The same exposure may be obtained on red-sensitive PPR in from 5 to 20 seconds, using a charge of 33 volts per micron of thickness of the PPR coating.

It should be understood that the speed of any light-sensitive material is difficult to define except for a specified set of conditions. The effective speed of a photographic film can be increased through special development or hypersensitization by a factor of ten times or more. The speed can also be reduced by desensitization and underdevelopment. In exactly the same way, the speed of PPR is not a fixed quantity, but depends on the charging stress and can be altered by changing the development time. It is possible to obtain considerably higher speed on PPR than that reported above by using a higher surface charge, but such slides were "frosty" or noisy and make poor spatial filters. (There have been substantial improvements.)

The conclusion on speed is that red-sensitive PPR is at least 50 to 100 times faster than the only satisfactory silver material presently available. This is an advantage in the case of poorly transmitting objects where the exposure can be reduced from an hour to 40 seconds.

Surface Quality of PPR Slides

The two separate optical systems used to make and use spatial filters are close to "perfect" systems which means that they are performing close to the limit to which light waves can be focused and controlled. It can be predicted from theory or easily confirmed by experiment that relatively minor departures from this perfection will cause a major reduction in the recognition signal-to-noise ratio.

These imperfections are easily introduced in the system by installing a glass plate that is not uniform in thickness or refractive index or which has obvious light-scattering defects on its surfaces such as scratches or roughness. This problem is common to silver-bearing and PPR materials, with one important difference; means has been found for compensating for the defects in silver-bearing amplitude materials, but no means of compensation is known in the case of PPR phase-modulating spatial filters.

If the glass plates on which silver filters are made are not flat or uniform in thickness they introduce deviations in the diffracted rays. It should be recalled that the diffraction angles realized in this system are small, only a few minutes of arc at most, and into this few minutes is crowded a tremendous amount of detail. The size of this detail is more or less determined by the diameter of the zero order diffraction image of the source, and in a typical instrument will be about two seconds of arc. As a result of this, any glass plate that randomly deviates or scatters an appreciable portion of the rays by two seconds of angle or more will appreciably degrade the system. In practical terms this means that a plate of clear glass which appears perfect to the eye may, when added to the system cause it to stop working. Most of the glass plates on which photographic emulsions are coated are not of a quality good enough to place in one of these optical systems. As result, liquid gates have been developed to "compensate" this effect. A liquid gate is a transparent cell with two parallel windows made of tested high-quality glass. The cell is filled with a liquid having the same refractive index as the glass and when a low-quality glass plate is placed in the cell the effect is to smooth out the irregularities in the glass surface. In effect, the cell windows, liquid and photographic plate all have the same index and so become optically a solid piece with two near-perfect surfaces, the cell windows.

We have tested several of the glass plates on which PPR is normally coated and all of the plates tested to date have been adequate for spatial filters. This does not mean they are "perfect", they usually show detectable degradation of the diffraction image, but this appears to be intermediate in amount between normal glass photographic plates which are mostly usable and "Microflat" glass which is the best material we can obtain and is virtually perfect. At present we believe that the surface quality of the glass plate or support is not a problem.

Such defects as we have noted in PPR slides were attributed to three causes:

1. Irregularities in the thickness of the coating, especially at the edges. This can be avoided by using only the center and masking the edges.
2. Dust embedded in the surface of the slide. This is rarely present in a new slide, but increases as the slide is used as described in a paragraph titled, "Reusability".
3. Overall roughness of the PPR surface which either cannot be erased or which returns on redevelopment.

At the present time these slides are handmade and a dust-free environment is not available for their production. It is expected that future improvements in coating technique will nearly eliminate these defects.

The conclusion surface quality is that selected PPR plates are adequate for any spatial filters that have been attempted. The selection process is simple and fast. About 75 percent of the first batch of slides was usable.

Resolution of PPR

One of the requirements for material for spatial filters is high resolution in order to be able to record fine interference detail.

The resolution of spectroscopic emulsion 649-F is so high that it cannot be measured optically. This means, that judged from measurements of the grain size and attempts to form very fine optical patterns with microscope lenses, the resolution is probably in excess of 1000 lines/mm. As mentioned earlier, this is the only completely satisfactory silver-bearing photographic material yet found.

The resolution of Kodak high contrast copy film when given ideal development is about 250 lines/mm. We have made many spatial filters of identical objects on both these materials and there is no question that the spectroscopic film produces a spatial filter with a higher modulation efficiency and one which results in a crisper reconstructed image.

When emulsions showing less than 150 lines/mm are used, the resulting spatial filters show very low efficiency, and have proven to be useless.

Spatial filters made on red-sensitive PPR appear to be equal to those made on spectroscopic emulsion in every test we have been able to make and also in general appearance of the detail when examined under a microscope at high power. The conclusion at present is that PPR has adequate resolution and this must be greater than 250 1/mm and probably is in the region of 1000 1/mm.

PPR Equipment

The special equipment for handling PPR consists of the following assemblies:

1. Charging and development station.
2. Charging head and power supply.
3. Development power supply and timer.
4. Mechanical traversing device.
5. Charge measuring head and meter.
6. Development microscope.
7. Slide evaluator.

1. Charging and Development Station

This equipment is essentially a holder for the PPR slide and is built on an optical bench carriage. The PPR slide is held in a vertical position which is not the normal practice, but which seems to have given no trouble.

Spring-finger contacts are provided to make electrical contact to the slide. The slide holder is designed to position the slide by its front surface so that variation in slide thickness will not affect the focus.

This station also supports the mechanical traversing device with its charging and measuring heads and the charge measuring meter.

2. Charging Head and Power Supply

The charging head consists of a fine tungsten wire surrounded on three sides by shields. When 5,000 to 10,000 volts is applied to this small wire it produces a corona discharge which charges the dielectric surface of the slide. A uniform charge is produced by traversing this head across the slide. Two passes are normally made.

The power supply consists of a calibrated variable transformer and a solid state 10 KVDC power pack. Normally voltages between 5,000 and 8,500 volts are used to charge the wire in the charging head. This will produce a surface charge on the slide between 400 and 800 volts. The chief control on surface charge is the charge on the head which can be varied by the variable transformer.

3. Development Power Supply and Timer

The power used to heat the PPR slide for development or erasure comes from a variable transformer. The total power used is 480 watts, the voltage being adjusted according to the slide resistance.

The development or erasure cycle is timed by a cycle timer developed by

25X1 [redacted] this is a solid state device which can be set to pass any number of full cycles of 60 cycle current from 1 to 24. A feature of the device is that it cuts on and off at the zero voltage point of the cycle so that not only is the number of cycles exact, but each one is exactly a full cycle.

In the experiments described, the recommended development times were as follows:

Development - 7 cycles

Erasure - 24 cycles

The development circuit also contains a 1 KW isolation transformer. This is necessitated by the fact that the conductive coating on the PPR slide is used for two purposes; to heat the slide and also to act as a ground plane for the surface charge. For this latter purpose it is absolutely necessary that one side of the slide be grounded to a real, not a nominal ground. In fact, one side of the high-voltage charging circuit, the electrostatic voltmeter and the corona shield all have to be directly connected to this same ground. Since it is unsafe to ground one side of an alternating current power line, the isolation transformer is used to separate this circuit.

4. Mechanical Traversing Device

This assembly consists of a pair of accurate rails, a motor-driven carriage supporting the charging head and charge measuring head. It is essential that these units maintain a constant distance from the slide and that the charging head move at a constant velocity. Minor variations in distance will produce major variations in the charge or the apparent measured charge.

5. Charge Measuring Head and Meter

The measuring head is a unit developed at this laboratory and is standard on all PPR equipment. For proper operation it is positioned .040" from the slide surface.

The meter is a Keithley electrostatic voltmeter, model 200B. It is installed on the charging and development station because the lead length from measuring head to meter should be as short as possible and not over three feet. When the surface charge on a slide is about 600 volts the charge induced in the measuring head is 0.5 volt. The measuring head has to be calibrated so that the meter readings can be converted to actual surface charge.

There are four quite different voltages in the charging system, all of which have to be correlated:

a. The voltage shown on the variable transformer input to the high voltage power supply. This is the primary control of charging voltage and varies between 50 and 85 volts.

b. The voltage on the charging head which varies between 5,000 and 8,500 volts.

c. The actual charge on the slide. This varies between 400 and 800 volts.

d. The actual voltage on the measuring head and indicated by the meter. This varies between .4 and .8 volts.

6. Development Microscope

Normally, PPR images are developed by inspection. An instrument for red-sensitive PPR has presented several serious problems and no solution was found in time for inclusion in this project.

7. Slide Evaluator

It is very difficult to see the diffraction image of a spatial filter on a PPR slide. This makes it impossible to look at the filter and determine whether or not it is properly exposed and developed, contains defects, etc.

The fine detail of the filter can be seen and photographed in a phase-contrast microscope. Since these instruments are not available at less than 100X this means that only a small area of the filter can be seen. A typical spatial filter is 20 mm in diameter, while the field of view of a 100X microscope is only about 2 mm.

One of the desirable measurements in evaluating spatial filters is the number of orders of diffraction recorded. A crude reflected-light schlieren device was made for this purpose and proved to be indispensible.

DESCRIPTION OF PHOTOS OF PPR EQUIPMENT

Figure 1 -

General view of complete PPR equipment on optical bench. PPR slide is shown in position on optical axis. Carriage supporting charging head is in extreme left position. Meter at top reads surface charge.

Under the bench the charging power supply has the high voltage control and motor traversing switch. The cycle timer regulates the length of the development cycle and is set to 7 cycles. The development power supply at left contains the variable and isolation transformers.

Figure 2 -

Closeup of the equipment surrounding the PPR slide. The slide surface is located by the Teflon guides on both sides. Electrical contact is made by spring finger contacts at top and bottom.

The carriage rides on two round rails at top and bottom. The reversible traversing motor is mostly hidden by the carriage, a pinion on the shaft engages the rack above the top rail. Attached to the carriage and moving with it are the charging head with high voltage wires leading to it and grounding shields surrounding it. To the left is the charge measuring head which can be positioned over the center of the slide when the carriage is traversed to the right.

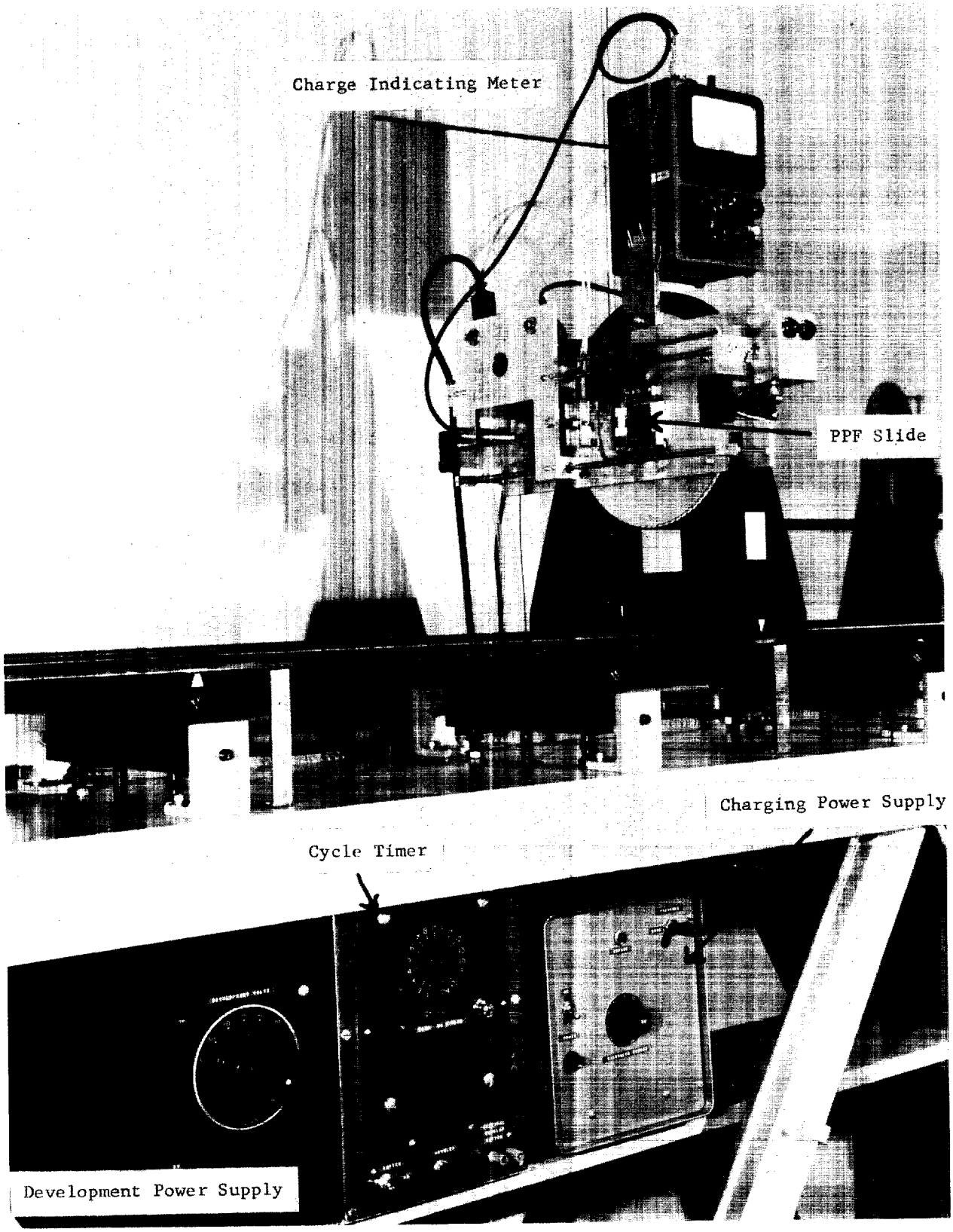

FIGURE 1 (ATL Photo 842401)

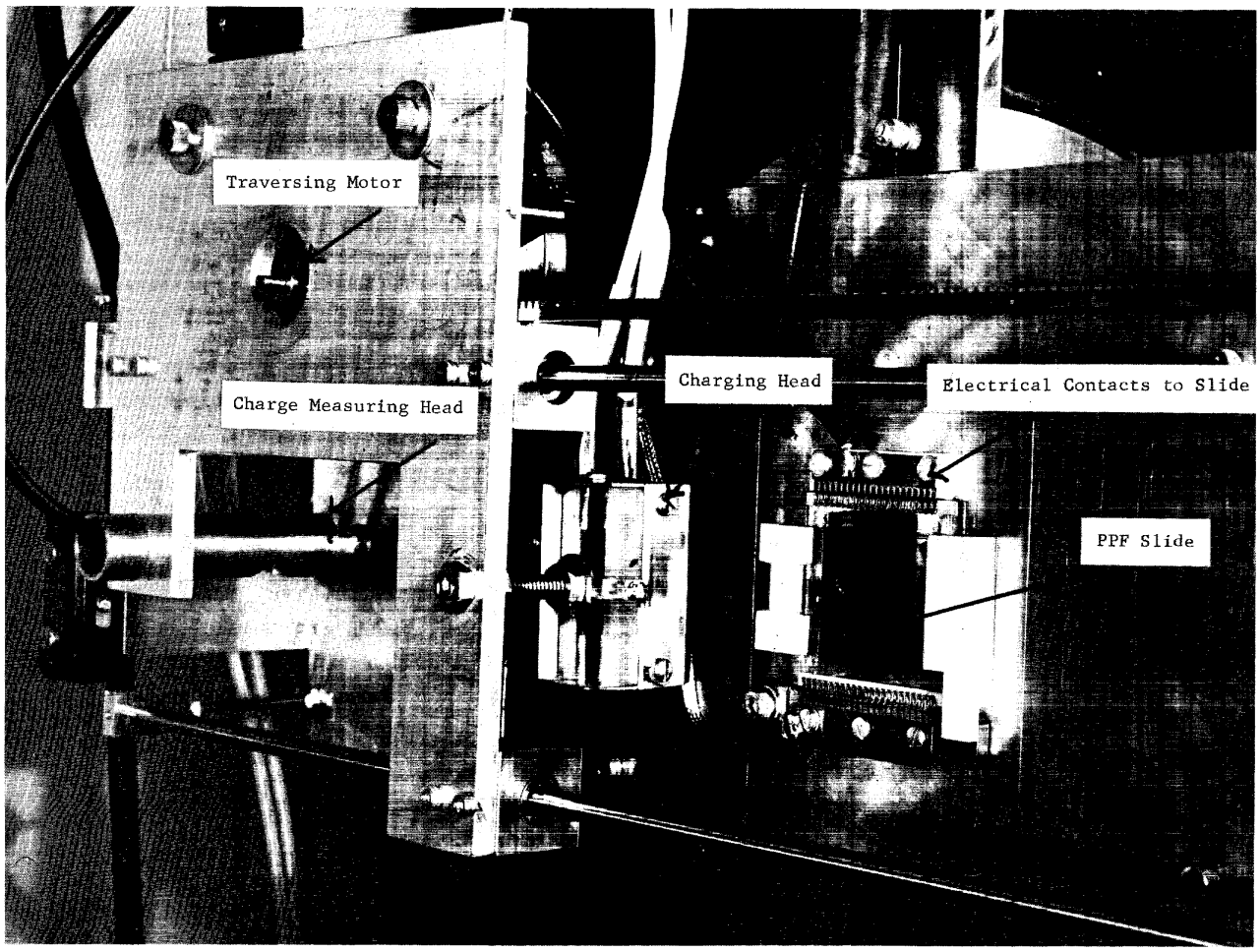

FIGURE 2 (ATL Photo 842402)

Making a PPR Spatial Filter

The process of making these filters has not been automated to the point where it is a matter of pressing a button. It appears to be entirely feasible to automate the process, but this was not considered in our experimental setup.

The first three steps are common to the process for making either a PPR or silver photographic filter, they are mentioned only to give an idea of the preparation required.

1. An object is selected and made into a transparency.
2. The object is placed in the sample beam and the reference beam is attenuated to a value which produces optimum interference in the desired diffraction order. This decision influences the selectivity of the final spatial filter.
3. The exposure is calculated to produce a properly exposed filter. Failure to achieve this results in a filter with low modulation efficiency.
4. A PPR slide is installed at the focus of the diffraction image.
5. The PPR slide is "cleared" if necessary. PPR coatings are hygroscopic and absorb moisture which produces a rough surface when the film is developed. To remove this moisture the slide is "cleared". The clearing process is erasure, except that in general, no image is present. The present clearing cycle is 21 cycles at 480 watts. To obtain this, the resistance value of the slide is converted by a chart to a voltage value to be applied to the development circuit

and this value is manually set on the variable transformer and the clearing or erasure cycle completed. If the slide has been erased within the previous 8 hours then it can be assumed that it has been cleared and this step is not required.

6. The PPR slide, if cleared, is cooled to room temperature. The time required depends on the heat sink available.

7. The PPR slide is charged. In total darkness, or using a tested safelight, the charge head is traversed across the slide twice while applying a high voltage to the head. The voltage is regulated by a calibrated variable transformer and is adjusted by experience to produce a surface charge of 33 volts per micron of thickness in the PPR coating. The thickness of the coating can be obtained from the slide container and the transformer is manually adjusted to the proper value.

8. The charge on the PPR is measured. This step should not be necessary in routine work, but it is essential at the present time. The charge measuring head is attached to the same carriage as the charging head. To make a measurement, the measuring head is first discharged of any stray atmospheric charge by pressing the shorting button on the electrostatic voltmeter, then the measuring head is moved over the center of the slide and the charge read. It is helpful to have a safe-lighted meter. The meter reading is converted by a chart to give the actual slide charge which should be close to that calculated in the last step. If the charge is too low it may be increased by extra charging passes or by increasing the charge on the head and making extra passes. It may be desirable

at this time to observe the meter for at least 15 seconds to determine if the charge is leaking. A decreasing charge can result from light leakage, a poor slide, or a slide that is not fully cooled. A warm slide will not hold a charge.

9. The charge measuring head is moved out of the way.
10. The PPR slide is exposed. At present this is done manually using a stop watch.
11. The PPR slide is developed. The voltage in the developing circuit is manually set at described under 5 above, and the timer set to recommended development time which is 7 cycles and the "start" button pressed.

This completes the PPR spatial filter. As can be seen, the operation at present involves a number of hand motions, decisions and corrections and may take about three minutes of elapsed time. This could be reduced to about 20 seconds plus exposure time.

Modulation Efficiency

1. Theoretical

The silver photographic process produces an "amplitude" spatial filter. The theoretical maximum modulation efficiency of such a filter is 16.4 percent. This calculation was based on a number of assumptions that are not necessarily correct:

a. The opaque lines are totally opaque.

b. The transparent lines are completely transparent.

c. The width of the opaque and transparent lines is equal.

In a photographic grating it is extremely difficult to meet these conditions exactly, and actual filters have shown measured modulation efficiencies between 2 and 10 percent. Actually, the situation is more complex, because there is usually a surface relief image on the silver film which acts as a phase grating. Thus, the usual silver photograph spatial filter is a combination phase and amplitude filter in which the opacity of the amplitude image attenuates the efficiency of the phase image. As a result, silver filters can have efficiencies higher than the theoretical 16.4 percent and 20 percent has been measured.

A completely transparent phase-grating such as produced on PPR can theoretically show a modulation efficiency over 40 percent, this being one of the advantages of this material. Actual samples of PPR tested on the two modulation efficiency instruments consistently show values in the neighborhood of 40 percent if correctly exposed and developed.

2. Actual Results on Spatial Filters

The first phase-modulating spatial filters were made by contact printing a silver filter on blue-sensitive PPR. These filters were "noisy" due to the mechanics of the contact printing process, but they showed modulation efficiencies of about 35 percent which was higher than we have ever obtained or can expect to obtain with silver filters.

The modulation efficiency of red-sensitive PPR filters has measured about 2 percent. The reason for this is that the 334 PPR formulation contains a red-absorbing sensitizer, which in typical slides has a transmission for laser light

of only 5 percent. This value can be obtained either from the spectrophotometric curve or by measuring the optical density of the slide in red light. If such a slide had an inherent modulation efficiency of 40 percent and a transmission for red light of 5 percent the measured modulation efficiency in the recognition setup would be only 2 percent which is the actual value obtained.

An attempt was made to increase the red light transmission of the slides by reducing the sensitizer content, but no images were obtainable on these slides. Apparently, there is a minimum sensitizer content below which the material fails to form a conducting chain through the dielectric film.

The conclusion on efficiency is that the inherent modulation efficiency of PPR is about twice as high as silver-bearing photographic film. This has been measured on PPR containing no absorbing material. The code 334 red-sensitive formulation contains a red-absorbing sensitizer which transmits only about 5 percent of the incident light resulting in a low efficiency. This is the first red-sensitive formulation tested. There is every reason to believe an improved material can be found.

Reusability of PPR

Theoretically, PPR is reusable indefinitely. At the end of considerable use the image tends to become "sticky" (difficult to erase); the modulation depth is less (lower efficiency). It is possible to predict that continued development and erasure heat cycles will evaporate the more volatile portions of the film and result in a thinner, denser coating. It is also possible that continued heating may degrade the sensitizer and cause a loss of sensitivity.

In practice, none of these effects has been of any importance because when the images are made and developed in air they attract dust which becomes part of the surface during the erasure cycle and after several cycles the slides become too dusty or "noisy" to use.

In our experiments, no attempt was made to exclude dust or determine the maximum reusability of a PPR slide. We found that a slide could be used about 15 times before the "noise" became objectionable. Several circumstances should be pointed out. First, the charging cycle places a strong static charge on the dielectric surface of the slide. This appears to attract the nearby dust, also the corona discharge probably accelerates the dust in the air between the charging head and the slide and drives it onto the slide with considerable force. Secondly, these slides are removed from the equipment for other tests and have ample opportunity to collect laboratory dust, more than they would if kept in the equipment for routine use.

It has been suggested that if the area around the charge and development station were enclosed and supplied with relatively dust-free air that the reusability of the PPR slides might be extended to a 100 or more uses.

PPR Experiments

A typical image of a model tank was selected as an object and spatial filters made on PPR and the best silver photographic material available, Kodak spectroscopic plates 649-F on Microflat glass. In each case the exposure was adjusted to give an image which showed the same amount of detail when examined under a suitable microscope. In the case of silver-bearing filters the maximum density was recorded and for PPR filters the modulation depth was measured.

The silver and PPR spatial filters were then used to recognize similar objects in other transparencies. The tolerance of alignment, the recognition signal strength and the signal-to-noise ratio were then measured for both cases. So far as could be told, the properties of a good PPR spatial filter are no different from those of a good silver-bearing filter.

The only difference between results obtained with the two kinds of filters was that the recognition signal strength was about one-tenth as high when PPR filters were used. This is contrary to the predicted higher efficiency of PPR filters and is due to the absorption of red light in the present red-sensitive PPR material. This is described separately under "Modulation Efficiency". We have calculated that if the PPR slides were colorless, their recognition signals would have been 2 to 3 times higher than that of the silver filters.

Results

1. The signal-to-noise ratio of the recognition signal is equal for equivalent silver and PPR spatial filters.
2. The absolute signal is stronger with non-absorbing PPR than the test silver filters. Red-sensitive PPR material has low transmission for red light and the signal is attenuated by this absorption.
3. PPR filters can be processed in much less time than silver filters.
4. PPR material has adequate resolution.
5. Red-sensitive PPR requires a much shorter exposure time than satisfactory silver material.
6. PPR material is reusable.

Section C-7

FEASIBILITY OF REAL-TIME FILTER GENERATION

In a strict sense "real-time" means instantaneous, but in connection with systems development it has come to mean any short time which is comparable to other necessary short delays in the process. It implies that the step under consideration is not the time bottleneck in the processing cycle. If we are willing to accept this more liberal interpretation of the term, then Photoplastic Recording (PPR) has been demonstrated as a successful means for real-time filter generation.

We have looked at this two ways:

1. The total elapsed time to make a silver-bearing filter on 649 material was two minutes exposure plus one hour processing. The total elapsed time to make a PPR filter of the same subject was 10 seconds exposure plus twenty seconds charging time plus a fraction of a second development. From this point of view, the PPR filter is finished before the silver filter was even exposed.

2. If we regard the exposure time as a separate item and count as the time for filter generation only the processing interval, then the present PPR processing time could easily be as short as 20 seconds, or less if the slides were pre-charged. Since this period is short compared to the exposure time, it can be regarded as not seriously delaying the process.

Section C-8

Television Readout of Recognition Signals

Introduction

Some sort of electrical readout is a necessity. Due to the high noise background of the image as a whole, it is not possible to use a simple photocell to detect the recognition signals. These recognition spots are bright, but they are so small that they add very little light to the total integrated light in the image. The only readout that appears feasible at present is a closed-circuit TV chain in which the camera scans the image and large increases in the video signal will be produced when the scan pattern crosses a recognition spot. In its simplest form, this signal would trip a counter when it was above a specified noise level. The TV chain used, without the counters is shown in Fig. 1.

In practice something more sophisticated is required. There are two reasons for this. First, tests to date indicate that a recognition spot appears not in one scan line only, but in two or more. The system we have used is non-interlaced to avoid the problems of successive lines occurring in different frames. Under ideal conditions, when the center of a recognition spot is coincident with the center of an individual horizontal scan line, a strong video signals is generated as the scan line passes through the spot. Successively weaker signals appear in the one or two lines immediately above and below the center of the spot. Alternatively, if the center of the recognition spot falls between scan lines, two pulses of more or less equal amplitude occur in the two adjacent lines, again with weaker pulses above and below. Throughout our tests, close inspection of the monitor screen as well as CRO traces of individual lines of video signal showed pulses on between one and five successive lines depending upon spot intensity and position. Fig. 2a shows the CRO traces of six successive scan lines. The recognition shows as a spike on the 3rd, 4th, 5th and 6th lines.

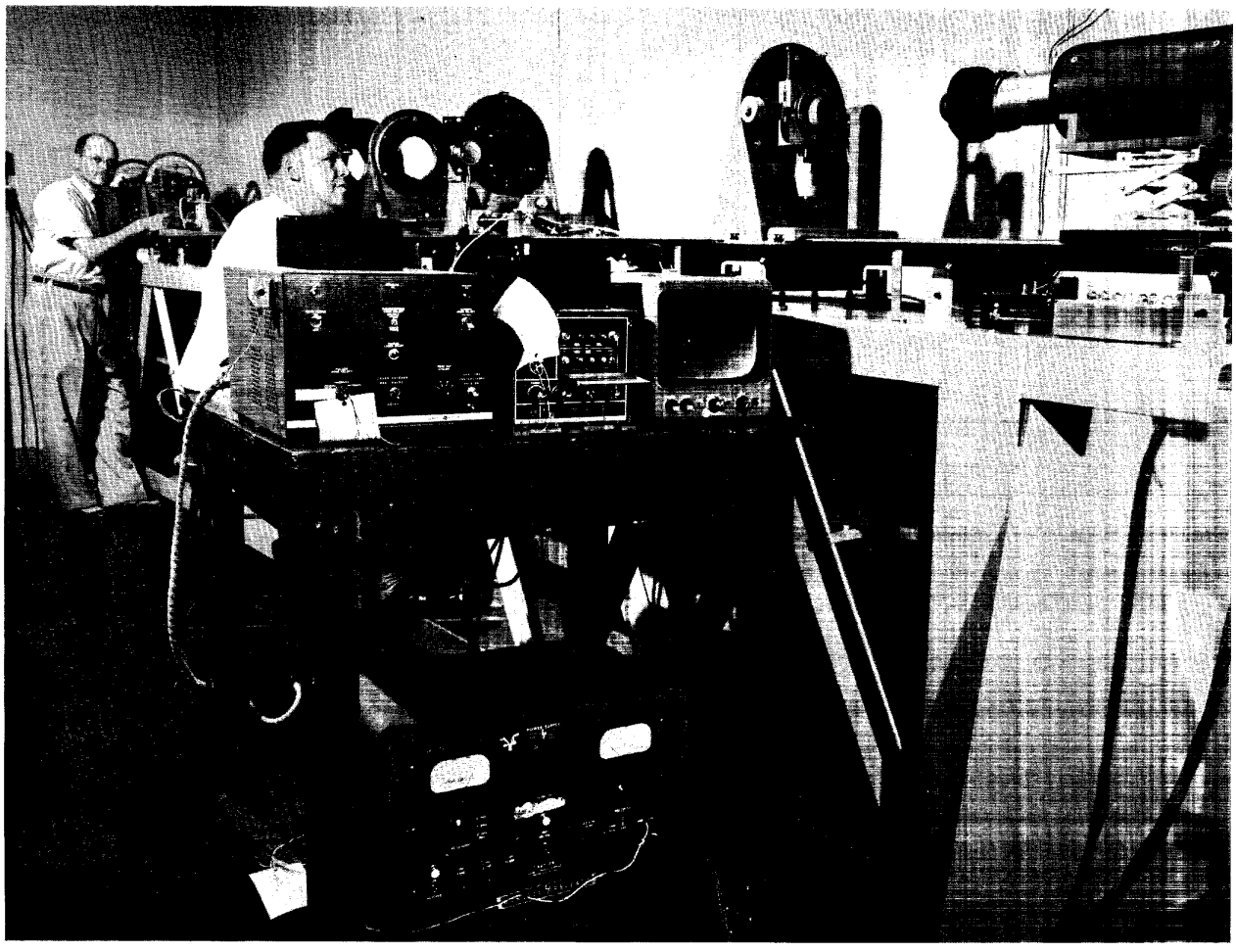

FIGURE 1 T.V. Readout System

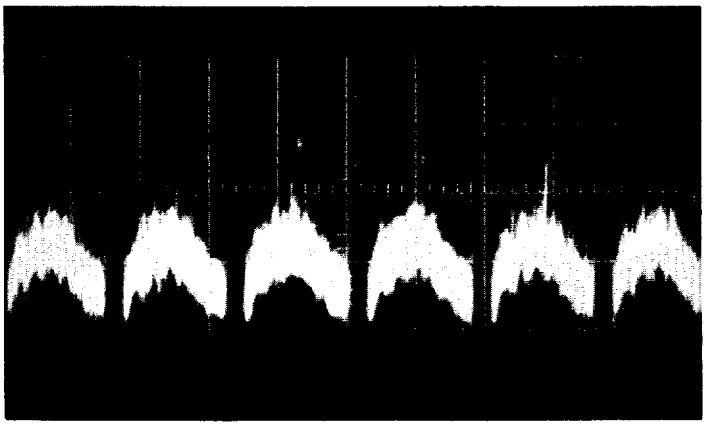

2a CRO Trace of 6 Line Scans

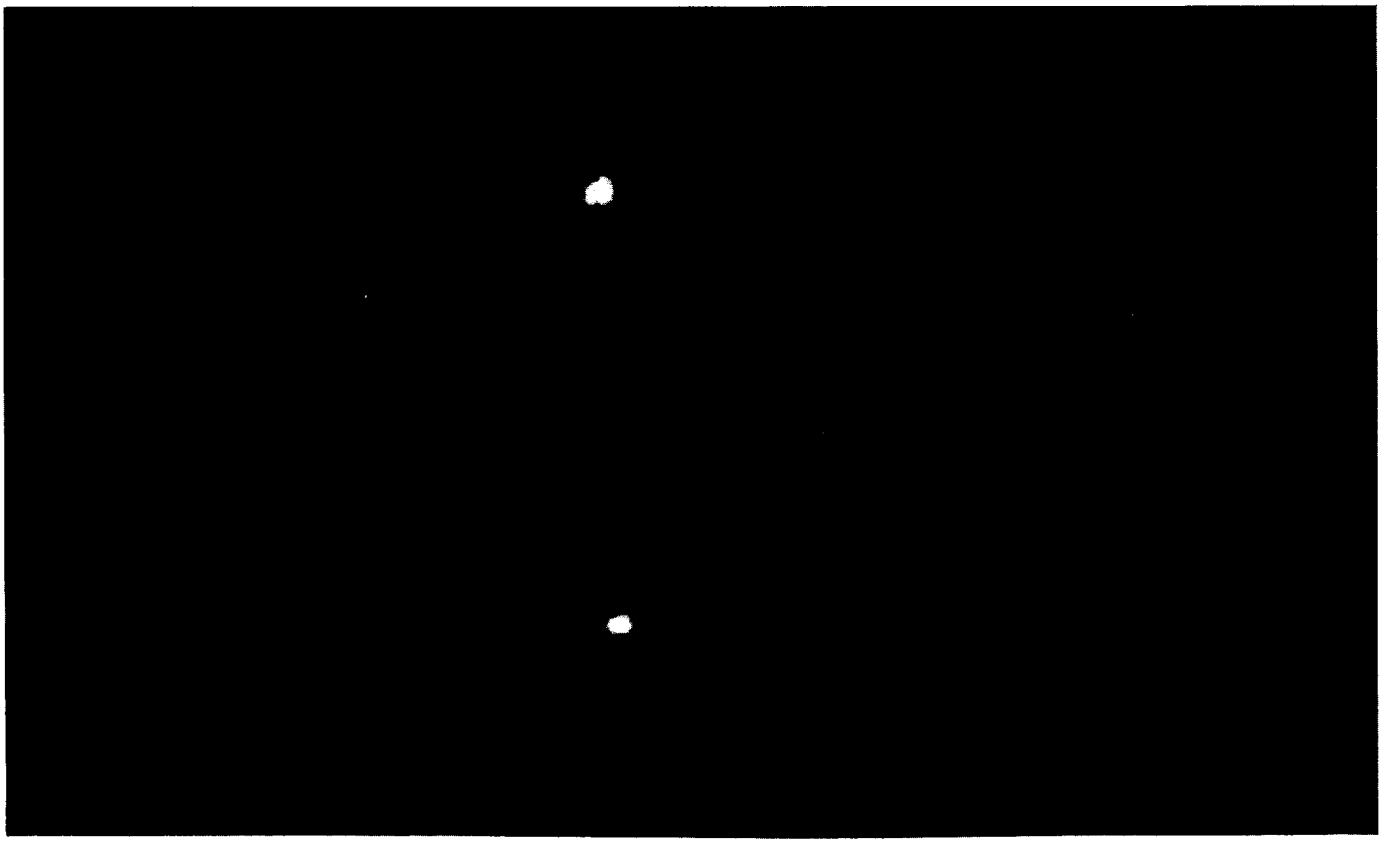

2b TV Monitor Showing Two Recognition Images
(Greatly Enlarged)

Figure 2

The first requirement, therefore, is a logic circuit to prevent multiple counting of a single recognition image which may appear in two or more lines. One way to do this would be to put the first signal in storage with a note of its horizontal position in the scan line. Successive signals in the next three scan lines are then placed in the same storage if they have the same horizontal position. At the end of four scans the memory is cleared and the stored signals read out as one count. This same logic circuit can also be used to provide a degree of immunity against false alarms by ignoring signals that occur in one line only.

The second requirement is a logic circuit to prevent multiple counting of a single recognition image which may appear in several successive frames during the orientation and scale search. Tests have shown that during orientation scan, for example, a recognition spot will appear at low, but detectible intensity as the filter becomes aligned with the target, in the next frame where the alignment is assumed to be optimum the signal is maximum intensity and in the third frame a weak signal is received. If we assume the object is stationary and the filter rotates, then these three recognition signals will all occur in the same place. To prevent reading the several recognition signals for one target as three or more targets it will be necessary to store the signals with information on their horizontal and vertical position for several frames. All signals with a position will go in the same storage and then periodically the storage will be cleared and read as one signal.

Tests Performed Using Television Chain

The image produced by the recognition system was viewed with an Image Orthicon Camera equipped with a tube having a highly red-sensitive (S-20) photosurface. This image tube has previously been found to perform quite well at the 6943 Å ruby laser wavelength when used for nighttime photography. Its sensitivity for the gas laser wavelength of 6328 Å should be even higher.

Two recognition spots were visible in the image. The maximum intensities for the two spots which were somewhat different occurred at two different angular positions. Fig. 2b is a photograph of the TV monitor screen when the object angular position was halfway between the two maxima. The CRO traces shown in Fig. 3a and b show the shape of the video pulse produced as the I-0 target is scanned through the spot. The amplitude of the recognition spot relative to background in 3a can be seen to be about 3.5 to 1. Since, in general, there is no information contained in the background signal, the video amplifier system can be adjusted so that almost all but the recognition spot signal is below the "black" level giving an effective signal-to-noise ratio of 20 to 1 as seen in 3b where the noise has been suppressed.

As mentioned above, close inspection of the monitor screen and the CRO traces show video pulses in from 1 to 5 scan lines depending on recognition spot intensity and position. Feeding the video signal into an electronic scaler using only amplitude discrimination indicated a count of from 2 to 4 per frame scan for the more intense spot and from 2 to 3 per frame for the less intense one. On the basis of the pulse count, the peak intensity points were found to be at an angular separation of about 3 to 4 degrees. The overall angular span in which the more intense spot was detected was 12 degrees while the less intense one was detected over a nine degree range. Outside the limits of detection the pulse count dropped quickly (less than 1 degree of rotation) from 2 per frame to zero.

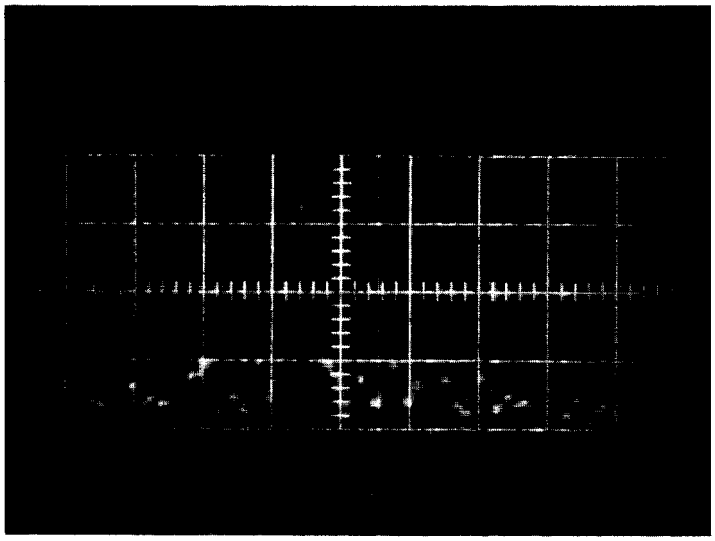

3a CRO Trace of Single Line Scan Expanded

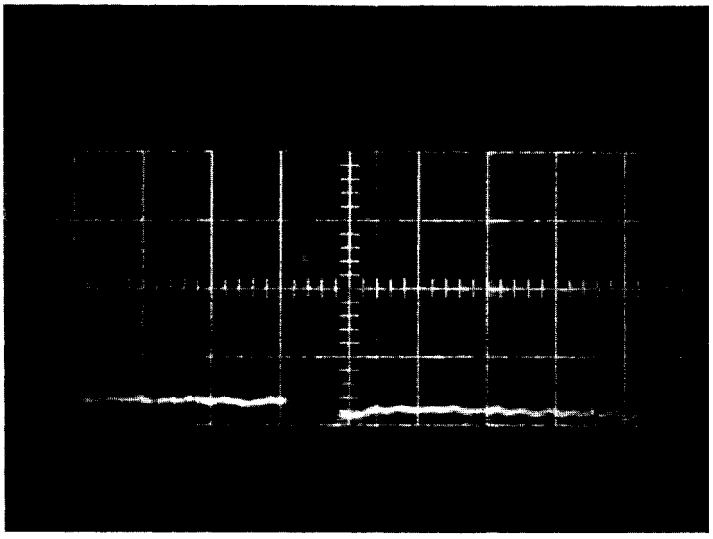

3b CRO Trace of Single Line Scan, Noise Suppressed

Figure 3

Section C

Conclusions

1. It appears feasible to make an automatic device to change spatial filters.
2. The curves of recognition signal strength as a function of orientation or magnification error are very favorable for machine recognition and provide data for calculating the time to scan a frame.
3. The time to scan a frame depends on the range of magnification to be covered. If this is assumed to be 2:1, then the time to scan one frame is less two minutes.
4. It is possible to make spatial filters by Photoplastic recording in a very short time and these filters perform practically the same as silver photographic filters.
5. The Photoplastic process is the only means we know of for real-time filter generation.
6. Television readout of the signals has been satisfactory, but will require some special circuits for automatic use.
7. The general conclusion is that answers or partial solutions have been found to several of the problems of automating the system and adapting it to operate in real-time. Considerably more work on automation remains to be done, but no serious problems have been uncovered.

Section D

Problems of the Photograph

This section was concerned with the effects of image variables on the detectability of targets. Typical problems were the effects of camouflage or low-contrast on the recognition system. These tests were all made using simulated aerial photographs and it is planned at some future time to check as many as possible of them on actual aerial camera film. The following topics were considered:

D-1 Properties of the Simulated Aerial Photographs

D-2 Effect of Target Size

D-3 Effect of Multiple Identical Targets

D-4 Multiple-Object Filter

D-5 Effects of Obscuration

D-6 Effect of Target Aspect

D-7 Effect of Shadows

Section D-1

Simulated Aerial Photographs

Purpose

The object of one part of this program was to find the effect of image variables such as the angle of illumination of the target. It would not be possible to measure the effect of this variable if the photographs to be tested also varied in density, contrast, sharpness, graininess or any of the other usual image parameters. For this reason it was decided to make these tests from simulated aerial photographs taken of models in our laboratory rather than try to find suitable frames on actual aerial films.

Procedure

There was no attempt to make the simulated aerial photographs resemble actual aerial films by building a set with trees, houses, roads and all the other usual items. In our opinion this would have been wasted effort. The only features that had to be simulated were the target, or several targets and the "noise" background.

In order to obtain a uniform signal from the target and noise background in a series of pictures it was necessary to control the following variables:

1. Contrast. This was adjusted to a contrast ratio of 1.5 which we believe is normal for aerial photographs.

2. Sharpness. All photographs were adjusted to show a resolution of about 150 lines per mm which we believed to be a high, but not unrealistic value.

3. Density. The photographs were adjusted to show approximately the same maximum density in any series, this was usually about maximum density 1.7.

4. Noise. The noise background was simulated by using fine sand, which when properly illuminated produced a noise reading very close to that of actual aerial photographs.

5. Graininess. The photographs were taken on very fine-grained spectroscopic plates, Kodak 649-F, but the graininess aerial film was simulated by the sand grains of the background.

The photographs were made on Kodak microflat glass so that the quality of the support would be as uniform as possible and there would be no necessity for liquid gates.

It proved to be more difficult than anticipated to make a set of photographs showing only one variable. For example, it was nearly impossible to make a set of photographs showing variable angle of lighting and still showing constant density. Also as the lighting angle changed the noise level of the background changed, but this is probably a natural condition.

Conclusions

The relative signal strength and noise background values obtained from the simulated aerial photographs were very close to the values obtained on original negative aerial films. We believe that the simulation was realistic and served its purpose in providing data for the picture variables studied.

Section D-2

Packing Density or Effect of Object Size

Purpose

The purpose of these tests was to determine the effect of the size which an object appears in the object transparency as it affects its recognition.

Discussion

25X1 It has been shown [redacted] and confirmed by many tests that the ideal size for the object to be recognized is about one-four hundredth the focal length of the focusing lens. The practical explanation is that an object this size makes the best diffraction image. If the object is very much larger than the ideal size and approaches the size of the field of view, then its diffraction angle will be so small that the resulting hologram will be crowded and difficult to photograph. In general the spatial filters made from these objects will be small and inefficient.

If the object is considerably smaller than the ideal size, the diffraction angles will be so large that the higher diffraction orders will fall outside the spatial filter area. The field of view of the lenses used in the system is small, and therefore the area which can be photographed and which will produce a good filter is also small. If an object is so small that the third and higher orders fall outside of the spatial filter area, then it will be impossible to make a high order spatial filter of this object.

Experimental Program

A series of 4 x 5 inch negatives was made of four model tanks on a "noisy" background resembling a ploughed field. The tank images on different negatives varied between 10 mm and 1 mm in length. In the classical recognition system in which the object transparency is in collimated light the object f value can be found from the familiar equation:

$$f = \frac{\text{focal length object lens}}{\text{length of object}}$$

In the overlapping system where the object is placed in a converging beam in order to vary its effective size, the object f value is calculated as follows:

$$f = \frac{\text{distance object to lens}}{\text{length of object}}$$

The object f value for the series of negatives tested is given below:

Image Size	Object f Value
10 mm	123
5 "	246
3 "	410
2 "	615
1 "	1230

It was the intention to make the five spatial filters as much alike as possible, but this did seem to be entirely practical. The observed differences between the filters was:

	Object Size				
	10 mm	5 mm	3 mm	2 mm	1 mm
Diffraction orders	33	23	19	14	7
Most efficient orders	10-12	4-8	7-15	4-7	2-5
Dia. spatial filter mm	12	16	24	24	18
Dia. diffraction orders mm	.10	.20	.3	.5	.8
Interference lines per order	10	20	33	50	100
Relative mod. eff.	.80	.80	1.0	.80	.80
Attenuation ref. beam	none	.20	.10	.02	.006
Exp. time 243 film sec.	.2	.5	1.0	3.0	16
Reconstruction detail	v. good	good	good	fair	poor

It can be seen from the Table that the five filters are not comparable, nor does it appear practical to make them so. The filter for the 10 mm object was most efficient in the 10-12th orders. If the 1 mm filter had extended to the 12th order it would have been larger than the camera we use to make filters or larger than the good image produced by the lenses. At the time the filter for the 10 mm object was made we had no way to make one showing a lower order of interference. The object is large, transmits a large amount of light and the diffracted orders are small and intense. This means there is a large amount of light in the higher orders. To produce a low-order filter would require attenuating the sample beam which is not recommended. The only other solution is to increase the intensity of the reference beam and at the time there was no way to do this; therefore the 10-12th order filter was the lowest we could make.

As the size of the object decreases the amount of light it transmits decreases and so the exposure time to make a filter increases. This is not a linear relation for two reasons:

a. It is usually necessary to attenuate the reference beam for small objects. This reduces the total light available at the filter plane.

b. As the size of the object decreases the diameter of the diffraction "spots" increases. This means that the light is spread over a larger area and the exposure is relatively longer.

Experimental Results

(a) 10 mm Images

Filter 1460 tested with two different transparencies, one at a moderately high contrast, the other at a fairly low contrast. The results were as follows:

	High Contrast	Low Contrast
	Signal Strength	
Tank A	90	95
B	96	110
C	46	85
D	85	90
Average Noise	.5	6
Max. Noise	10	14
Min. Signal/Max. Noise	4.6:1	6:1

The higher contrast transparency did not improve the results in this test.

(b) 5 mm Images

	Signal Strength
Tank A	110
B	100
C	96
D	100
Average Noise	.03
Max. Noise	.08
Min. Signal/Max. Noise	12:1

(c) 3 mm Images

	Signal Strength
Tank A	90
B	120
C	160
D	140
Average Noise	3
Max. Noise	5
Min. Signal/Max. Noise	18:1

(d) 2 mm Images

	Signal Strength
Tank A	40
B	50
C	40
D	42
Average Noise	15
Max. Noise	25
Min. Signal/Max. Noise	1.6:1

(e) 1 mm Images

	Signal Strength
Tank A	10
B	12
C	10
D	9
Max. Noise	7
Min. Signal/Max. Noise	1.3:1

Discussion of Results

These examples show the best signal-to-noise ratio for objects having a size close to the ideal, or for 5 and 3 mm objects in this case. Larger and smaller objects gave poorer signals. Of course, the filters of the different size objects were not comparable, nor did it appear practical to make them so.

We feel that at least part of the trouble was the filters. The poor result with the large 10 mm object was probably due partly to the use of a very high order filter which is quite dense at the center. The poor results with the small 1 and 2 mm objects was due partly to the low order of the filter and partly to the small size of the object. Only light transmitted by the object can contribute to the recognition spot. As the object becomes smaller there is less light available and so the signal strength does down. The noise, however, is approximately constant, so that the signal-to-noise ratio decreases as the object size decreases.

A final test was made to determine if the decrease in signal observed in the case of the small objects was due primarily to the filter or the object size. In this test, the filter for the 3 mm object which had given good results with the appropriate transparency was compared to the transparency with the 2 mm objects at the proper magnification. The results were slightly better than when the 2 mm filter was used, but not enough to make any difference. Our interpretation is that the primary difficulty is the small size of the object and not the filter.

Conclusions

The optimum signal-to-noise ratio in continuous tone pictures was obtained for objects close to the recommended size (one-four hundredth the focal length of the imaging lens). Objects 2 mm or less gave poor recognition. This appears to be a limitation of the process though it is not necessarily applicable to high contrast objects such as microfilm copies of documents.

Smaller objects could be processed in a different setup using shorter focal length lenses, but in this case the entire 4 x 5 inch transparency could not be covered at one time.

In the theoretical section A-6 it was shown that objects as small as .3 mm should be detectable. In the theoretical analysis no assumption was made as to the design of the optical system or the focal length of the lenses, it was assumed that the lens focal lengths were completely flexible which they are not in practice.

Section D-3

Effect of Multiple Identical Targets

Object

The purpose of this test was to determine if the presence of several identical targets in the same field of view would decrease the liklihood of their detection.

Discussion

The theory of the process indicates that the number of targets should have no effect and experiments with alphanumerics tended to prove this. It is less easy to visualize the diffraction effects due more complex objects particularly when they arranged in uniform and slightly random patterns. For example, if two identical vehicles were oriented so that the angle between them was about 5 degrees, the two differently oriented diffraction images would both be symmetrical about the optical axis and the various diffraction orders would overlap and interfere. It can be predicted that this phase interference will produce a phase shift and this will vary the strength of the recognition signal through this particular order of the filter.

A similar but different problem arises when a number of vehicles are parked in a close array as in a motor pool or parking lot. In this case the edges or ends of the vehicles are often close together so that their outline cannot be directly seen or is in very low contrast, as in the case of a group of black automobiles parked closely together. From a study of spatial filters we have made, it appears that the outline is one of the most important features in recognizing an object such as a vehicle. If this outline is lost by being merged with other vehicles it is easy to see that the recognition may be lost or reduced.

Experimental Procedure

The test was divided into two parts; random orientation effects and close-packing effects.

1. Random Orientation

For this test a simulated aerial photograph was used showing eleven model tanks of the same type distributed over the picture area. The orientation angle between these varied from one-half to ten degrees. While these vehicles were all initially "identical" in that they were made in the same mold, all of them had been sandblasted to a dull, dusty finish and each was dirty in a different way. The turrets of the tanks and other minor parts were differently orientated on different models. Also, because the photograph was not exactly vertical and the field angle was about 30 degrees all of the tank images were not seem in the same perspective nor did they have the same shadows around them. Therefore, the objects were "identical", but their images on the negative were not. This is a situation similar to real life where vehicles leave the factory in identical condition, but soon acquire an individuality of their own.

Results of Random Orientation Test

In most cases the signal measured for each vehicle was identical regardless of its position in the picture or its orientation in relation to other vehicles. The only exceptions were vehicles orientated at small angles, of about two degrees to each other. We interpret this as due to phase interference between the diffraction images. This angle is of two degrees is correct to cause overlap of the most important diffraction orders in the apparatus used. In this case one of the two recognition signals was reduced to about 70 percent of its normal value.

Larger and smaller angles produced negligible loss of signal.

Numerical Results

Effect of Relative Orientation Angle

Angle Between Vehicles	Signal Strength	
	Vehicle A	Vehicle B
10	100	97
8	100	96
6	100	98
4	100	96
3	100	95
2	100	72
1	100	98
1/2	100	98
0	100	98

2. Close-Packing Effects

For this test a simulated aerial photograph was made showing vehicles of the same types in groups of two, threes and sixes. Recognition signals were measured for all the images.

Results of Close-Packing Tests

The outer vehicles in a close-packed group give normal or nearly normal signals while the inner vehicles tend to give weak signals which may be as low as 47 percent of the normal values. This is interpreted as a loss of outline of the inner vehicles. The outline is a major contributor to the total signal.

Numerical Results

Effect of Close Packing

Array	Signal Strength Vehicle A	Signal Strength Vehicle B
Two end to end	100	96
Two side by side	100	94
Three end to end, A is end, B Center	100	92
Three side by side, A is side, B Center	100	54
Six in a square, A is outside, B Center	100	47

Conclusions

1. Multiple identical targets in the same photograph can result in some loss of detection signal for some of these targets. If these vehicles are oriented at certain small angles to each other which result in phase interference in the most important parts of their diffraction pattern, then one or more of these vehicles will produce a weak signal. Close-packed vehicles lose part of their outline and the inner vehicles show some loss of detection.
2. In none of the cases we have tested has the relative signal strength fallen below 47 percent that of a single vehicle.
3. We feel that this test shows an interesting shortcoming of the process, but represents a rather unusual condition that should give little trouble in actual use.

Section D-4

Multiple Object Filter

Discussion

In the normal use of the recognition process a spatial filter is made for a single object and this filter is used to detect this object in the transparencies. The readout then presents two kinds of information, the type of object and its location in the picture area.

It is also possible to make a filter of several objects at the same time called a multiple-object filter and recognize any of these. The readout is now ambiguous, we can examine the entire transparency and obtain position information without knowing which of the objects has been detected, or we can restrict the area under examination to an area no greater than one object and obtain information on which object was detected by the angle at which it reads out through the filter. This is another kind of position information which, when referred to the positions of the objects in the filter tells which object was detected.

The use we have considered for multiple-object filters is a filter which would contain several objects and thereby speed the search process. If the filter contained ten objects and the use of the multiple-object filter did not change the time constants of the search process, then a roll of film could be scanned for ten objects in one-tenth the time it could be scanned with ten single-object filters separately.

Purpose

The purpose of these tests was to test the features of a multiple-object filter which would speed the process of scanning a large amount of film.

Previous Experience

In earlier experiments with character recognition it was shown that a filter could be made for ten digits which would recognize any one of these with signal-to-noise ratio of 40:1. Elsewhere, filters were made for 36 different characters which produced satisfactory recognition at an unspecified signal-to-noise ratio.

It might therefore appear that ten vehicles could be placed in a multiple object with the same results. Our experiments have shown that there are several important differences between the two cases:

1. In the case of characters on an opaque background the contrast is practically infinite and the "noise" is negligible. The multiple object filter is always more complex and denser than a single object filter. The strength of the recognition signal obtained from a multiple-object filter is therefore always less than the signal obtained with a single-object filter. For characters on a noise-free background we can afford loss of signal and still have an acceptable signal-to-noise ratio. For aerial photographs which show a "noisy" background not much loss of signal can be tolerated.

2. Characters are relatively simple shapes and produce simple spatial filters. Vehicles and other aerial photograph "targets" tend to be more complex and produce filters with a great deal of detail in them. For example, the filter of a single tank appears to have as much or more detail than a multiple-object filter for ten letters or numbers. This means that multiple-object filters for vehicles will be packed with detail, dense and show lower modulation efficiencies.

3. In character recognition there is no orientation or scale scanning and therefore no opportunity for "false-alarms" due to inverted letters or letters of a different size. A filter made from several vehicles of different sizes, all of which tend to be more or less rectangular or to have common features such as turrets or guns will show partial recognition or "false-alarms" as the orientation is changed and the scale varied. In a sense, these many false alarms tend to raise the noise level of the recognition image so that in the case of aerial photographs, scanned with multiple-object filters the signal is less and the noise greater so that the signal-to-noise goes down very fast as objects are added to the filter.

Experiment with Ten Vehicles

Ten models of different army vehicles were selected and a spatial filter made of them. The vehicles were of assorted sizes from a large tank to a jeep. The objects were not arranged in straight rows or aligned parallel because it was felt that the many parallel sides would act as a multiple line grating and produce a confusing effect in the filter. Different filters were made which showed the optimum interference in the 4th to the 10th diffraction order by attenuating the reference beam different amounts. All of these filters tested very good and showed sharp reconstruction images. A multiple-object filter tends to be denser than a single object filter and the high order multiple-object filters were quite dense.

One of these multiple-object filters was tested in detail. When used to recognize the object from which it was made it showed a very strong recognition spot in the exact center of the pattern where no vehicle existed. This is interpreted as a recognition of the entire pattern of several vehicles and since the spot is at the center of the pattern it does not represent the recognition of any specific vehicle. The

intensity of the recognition was then measured for each individual vehicle by masking off all the others in the object transparency. In this case, the recognition spot also appeared at the center of the pattern. The results were as follows:

	Signal Strength (arbitrary units)
All vehicles	2500
German tank 2108	100
German Panzer tank-S	100
Rocket launcher	100
German tank T-34	110
10 wheel tractor unit	100
Tank M-47	60
Heavy gun carrier	45
German tank 077	20
Jeep	17
Tank M-48	90

It can be seen that the recognition for the whole pattern was about three times as high as the total recognition for all the objects in it. This is some accumulative effect we cannot explain. Most of the vehicles were approximately the same size and produced the same strength signal or 100 units. It is normal to expect the jeep which is small to produce a lower signal. The area of the jeep image on the transparency measures about one-fifth that of the tanks and so regarding the image as a window, the light transmitted will be only one-fifth. Since the recognition signal is derived from this light we would expect the signal to be about 20 units. The low values for the tank M-47, German tank 077 and Heavy gun carrier are due to the lighter color of the models. These had a different color of "camouflage" paint which photographed much darker on the negative transparency. The effect of dense images in the transparency is like adding a neutral density filter to the object or its recognition spot. The observed density of the images and strength of recognition spots shows reasonable agreement.

One feature that this test showed was that if multiple-object filters are to be made, all of the objects should have approximately the same size and reflectance or there will be a large disparity in the recognition signals for these objects.

An object transparency containing these same 10 vehicles, but in different positions and on a "noisy" background was compared to the three best multiple-object filters. The vehicles could be detected, but at such a low signal-to-noise ratio and with so many false alarms that automatic recognition was considered impractical. Typical values were:

	Signal
Large vehicles	40
Small vehicles or dense images	16
Noise	10
False-alarms	20

The signal strength measured above is reported in the same units as in the previous Table. The reason for the lower values in this case was the low-contrast images in the simulated aerial photograph which produced weaker diffraction. Thus, a high-contrast image of a tank might produce 100 units of signal, while a medium contrast image produced 40 or less. The small and dense images produced still lower signals for obvious reasons. The false-alarms came from all the partial recognitions of similarly shaped vehicles at various combinations of orientation and scale. Even if there had been but one vehicle in the transparency we would probably have obtained false-alarms for rectangular buildings, shadows of telephone poles and other normally occurring objects which would have the same shape as tanks, turrets, guns or other parts of the vehicles.

Alignment Tolerances of a Multiple Object Filter

1. Displacement. The measured horizontal alignment tolerance was no different than a single object filter. The vertical alignment tolerance was slightly tighter, but within the usual experimental variation.

2. Rotation. The rotation tolerance for multiple object filter 1546 was half that of a good single object filter for the same object as shown below:

Signal	Rotation Tol. Single Object Filter	Rotation Tol. Mult. Object Filter
100	.5 degree	.3 degree
90	1.2 "	.7 "
80	1.9 "	1.0 "
50	3.9 "	2.0 "

This can be explained as due to the higher order of the filter. The single object filter operated mostly in the 5th to 7th diffraction orders, the multiple object filter operated mostly in the 10th to 16th diffraction orders. The reason for this was that the multiple object filter showed very poor efficiency and selectivity at a lower order.

Referring to the geometrical explanation for rotational alignment tolerance, it can be seen that if the effective diffraction order is twice as high, these orders will be twice as far from the axis and the same amount of rotation angle will cause them to be misaligned twice as much, or to put it another way; the angle error to produce the same signal will be half as much.

3. Magnification. The magnification tolerance for multiple object filter 1546 was also about half that of a single object filter for the same object.

Signal	Magnification Tol. Single Object Filter	Magnification Tol. Multiple Object Filter
100	1.0%	.2%
90	2.2%	.6%
80	3.2%	1.4%
50	6.0%	2.6%

The explanation again is probably the higher diffraction order which apparently was required by the greater complexity of the filter.

Conclusion on Alignment Tolerance

1. The x and y displacement tolerance of multiple object filters is the same as single object filters.

2. The rotation and magnification alignment tolerances are the same if the filter is made in the same diffraction order.

3. In general, multiple object subjects will require a higher order filter. Since the higher order filter has "spots" at greater radial distances from the axis the rotation and magnification tolerances are reduced proportionately.

Effect on Time Constants

It is impossible to predict anything from the few experiments described. However, if a ten object filter requires a diffraction order twice as high as a single object filter, then the time to make the orientation and scale search will each become twice as long and the product will be four times as long. Thus, the time to make a complete search with a ten object filter will be four times as long as the time to make the search with a single object filter. This is still considerably less than the time required to make a search with ten single object filters.

Conclusions for 10 Object Filter

1. Ten vehicles are too many for any multiple-object filter we have been able to make because this filter produces a lower signal strength and many false alarms.

2. The problem is different from the multiple-object character filter because in that case we do not perform a scale and orientation search. For the case described, a complete scan with the ten object filter would result in about 60 false-alarms.

3. Due to changed alignment and time constants the ten object filter would require four times as long to make a search as a single object filter.

Experiment with Two Vehicles

Two tank models M-47 and a German Panzer IV S were selected and a spatial filter made for both of them. This filter was then used to recognize these targets in a photograph containing these and eight other similar vehicles and some model trees.

The two tanks in the filter recognized the similar tanks in the photograph with a signal-to-noise level of ten to one which is considered satisfactory. False alarms were also obtained for other vehicles as follows:

	Signal Strength
M-47	100
Panzer IV S	90
M-48	40
M-48 inverted	30

	Signal Strength
German Tank T-34	20
German Tank T-34 inverted	20
Heavy gun carrier	30
Heavy gun carrier inverted	20

Conclusions for Two-Object Filter

1. Two objects as complex as tanks can be handled by a multiple object filter.

2. The alignment tolerance and time constants for search were the same as for a single object filter.

3. In the experiment described, there could have been six false alarms. Four of these were for very similar tanks, the other two were for an entirely different vehicle that bears no obvious similarity to the tanks for which the filter was made.

Experiment with Three Vehicles

The previous experiment was repeated, adding a German 2108 tank to the spatial filter. The average signal-to-noise level for the detection of the tanks was seven to one for the maximum noise. Twelve false alarms were obtained which was twice the number obtained with the two-object filter.

The conclusion is that three or four tanks probably represent the maximum we can put in a filter at the present time.

General Conclusions on the Multiple-Object Filter

1. For simple objects such as characters on a noise-free background, 20 or 30 can be used, certainly ten are not too many. For more complex objects such as vehicles and on a noisy background the present limit appears to be three or four.

2. In these experiments the signal-to-noise ratio decreased as the number of objects in the filter increased.

3. The number of false-alarms for similar objects increased as the number of objects in the filter increased.

4. It is possible that improved techniques in making filters will change this situation.

5. Multiple-object filters appear to required a higher order of diffraction than single object filters and this will tighten the magnification and orientation tolerances. This in turn increases the time required to make a search with a multiple-object filter. The exact relation between number of objects and increase in time is not yet known.

EFFECTS OF OBSCURATION - 1 Contrast

Purpose

Objects can be obscured or made difficult to find in a photograph if they appear either in low-contrast with their surroundings or if the entire photograph has a low-contrast.

Low-contrast aerial photographs can result when pictures are made on cloudy, overcast or rainy days; or when the film is underexposed or improperly developed. To test the effect of overall contrast we made a series of photographs identical except for density range.

Experimental Program

Each photograph contained four tanks agains a "noisy" background. Included in the photograph was a piece of white cardboard which acted as a brightness standard to measure the contrast of the negative. The contrast ratio was defined as the density difference between the image of the white standard and the unexposed edge of the plate, and was therefore the total contrast range of the entire photograph, and not the contrast of the tank against its background. Since the tanks and background were both fairly dark in the scene, the contrast of the tanks was considerably less, about half the contrast of the photograph.

The low-contrast images were made by reducing the normal development of the plates. It was necessary to mix special developers and use a two-bath system to obtain satisfactory low-contrast images on the material we used.

As a normal photograph we used one with a total contrast of 1.5, since we believe this is an average value for aerial photographs taken on a bright day. In any case, this negative looked very much like aerial negatives we have seen.

The 1.3 contrast negative was noticeably weaker, but still an acceptable photograph.

The 1.1 density negative was the kind a photographer would call a "thin" negative and the tanks were less obvious than in the higher contrast photographs.

The .7 contrast negative was quite thin and the images difficult to find.

The .3 contrast negative, unless looked at carefully appeared blank. The tank images were very difficult to find. Most observers would find it difficult to use such a negative.

The recognition signal for each tank and the noise background was measured in each photograph.

Results

Contrast	Signal	Max. Noise	S/N
1.5	140 - 160	19	7:1
1.3	100 - 120	15	7:1
1.1	58 - 80	8	7:1
.7	27 - 40	4	7:1
.3	17 - 25	3	7:1

These figures show that the inherent noise in the film decreases in the same ratio as the contrast, so that low-contrast images show practically the same signal-to-noise as high contrast images. These are exceptions to this of course. All of these photographs had practically perfect surfaces with no scratches or defects. The diffraction caused by a scratch is constant and therefore a scratch is much

more serious on a low-contrast negative than a normal contrast negative. In one test a fingerprint was put on the back of the glass plate. The noise level rose from 4 units to 27 units which was equal to the strength of the weakest signal in this case. Therefore, while it is feasible to find images in very low-contrast photographs, it may prove to be impractical if the film is scratched or finger-marked.

These tests indicate that a machine should be able to find low-contrast images as easily as high-contrast images, but these tests were performed manually and it was necessary to scan the field for recognition images by eye and then align the measuring microscope with them. The actual tests were much more difficult to perform on the low-contrast negatives because of the difficulty of locating and orienting the low-contrast images by eye. Figure 1 shows a low-contrast photograph.

Conclusions

1. If the negatives are in perfect condition, with no scratches or flaws, the automatic recognition process will locate images of objects at extremely low-contrast and at the same signal-to-noise ratio as obtained in normal contrast negatives. This potentially makes the process suitable for locating images too weak to see. In this experiment good recognition was obtained for images that had a density difference from this background of .15 or less.

2. The intensity of the recognition signal is less in low-contrast photographs, therefore defects which raise the noise level are relatively more serious.

3. The results of this experiment cannot be directly related to a normal contrast photograph in which the targets appear in low-contrast due to camouflage or other reasons. In this case the object is at a low-contrast and will produce a

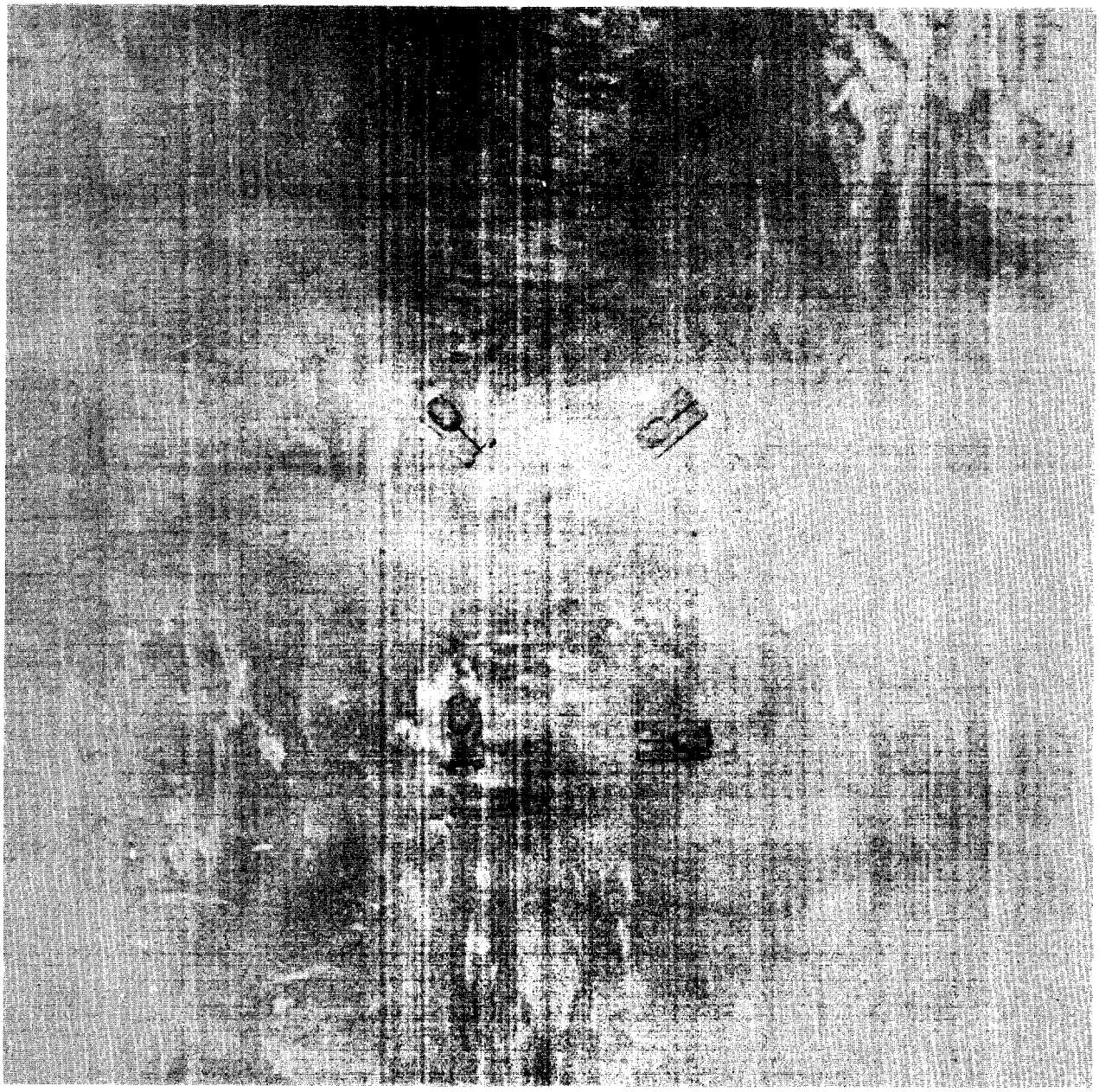

Overall Contrast .15

Figure 1 - Low Contrast

weak signal, but the average noise level will be that of a high-contrast photograph. For example, if the target were camouflaged to show a density difference of only .15 from its surroundings, but the photograph as a whole showed normal contrast, then we would expect the signal and maximum noise to be about equal.

EFFECTS OF OBSCURATION - 2 Camouflage

Purpose

This test was to determine the effect of a confusing background, especially one in which the major color was the same as the vehicles and therefore provided little or no contrast, while the background itself contained many similar patterns in high contrast. This was the principle of "dazzle camouflage" used in World War I.

Discussion

The tanks used in this test were a dusty olive drab color. Four of them were placed on a piece of "camouflage cloth" purchased from a surplus store. This material has an irregular design in three colors, one of which was an olive drab that matched the tanks almost perfectly. Also, the general pattern of the cloth produced differently colored areas each about the size of a model tank. The photograph was diffusely illuminated so there would be no shadows to outline the tanks. The resulting photograph was a good example of "dazzle camouflage" in that the tanks were difficult to find and the eye was misled by the overall pattern.

Results

When the area around any tank was masked the intensity of the recognition signal for that tank was normal for a low-contrast target. Diffusely illuminated objects lack the sharp shadows which are one of the chief causes of diffraction and an important aid in recognition. If the normal recognition intensity for a sunlighted tank was 100 units, the value for a diffusely lighted tank simulating a photograph taken on a cloudy day would be 30 units. The four different tanks gave recognition signals between 23 and 40 units. However, when the area around the tank was uncovered and the entire photograph used, the intensity of the recognition spot dropped to as low as 8 units. This is the first time that this has been observed. Normally, if the area around an object is masked, the intensity of the recognition spot does not

change enough to measure. In this case the average size of the camouflage color areas was close to the size of the tanks and we theorize that the diffraction of these many areas produced a strong "noise" diffraction in spatial frequencies close to that of the object. Apparently the energy in these frequencies optically interferred with the energy diffracted by the tanks and reduced their intensity. The same result was noticed for all four tank images.

The noise in this photograph was very strong and "spotty" so that it was difficult to choose the maximum noise to measure, but values as high as 23 units were found. The result of viewing the photograph as a whole was as follows:

Signals for tanks	6 - 8 units
Maximum noise	23 units
Average noise	8 units

In other words, the signals for the tanks in this case were below the average noise level and therefore undetectable except when the operator knew where to look for them. Figure 2 shows the photograph used.

Conclusions

1. Dazzle camouflage produces strong diffraction noise. If the average frequency of this noise is close to that of the chief spatial frequency of the target, then the target may be obscured by noise and be undetectable by this process.

2. For reasons not entirely understood, the presence of a confusing background actually reduced the intensity of the recognition signals.

Camouflage - Dazzle Effect (Tank at upper right was isolated as shown after tests were made)

Figure 2

3. The target in these photographs was diffusely lighted (no shadows) and showed a maximum density variation of .55 which simulated the situation of a cloudy day.

Section D-5-3

EFFECTS OF OBSCURATION - 3 Low Contrast

Purpose

Previous tests showed effects of a low-contrast image on a plain "non-noisy" background and the effects of a low-contrast image on a background of noise having a high intensity and a mean spectral density close to that of the signal. This test was to find the effect of a low-contrast target on a background of high frequency noise of the same intensity.

Discussion

Four similar tank models were photographed on a finely mottled background. The average contrast of the tank images and background were both close to density .65 and the scene was flat lighted to eliminate shadows. As result, the entire photograph is in low-contrast and the tanks are fairly difficult to see.

Results

The recognition signals for the four tank images varied between 70 and 100 units. The background showed a strong noise area which had a maximum value as high as 33 units though most of the noise measured about 10 units. The cause of the high noise area was a scratch in the emulsion. This shows the severe effect that scratches can have, especially in low-contrast pictures.

Results with Scratch

Signal	Noise	S/N
70 - 100	33	2.1:1

Results without Scratch

70 - 100	10	7:1

Conclusions

1. All low-contrast subjects give a lower signal-to-noise ratio than high contrast subjects. The addition of defects to the film, a scratch in this case is relatively more serious in the case of low-contrast subjects.

2. In this case where the "noise" background had the same contrast as the target, the detection was fair, much better than the case where the noise was at high contrast.

Section D-5-4

EFFECTS OF OBSCURATION - 4 Noise Background

Purpose

This test was to determine the effect of a high-contrast noisy background on the recognition of normal contrast objects.

Discussion

Four similar tanks were photographed on a spotted background made by putting dark colored random size spots on brown paper. The result was what might be called a "spattered paint" effect. In the photograph the tanks appear at the contrast they would have in a normal aerial photograph and they are seen the very noisy background or random size spots. All of the spots are smaller than a tank and therefore the noise spectrum consists chiefly of frequencies higher than the tank outline, but about the same as the tank details.

Results

The intensity of the signal for these normal contrast tank images was about five times the signal obtained for low-contrast images in the previous tests. While the background produced strong "noise" at random frequencies it did not interfere with the detection of the signals.

Signal	Noise	S/N
350 - 520	15	22:1

Conclusions

1. If the targets appear in average contrast, then they can be detected against a "noisy" or confusing background, especially if the peak noise spatial frequency is not the same as that of the targets.

Section D-5-5

EFFECTS OF OBSCURATION - 5 Overlap

Purpose

This test was to determine the detectability of objects when they are partly concealed by opaque covering.

Theoretical Background

It is clear from theory that the strength of the recognition signal should not decrease linearly with the unobscured area when an object is partly covered. The exact relation is unknown at present and may have to be determined experimentally. As long as five years ago the mathematician Van Heerden tried to calculate two cases for us and reported that the mathematics was not simple nor the results definite; but to his best guess, when 90 percent of the object was visible the signal should be practically the same as for an unobscured object and when 50 percent of the object was visible the signal should be close to .9 the normal signal. Even when only 10 percent of the object was visible the signal should be fairly high. These calculations were made on the basis of letters and words of the English language and do not necessarily apply to other objects, though the general conclusions probably do.

If this proves to be true, then this system would be useful for detecting partly hidden objects and should find them even when only a small portion is visible, or in more practical terms until the reduced signal approaches the noise level. As in all these other situations, the ability to detect hidden objects will depend on the noise background.

Discussion

Four similar model tanks were photographed on a "noisy" background of rough sand. One tank was not concealed and used as a control; the other three were covered by model trees made of lichen and a different part of each tank was covered. There were four photographs made in the first about 20 [illegible] covered,

in the others, 40, 60 and 80 percent. Figure 3 shows a typical photograph.

Results

		Signal
1.	Tanks 20 percent covered	
	a. Control (not covered)	100
	b. Left rear covered	100
	c. Left front covered	90
	d. Rear end covered	90
2.	Tanks 40 percent covered	
	a. Control	100
	b. Left side covered	80
	c. Front end covered	83
	d. Rear end covered	93
3.	Tanks 60 percent covered	
	a. Control	100
	b. Left side covered	97
	c. Front and left side covered	70
	d. Rear end covered	90
4.	Tanks 80 percent covered	
	a. Control	100
	b. Only little of left side visible	58
	c. Only little of right side visible	50
	d. Only left front visible	60

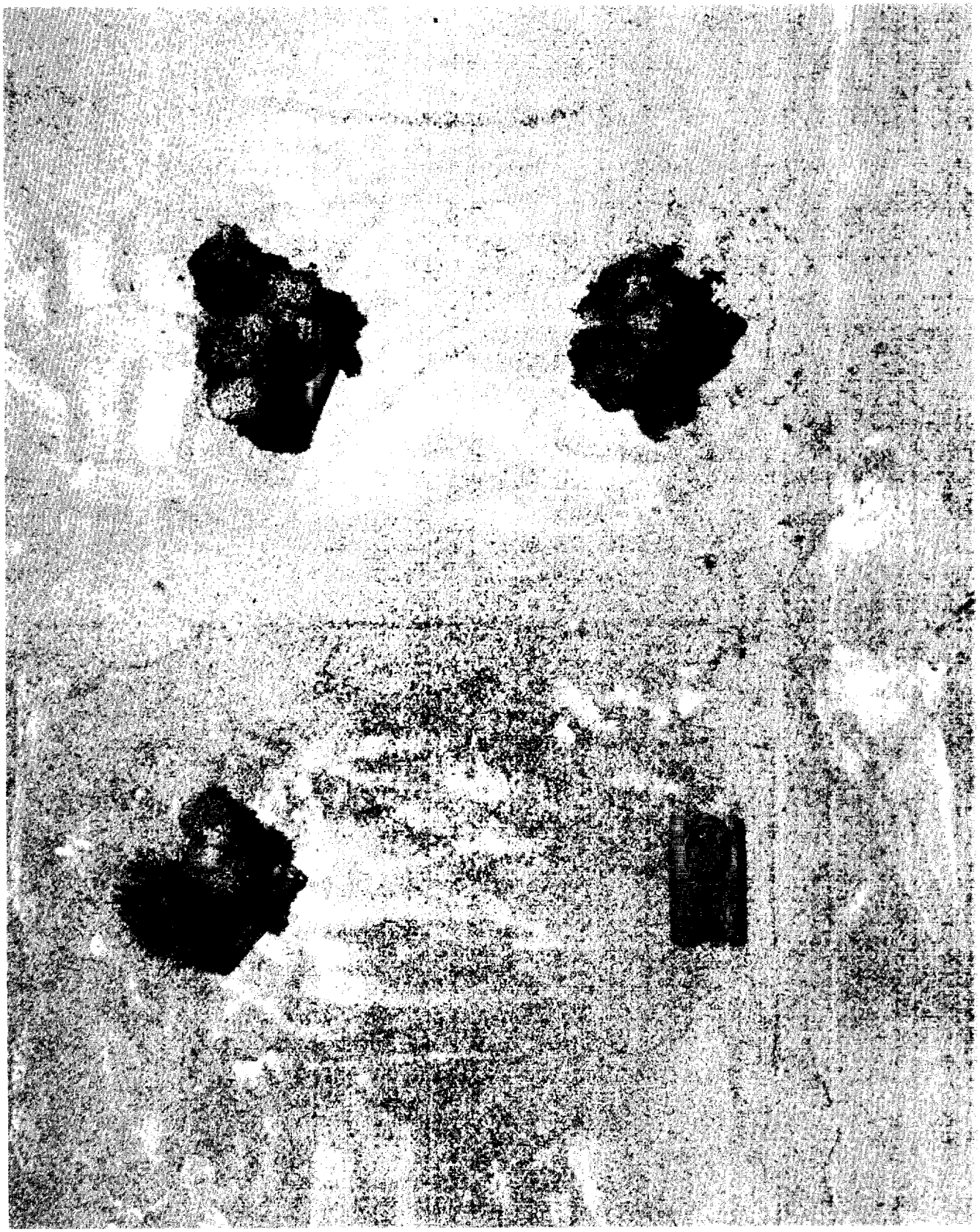

Obscuration - 80 percent Concealed

Figure 5

These photographs are not strictly comparable because the noise level was not constant. For reasons not known entirely at present, the noise level in all of them was higher than normal and increased from about 10 units in photograph 1 to 15 units in photograph 3 and 20 units in photograph 4. This may be partly due to the fact that it was necessary to move the lights in the last picture and this may have put more shadow detail or noise on the sand background. If this is taken in account then the average signal-to-noise ratio for the four cases is:

Percent Concealed	Signal/Noise
20	10 :1
40	8.5:1
60	6 :1
80	2.8:1

There should have been no difference in the noise background of the four photographs and the only variable should have been the degree of concealment. Also, the noise level of all the pictures is about twice as high as that of most of our photographs, so that if a normal noise level had been obtained the signal-to-noise values would be at least twice that shown.

Conclusions

1. The recognition signal is not proportional to the visible area of the object. It is not logical to expect half of the object to give a half strength signal.

2. The present tests were confused somewhat by a variable noise background, but they indicate that good recognition should result when 60 percent or more of the target is obscured. Some recognition was obtained for targets 80 percent obscured.

EFFECTS OF OBSCURATION - General Conclusions

1. The recognition signal comes from light diffracted by the image of the target and then again selectively diffracted by the spatial filter. In all aerial photographs it is necessary to detect this signal against a background of noise which results from all the random shapes and textures which give rise to diffracted light representing many spatial frequencies in the scene. In general, a natural background does not seem to present a high noise level at frequencies that interfere with detection of man-made objects. The introduction of a background filled with human artifacts such as roads and buildings produces a higher level of noise at frequencies close to those of typical man-made objects that might be considered as targets. Therefore, the effective signal-to-noise obtainable will probably be less in urban scenes than rural scenes.

2. Since the recognition signal is basically derived from light diffracted by the image of the target, any circumstance which reduces this diffraction will result in loss of signal. Typical circumstances are low-contrast, lack of sharpness and obscuration.

a. Overall low-contrast of the entire photograph is not a problem because in this condition the noise diffraction reduces in the same ratio as the target diffraction.

b. A low-contrast object on a normal-contrast background is difficult to detect.

c. A low-contrast target on a high-contrast background is impossible to detect when the spatial frequencies of the background or camouflage are close to that of the target.

Section D-6

Effect of Target Aspect

Introduction

Objects on the ground which appear at the center of a vertical photograph are seen exactly from above. The same object at the edge of a wide-angle photograph will show a different aspect or perspective and portions of the sides or ends will appear in the photograph. Oblique and panoramic photographs show objects from many aspects.

If we assume that the spatial filter for a target is made from an image showing a vertical aspect, then it can be predicted that objects appearing in other aspects will not match the filter perfectly and there will be some loss of recognition.

The purpose of this test was to determine the effect of reasonable aspect angles on recognition.

Experiment

Four model tanks, turned in different directions were photographed with a long focal length lens. One picture was made directly above and others at various angles. Each of the tanks in any one photograph was seen from the same aspect angle, though due to its orientation each tank presented a different appearance. The signal-to-noise ratio was measured for each photograph and also the relative signal strength of each tank in each photograph.

In the first test, normal recognition signals were obtained for the vertical images, fair results for ten degrees of obliquity but poor and erratic results for larger angles.

Section D-7

Effect of Shadows

Introduction

On a cloudy or rainy day there are no shadows in aerial photographs. On sunny days there are shadows on the ground and for any particular object the size of the shadow will vary with the position of the sun. For high sun angles the shadows are small and close to the objects and serve to outline them and make them more visible. It appears that these small, sharp shadows improve the recognition signal because we have always obtained better results with such photographs than ones taken with diffuse light to simulate a cloudy day.

However, as the sun angle becomes lower the shadows become larger and extend to greater distances and often assume peculiar shapes. Since the shape of a shadow depends on the sun angle and orientation of the target, the shape is quite variable. It appears that these shadows do not aid the recognition process and may hinder it to some degree.

A second effect of a low sun angle is loss of detail on the target. When lighted from above, all of the detail on the top surface is visible and hence comparable to the filter which is assumed to be made from a diffusely illuminated object. As the sun angle becomes low many of the areas on the top surface fall into shadows and the detail on them disappears.

Experiment

Four model tanks turned in different directions were illuminated with a lamp which simulated the shadow contrast produced by sunlight. Vertical photographs were made with the "sun" at various angles to the camera. In any one photograph the four tanks were all illuminated at the same angle, but showed different shadows due to their orientation.

Section D

Conclusions

Only a few of the possible image variables were studied and these were measured by means of laboratory made simulated aerial photographs.

The general conclusion is that the recognition process should be capable of finding any object a human operator would normally find. It is also possible to have objects too small to detect with a particular instrument, and certain types of camouflage confuse the recognition process. On the other hand, the process has shown good performance on low-contrast and partially hidden objects. An exception is deliberate camouflage which may alert a human operator to look for additional clues. Human beings have intelligence to cope with all sorts of difficult situations when necessary, but the recognition process has no intelligence.

Section E-1

Test of Recognition on Aerial Film - 1

Introduction

Aerial camera film was tested for recognition of vehicles and airplanes appearing in the pictures. Very poor recognition was obtain on the first roll of film in which the intensity of the recognition spots was approximately equal to the strongest noise in the scene. This is considered unsatisfactory for automatic recognition.

A preliminary analysis of the cause was made and the experiments are described.

The film consisted of a strip of 78 9 x 9 inch frames and 33 panoramic negatives.

All of the film was apparently a reversal processed duplicate negative. While these are very good duplicates, it was our idea that the recognition process would work best on the original negative.

As will be described later in the experiments, we were unable to obtain good recognition in any of the frames tested. Definite recognition was obtained in almost every case, but the recognition spots were never as much as 1.5 times the maximum noise in the picture. Since we believe that a signal-to-noise at least 2:1 and preferably 5:1 or higher is necessary for automatic operation, the recognition was considered unsatisfactory.

4. Use of a less than perfect optical system.

5. Use of less than perfect liquid gates.

Each of these will be explained in some detail.

1. Loss of low-contrast diffraction detail. The earliest spatial filtering experiments conducted by Marechal and Toraldo di Franca showed that it was possible for a negative to contain an image of the light diffracted by objects too small to be imaged by a lens. This diffraction detail was recorded over a large area at very low contrast something like a hologram. The spatial filtering apparatus duplicated the Abbe condition where the geometrical image and the reconstructed diffraction image were superimposed and it was then possible to see fine detail in the processed picture that could not be found in the original negative. We have assumed that something of this sort took place when original negatives were used as the objects for recognition experiments. We have also assumed that this detail was recorded at such a low contrast that it would be practically impossible to copy it.

2. Loss of sharpness. There is inevitable loss of sharpness in any copying process. The best diffraction is produced by sharp edges.

3. Weak diffraction due to grain noise. Edges that are diffuse or rough produce weak and complex diffraction compared to sharp, high contrast edges. The copying process inevitably superimposes the grain pattern of the copy film on that the original film resulting in a grain pattern that is worse than either film above.

Description of Experiments

Several frames were selected for recognition experiments. Using two frames which showed the same or a similar vehicle or airplane, a spatial filter was made from the object in one frame and used to recognize the same object on another. In no case was a filter used to recognize the object from which it was made. We feel that to do this would be dishonest.

The spatial filters were made in several ways:

1. From objects taken from adjacent frames as described above.

2. From models of similar vehicles.

3. From drawings made from the objects in the aerial films.

The filters were aligned with the axis and a search made for the objects. In every case a recognition spot was obtained, but it was so weak in comparison to the general noise level that it could only be recognized because the operator knew where to look and what to look for. Recognition spots have a distinctive appearance and surround. For example, a very weak recognition spot for a rectangular tank shows a small circular spot with four thin rays aligned with the principle dimensions, a dark area representing the area of the tank and a faint bright outline of the tank itself. These visual clues aid a human operator to find the recognition spot though they do not aid in machine recognition.

Experiment 1. Images of a Patton tank were compared to a filter made from another frame. Using either the full aperture, 2 1/4 inch aperture or 1 inch aperture of the film with or without a liquid gate the recognition spot measured about .8 to 1. times as high as the highest noise in the picture. This was about 30 times as high as the average noise.

Experiment 9. Images of the Beechcraft airplane were compared to a filter made from a photograph of a model. The recognition of high contrast images was fair, 2-3 times above the noise level, but low contrast images gave recognition at the noise level. High contrast images were produced when the aircraft, normally painted white, was on a dark runway. In this case the outline was very clear and there were no confusing shadows. Low contrast images were produced when the aircraft was on a clean concrete runway in which case all that showed was the shadow which was a different shape than the airplane; or when the aircraft was painted a dark color and standing on a dark runway.

False alarms equal in intensity to about half the recognition signal were produced by other smaller airplanes, even single engine aircraft.

Experiment 10. The previous experiment was repeated using spatial filters showing a higher order of diffraction. The filters used in Experiment 9 were 1st and 2nd order. In this experiment several filters combining 3rd and 4th and 5th and 6th orders were tried. The general noise level and the false alarms were reduced but not enough to insure reliable detection. In this experiment it appeared that there was a direct relation between the contrast visibility of the airplanes and the strength of the recognition signal. As we understand it, this is not supposed to be true in a properly operating system, though there will be some reduction of recognition with loss of contrast.

Experiment 11. Images of the Beechcraft airplane was compared to a filter made from an enlarged section an aerial film in which the airplane was cut out with scissors. This is equivalent to a drawing of the object. Actually, two cutouts were made of different images. The results were practically the same as the experiment using the model as an object for the spatial filter.

In these experiments, vehicles had to be isolated from the aerial film. Taking as an example a tank which appeared dark on a light background the negative showed a transparent tank on a darker transparent background. This image was contact printed on a glass plate to make a positive. The glass plate was fine-grained and developed to give the same contrast as the negative. This positive was then contact printed to make a negative and this image was the one used to make the filter. On large images such as 5 mm tanks, the background around the vehicle was painted with opaque paint and masked with tape to produce a plate in which the only transparent image was the vehicle. This plate was then used as the object to make the spatial filter. When these images were enlarged 6 times they looked good, but when enlarged 40 times the outlines were indistinct and the image grainy. It could be seen that the major detail in the image was shadow detail, and of course, this varied with the aspect of the sun. Therefore when filters made from these vehicles were used to recognize other vehicles, the shadow detail was quite different.

On the other hand, our laboratory pictures could be enlarged 40 times and still remain sharp and grainless, and due to the fact that they were diffusely lighted, the shadow detail was not distinctive of any particular angle of lighting.

In the case of models it is necessary to eliminate any shiny surfaces which would produce highlights distinctive of the lighting. We therefore either sandblasted the models or spray painted them with dull gray paint. If it is necessary to produce a very opaque background in the photograph it is not enough to make the picture on a white background, in general it will be found that sufficient exposure to produce a background of density 3.0 plus will result in a fairly high density vehicle image also. Such poorly transmitting object transparencies are difficult subjects for spatial filters and require long exposures. Instead, the model is placed on trans-

Conclusions First Roll Aerial Film

1. Recognition obtained on the submitted aerial film was poor. This was chiefly due to loss of signal strength and not gain in noise, though in at least two instances minor damage to the film resulted in high local noise.

2. The film was apparently reversal processed duplicate negative and showed no detectable relief image.

3. The diffraction images produced by the objects on the film were very weak compared to images made in our laboratory.

4. The spatial filters do not appear to be at fault.

5. Recognition on contact prints from the aerial negatives was considerably improved, but still less than anticipated.

6. Spatial filters made from sharp originals such as models and cut-outs gave slightly better recognition than filters made from images taken from the aerial film.

Section E-2

SECOND ROLL OF AERIAL FILM

Purpose

These tests were to determine the detectability of objects on aerial film.

Introduction

Earlier tests made on duplicate negative film showed poor results. The film was fine-grained, the images were reasonably sharp and in good contrast, but the images on the film showed very weak diffraction. We therefore requested an original negative. The new film used in the tests reported in this section was 5 inches wide and designated "High Resolution Test Film, Can 24".

The film was very long, containing many duplicate and overlapping frames produced by the camera plane flying over the same course several times. Two frames near the end, Numbers 47366 and 47365 were chosen for tests. These two overlapping pictures showed a corner of an airfield with several airplanes of three types. The images were sharp, but somewhat smaller than desirable. As shown in earlier tests, the apparatus we use gives optimum recognition for objects between the sizes of 10 and 2.5 mm, or for larger objects if they contain small details. The sizes of the three types of airplanes on the negative were:

Airplane	Wingspan
Small	.97 mm
Medium	1.90 mm
Large	2.12 mm

We would therefore predict on the basis of previous tests that the small airplanes would give weak or marginal signals, while the two larger planes would provide a reasonably satisfactory signal. For best results, this film should have been examined in an instrument with shorter focal length lenses, or the negative could have been enlarged to fit the apparatus. neither was done.

have been used to search the original negative which appears to be the optimum condition for two-beam spatial filters. However, to do this would have required a vignetting mask around the object. When the airplane is dark and the surrounding transparent there has to be an edge or border to the illuminated transparency. If this edge is sharp, square for example, it will produce the diffraction of a square as well as the diffraction of the airplane. The resulting filter will then attempt to recognize an airplane in a square. To avoid this and to prevent diffraction of the edges of the field it is necessary to use a vignetting mask, a glass plate or film with a clear spot at the center and a gradually tapering density out to the edges where it becomes totally opaque or at least density 3.0. No such mask was available at the start of the tests and so in the first experiments the spatial filter was made from a positive and used to recognize airplanes on a negative film.

This situation, which frequently arises is known as using a filter of the oppositive polarity. In previous experiments with characters, the polarity of the filter appeared to make little difference. We have assumed that for more complex objects, the best recognition would be obtained if the film and filter had the same polarity. The situation is complicated, the amplitude portion of the filter certainly shows polarity, but at present we believe the phase portion does not; there is no difference between negative and positive phase. Therefore, when we speak of a filter of the opposite polarity, probably only one part of it is opposite.

Making the Vignetting Filter

As explained above, this item is required to make spatial filters of objects that are dark and have transparent surroundings. For a 2 mm diameter airplane image the filter should have a transparent center 2 mm in diameter and gradually decreasing transmission to practically zero at a diameter of about 10 mm. Making this filter proved to be difficult. Three different means were used and several tries of each one and none of them produced a really good filter. The best one was

Most of the airplanes were on a high contrast background and were easy to see (though quite small), one airplane was on a white concrete runway apparently in motion and perhaps airbourne. It showed very low contrast against the runway and a different aspect (foreshortened). Poor recognition was obtained, the strength of the signal was only one-fifth that of the other airplanes.

The small airplanes gave weak recognition signals due to their small size. The signals were about twice the maximum noise.

When tested with three different "negative" spatial filters made with a rather poor vignetting mask, the large and medium airplanes gave good recognition. The ratio of the signal to the maximum noise was 6 to 1 and the ratio of signal to most of the noise was 100 to 1. False alarms similar to the earlier tests were also obtained. There seemed to be very little difference between the performance of the two sets of filters.

Figure 1a shows the area covered by the negative and the actual size of the airplane images. Figure 1b is an enlargement of a small area to show the quality of the airplane images.

Figure 2 is an enlargement of the hangar area showing the relative positions of the four large airplanes.

Figure 3 is an enlargement of the recognition image of this same area and shows four recognition images where the airplanes were located. This photograph was made by stopping the scale and orientation search at three different times and making successive exposures on the same film.

Liquid Gates

Both surfaces of the aerial negative were crisscrossed with scratches, some as much as half a micron deep. There were also a number of other minor surface

Figure 1 a Contact Print of Aerial Negative

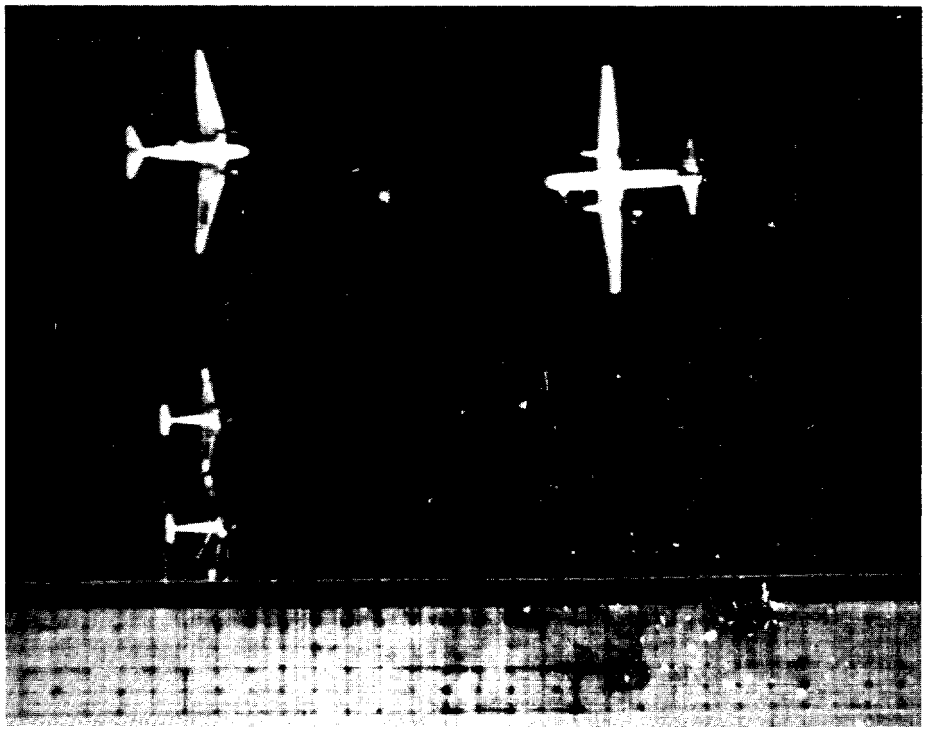

Figure 1 b Portion of Above Enlarged 16 Times to Show Image Quality

Figure 1

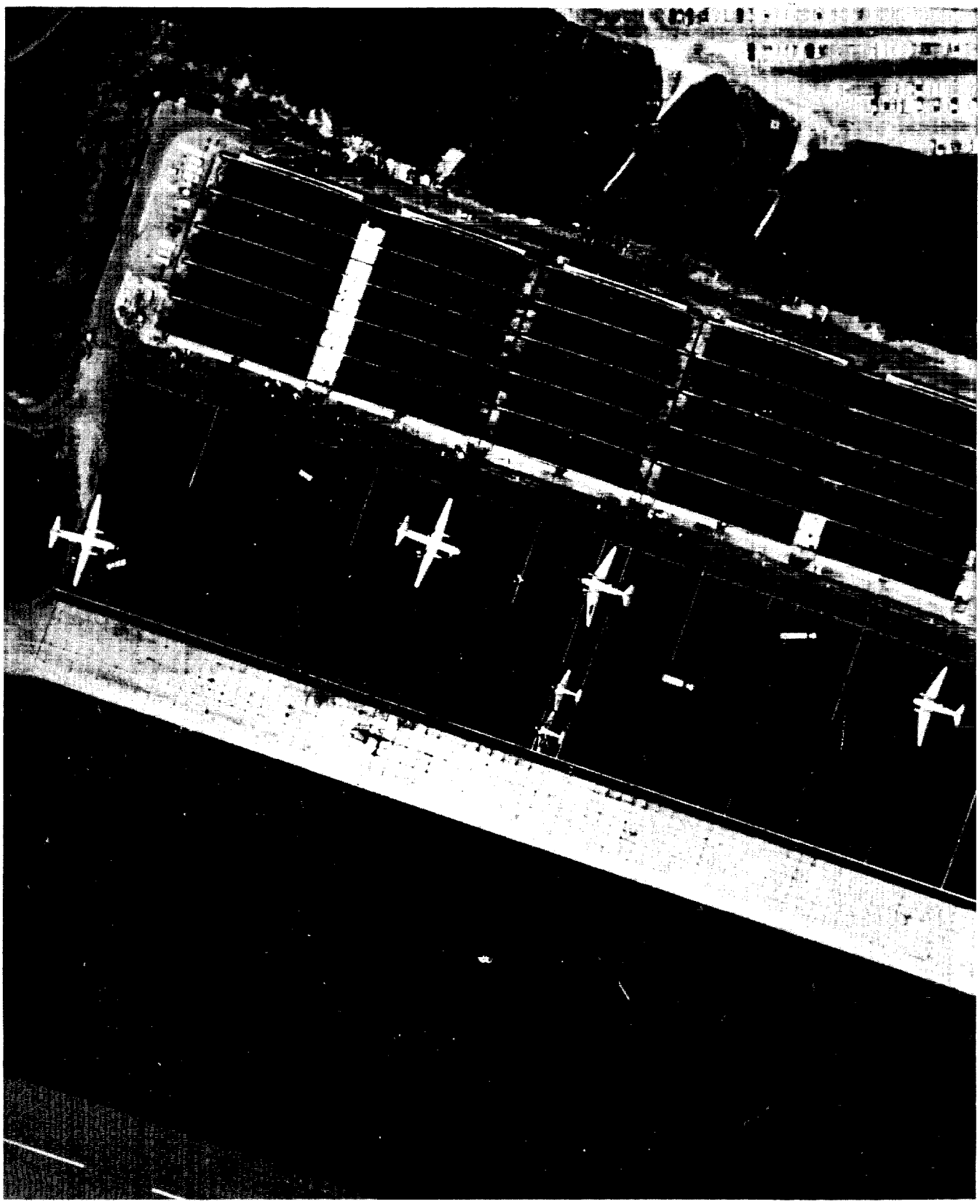

Enlargement of Hangar Area

Figure 2

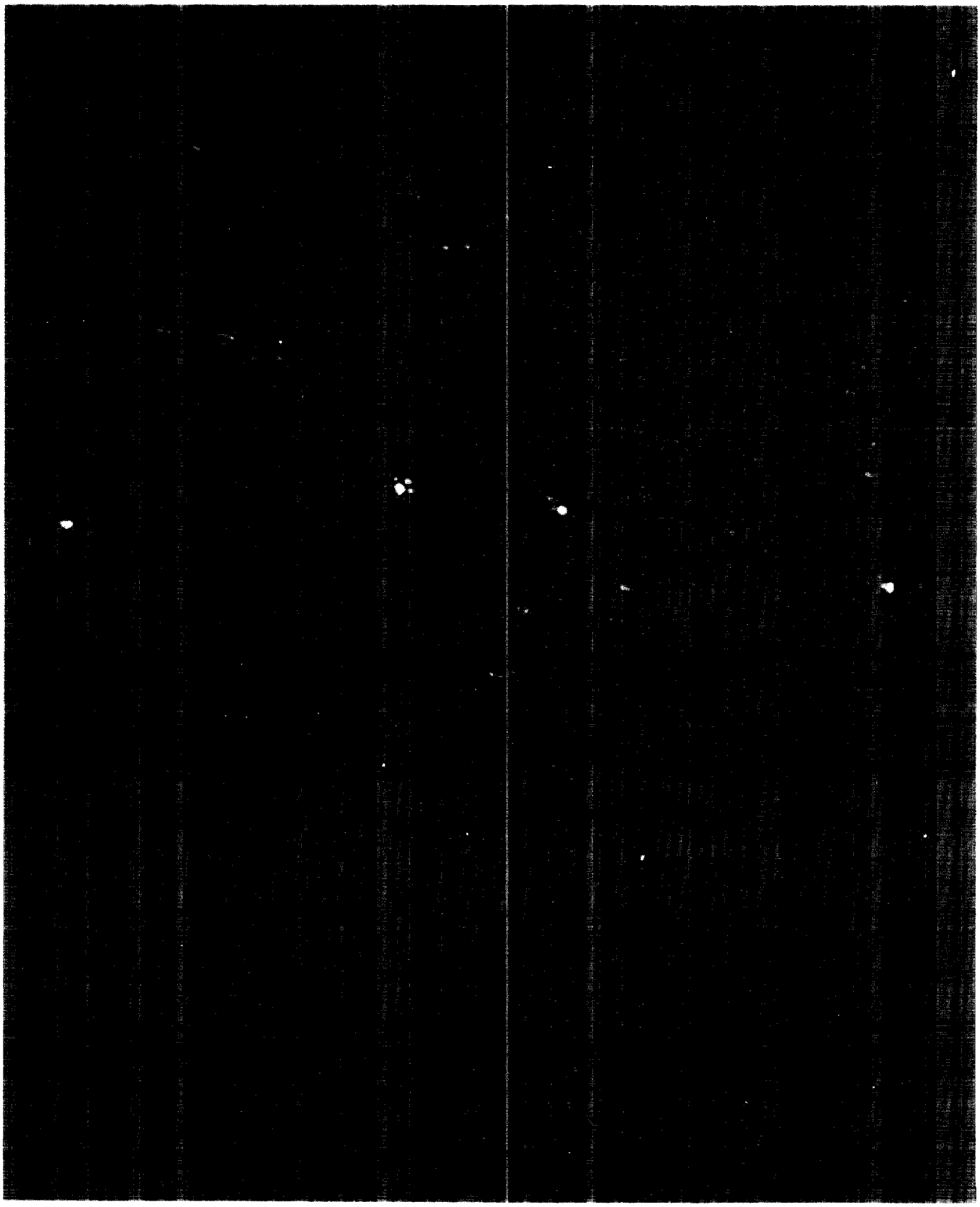

Four Recognition Images for Four Planes - Area is Same as Figure 2

Figure 3

defects. Supposedly, these defects produce diffraction which contributes to the noise, and one of the purposes of a liquid gate is to eliminate the diffraction effects of these scratches. The experiment was repeated with the negative in a gate filled with mineral oil and there was no detectable difference either in the absolute signal strength or the noise. This is the first time this has been noticed. Usually, immersion in a liquid gate reduces the signal by suppressing the relief image and also reduces the noise.

Relief in the Negative

Negative 47366 was examined for relief. It was normal for a fine-grained image. The edges of the runways showed a relief of .15 microns, the airplanes showed about the same. Some high-contrast details showed .30 micron. In contrast to this the back side of the negative showed many scratches at least .5 micron deep.

Conclusions

1. Large (2 mm) and medium (1.9 mm) airplanes were easily detected at a satisfactory signal-to-noise ratio as long as they were on contrasting backgrounds.
2. A similar plane on a very low-contrast background would probably not have been detected.
3. Small (.9 mm) airplanes were detected with a marginal signal-to-noise ratio. These objects are really too small for our equipment.
4. The use of a liquid gate in this case made no difference.
5. The polarity of the filter seemed to make little difference. This means that negative images on the film were detected almost as well with filters made from negatives as positives. Actually, better results were obtained with positives and the probable reason is our limited experience in working with the vignetting filter.